universität wien

DISSERTATION

Titel der Dissertation

„The SWI/SNF complex regulates the Prdm protein Hamlet to ensure lineage directionality in *Drosophila* neural stem cells“

Verfasserin

Elif Eroglu

angestrebter akademischer Grad

Doctor of Philosophy (PhD)

Wien, 2014

Studienkennzahl lt. Studienblatt: A 094 490

Dissertationsgebiet lt. Studienblatt: Molekulare Biologie

Betreut von: Mag. Dr. Juergen A. Knoblich

Table of Contents

1. SUMMARY

Stem cell lineages often contain a transit amplifying (TA) progenitor pool that multiplies the number of differentiating progeny. Unlike in stem cells, the ability to self-renew has to be limited in TA-progenitors to prevent uncontrolled proliferation. Understanding the mechanisms that control the progression from unlimited to limited self-renewal and ultimately to differentiation is therefore important for the treatment of stem cell originated tumors.

Members of the SWI/SNF chromatin-remodeling complex are among the most frequently mutated genes in human cancer but how they suppress tumorigenesis is currently unclear. Here, we use *Drosophila* neural stem cells, called neuroblasts (NBs) to investigate the role of SWI/SNF complex in lineage progression and tumor formation. Knockdown of SWI/SNF complex subunits *osa*, *brahma*, *moira* and *snr1* in type II NB lineages results in formation of ectopic NB-like cells that cause transplantable tumors. Detailed analysis of *osa* mutant clones demonstrate that this is due to dedifferentiation of progenitors, indicating that Osa prevents tumorigenesis in stem cell lineages by ensuring correct lineage progression. We show that Osa acts after asymmetric stem cell division to initiate a progenitor program limiting self-renewal in the TA-population. We identify the Prdm protein Hamlet (Ham) as a key component of this program.

Ham is directly activated by Osa in progenitors and limits the number of asymmetric divisions in *Drosophila* NB lineages. Ham overexpression in NBs causes premature differentiation and underproliferation. Conversely, loss of *ham* function in type II lineages results in formation of ectopic progenitors. We show that Ham is required for correct temporal patterning of progenitors and loss of Ham function blocks the transition from middle-aged to old progenitors, extending their life span. As Prdm family proteins belong to SET domain family of histone methyltransferases it will be interesting to investigate whether Ham mediates the progression of temporal patterning via epigenetic modifications at the temporal transcription factor loci. In the final chapter of this thesis a protocol for performing histone mark chromatin immunoprecipitation followed by sequencing from limited number of FACS sorted cells is described to test this hypothesis.

As composition of SWI/SNF complex is relevant to its tissue specific functions, we performed affinity purifications followed by mass spectrometry to define the complex composition in *Drosophila* larval brain. We identified potential novel binding partners of the complex. Future studies will determine the function of these binding partners.

Collectively, our data provide a mechanistic explanation for the widespread tumor suppressor activity of SWI/SNF. As the Ham homologs Evi1 and Prdm16 are frequently mutated in cancer, this mechanism could well be conserved in human stem cell lineages.

2. ZUSAMMENFASSUNG

Die direkte Nachkommenschaft einer Stammzelle besteht oftmals aus einer transienten Population von Vorlaeuferzellen, die sogenannten transit amplifying Zellen (TA-Zellen). Diese Zellen durchlaufen mehrere Zellzyklen und koennen so in kurzer Zeit eine große Anzahl von Nachkommenzellen erzeugen. Waehrend die Faehigkeit zur Zellteilung bei gleichzeitiger Erhaltung der Identitaet bei Stammzellen als unlimitiert angesehen wird, muss dies in den TA-Zellen limitiert werden, um eine unkontrollierte Proliferation zu verhindern. Wenn man also die Rolle verstehen moechte die Stammzellen bei der Tumorgenese spielen, muessen die Mechanismen untersucht werden, die die unidirektionale Progression von einer unlimitierten ueber eine limitierten Faehigkeit zur Zellteilung bis hin zur terminalen Differenzierung kontrollieren.

Einige Mitglieder aus dem SWI/SNF Komplex, ein Proteinkomplex der in die Remodellierung von Chromatin involviert ist, gehoeren zu den am meisten mutierten Genen in humanen Krebsen. Es wurde gezeigt, dass der SWI/SNF Komplex eine Rolle bei der Kontrolle der Selbsterhaltung der Stammzellidentitaet und Differenzierung spielt; inwiefern dies allerdings zur Entstehung von Krebs fuehren kann ist noch unklar. In der vorliegenden Arbeit nutzen wir neuronale Stammzellen, sogenannte Neuroblasten, aus der Fruchtfliege *Drosophila melanogaster* um die Rolle des SWI/SNF Komplexes bei der Progression der Stammzellnachkommenschaft zu einer immer limitierteren Faehigkeit zur Selbsterhaltung zu untersuchen. Der Knockdown einiger Untereinheiten des SWI/SNF Komplexes (*osa*, *brahma*, *moira* und *snr1*) in einem speziellen Subtypen von Neuroblasten, Typ II Neuroblasten, und deren Nachkommen resultiert in einer Expansion von Neuroblasten-aehnlichen Zellen. Diese Zellen koennen entnommen werden, und wenn in gesunde Fliegen injiziert, proliferieren weiter und haben die Ausbildung von transplantierbaren Tumoren zur Folge. Eine detaillierte Analyse des *osa* Knockdown Phaenotyps ergab, dass dies auf eine Reversion von TA-Zellen zurueck zu Neuroblasten, also Zellen mit unlimitiertem Selbsterhaltungspotential, zurueck zu fuehren ist. Dies deutet darauf hin, dass Osa die Entstehung von Tumoren verhindert, indem es die korrekte unidirektionale Progression der Stammzellnachkommen zu einer immer staerker

differenzierten Indentitaet sicher stellt. Wir zeigen in dieser Arbeit, dass Osa erst nach der asymmetrischen Teilung des Neuroblasten in den TA-Zellen ein Programm ausloest, welches deren Faehigkeit zur Selbsterhaltung, und damit die Anzahlt der Zellzyklen die durchlaufen werden koennen, limitiert. Wir haben das Prdm Protein Hamlet (Ham) identifiziert, welches hauptverantwortlich fuer die Initiierung dieses Programms ist.

In Neuroblasten ist Ham nicht exprimiert, waehrend seine Expression in TA-Zellen direkt durch Osa aktiviert wird. Ham ist sowohl notwendig als auch ausreichend um die Anzahl an Zellteilungen bei denen eine Tochterzelle ihre Indentitaet beibeihaelt und sich weiterhin teilen kann, zu limitieren. Eine Ueberexpression von *ham* in Neuroblasten resultiert in deren verfruehter Differenzierung und damit einem Unterproliferationsphaenotyp. Auf der anderen Seite bedeutet ein Verlust des Ham Proteins in Typ II Neuroblasten und deren Nachkommen eine Akkumulierung von ektopischen Vorlaeuferzellen. Wir zeigen, dass Ham fuer die Etablierung der korrekten zeitlich bedingte Identitaet von Vorlaeuferzellen notwendig ist, und dass die Abwesenheit von Ham den Wechsel von mittelalten zu alten Vorlauefern blockiert. Dies resultiert in einer Verlaengerung ihrer Lebensdauer und damit zu mehr Zellteilungen. Da Prdm Proteine zur Familie der Histonmethyltransferasen mit einer SET Domaene gehoeren, waere es interessant zu untersuchen ob Ham die Progression der zeitlichen Vorlaeuferzellidentitaet vermittelt, indem es auf epigenetischer Ebene die Expression der temporalen Transkriptionsfaktoren modifiziert. Um dieses Experiment Zelltypspezifisch durchfuehren zu koennen, beschreiben wir im letzten Kapitel dieser Arbeit ein Protokoll mit dem von einer limitierten Anzahl an Zellen, die durch FACS gewonnen werden, Chromatin Immunopraezipitationen fuer Histonmarkierungen, gefolgt von deren Sequenzierung, durchgefuehrt werden koennen.

Zusammengefasst bieten unsere Daten eine mechanistische Erklaerung fuer die weitverbreitete Tumorsuppressoraktivitaet des SWI/SNF Komplexes. Da auch die Ham Homologe Evi1 und Prdm16 haeufig in humanen Krebsen mutiert sind, ist es moeglich dass der von uns beschriebene Mechanismus auch in humanen Stammzellen und deren Nachkommen konserviert ist.

3. GENERAL INTRODUCTION

Stem cells have the unique ability to go through several self-renewing divisions, while producing progenitor cells that are more restricted in their developmental potential and can undergo only limited number of divisions before they terminally differentiate. Control over these transit-amplifying divisions and unidirectional establishment of various cell types is crucial for tissue homeostasis, as its defects can lead to tumorigenesis.

Neural stem cells of *Drosophila* have emerged as an attractive model for studying asymmetric cell division and lineage progression (Brand & Livesey, 2011; Homem & Knoblich, 2012; Reichert, 2011; Weng & Lee, 2011). These cells go through several rounds of asymmetric cell divisions, producing an invariant lineage that can be analyzed precisely based on marker expression and the birth order of cells (Brand & Livesey, 2011; Homem & Knoblich, 2012; Reichert, 2011; Weng & Lee, 2011). This introduction will provide background on the origin and characteristics of the *Drosophila* neural stem cells and describe the mechanisms that ensure the balance between self-renewal and differentiation.

3.1 Development of *Drosophila* central nervous system

Central nervous system of *Drosophila* consists of a brain and ventral nerve chord (VNC) that arise from roughly 1000 neural stem cells called neuroblasts (NBs) in three developmental phases (Hartenstein, Spindler, Pereanu, & Fung, 2008; S. Lin & Lee, 2012). During early embryonic development (stages 9 to 11), around 30 cells per thoracic/abdominal hemisegment are specified to become NBs by lateral inhibition and delaminate from a monolayer of bilaterally symmetrical neuroectoderm (Fig. 1) (Homem & Knoblich, 2012; Udolph, 2012). They gain specific identities based on the positional information within the neuroectoderm, temporal cues and repertoire of genes that they express.

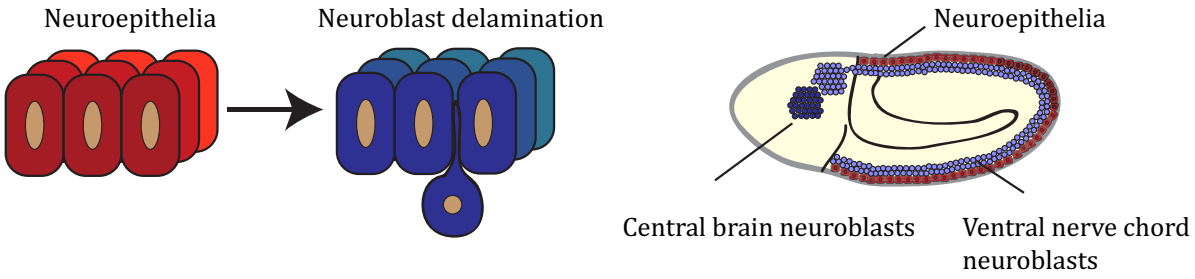

Figure 1: *NBs delaminate from the neuroectoderm at the onset of neurogenesis.*

Each NB generates an invariant lineage by dividing asymmetrically to self-renew and to generate a smaller cell called ganglion mother cell (GMC). GMC divides once to generate two post-mitotic cells that differentiate into neurons or glia that will constitute the larval brain (Knoblich, 2008; P.-S. Wu, Egger, & Brand, 2008). During embryonic stages NBs shrink in size with each cell division. Towards the end of embryogenesis (stages 14-15), most of the abdominal NBs undergo apoptosis, while the cephalic and thoracic NBs (with the exception of mushroom body NBs) cease proliferation through combined activity of Hox proteins and temporal identity factors (described in more detailed below) (Abrams, White, Fessler, & Steller, 1993; Peterson, Carney, Taylor, & White, 2002; Tsuji, Hasegawa, & Isshiki, 2008; White et al., 1994).

With the initiation of food intake during larval stages, a cascade of physiological events is triggered. Due to the increase in circulating amino acids, TOR pathway is activated in the fat body of the larvae (Sousa-Nunes, Yee, & Gould, 2011). The fat body, being the equivalent of the mammalian adipose tissue with endocrine functions, releases an unknown signal that activates PI3K and TOR pathways in glial cells of the larval brain (Chell & Brand, 2010; Colombani et al., 2003; Sousa-Nunes et al., 2011). Glial cells surrounding the NBs then release insulin-like peptides that activate proliferation in the NBs and end the quiescence at the beginning of the second-instar larval stage (Britton & Edgar, 1998; Chell & Brand, 2010; Homem & Knoblich, 2012; Sousa-Nunes et al., 2011). Once NBs re-enter mitosis they divide around 50 times, re-growing after each division until early pupal stages (Almeida & Bray, 2005; Homem & Knoblich, 2012; Maurange, Cheng, & Gould, 2008; Truman & Bate, 1988; White & Kankel, 1978). Almost 90% of the neurons that

form the adult brain are generated during this second wave of neurogenesis during the larval stages and their maturation is completed during pupal stages (Hartenstein et al., 2008).

3.2 Neuroblast lineages of *Drosophila* larval brain

Larval NBs can be classified based on their location and the type of progeny that they produce. Type I, type II, optic lobe and mushroom body NBs generate the lineages of the brain lobes, while abdominal and thoracic NBs generate the lineages of the VNC (Fig. 2A). All larval NBs express the transcription factors (TF) Deadpan (Dpn), Helix-loop-helix mγ (HLHmγ) and Klumpfuss (Klu) (Bello, Izergina, Caussinus, & Reichert, 2008; Berger et al., 2012; Boone & Doe, 2008; Bowman et al., 2008; San-Juán & Baonza, 2011; Xiao, Komori, & Lee, 2012; Zacharioudaki, Magadi, & Delidakis, 2012). The Ets-family transcription factor Pointed (P1 isoform), however, is only expressed in a small subset of so-called type II NBs, where it represses the expression of another TF called Asense (Ase) (S. Zhu, Barshow, Wildonger, Jan, & Jan, 2011). In contrast to the more abundant type I NB lineages, type II NB lineages contain a transit amplifying population and are therefore particularly suitable for the analysis of lineage progression (Fig. 2B). Asymmetric division of type II NBs generates an immature intermediate neural progenitor (imINP) cell that does not express Dpn, HLHmγ and Klu. In a precisely defined, reproducible manner, the imINP subsequently goes through several maturation steps, first turning on Ase and then re-initiating the expression of the NB specific TFs Dpn, HLHmγ and Klu (Bello et al., 2008; Berger et al., 2012; Boone & Doe, 2008; Bowman et al., 2008; Song & Lu, 2011; Xiao et al., 2012; Zacharioudaki et al., 2012) (Fig. 2B). In addition, INPs but not NBs express the TF Earmuff (Erm) (Weng, Golden, & Lee, 2010). Subsequently, the INP resumes self-renewing divisions, always producing another INP and a ganglion mother cell (GMC) that divides symmetrically into two post-mitotic neural cells (Bello et al., 2008; Boone & Doe, 2008; Bowman et al., 2008). In contrast to NBs, however, that divide many times, INPs undergo differentiation after around five rounds of asymmetric division. How the unidirectional establishment of the various cell types in type II lineages is controlled, is currently unclear.

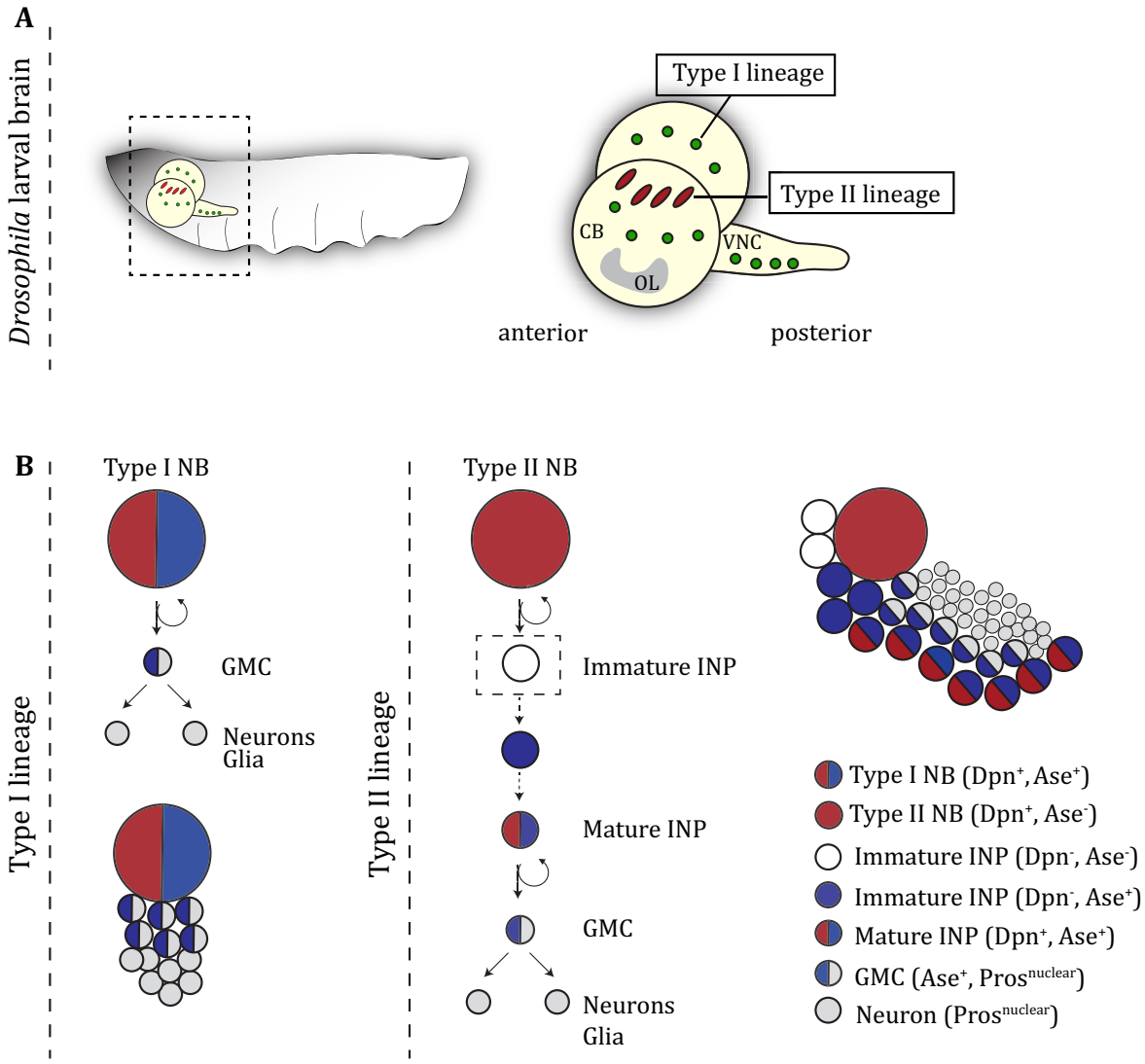

Figure 2: Drosophila larval brain

(A) *The Drosophila larval brain is composed of central brain (CB), optic lobes (OL) and ventral nerve chord (VNC). Type I, type II and mushroom body (not shown) NB lineages in the CB.* ***(B)*** *Type I lineages are characterized by the expression of TFs Dpn and Ase. Their asymmetric division generates another type I NB and a ganglion mother cell (GMC), which divides once to form two differentiated cells (neurons or glia). GMCs express Ase and show nuclear Pros staining. Ase expression is shut down in neurons.* ***(C)*** *Type II lineages contain a transit-amplifying progenitor pool. Type II NB expresses Dpn, but not Ase. Its asymmetric division generates a Dpn-negative, Ase-negative immature intermediate neural progenitor (imINP) that undergoes a maturation step, first turning on Ase and then Dpn before they resume self-renewing divisions.*

3.3 Temporal patterning in *Drosophila* neural stem cells and progenitors

How is the great neural diversity of the adult brain achieved from this seemingly homogenous population of neural stem cells and progenitors? Spatial information elicited by morphogen gradients and their signaling cascades contributes to the generation of neural diversity (Bhat, 1999; Dessaud, McMahon, & Briscoe, 2008; X. Li, Chen, & Desplan, 2013). However, even when progenitors are cultured *in vitro* in the absence of morphogens, they are able to recapitulate the stereotyped generation of neurons observed *in vivo*, indicating that intrinsic mechanisms are involved (Gaspard et al., 2008; Naka, Nakamura, Shimazaki, & Okano, 2008; Shen et al., 2006). Indeed, *Drosophila* NBs, and most recently progenitors, have been shown to express a series of transcription factors that confer them temporal identity, determining the fate of neurons and glia generated in each of these temporally defined competence windows (reviewed in (Jacob, Maurange, & Gould, 2008; Kohwi & Doe, 2013)).

During the embryonic stages of neurogenesis, a subset of NBs expresses the transcription factors Hunchback (Hb), Kruppel (Kr), Pdm1/2 (Pdm) and Cas (Cas) in a sequential manner (Grosskortenhaus, Robinson, & Doe, 2006; Homem & Knoblich, 2012; Isshiki, Pearson, Holbrook, & Doe, 2001; Kambadur et al., 1998; X. Li et al., 2013) (Fig. 3). While the expression of these factors is transient in the NBs, post-mitotic progeny maintains the expression of the TF that is present at their birth. Feedback and feed-forward loops, as well as yet unidentified mechanisms, ensure timely progression of the temporal identity, defining the competence of NBs as they age (Homem & Knoblich, 2012; Isshiki & Doe, 2004; X. Li et al., 2013). It has been recently demonstrated that NBs re-express Cas at the post-embryonic stages of neurogenesis, upon resuming self-renewal divisions, which is followed by a second pulse of Svp expression (Bayraktar & Doe, 2013; Maurange et al., 2008).

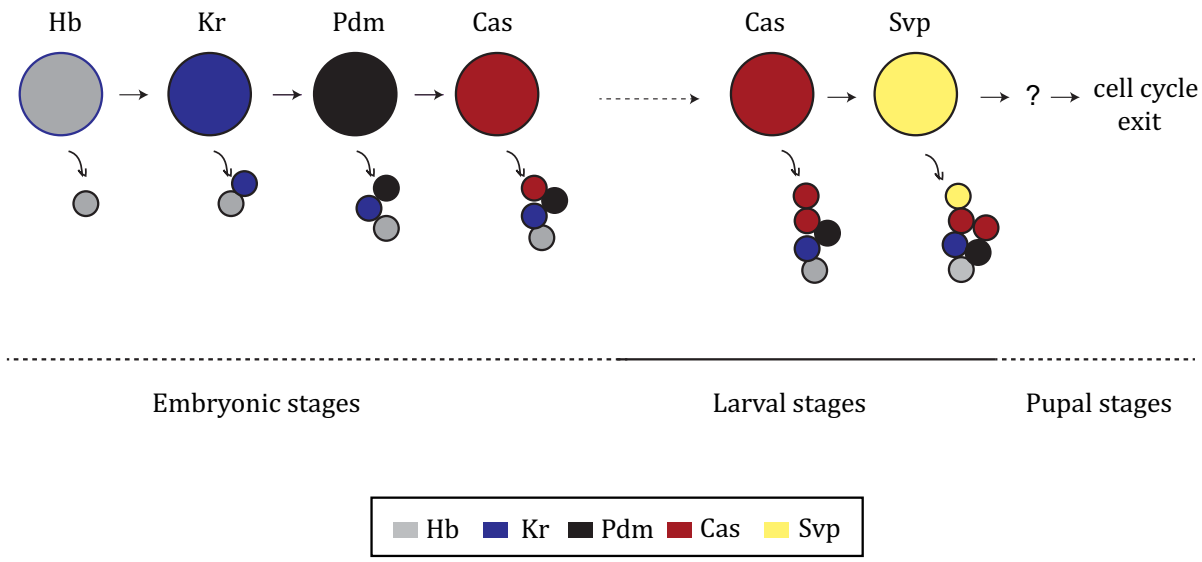

Figure 3: Temporal patterning of Drosophila neural stem cells

A subset of the NBs expresses the TFs Hb, Kr, Pdm and Cas in a sequential manner throughout embryonic neurogenesis. After a quiescence period at the end of embryogenesis, NBs resume Cas expression, followed by a pulse of Svp expression. Currently, TFs that follow Svp expression and eventually lead to NB cell cycle exit at pupal stages are not known. Adapted from (Homem & Knoblich, 2012).

A second axis of temporal patterning has recently been identified in type II NB lineages (Fig. 4) (Bayraktar & Doe, 2013). Elegant work by Bayraktar and Doe demonstrated that in addition to the NBs, INPs also harbor an internal clock. They sequentially express the TFs Dichaete (D), Grainy head (Grh) and Eyeless (Ey) to specify the type of neural progeny generated. Moreover, expression of these factors controls the life-span of INPs, as loss of Ey results in accumulation of progenitors (Bayraktar & Doe, 2013).

What drives this transcriptional clock that ultimately limits self-renewal activity in INPs is currently unclear. However, a recent study shows that regulation of stem cell competence is not achieved merely by a transcriptional on/off switch, but involves larger scale chromatin re-organization (Fig. 5). It has been demonstrated that a two-step process is required for limiting the early competence window in the embryonic NB7-1 lineage;

initial transcriptional downregulation of the *hb* gene and subsequent relocalization of the *hb* locus to the nuclear periphery for permanent silencing (Kohwi, Lupton, Lai, Miller, & Doe, 2013). This suggests a role for epigenetic regulators in the regulation of competence. Previously it has been shown that the window of responsiveness to Kr is regulated by the Polycomb repressor complex (Touma, Weckerle, & Cleary, 2012), supporting the fact that epigenetic changes are crucial in determining stem cell and progenitor competence. Whether a similar genomic re-organization is responsible for the progression of the INP transcriptional clock remains to be determined.

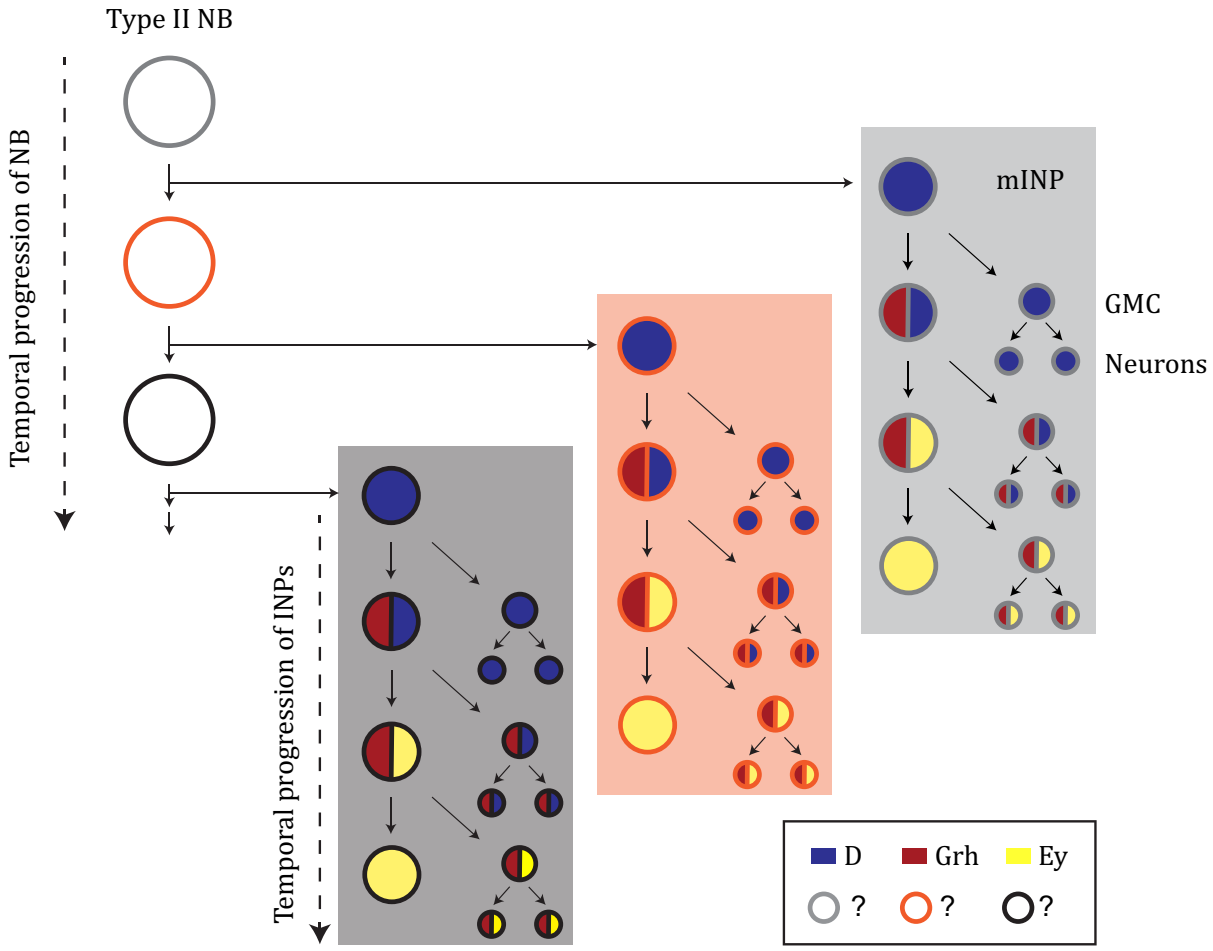

Figure 4: Temporal progression in type II lineages

Temporal patterning in type II lineages is two-dimensional. In addition to the type II NB, which expresses a series of TFs that are not yet fully characterized, mature INPs express the TFs D, Grh and Ey in a sequential manner at larval stages. Adapted from (Kohwi & Doe, 2013).

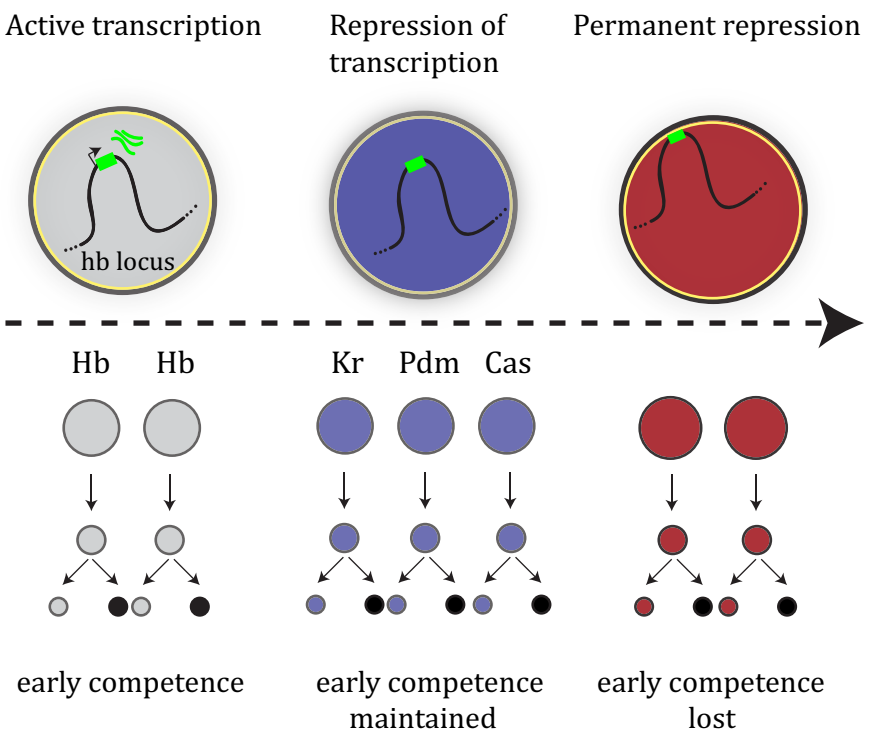

Figure 5: Stem cell competence is regulated through subnuclear genome re-organization.

As the NB proceeds to the next temporal window, expression of the hb gene is turned off. However, the NB is still competent to generate ealy-born neural progeny upon Hb overexpression. When the hb locus moves to the nuclear periphery and gets permenantly silenced, the NB loses its competence to generate early born neural progeny. Adapted from (Cayouette, Mattar, & Harris, 2013).

3.4 Asymmetric cell division in *Drosophila* neuroblasts

A key feature of stem cells is their ability to self-renew as they give rise to a differentiating daughter cell. Generation of two cells with different cell fates could be completely stochastic, enforced by exposure to differential extrinsic signals from a niche, or could be due to unequal segregation of intrinsic cell fate determinants (Fig. 6). Both extrinsic and intrinsic mechanisms of asymmetry are observed in different tissues of *Drosophila* (S. Chen, Wang, & Xie, 2011; Knoblich, 2008; Simons & Clevers, 2011). While germline stem cells have been extensively studied to understand extrinsic regulation of

asymmetric cell fate establishment, NBs have been utilized as a model to investigate the intrinsic mechanisms (Brand & Livesey, 2011; Ceron, Tejedor, & Moya, 2006; S. Chen et al., 2011; Knoblich, 2010; Rebollo, Roldán, & Gonzalez, 2009; Tulina & Matunis, 2001).

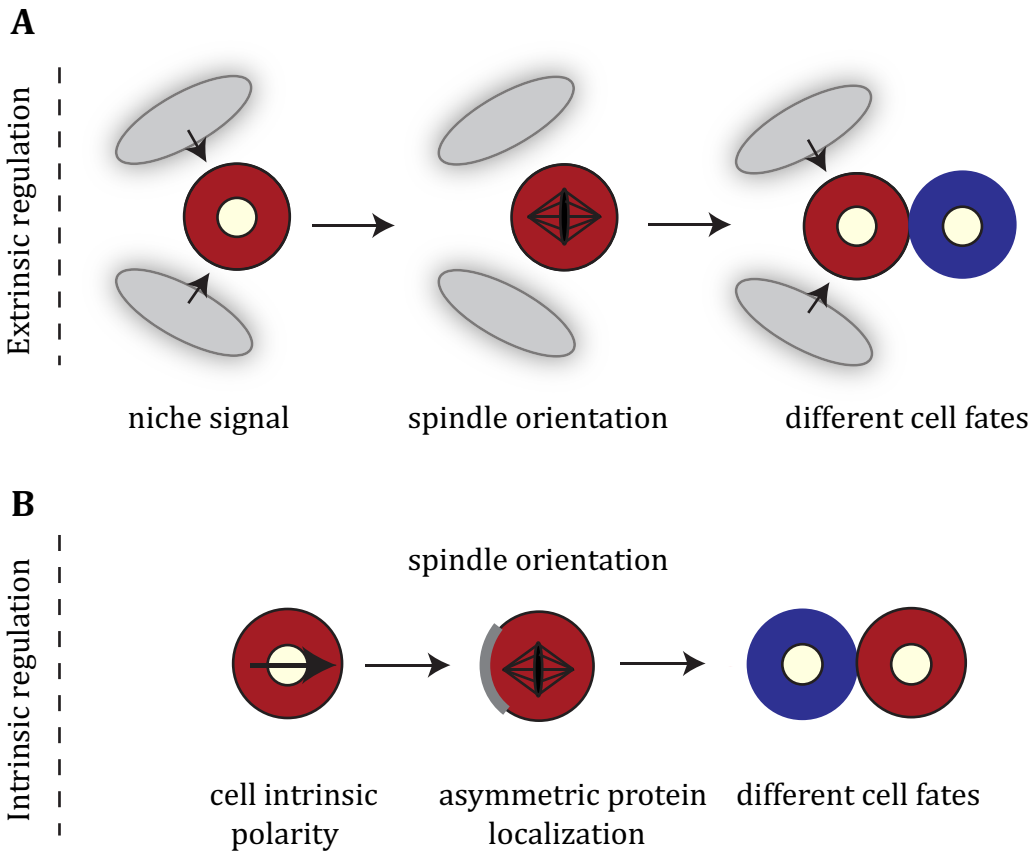

Figure 6: Extrinsic and intrinsic regulation of asymmetric stem cell division

(A) *Extrinsic regulation of stem cell self-renewal. A signal from the niche maintains the self-renewal capacity. Perpendicular spindle orientation ensures that the daughter cell is not in contact with the niche.* ***(B)*** *Intrinsic regulation of stem cell self-renewal. Intrinsic polarity ensures asymmetric segregation of cell fate determinants and generation of different cell fates. Adapted from* (Knoblich, 2008).

Establishment of different cell fates through the intrinsic mechanism in the *Drosophila* NBs depends on the successful execution of the following steps: establishment of axis polarity, correct orientation of the mitotic spindle along the polarity axis, localization of the cell fate determinants asymmetrically and differential segregation of these determinants into the daughter cells (reviewed in (Knoblich, 2010)). Par proteins and localized phosphorylation events have been identified as key components in orchestrating these steps during different phases of the cell cycle (C. A. Smith et al., 2007; Wirtz-Peitz, Nishimura, & Knoblich, 2008).

Par proteins are involved in the establishment of apicobasal polarity in epithelial cells (Suzuki & Ohno, 2006). As NBs delaminate from the ventral neuroectoderm, their apical polarity is maintained. Before mitosis, PDZ-domain-containing proteins Partition defect-3 (Par3 or Bazooka) and Par6, along with the protein kinase atypical PKC (aPKC) accumulate at the apical cell cortex, mediating the basal localization of the cell fate determinants Numb, Prospero (Pros) and Brain tumor (Brat) (Fig. 7A) (Kuchinke, Grawe, & Knust, 1998; Petronczki & Knoblich, 2001; Wodarz, Ramrath, Grimm, & Knust, 2000; P.-S. Wu et al., 2008). Numb has a high affinity for the plasma membrane due to its positively charged N-terminus, making it uniformly cortical in interphase (Knoblich, Jan, & Jan, 1997). There are three aPKC phosphorylation sites in this N-terminal region. Phosphorylation by aPKC neutralizes and therefore disrupts the plasma membrane association of Numb at the apical cortex during mitosis, ensuring its segregation only into the small daughter cell (C. A. Smith et al., 2007).

The fact that aPKC itself is asymmetric already in interphase raises an important question: why is Numb only asymmetric in mitosis? It has been demonstrated that aPKC is in two different complexes depending on the phase of the cell cycle. In interphase, aPKC associates with Par6 and Lethal (2) giant larvae (Lgl) and has reduced substrate specificity. At the onset of mitosis, mitotic kinase Aurora-A phosphorylates Par-6, altering its binding to aPKC and therefore resulting in conformational changes that increase aPKC activity. aPKC phosphorylates Lgl. This releases Lgl from the complex, allowing Par3 to bind aPKC. Par3 acts as an adaptor protein between aPKC and Numb, mediating the phosphorylation that releases Numb from the apical cortex (Fig. 7B) (Wirtz-Peitz et al., 2008). A similar

phosphorylation event by aPKC is also responsible for the basal localization of Miranda, the adaptor protein for Pros and Brat (Atwood & Prehoda, 2009).

aPKC and Aurora-A are not the only kinases that are important for the establishment of the cortical polarity. Phosphorylation of Partner of Numb (Pon), the adaptor protein for Numb, by Polo is crucial for basal localization of Numb (H. Wang, Ouyang, Somers, Chia, & Lu, 2007). Additionally, the G2/M mitotic kinase, cdc2, has been shown to be important for not the initiation, but the maintenance of the apical complex (Tio, Udolph, Yang, & Chia, 2001). What are the phosphatases that reverse the activity of these kinases during mitosis? Mutations in Protein Phosphatase 4 (PP4) complex and its regulatory subunit *falafel* (*flfl*) have been shown to disrupt the basal localization of Mira and its cargo proteins Pros and Brat in metaphase/anaphase NBs (Sousa-Nunes, Chia, & Somers, 2009). Similarly, mutations in *microtubule star* (*mts*), the catalytic subunit of protein phosphatase 2A (PP2A) and *twins*, the regulatory subunit of PP2A complex have been shown to disrupt the asymmetric localization of aPKC, Numb and Pon (Chabu & Doe, 2009; Sousa-Nunes & Somers, 2010; C. Wang et al., 2009). Molecularly, PP2A complex dephosphorylates Par-6 and indirectly suppresses aPKC function (Ogawa, Ohta, Moon, & Matsuzaki, 2009). To sum up, the balance between kinases and phosphatases is key for the timely establishment of cortical polarity.

In addition to establishing the cortical polarity, NBs have to orient their mitotic spindle to specify the cleavage furrow position. This is achieved by the interaction of aPKC-Par complex with the Inscuteable (Insc) protein via Par-3 (Fig. 7C) (Kraut, Chia, Jan, Jan, & Knoblich, 1996; Schober, Schaefer, & Knoblich, 1999). Insc binds to a second protein complex containing the adaptor protein Partner of Inscuteable (Pins) and Gαi (Schaefer, Shevchenko, Shevchenko, & Knoblich, 2000; Siller, Cabernard, & Doe, 2006). Lipid modifications of Gαi tethers the complex to the plasma membrane (Sprang, 1997). On the other hand, Pins mediates microtubule attachment via two spindle orientation pathways. Linker domain of Pins interacts with Discs large (Dlg), which recruits the plus end directed kinesin Khc-73 (Johnston, Hirono, Prehoda, & Doe, 2009; Siegrist & Doe, 2005). TPR motifs of Pins interact with the dynein binding protein Mushroom body defect (Mud), acting as a cortical dock for astral microtubules (Siller et al., 2006; Siller & Doe, 2008). Taken together,

the interaction of the aPKC-Par complex with microtubules and the plasma membrane ensures correct spindle orientation.

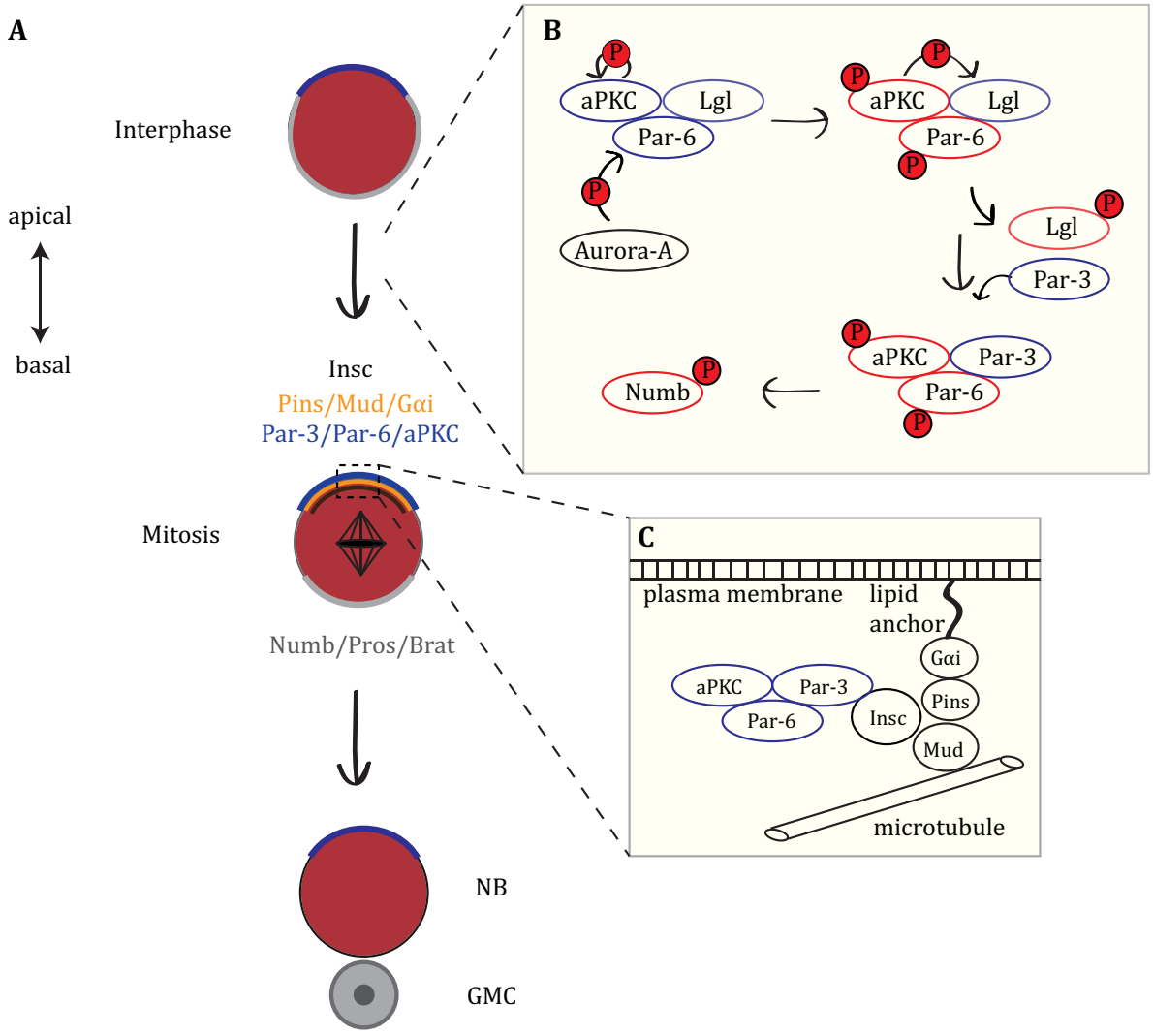

Figure 7: Asymmetric division of Drosophila neuroblasts

(A) *At the onset of mitosis Brat, Numb and Pros are localized basally as a result of phosphorylation events induced by the apical complex. Asymmetric inheritance of the cell fate determinants generates two cells with different fates.* ***(B)*** *Cascade of phosphorylation events leads to subunit exchange in the apical complex, activating aPKC and resulting in phosphorylation of Numb, excluding it from the apical cortex. Adapted from* (Wirtz-Peitz et al., 2008). ***(C)*** *Inscuteable (Insc) mediates the interaction between the apical aPKC-Par complex and the Gαi-Pins-Mud complex. This interaction ensures spindle alignment along the cortical polarity axis.*

3.5 Specifying NB vs. progenitor fate - cell fate determinants and beyond

What is the outcome of asymmetric segregation of the cell fate determinants, Pros, Numb and Brat into the future GMC or INP? Are they sufficient to induce differentiation or is it the exclusion of a mysterious self-renewal factor that drives differentiation? It is necessary to describe the function of the so-called cell fate determinants to start answering these questions.

Numb is a membrane-associated, phoshotyrosine binding (PTB) domain protein that acts as a tissue specific repressor of Notch signaling (Bork & Margolis, 1995; Le Borgne, Bardin, & Schweisguth, 2005; Rhyu, Jan, & Jan, 1994). It was initially identified as an asymmetrically segregating cell fate determinant in sensory organ precursor (SOP) cells of the peripheral nervous system (Rhyu et al., 1994). Its mutation leads to the loss of neurons due to cell fate transformation (Rhyu et al., 1994; Uemura, Shepherd, Ackerman, Jan, & Jan, 1989). In type II lineages of the larval brain, loss of Notch signaling in NBs results in complete loss of type II lineages (Bowman et al., 2008; H. Wang et al., 2006). Conversely, failure to repress Notch signaling in the imINPs results in overproliferation (Bowman et al., 2008; Weng et al., 2010; Xiao et al., 2012). Therefore, it is critical to establish differential Notch responsiveness to maintain the balance between self-renewal and differentiation. Previous studies suggested that interaction of Numb with the endocytic AP-2 complex member α-Adaptin and endocytosis of Notch is critical for this balance (Berdnik, Török, González-Gaitán, & Knoblich, 2002; Song & Lu, 2012). However, recent studies that utilize advanced imaging techniques suggest that in SOP cells Numb antagonizes Notch signaling by preventing the recycling of Notch to the plasma membrane (Cotton, Benhra, & Le Borgne, 2013; Couturier, Mazouni, & Schweisguth, 2013). It will be interesting to see how this model fits with the previous findings and whether it holds true in neural stem cells.

Pros is a homeodomain TF that can act both as a repressor and an activator (Chu-LaGraff, Wright, McNeil, & Doe, 1991; Doe, Chu-LaGraff, Wright, & Scott, 1991). It is expressed in the NB, but only becomes nuclear in the smaller daughter cell following its asymmetric segregation. *In vivo* binding site-mapping experiments performed in embryos showed that Pros directly regulates the expression of cell cycle genes, as well as NB self-

renewal genes, limiting the mitotic potential of GMCs (Choksi et al., 2006; L. Li & Vaessin, 2000). Additionally, Pros binds to the loci of differentiation genes and initiates a transcriptional program required for neuronal or glial fate (Choksi et al., 2006). Surprisingly, forced nuclear localization of Pros in NBs is not sufficient to induce neuronal fate, indicating that there might be an unknown co-activator (Choksi et al., 2006). *pros* mutant embryonic NBs generate unstable GMCs that revert to NBs and gain increased proliferation capacity (Choksi et al., 2006). Similarly, *pros* mutant larval NBs cause stem-cell derived tumors (Bello, Reichert, & Hirth, 2006; Betschinger, Mechtler, & Knoblich, 2006; Caussinus & Gonzalez, 2005; C.-Y. Lee, Wilkinson, Siegrist, Wharton, & Doe, 2006a).

Brat is a translational repressor that belongs to the NHL domain family (Slack & Ruvkun, 1998; Sonoda & Wharton, 2001). *brat* mutants have been identified to die at late larval stages with enlarged brains long before Brat was shown to be an asymmetrically segregated fate determinant (Arama, Dickman, Kimchie, Shearn, & Lev, 2000). Unlike the *pros* mutant phenotype, *brat* mutant phenotype arises strictly from type II lineages (Bowman et al., 2008). Brat has been shown to act at several different developmental stages and tissues as a translational repressor. In the embryo it regulates abdominal segmentation by co-operating with Nanos and Pumilio to repress translation of *hunchback* mRNA (Sonoda & Wharton, 2001). Similarly, it has been shown to repress the translation of *paralytic* mRNA in motoneurons (Muraro et al., 2008). In ovarian germline stem cell lineages, it acts with Pumilio to repress *Mad* and *dMyc* mRNA translation and alter responsiveness to Dpp signaling to promote differentiation (R. E. Harris, Pargett, Sutcliffe, Umulis, & Ashe, 2011). However, a similar translational repression function in the larval brain has not been shown so far. A recent study suggests that downregulation of Wnt signaling by Brat is crucial for the specification of imINP fate (Komori, Xiao, McCartney, & Lee, 2013). Further studies will be required to shed light on the molecular mechanism of Brat function in the type II lineages.

Brat, Numb and Pros are important in establishing the progenitor fate, but how is the NB identity maintained? A recent study from our laboratory identified 28 NB specific TFs and proposed a hypothetical transcriptional network for the maintenance of NB self-renewal capacity (Berger et al., 2012). While there is a great redundancy within this

network, three of these TFs, Deadpan (Dpn), HLHmγ and Klumpfuss (Klu) are necessary and sufficient for the establishment and maintenance of the NB identity. Dpn and HLHmγ belong to the basic helix-loop-helix protein family (Bier, Vaessin, Younger-Shepherd, Jan, & Jan, 1992; Knust, Schrons, Grawe, & Campos-Ortega, 1992). Klu belongs to the EGR transcription factor family (Klein & Campos-Ortega, 1997). All of these three factors act as repressors, however their exact mechanism of action is undefined (Bier et al., 1992; Jennings, Preiss, Delidakis, & Bray, 1994; Klein & Campos-Ortega, 1997).

3.6 *Drosophila* neuroblasts as a tumor model

In recent years importance of tumor "cell of origin" has become evident. However, at the stage of clinical presentation these tumors often display a great level of heterogeneity in genetic composition, cellular morphology, proliferative capacity and response to therapeutics, making it difficult to distinguish the tumor initiating vs. tumor propagating events (Visvader, 2011). Even though technological advances allow rapid sequencing of patient tumors, molecular mechanisms giving rise to these tumors remain elusive. *Drosophila* NB lineages provide an excellent model system where each cell in the lineage can be unambiguously identified and modified by sophisticated genetic tools and the molecular mechanisms of tumor formation can be studied.

Indeed malignant neoplastic transformations in *Drosophila* have been recognized as early as 1960's. Mutations that cause excessive growth in the brain, imaginal discs and hematopoietic system were identified in various genetic screens. Surprisingly, among these were genes such as *brat*, *lethal giant larvae* (*lgl*) and *discs large* (*dlg*), which were later identified as key components of asymmetric stem cell division machinery (Gateff, 1978). Further support for a close link between the asymmetric stem cell division and tumor formation was provided by transplantation experiments, where pieces of larval brain tissue mutant for *pins*, *mira*, *pros* or *numb* were injected into the abdomen of host flies. These host flies developed tumors that were 100-fold bigger than the original tumor, metastasized to secondary sites and caused lethality (Caussinus & Gonzalez, 2005). Additionally, centrosome dysfunction has been shown to compromise asymmetric division in NBs causing transplantable tumor formation (Basto et al., 2008; Castellanos, Dominguez, &

Gonzalez, 2008; Gonzalez, 2013). More recently, factors that are not involved in asymmetric stem cell division machinery, but required downstream of these factors to mediate lineage progression have been identified as potential tumor suppressors (Weng et al., 2010; S. Zhu et al., 2011). Unlike wild type NBs, which exit cell cycle at pupal stages, ectopic NBs resulting from defects in asymmetric division machinery or lineage progression can continue to proliferate even throughout adulthood. Therefore, tumorigenesis in NB lineages is not merely an excess of NBs at the expense of neurons, but involves a transformation where ectopic NBs gain proliferative capacities beyond their cell of origin.

3.7 Genome-wide RNAi screen for novel stem cell self-renewal regulators identified the SWI/SNF complex

Cell fate determinants initiate the progenitor fate upon their asymmetric inheritance; however how this fate is maintained and how progenitors can transform into tumor initiating cells is currently unclear. A genome-wide RNAi screen was performed in our laboratory to identify novel regulators of stem cell self-renewal (Neumüller et al., 2011). In order to drive cell type specific expression of RNAi lines, GAL4/UAS system was employed (Fig. 8A). In this system, the yeast activator protein GAL4 recognizes UAS sequences. By fusing a transgene of interest to these sequences, it is possible to achieve spatial gene expression control (Brand & Perrimon, 1993). For the screen a driver line was generated by recombining *insc*-GAL4 with UAS-m*CD8::GFP*. *insc*-Gal4 drives the expression of membrane-bound GFP and the RNAi line specifically in type I and type II lineages of the larval brain. Moreover, since the GFP labels the entire lineages, initial analysis could be performed without a need for antibody staining.

Loss of function of known self-renewal regulators such as *brat* and *numb,* causes lethality before adulthood. Therefore, a primary screen was performed by crossing all the available RNAi lines from the Vienna *Drosophila* RNAi Collection (VDRC) GD library to the *insc*-Gal4 driver line and assessing their effect on survival (Fig. 8B). Out of the 17,362 RNAi lines (corresponding to 12,314 individual genes), 4182 caused lethality. The analysis of larval brains by confocal microscopy based on the m*CD8::GFP* expression identified 832

RNAi lines (687 genes). Further consideration of RNAi line quality narrowed this number down to 620, corresponding to 4.5% of all protein coding genes in *Drosophila*. Lineages were analyzed based on the number of NBs and daughter cells, the size and shape of NBs and daughter cells and GFP aggregates. Alternative secondary RNAi lines were processed in the same way to confirm the phenotypes. Knockdown of most of the genes either caused "underproliferation" defined by loss of NBs and their progeny, or "overproliferation" defined by amplification in the number of NBs and their undifferentiated progeny (Fig. 8C). 538 genes out of 620 fit into the underproliferation category. In addition to novel genes that promote stem cell self-renewal, housekeeping genes required for cell survival are also expected to be in this category. In contrast, the screen identified only 18 genes in the overproliferation category. Interaction network analysis of these genes revealed two protein complexes (Fig. 8D). The first complex contains the previously identified asymmetric cell division machinery components such as the segregating cell fate determinants, Brat, Numb and Prospero. Interestingly, the second complex contains transcriptional regulators such as the genes *Ssrp* and *barc,* that are thought to be involved in transcriptional elongation and subunits of the SWI/SNF complex *brahma (brm)*, *moira (mor)*, *osa* and *snr1.* These transcriptional regulators provide great candidates for understanding the molecular events that lead to the establishment of stable cell fates in neural stem cell lineages. This thesis will focus on the role of the SWI/SNF complex in *Drosophila* NB lineages.

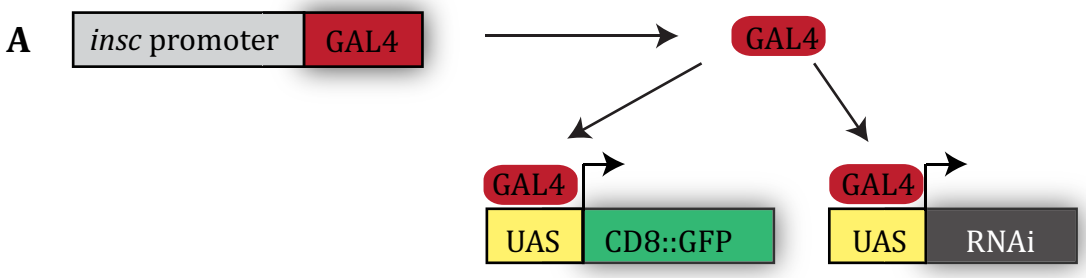

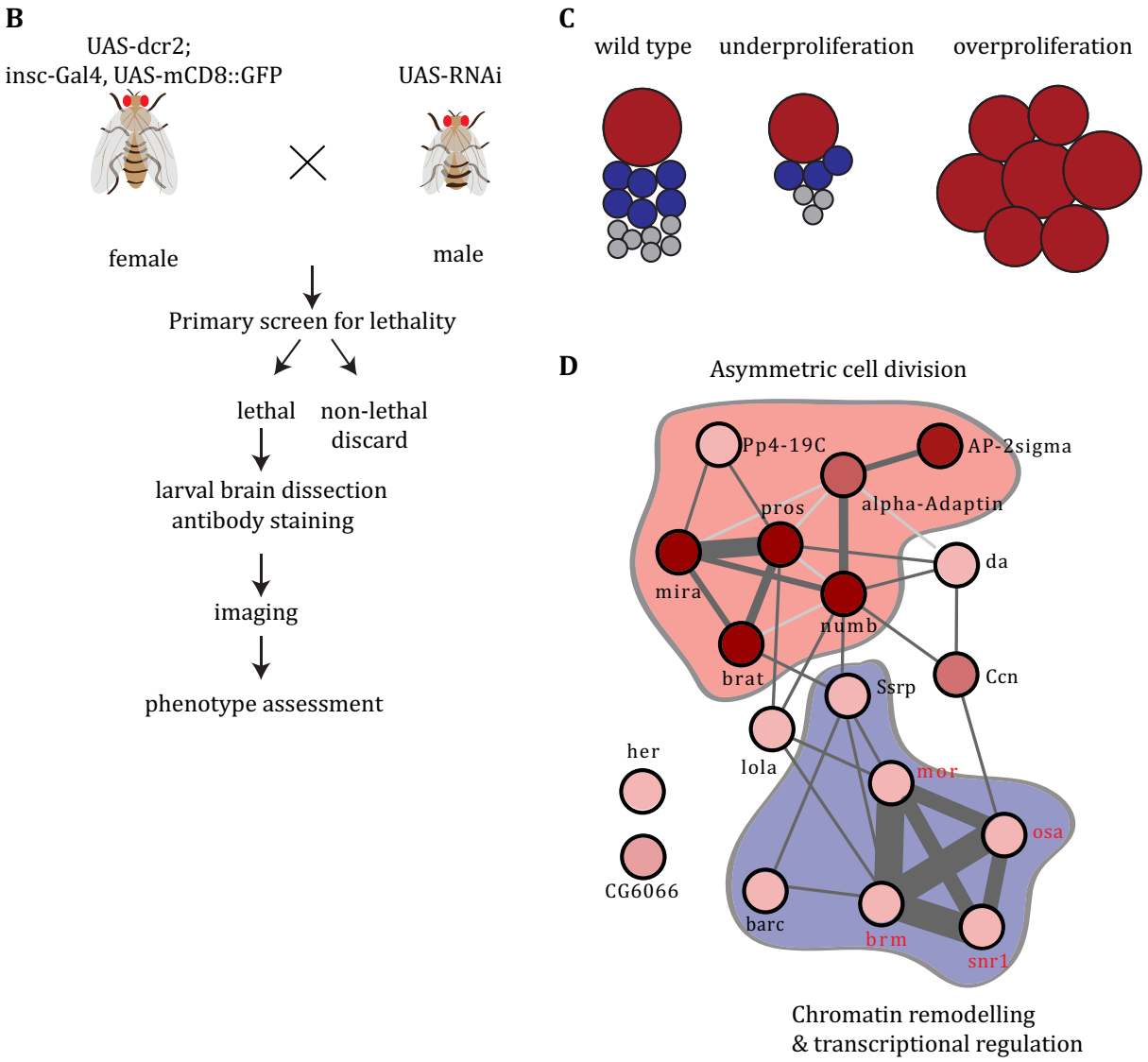

Figure 8: Genome-wide RNAi screen to identify novel stem cell regulators.

(A) *UAS-GAL4 system used for the screen. Insc promoter drives the expression of Gal4, which binds to UAS sequences, leading to the expression of membrane-bound GFP and RNAi specifically in NBs.* ***(B)*** *Flow chart showing the principle of the screen. A primary screen was performed based on lethality. A secondary screen was performed by immunostaining followed by microscopy.* ***(C)*** *Phenotypic outcomes of interest are illustrated. Underproliferation can be observed upon loss of a stem cell maintenance gene. Overproliferation can be observed upon loss of a differentiation gene.* ***(D)*** *Interaction network showing the genes that cause overproliferation upon knockdown. Nodes represent genes and thickness of the lines demonstrates the strength of the interaction (based on biochemical or genetic interactions and literature association). Adapted from* (Neumüller et al., 2011)*. Note that snr1 was identified in an independent screen by Catarina Homem.*

3.8 The SWI/SNF complex

The SWI/SNF complex is an evolutionarily conserved multi-subunit chromatin-remodeling complex, that uses the energy released from the hydrolysis of ATP to mobilize nucleosomes (Roberts & Orkin, 2004). Subunits of the SWI/SNF complex were initially identified in yeast by two independent screens. The first screen was for mutants defective in mating type switching (SWI) and the second screen was for mutants defective in sucrose fermentation (SNF - sucrose non-fermenting) (Neigeborn & Carlson, 1984; Stern, Jensen, & Herskowitz, 1984). In both cases the phenotypes were linked to perturbed transcriptional activation of the genes required for the switching process (*HO* gene) and sucrose fermentation (*SUC2* gene), respectively. Microarray analysis in yeast confirmed the role of the SWI/SNF complex in the transcriptional regulation, acting both as an activator and a repressor (Sudarsanam, Iyer, Brown, & Winston, 2000). Identification of histones and other chromatin components as suppressors of the SWI/SNF complex mutations suggested a link between the chromatin structure and the transcriptional regulation (Hirschhorn, Brown, Clark, & Winston, 1992; Kruger et al., 1995). Further studies showed the recruitment of the SWI/SNF complex to the chromatin and the hydrolysis of the ATP used for the mobilization of the nucleosomes (Imbalzano, Kwon, Green, & Kingston, 1994; Kwon, Imbalzano, Khavari, Kingston, & Green, 1994; Logie & Peterson, 1997; Owen-Hughes, Utley, Côté, Peterson, & Workman, 1996; Phelan, Sif, Narlikar, & Kingston, 1999; SCHNITZLER, Sif, & Kingston, 1998).

In *Drosophila*, there are two evolutionarily conserved subclasses of the SWI/SNF complex. These two subclasses, BAP (Brahma-associated proteins) and PBAP (Polybromo-associated BAP), share seven core subunits. While BAP complex is defined by the presence of a signature subunit called Osa, PBAP complex is defined by the presence of Polybromo, BAP170 and SAYP (Chalkley et al., 2008; Mohrmann et al., 2004). It is thought that the core subunits of the complex are required for the enzymatic and architectural functions, while the signature subunits give the complex the functional specificity. The ATPase subunit Brahma, the signature subunit Osa and the assembly subunit Moira were originally identified as dominant suppressors of Polycomb mutations and are classified as Trithorax-group proteins (Collins, Furukawa, Tanese, & Treisman, 1999; Crosby et al., 1999;

Kennison & Tamkun, 1988; Tamkun et al., 1992), underlining the importance of the complex function in developmental processes.

The SWI/SNF complex is well conserved in mammals and called the BAF complex. Most subunits of the BAF complex are encoded by gene families, increasing the variety and allowing combinatorial assembly. Transcriptional changes arising from the complex activity have been implicated in controlling mammalian stem cell self-renewal and differentiation (Ho et al., 2011; Kidder, Palmer, & Knott, 2009; la Serna, Ohkawa, & Imbalzano, 2006; Lessard & Crabtree, 2010). Deletion of several BAF complex subunits causes early embryonic lethality and defects in the formation of pluripotent cells in mice (Gao et al., 2008; Guidi et al., 2001; Kim et al., 2001; Klochendler-Yeivin et al., 2000; Lessard & Crabtree, 2010). An embryonic stem cell (ESC) specific BAF complex (esBAF), specified by the presence of the ATPase Brg1, BAF155 and BAF60a and absence of the ATPase Brm, BAF170 and BAF60c, is essential for ESC self-renewal (Ho et al., 2009). Osa homologues BAF250a and BAF250b are also crucial for maintaining ESC pluripotency. Furthermore, they are differentially required for differentiation of ESCs into distinct germ layers. Mutations in BAF250a cause defects in gastrulation and failure to generate mesoderm derived cardiomyocytes, while differentiation towards primitive endoderm and ectoderm-like cells is unaffected. Conversely, ESCs mutant for BAF250b show upregulation of mesoderm lineage-specific genes (Gao et al., 2008; Yan et al., 2008). Molecularly, the esBAF complex has been shown to interact with the core pluripotency factors Oct4 and Sox2 and mediate LIF signaling by opposing PcG repression of target genes (Ho et al., 2009; 2011).

The SWI/SNF complex is also required at different stages of neural development, its functions ranging from the control of neural stem cell/progenitor self-renewal and proliferation (Lessard et al., 2007; Matsumoto et al., 2006; Seo, Richardson, & Kroll, 2005), to dendritic development and neural circuit formation (Parrish, Kim, Jan, & Jan, 2006; Tea & Luo, 2011; J. I. Wu et al., 2007). Targeted deletion of Brg1 in neural stem cells decreases the cortex thickness, giving rise to mice with smaller brains (Lessard et al., 2007). Heterozygous BAF155 mutant embryos show defects in neural tube closure, resulting in severe brain malformation (Kim et al., 2001). Furthermore, exome sequencing data reveal

roughly 100 mutated BAF subunit alleles associated with human mental disorders, underlining the importance of the BAF complex in neural development. More mechanistic studies are emerging to explain the underlying cause of these disorders. For example, a recent study shows a critical role for BAF170 in modulating direct vs. indirect neurogenesis (Tuoc et al., 2013). As ESCs give rise to neural progenitors, BAF170 replaces one of the BAF155 in the esBAF (Ho et al., 2009; Lessard et al., 2007; Yan et al., 2008). Conditional BAF170 deletion promotes indirect neurogenesis that results in expansion of intermediate progenitor pool and ultimately leads to an increase in the cortex thickness. It has been demonstrated that this is via interaction of the BAF complex with the REST corepressor complex and repression of Pax6 target genes (Tuoc et al., 2013). Surprisingly, many of the mutations observed in neurodevelopmental disorders are similar to mutations detected in human cancers (Ronan, Wu, & Crabtree, 2013).

3.9 The role of the SWI/SNF complex in tumorigenesis

The mammalian SWI/SNF complex is the most frequently mutated chromatin remodeler in human tumors. A recent study analyzing the exome and whole-genome sequencing data from primary human tumors showed that 19.6% of all reported human tumors have mutations in the SWI/SNF complex subunits (Kadoch et al., 2013). Interestingly, it has been observed that different subunits are mutated in tumors originating from different tissues. For example, the first subunit to be recognized for its tumor suppressive role, hSNF5 (mammalian homolog of the *Drosophila* Snr1), is homozygously inactivated in almost all rhabdoid tumors (aggressive pediatric maliganancy) (Versteege et al., 1998). Osa homolog, ARID1A, is deleted in 10% of breast carcinomas, 30% of renal carcinomas and 57% of primary ovarian clear cell carcinomas (Hargreaves & Crabtree, 2011; S. Jones et al., 2010; X. Wang et al., 2004). Biallelic loss of the ATPase subunit SMARCA4/BRG1 is associated with prostate, lung, breast and pancreatic cancers, as well as medulloblastomas (Hargreaves & Crabtree, 2011; D. T. W. Jones et al., 2012). Even though mounting evidence suggests a crucial role for the SWI/SNF complex in tumor suppression, the molecular mechanim behind has been elusive. Initially it has been suggested that the SWI/SNF complex antagonizes the Polycomb mediated repression of cell cycle checkpoint genes (Kia, Gorski, Giannakopoulos, & Verrijzer, 2008). However, a

following study shows not only antagonizing but also synergistic relation between the SWI/SNF complex and the Polycomb-group proteins, revealing a new level of complexity (Ho et al., 2011). *Drosophila* neural stem cells offer an attractive model system to study the tumors originating from the SWI/SNF complex subunit mutations, due to the well-characterized cell types that can be followed unambiguously *in vivo*.

3.10 Hamlet belongs to the Prdm family of transcription factors

Our studies identified Hamlet (Ham) as a key target of the SWI/SNF complex in type II lineages. Ham belongs to the Prdm family of transcription factors. Members of this family are defined by an N-terminal PR-domain that is related to the SET domain of histone lysine methyl-transferases. In addition to the PR-domain, Prdm proteins have multiple zinc fingers that mediate DNA binding and/or protein-protein interactions (Fig. 9). Some of the Prdm proteins also contain a proline-rich sequence, whose role is less well understood. Even though all the Prdm proteins contain a PR domain, not all of them show enzymatic activity in *in vitro* assays. This raises the possibility that there might be non-histone substrates that can be methylated by the Prdm proteins. Additionally, Prdm proteins can bind and recruit a variety of histone modifiers to target loci in a cell type specific manner.

The mammalian Prdm family has 17 members. These members are involved in a diverse array of biological processes such as vascular development, brown fat differentiation, maintenance of human embryonic stem cells and early hematopoiesis. Not surprisingly, gain or loss of Prdm protein function has been associated with tumor formation. While some Prdm proteins are proto-oncogenes (Prdm3, Prdm13, Prdm14 and Prdm16), some are tumor-suppressors (Prdm1, Prdm2, Prdm5 and Prdm12).

Prdm3 and *Prdm16* are the closest mammalian orthologs of the *Drosophila hamlet* (*ham*) gene. Misexpression of either Prdm3 or Prdm16 causes myeloid malignancies. *Prdm3* knockout mice lose the quiescent long-term hematopoietic stem cells. *Prdm16* is expressed exclusively in the hematopoietic stem cells and early multipotent hematopoietic cells, as well as neural stem/progenitor cells. Chuikov et. al. showed that loss of Prdm16 function results in loss of the stem cells, as well as an increase in apoptosis. The authors

identified altered levels of reactive oxygen species upon loss of Prdm16 function (Chuikov, Levi, Smith, & Morrison, 2010).

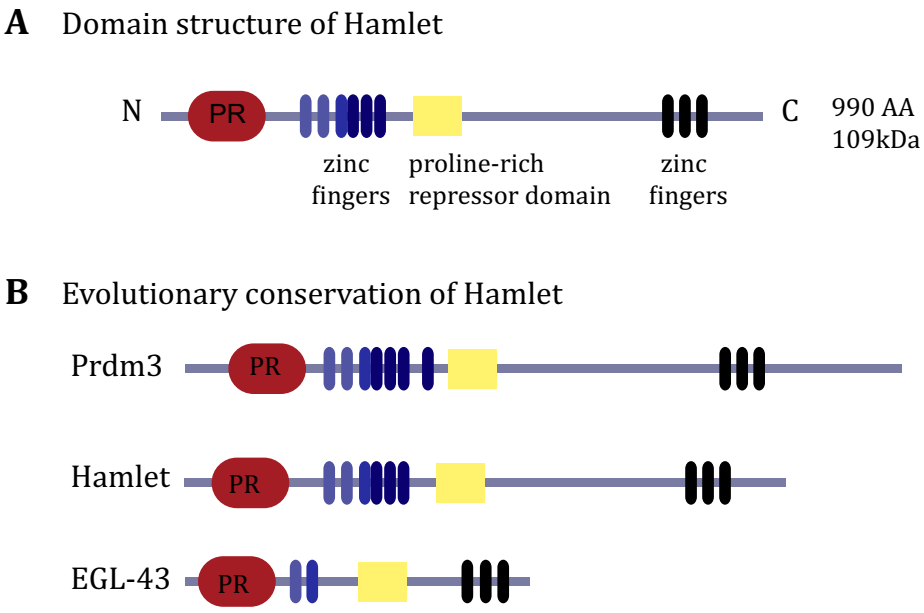

Figure 9: Hamlet is a well-conserved Prdm family transcription factor

(A) *Domain structure for Hamlet is illustrated. Hamlet has N-terminal PR domain followed by multiple zinc fingers and proline-rich repressor domain.* ***(B)*** *Domain structure of mouse and C. elegans homologs of Ham, Prdm-3 and EGL-43 are illustrated. Adapted from* (Hohenauer & Moore, 2012).

A recent publication by Pinheiro et. al. identifies *Prdm3* and *Prdm16* as H3K9 mono methyltransferases that are required for the establishment of heterochromatin. According to this study Prdm3 and Prdm16 redundantly monomethylate H3K9 in the cytoplasm. This precedes the di- and tri-metylation of H3K9 in the nucleus by Suv39h enzymes (Pinheiro et al., 2012).

Ham was first identified in a genetic screen looking for factors affecting the dendrite morphology of neurons arising from the embryonic sensory organ precursor. Moore et. al. showed that Ham acts as a binary switch controlling the formation of external

sensory neurons (with single non-branched dendrite) versus multidendritic neurons (Moore, Jan, & Jan, 2002). Furthermore, loss of Ham function in the adult external sensory organs results in re-specification of an internal cell-fate to an external cell-fate. The role of Ham in cell fate decisions seems to be well conserved, as the mammalian ortholog *Prdm16* has also been shown to act as a bi-directional switch mediating the cell fate decisions between skeletal myoblasts versus brown fat cells.

How does Ham control cell fate at the molecular level? In a recent study, Endo et. al. show that Ham is required in the olfactory receptor neuron diversification by acting at the Notch signaling pathway target loci. The authors argue that Ham re-sets the expression levels of Notch targets through epigenetic modifications of these loci, thereby, allowing the cells to respond to an upcoming Notch signal (Endo et al., 2012). The role of Ham in the central nervous system has been so far elusive.

Here, we make use of the type II NB lineages to ask, how loss of SWI/SNF activity can lead to tumor formation. We show that loss of Brm, Mor, Snr1 or Osa leads to the formation of lethal brain tumors that proliferate indefinitely upon transplantation. Tumors arise, because mutant type II NBs fail to generate the correct cell types in a unidirectional order, a phenomenon we call lineage directionality. Instead of progressing to the mature INP (mINP) stage, *osa* mutant imINPs revert back to type II NBs. We identify a transcriptional program activated by Osa in INPs that is required for temporal patterning and self-renewal control. Ham is an integral part of this program. It is required for the progression of temporal patterning in INPs and ensures timely cell cycle exit. As Ham is both necessary and sufficient for limiting self-renewal in stem cell lineages, we propose a model where Osa ensures that a self-renewal restriction program is initiated before transit amplifying cells resume asymmetric division and a failure to do so leads to the formation of stem cell derived tumors.

3.11 Structure and aim of this study

This study is presented in three Chapters as outlined below.

Chapter I

Investigation of the role of SWI/SNF complex in ensuring lineage directionality and characterization of tumors arising from its defects identify Ham as a key progenitor specific target gene required to restrict INP self-renewal capacity.

Chapter II

Chapter II describes the efforts to characterize the composition of SWI/SNF complex in *Drosophila* larval brain tissue to determine novel, tissue-specific binding partners and to investigate whether there is a subunit switch accompanying lineage progression.

Chapter III

Chapter III describes the establishment of a method to perform histone mark ChIP-Seq from limited number of FACS sorted NBs and neurons to investigate the *in vivo* chromatin profile of well-defined self-renewing vs. differentiated cell populations.

4. CHAPTER I – SWI/SNF COMPLEX ENSURES LINEAGE DIRECTIONALITY IN *DROSOPHILA* NEURAL STEM CELLS

4.1 RESULTS AND DISCUSSION

4.1.1 Osa is a tumor-suppressor in the *Drosophila* brain

A genome-wide RNAi screen for defects in NB self-renewal identified the subunits of the SWI/SNF complex, Osa, Moira (Mor) and Brahma (Brm) (Neumüller et al., 2011). RNAi of either *osa*, *mor* or *brm* in the type II lineages results in an excess of self-renewing Miranda (Mira)-positive cells at the expense of Prospero (Pros)-positive neurons (Fig. 10A) (Neumüller et al., 2011). Another subunit of the complex, *snr1*, was identified in an independent screen performed in our laboratory to cause a similar overproliferation phenotype (Fig. 10A).

To determine whether the overproliferation caused by loss of SWI/SNF complex subunits is due to an expansion of type II NBs or progenitors, we performed Dpn and Ase staining. Larval brains expressing RNAi against *osa*, *mor*, *brm* or *snr1* in type II lineages contained supernumerary Dpn-positive, Ase-negative NB-like cells (Fig. 10B).

To test whether these ectopic Dpn^{+}, Ase^{-} NB-like cells cause tumor formation, we transplanted fragments from control brains or brains in which RNAi of *osa*, *mor*, *brm* or *snr1* was induced by *insc*-Gal4, into the abdomen of adult host flies (Fig. 11A). While none of the control transplants (0 flies out of 68) caused tumors, 29% of the adult hosts transplanted with the *osa* RNAi brain tissue (8 flies out of 28), 58% of the adult hosts transplanted with the *mor* RNAi brain tissue (23 flies out of 40), 66% of the adult hosts transplanted with the *brm* RNAi brain tissue (36 flies out of 55), and 43% of the adult hosts transplanted with the *snr1* RNAi tissue (26 flies out of 60) developed tumors between 14 and 28 days after the transplantation (Fig. 11B). Thus, the widespread tumor suppressor function described for the mammalian SWI/SNF complex is conserved in *Drosophila*.

Although PBAP complex specific subunits, Polybromo, SAYP and Bap170 are expressed in the larval brain, RNAi knockdown showed no phenotype (Berger et al., 2012; Neumüller et al., 2011) (data not shown), underlining a function for the BAP, but not the PBAP complex in NB self-renewal control. In order to study the BAP complex function, we

focused on Osa for in depth analysis. To confirm the *osa* RNAi phenotype, we used the MARCM system to generate *osa* mutant type II NB clones and stained for the markers Dpn and Ase (Lee and Luo, 1999). After 98 hrs, control clones contained only one Dpn^{+}, Ase^{-} primary NB (Fig. 12A) (Bello et al., 2008; Boone & Doe, 2008; Bowman et al., 2008). *osa* mutant clones, however, were significantly larger and contained multiple Dpn^{+}, Ase^{-} ectopic NB-like cells, recapitulating the overproliferation phenotype observed upon *osa* RNAi (Fig. 12A). This phenotype is not due to defects in asymmetric cell division as the asymmetric localization of the apical marker aPKC and the basal markers Mira, Numb and Brat was unaffected by *osa* RNAi (Fig. 12B-D). Similarly, Notch signaling was successfully suppressed in imINPs as revealed by mγ-GFP reporter (Fig. 12E-F). Thus, the BAP complex acts after asymmetric cell division to inhibit the generation of supernumerary type II NBs and prevents tumor formation.

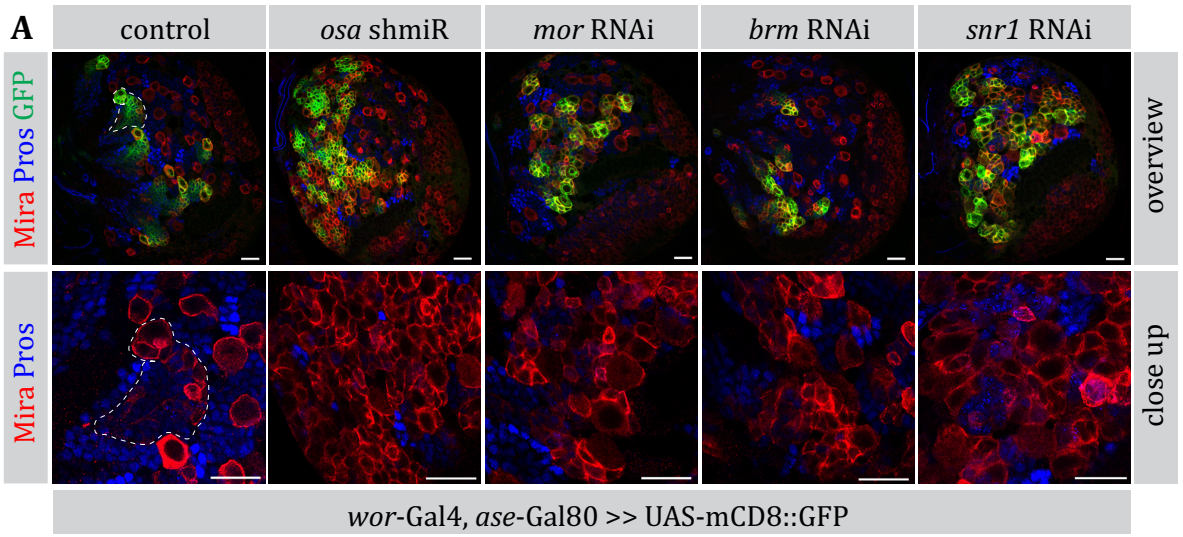
A
control
osa shmiR
mor RNAi
brm RNAi
snr1 RNAi
Mira Pros GFP
overview
Mira Pros
close up
wor-Gal4, ase-Gal80 >> UAS-mCD8::GFP

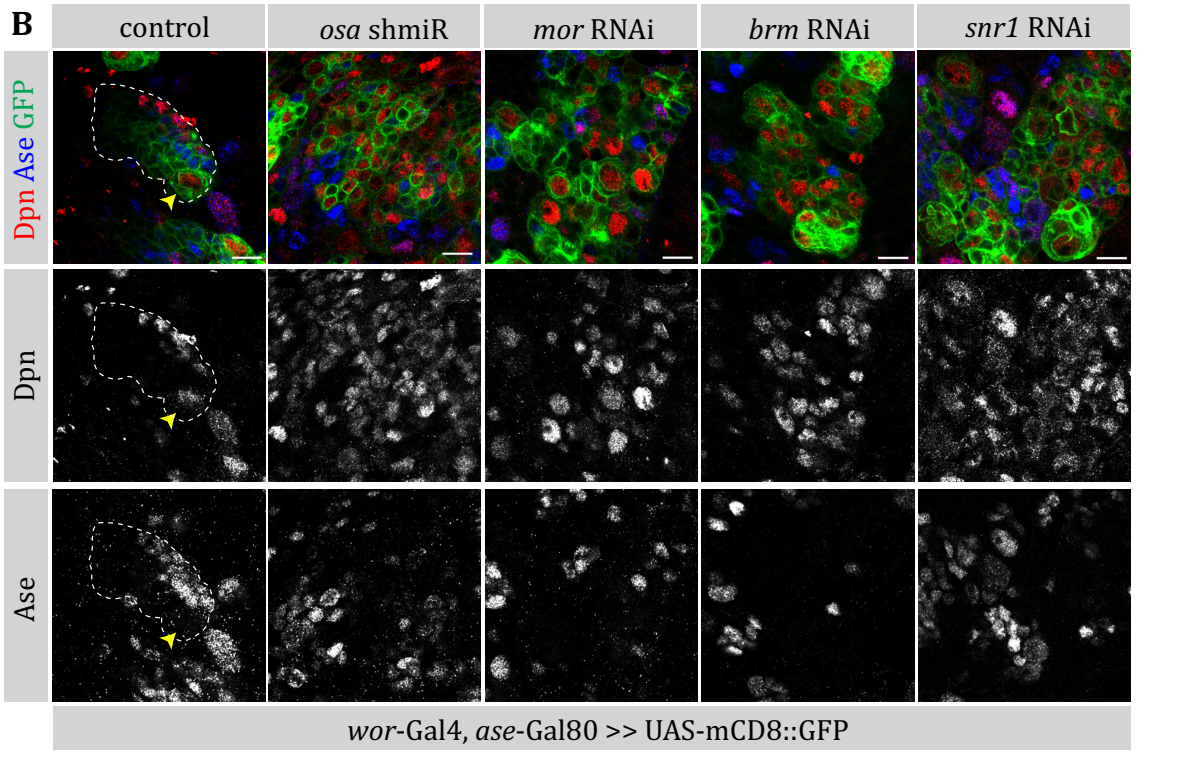
B
control
osa shmiR
mor RNAi
brm RNAi
snr1 RNAi
Dpn Ase GFP
Dpn
Ase
wor-Gal4, ase-Gal80 >> UAS-mCD8::GFP

Figure 10. Knockdown of SWI/SNF complex subunits causes formation of ectopic type II NB-like cells.

(A) *Larval brains expressing shmiR/RNAi against osa, mor, brm or snr1 in type II NB lineages by wor-Gal4, ase-Gal80, stained for Mira and Pros. Knockdown of these subunits causes ectopic Mira^{+} cells (overview images on top panels and close up images on the bottom panels) at the expense of neurons (Pros staining). Scale bars: 20 μm.* ***(B)*** *Close up images of larval brains expressing shmiR/RNAi against osa, mor, brm or snr1 in type II NB lineages, stained for Dpn and Ase. Control type II lineage (outlined) contains a single Dpn-positive, Ase-negative NB (indicated by a yellow arrowhead). RNAi of osa, mor, brm or snr1 causes ectopic Dpn^{+}, Ase^{-} type II NB-like cells. Scale bars: 10 μm.*

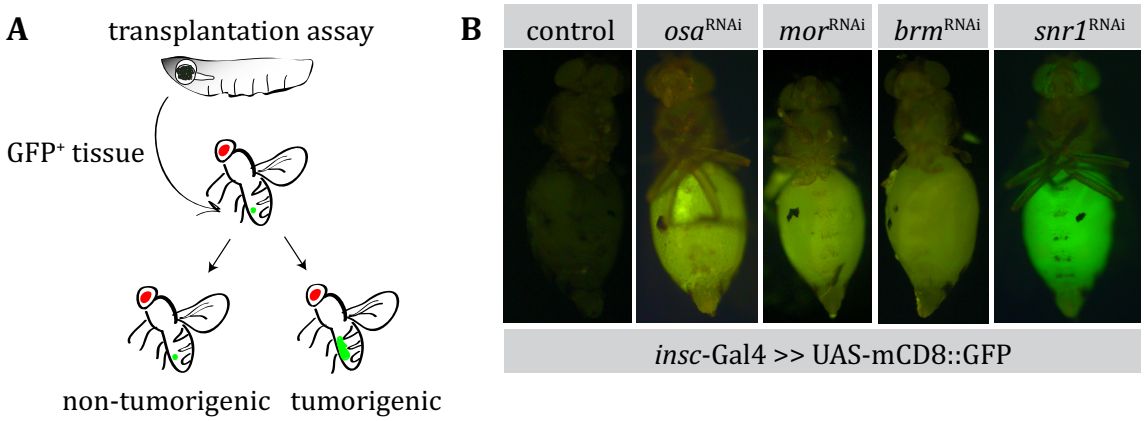

Figure 11. Overproliferating tissue upon RNAi of osa, brm, mor or snr1 cause transplantable tumors.

(A) *Cartoon showing the transplantation assay. Control or RNAi expressing larval brain tissue marked by GFP is implanted into the abdomen of adult host flies. Abdomen of the host fly is filled with GFP⁺ tissue upon tumor formation.* ***(B)*** *GFP-positive overproliferating tissue from larval brains expressing RNAi against osa, mor, brm or snr1 transplanted into the abdomens of host flies cause tumor formation in the adult flies (green abdomen).*

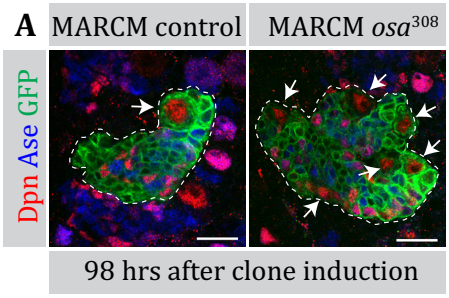
A
MARCM control
MARCM osa308
Dpn Ase GFP
98 hrs after clone induction

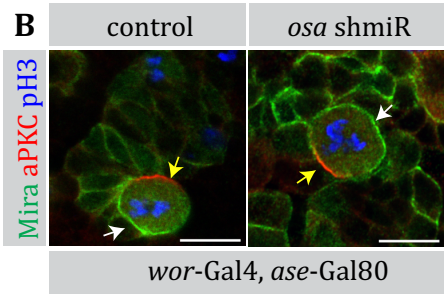
B
control
osa shmiR
Mira aPKC pH3
wor-Gal4, ase-Gal80

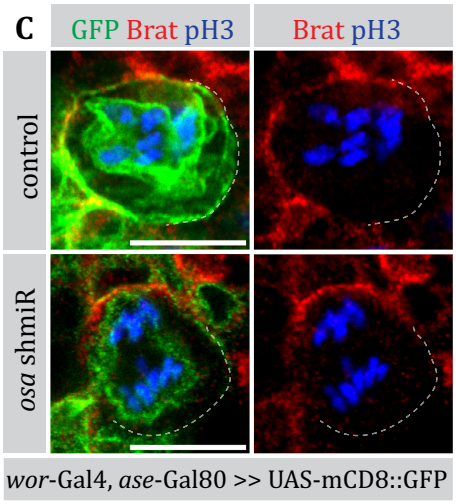
C
GFP Brat pH3
Brat pH3
control
osa shmiR
wor-Gal4, ase-Gal80 >> UAS-mCD8::GFP

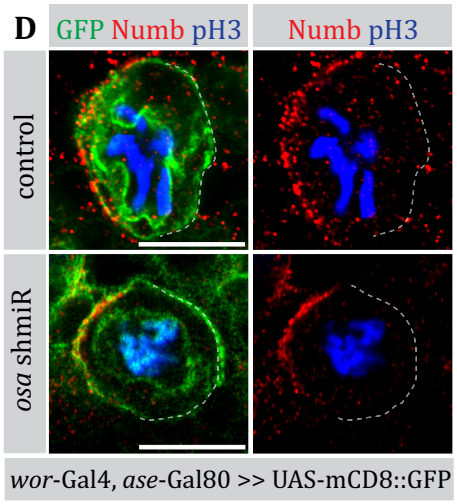
D
GFP Numb pH3
Numb pH3
control
osa shmiR
wor-Gal4, ase-Gal80 >> UAS-mCD8::GFP

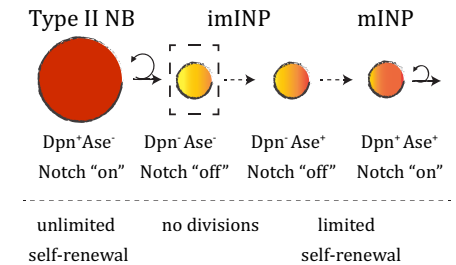
E
Type II NB
imINP
mINP
Dpn+Ase-
Notch "on"
Dpn-Ase-
Notch "off"
Dpn-Ase+
Notch "off"
Dpn+Ase+
Notch "on"
unlimited
self-renewal
no divisions
limited
self-renewal

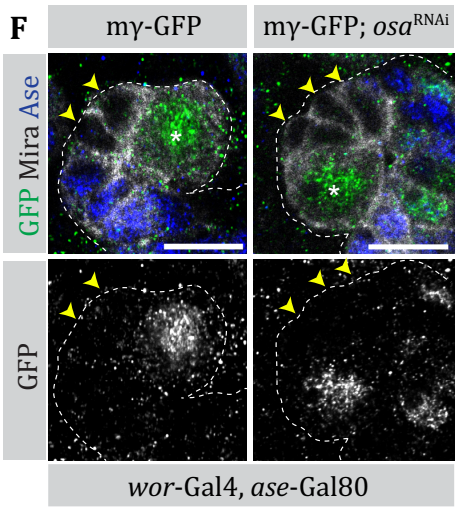
F
mγ-GFP
mγ-GFP; osaRNAi
GFP Mira Ase
GFP
wor-Gal4, ase-Gal80

Figure 12. imINP fate is correctly established in type II NB progeny upon osa RNAi.

(A) *osa mutant clones recapitulate the RNAi phenotype. Control clone has only one Dpn$^+$, Ase$^-$ type II NB (left panel, indicated by an arrow). osa^{308} clone, analyzed 98 hrs after clone induction contain multiple Dpn$^+$, Ase$^-$ type II NB-like cells (right panel, marked with arrows). Scale bars: 15 μm.* ***(B-D)*** *As in control type II NBs, pH3$^+$-mitotic NBs expressing osa shmiR show asymmetric localization of* ***(B)*** *aPKC (apical marker, yellow arrow) and Mira (basal marker, white arrow)* ***(C)*** *Brat (basal marker) and* ***(D)*** *Numb (basal marker). Scale bars: 10 μm.* ***(E)*** *Cartoon showing the self-renewing cells of the type II lineage and their characteristics. Type II NBs are Dpn$^+$, Ase$^-$ with long-term self-renewal capacity. Expression of the self-renewal factors (Dpn and others not mentioned here) is shut down rapidly in the imINP, followed by a maturation step marked by Ase expression and re-activation of the self-renewal genes as well as Notch signaling.* ***(F)*** *As in control imINPs, Notch signaling (monitored by mγ-GFP reporter) is repressed in osa RNAi expressing imINPs. Both control and osa RNAi type II NBs (indicated by an asterisk) show strong mγ expression (also shown as a single channel in the bottom panels), which is repressed in imINPs (identified as Ase$^-$ cells adjacent to type II NBs, indicated by yellow arrowheads). Scale bars: 10 μm.*

4.1.2 *osa* mutations cause lineage reversion

To define the origin of the supernumerary NBs, we analyzed *osa* mutant MARCM clones at various time-points. 50 hrs after clone induction, control type II lineages contained a single Dpn^+, Ase^- NB and this was unchanged in *osa* mutant clones (Fig. 13A). In addition, control clones contained 2-3 Dpn^-, Ase^- and 3-4 Dpn^-, Ase^+ imINPs and this number was slightly but significantly increased in osa^{308} clones (for example: Dpn^-, Ase^- imINPs: control: 2.62 ± 0.18 s.e.m., n=13 clones, osa^{308}: 3.5 ± 0.26 s.e.m., n=12 clones, Student's t test *P* value=0.01) (Fig. 2A). Thus, although there may be a slight delay in differentiation, Osa is not required for initial lineage progression. This was not due to protein perdurance as Osa protein was undetectable by immunofluorescence in 50 hrs mutant clones (Fig. 13B). 75 hrs after clone induction, however, *osa* mutant clones contained ectopic Dpn^+, Ase^- cells (2.24 ± 0.55 s.e.m, n=21 clones) (Fig. 13C), although the number of Dpn^-, Ase^- imINPs was no longer significantly different from the control (control 2.64 ± 0.34 s.e.m., n=14 clones, osa^{308} 3 ± 0.27 s.e.m., n=21 clones, Student's t test *P* value=0.42). Similarly, there was no significant difference in the number of mINPs (control 28.57 ± 2.44 s.e.m, n=7, osa^{308} 23.75 ± 2.35 s.e.m, n=21, Student's t test *P* value=0.18). All of the ectopic Dpn^+, Ase^- cells were several cell diameters away from the primary NB (Fig. 13C, lower panels). As there is no cell migration, these results suggest that Osa is required for stabilizing cell fate and in its absence, INPs revert back to the type II NB fate.

To determine the precise origin of the reverting cells, we depleted Osa by RNAi in the Dpn^-, Ase^- imINPs by *erm*-Gal4 (II) (Xiao et al., 2012) or in the Dpn^-, Ase^+ imINPs by *erm*-Gal4 (III) (Pfeiffer et al., 2008; Weng et al., 2010). *osa* RNAi in the Dpn^-, Ase^- imINPs caused formation of ectopic $Mira^+$, Ase^- cells, some of which were GFP-negative, confirming the loss of INP identity (Fig. 13D-E). These ectopic cells caused tumors upon transplantation (control 0/40 flies, *osa* shmiR 6/59 flies, 5 weeks) (Fig. 14A-B), suggesting that reverting Dpn^-, Ase^- imINPs are the origin of tumor. *osa* RNAi in the Dpn^-, Ase^+ imINPs, in contrast, did not cause formation of ectopic $Mira^+$, Ase^- cells or transplantable tumors (Fig. 14C).

To investigate whether revertant NB-like cells behave akin to NBs, we developed a long-term cell culture method coupled to live imaging to follow the effect of *osa* knockdown in real time. As expression of *erm*-Gal4 (II) line is not restricted to the type II lineages, we used *wor*-Gal4, *ase*-Gal80 to mark the cells of type II lineages with nuclear RFP and express *osa* RNAi. There were no significant changes in cell cycle time, INP maturation time or the lineage generated upon *osa* knockdown (Fig. 15A-C), suggesting that revertant cells behave similar to wild type NBs.

To confirm that Osa functions in the BAP complex to exert its effect on lineage directionality, we analyzed *snr1* mutant clones. Analysis of *snr1* mutant clones 122 hrs after clone induction revealed the presence of ectopic Dpn^{+}, Ase^{-} cells (9 ± 0.95 s.e.m., n=9 clones, *P* value < 0.001, Student's t test) (Fig. 16A-B). Moreover, RNAi of *snr1* in Dpn^{-}, Ase^{-} imINPs caused ectopic $Mira^{+}$, Ase^{-} cells (Fig. 16C). Thus, the BAP complex is required for the transition from the immature to mature INP stage. In its absence, INPs revert to NB-like cells upon re-expression of the self-renewal program, indicating that BAP ensures lineage directionality in type II NBs.

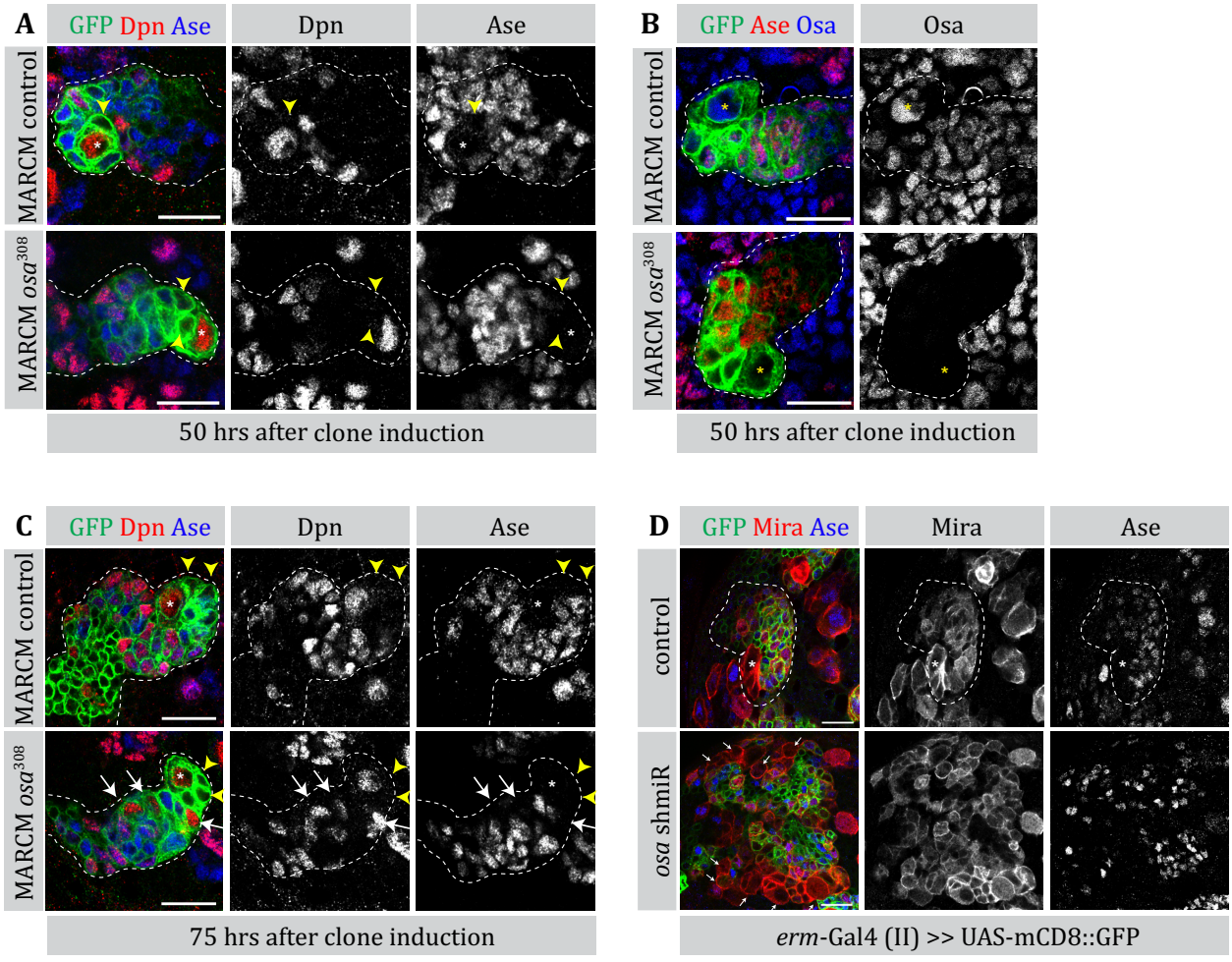
A
GFP Dpn Ase
Dpn
Ase
MARCM control
MARCM osa308
50 hrs after clone induction
B
GFP Ase Osa
Osa
MARCM control
MARCM osa308
50 hrs after clone induction
C
GFP Dpn Ase
Dpn
Ase
MARCM control
MARCM osa308
75 hrs after clone induction
D
GFP Mira Ase
Mira
Ase
control
osa shmiR
erm-Gal4 (II) >> UAS-mCD8::GFP
E
control
osa308
6
5
4
3
2
1
Type II NB (Dpn+ Ase-)
Immature INP (Dpn- Ase-)
Immature INP (Dpn- Ase+)
Mature INP (Dpn+ Ase+)
GMC (Ase+ Prosnuclear)
Neuron (Prosnuclear)

Figure 13. osa mutant imINPs revert to NB-like cells.

(A) *Control and osa^{308} MARCM clones (lower panels, outlined), stained for Dpn and Ase, analyzed 50 hrs after clone induction. Mutant clone (lower panel, outlined) has a single parental Dpn^{+}, Ase^{-} type II NB (lower panel, marked with an asterisk), indistinguishable from the control clone (upper panel, outlined).* ***(B)*** *Control and osa mutant MARCM clones stained for Osa and Ase, 50 hrs after clone induction. Every cell in the control clone (upper panels) is Osa-positive, while the mutant clone shows a complete loss of Osa protein (lower panels). Asterisks indicate NBs.* ***(C)*** *Control and osa^{308} MARCM clones (lower panels, outlined), stained for Dpn and Ase, and analyzed 75 hrs after clone induction. Ectopic Dpn^{+}, Ase^{-} type II NB-like cells emerge in the mutant clone (marked with white arrows, lower panel). Most recently born daughter cells (marked with yellow arrowheads) are correctly specified (Dpn^{-}, Ase^{-}). Parental NB is marked with an asterisk.* ***(D)*** *Close up images of larval brains expressing osa shmiR in imINPs by erm-Gal4 (II) and stained for Mira and Ase, showing ectopic of Mira^{+}, Ase^{-} cells (lower panel, white arrows).* ***(E)*** *Cartoon showing the mutant lineage compared to the control lineage. Cells are numbered according to the birth-order. Scale bars (A-D): 15 μm.*

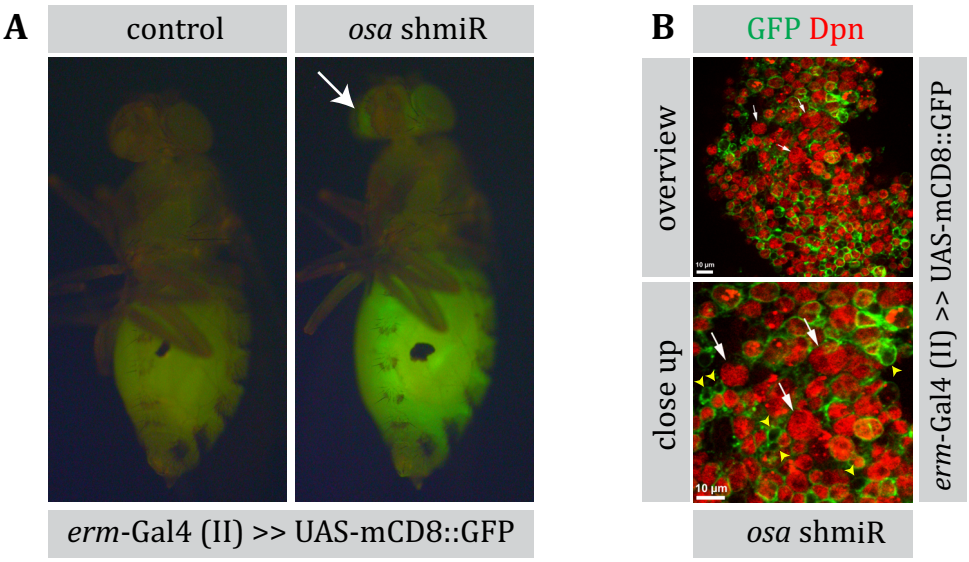

C

Driver line	*erm*-Gal4 (II)		*erm*-Gal4 (III)	
Genotype of implanted cells	control	*osa* shmiR	control	*osa* shmiR
Hosts that developed tumors % (number of hosts injected)	0 (40)	10 (59)	0 (59)	0 (39)

Figure 14. Reversion of imINPs to NB-like cells is tumorigenic.

(A) *GFP-positive overproliferating tissue from larval brains expressing osa shmiR by erm-Gal4 (II) transplanted into the abdomens of host flies cause tumor formation (green abdomen, green spots in the eye indicated by a white arrow. Note that the GFP levels are not high due to loss of GFP expression in revertant cells).* ***(B)*** *Overview and close up images of extracted tissue from the transplanted host stained for Dpn reveals the presence of large Dpn$^+$, GFP$^-$ revertant cells (indicated by white arrows), neighbored by Dpn$^-$, GFP$^+$ imINPs (indicated by yellow arrowheads). Scale bars: 10 µm.* ***(C)*** *Table showing the frequency of host flies that show tumors 5 weeks after transplantation. Osa is depleted in imINPs (erm-Gal4 (II) or erm-Gal4 (III)).*

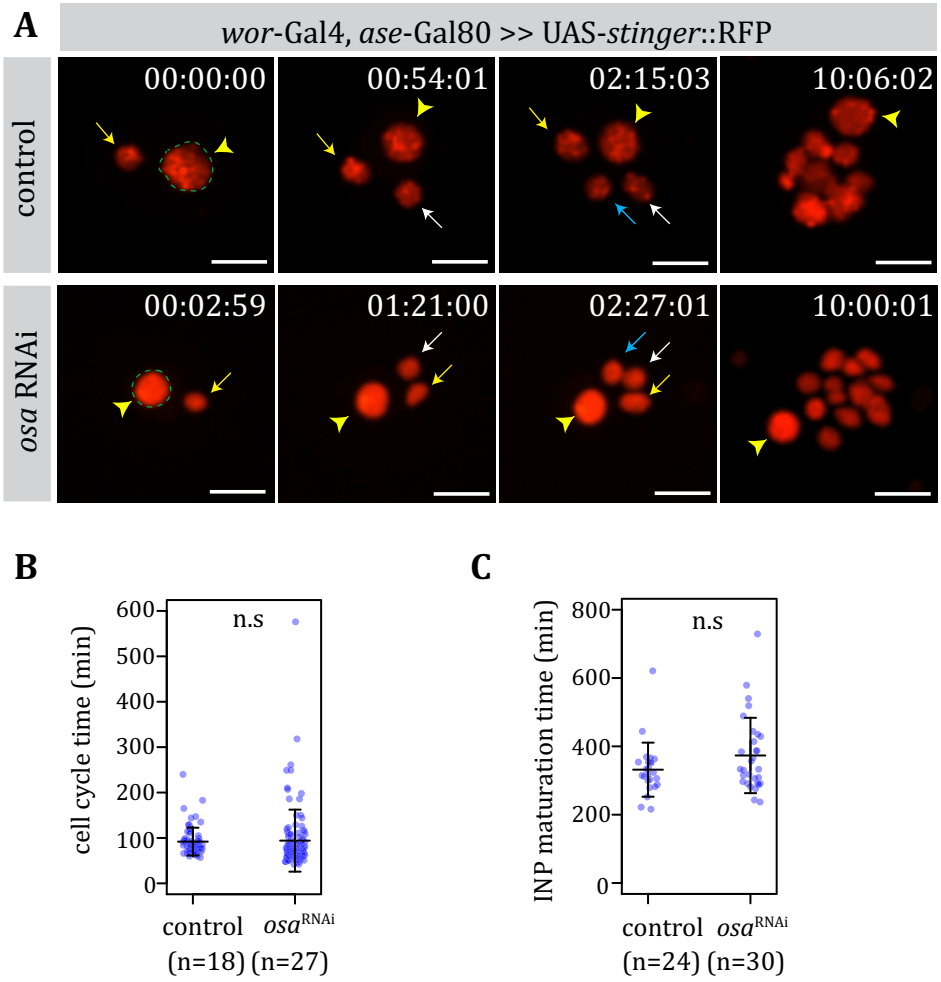

Figure 15. Revertant NB-like cells behave akin to NBs

(A) *Stills from live imaging movies of a control NB (top panels, circled and indicated by yellow arrowhead) or a osa RNAi expressing NB-like cell (bottom panels, circled and indicated by yellow arrowheads, note the smaller size). wor-Gal4, ase-Gal80 was used to drive the expression of nuclear RFP and RNAi. INPs are indicated by differently colored arrows based on birth order (yellow (1.INP), white (2.INP), blue (3.INP)). osa RNAi expressing NB-like cell generate a similar sized lineage after 10 hrs.* ***(B)*** *Scatter plot showing the cell cycle time of control or osa RNAi expressing NBs (control n=18, osa RNAi n=27 NBs followed for 5 subsequent divisions). Error bars represent SD. No significant difference is observed between control and osa RNAi (P value= 0.80, Student's t-test)* ***(C)*** *Scatter plot showing maturation time of INPs in control or osa RNAi expressing NB lineages (control n=24, osa RNAi n=30 INPs). Maturation time has been defined as the time between the generation and the first division of the first-born INP. Error bars represent SD. No significant difference is observed between control and osa RNAi (P value= 0.1, Student's t-test)*

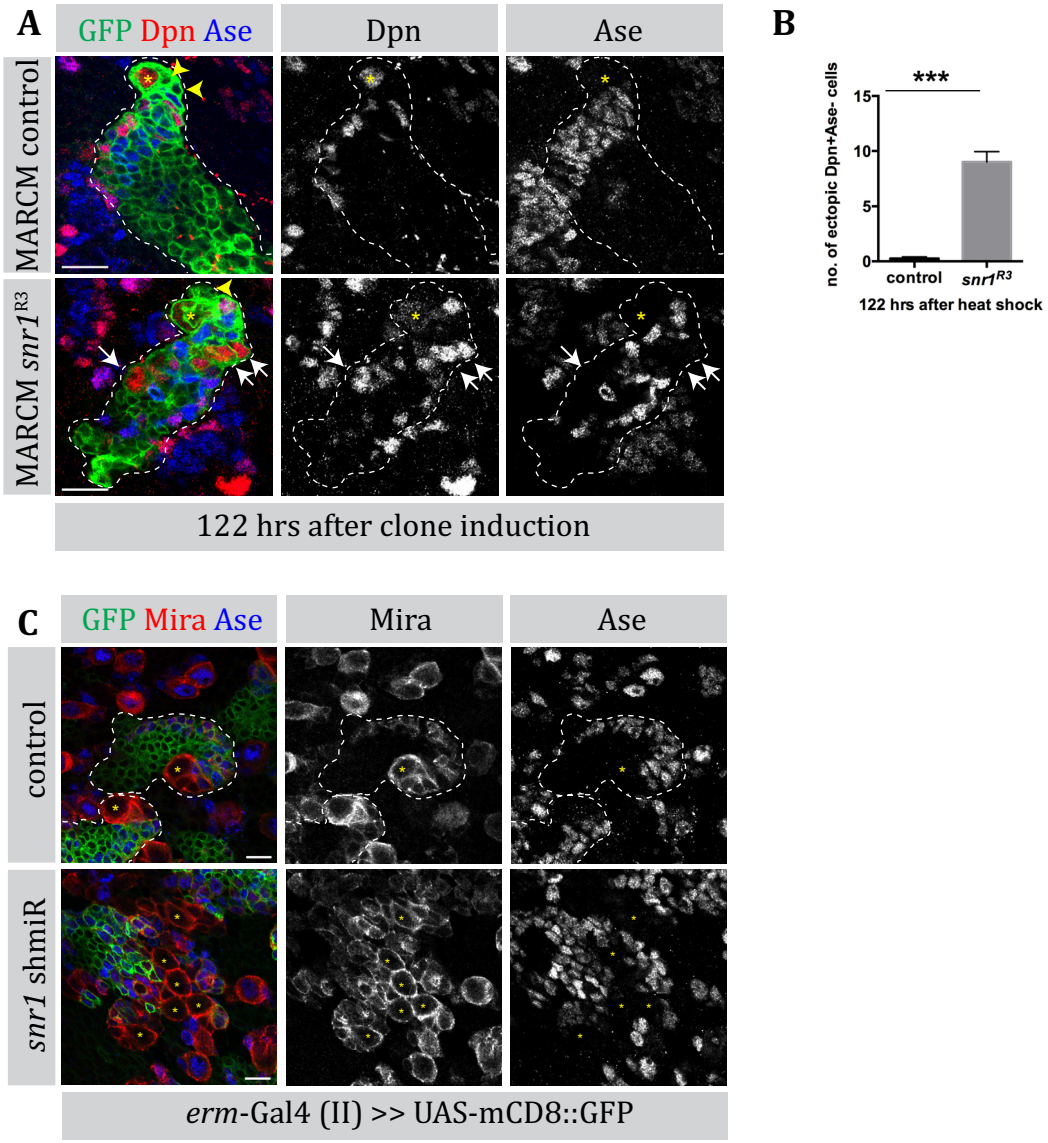

Figure 16. snr1 mutation in type II lineages recapitulate osa mutation.

(A) *Control and snr1^{R3} MARCM clones (outlined), stained for Dpn and Ase, analyzed 122 hrs after clone induction. Parental NBs are indicated by asterisks and imINPs are indicated by yellow arrowheads. Unlike the wild type clone (top panels), snr1 mutant clone (bottom panels) has several ectopic Dpn$^+$, Ase$^-$ NB-like cells (indicated by white arrows). Scale bars: 15 μm.* ***(B)*** *Graph showing the number of ectopic Dpn$^+$, Ase$^-$ NB-like cells in snr1^{R3} mutant clones 122 hrs after clone induction. Error bars represent s.e.m. P value < 0.001. Student's t-test.* ***(C)*** *Close up images of larval brains expressing snr1 shmiR in imINPs by erm-Gal4 (II) and stained for Mira and Ase, reveals ectopic, Mira$^+$, Ase$^-$ cells (lower panel, yellow stars). Control type II lineages are outlined in the top panels. Scale bars: 10 μm.*

4.1.3 Identification of Osa regulated transcriptional targets

To understand how Osa prevents imINP reversion to a NB-like cell, we characterized the transcriptome in type II lineages with and without Osa. As type II NBs are too rare for transcriptome analysis (Bello et al., 2008; Boone & Doe, 2008; Bowman et al., 2008), we developed a FACS strategy that would allow us to isolate wt and *osa* mutant type II lineages of approximately similar cell type composition. For this, we expressed membrane-tethered green fluorescent protein (GFP) from *wor*-Gal4, *ase*-Gal80 in the entire type II lineage, with decreasing levels of GFP in neurons (Fig. 17A-B). As tumors arising from *osa* RNAi are enriched for type II NBs and INPs and contain less neurons, we separated GFP^{high} and GFP^{low} populations to exclude neurons. Indeed, staining for the neuronal marker Elav confirmed that the GFP^{high} population was devoid of neurons (Fig. 17C), whereas Osa staining confirmed that RNAi results in depletion of the protein to undetectable levels (Fig. 17D).

We isolated mRNA from the wild-type (wt) and Osa depleted GFP^{high} fractions and used deep sequencing for expression analysis. This identified 50 genes whose transcript levels were significantly altered in *osa* tumors (assuming a false discovery rate of 0.1, $P < 0.1$, Supplemental Table 1). Even though overactivation of Notch signaling in INPs cause NB-like reversion (Bowman et al., 2008; Weng et al., 2010; Xiao et al., 2012), Notch target genes were not among these 50 genes (Fig. 17E), indicating that Osa acts independently to prevent NB-like reversion. GO term analysis of the differentially expressed genes revealed a strong enrichment for transcriptional regulators (Supplemental Table 2). As expected, known self-renewal factors Pointed and Grainyhead were among the most highly upregulated genes (Supplemental Table 1) (Almeida & Bray, 2005; S. Zhu et al., 2011). The homeodomain-containing TF Optix, expressed primarily in type II lineages (T. D. Carney et al., 2012) and the Myc-type basic helix-loop-helix domain proteins Oli, Tap and Fer2 were also among these genes (Supplemental Table 1) (Bush, Hiromi, & Cole, 1996; Moore, Barbel, Jan, & Jan, 2000). Based on these transcriptional changes and INP reversion phenotype, we hypothesized that Osa might activate a transcriptional program required to maintain INP identity. TFs that are part of this program should be downregulated upon *osa* RNAi but also activated as INPs progress to maturation. To identify these TFs, we separated

GFP^{high} cells according to cell size to obtain pure populations of larger type II NBs and smaller INPs/GMCs (Fig. 18A). We used qPCR to test the expression of various TFs in these two cell populations. As expected, *dpn, mira, klu and HLHmγ* were expressed in both populations, whereas *ase* and *erm* were upregulated in the INPs (Fig. 18B). Of the 13 TFs that were downregulated upon *osa* RNAi (Supplemental Table 1), five were more than 10-fold upregulated in INPs. These were *ham*, *oaz*, *opa*, *D* and *ap* (Fig. 18B) and are likely components of a transcriptional program induced by Osa to stabilize the INP fate and prevent reversion of INPs to NBs. As RNAi knockdown of *oaz*, *opa*, *D* and *ap* did not show any overproliferation phenotype (Neumüller et al., 2011) (data not shown), the components of this program are likely to act redundantly. For *ham*, however, we observed a specific phenotype (see below). As this might indicate a non-redundant function in performing a specific aspect of this program we focused on *ham* for further analysis.

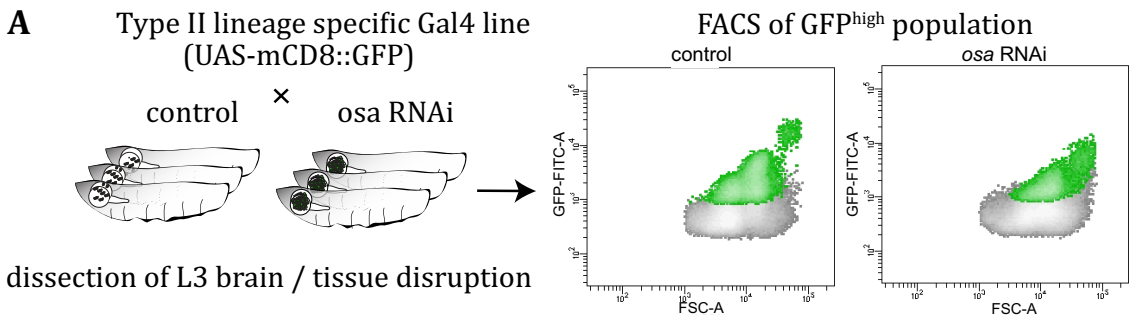
A
Type II lineage specific Gal4 line
(UAS-mCD8::GFP)
control
×
osa RNAi
dissection of L3 brain / tissue disruption
FACS of GFPhigh population
control
osa RNAi
GFP-FITC-A
FSC-A

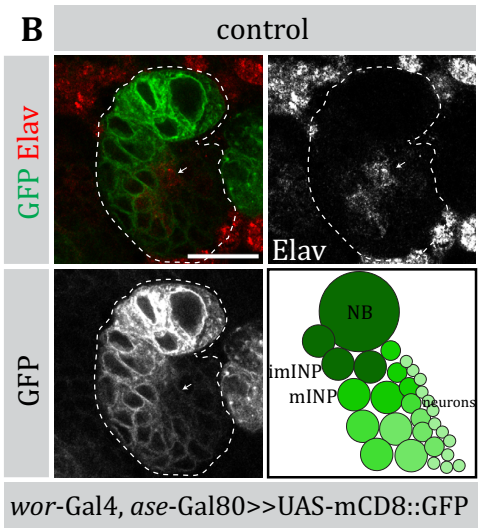
B
control
GFP Elav
Elav
GFP
NB
imINP
mINP
neurons
wor-Gal4, ase-Gal80>>UAS-mCD8::GFP

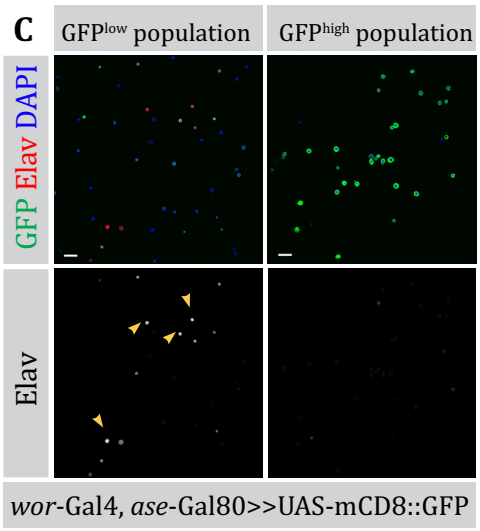
C
GFPlow population
GFPhigh population
GFP Elav DAPI
Elav
wor-Gal4, ase-Gal80>>UAS-mCD8::GFP

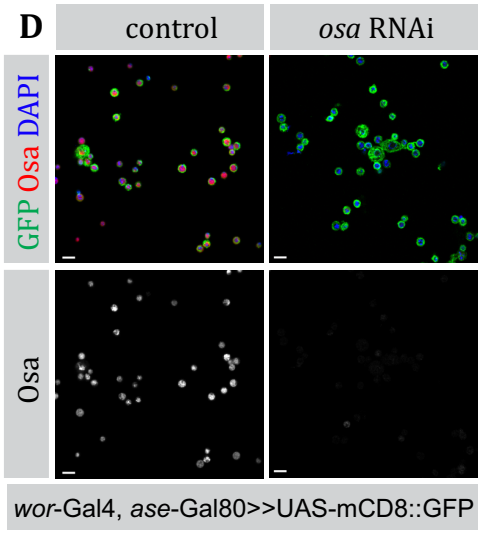
D
control
osa RNAi
GFP Osa DAPI
Osa
wor-Gal4, ase-Gal80>>UAS-mCD8::GFP

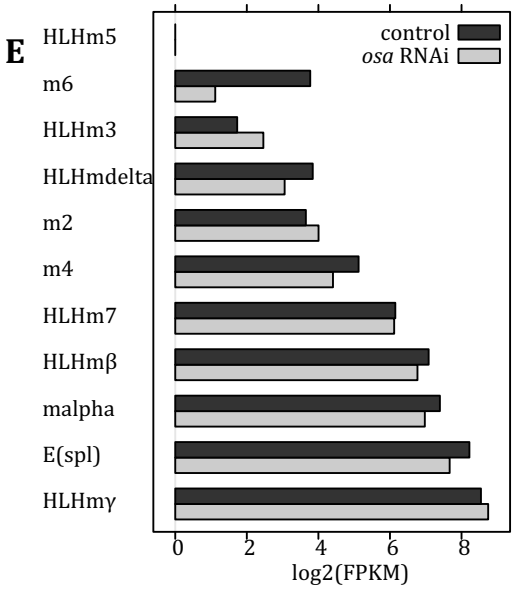
E
HLHm5
m6
HLHm3
HLHmdelta
m2
m4
HLHm7
HLHmβ
malpha
E(spl)
HLHmγ
control
osa RNAi
0
2
4
6
8
log2(FPKM)

Figure 17. FACS sorting of type II lineages expressing osa RNAi

(A) *Membrane-bound GFP and osa RNAi was expressed in the type II lineages by wor-Gal4, ase-Gal80. Control and osa RNAi larval brains were dissected and dissociated. Cells were FACS sorted into* GFP^{low} *(grey) and* GFP^{high} *(green) populations. GFP intensity (vertical axis) vs. size (horizontal axis) plot shows the shift in the cell size and GFP intensity upon osa RNAi.* ***(B)*** *Close up view of a control type II lineage marked with GFP driven by wor-Gal4, ase-Gal80 and stained for Elav. An* $Elav^{+}$ *neuron is marked with a white arrow. Schematic showing the decrease in GFP levels throughout the lineage. Scale bars: 15 μm.* ***(C)*** GFP^{high} *population is devoid of neurons. Elav staining (neuronal marker) in FACS sorted control* GFP^{low} *and* GFP^{high} *populations. Neurons are marked with arrowheads. Scale bars: 20 μm.* ***(D)*** *Osa is efficiently knocked down in sorted cells. Osa staining of FACS-sorted* GFP^{high} *populations from control and tumor tissue. All the DAPI-positive cells in the control are* Osa^{+} *(left panel). All the DAPI-positive cells expressing osa RNAi are* Osa^{-} *(right panel). Scale bars: 10 μm.* ***(E)*** *Notch target genes are not misregulated upon osa knockdown. Plot showing the log2 fold change of the expression of Notch target genes (E(spl) complex genes) upon osa knockdown. FPKM stands for fragments per kilobase of exon per million fragments mapped.*

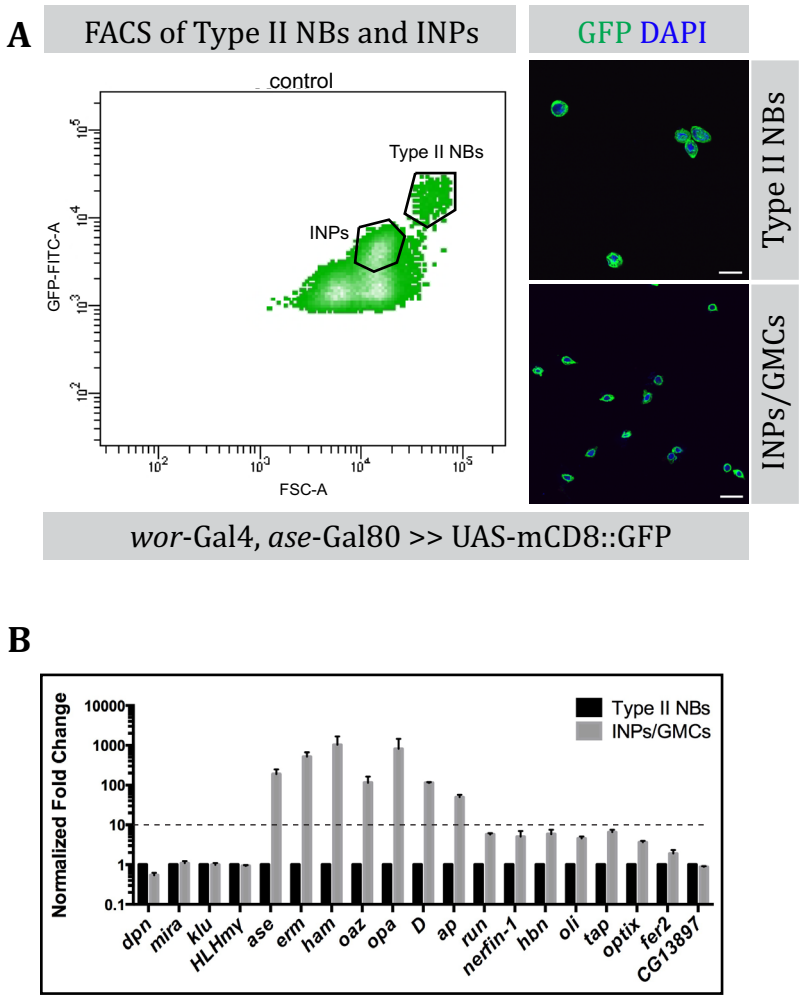

Figure 18. Identification of progenitor specific Osa target genes.

(A) *FACS sorted control type II NBs and INPs. GFP-intensity (vertical axis) vs. cell size (horizontal axis) plot shows a small population of large cells with high GFP intensity (type II NBs). To obtain the INP population we sorted the second largest cell population that showed the second highest GFP intensity. The cells were sorted on cell culture dishes and cell size was measured. Scale bars: 15 μm.* ***(B)*** *qPCR analysis of candidate target gene expression levels in FACS-sorted control Type II NBs vs. INPs/GMCs. dpn, mira, klu and HLHmγ are included as control genes expressed both in the NBs and the INPs. ase and erm are included as control genes not expressed in the NBs, but expressed in the INPs. Error bars represent s.e.m.*

4.1.4 Ham is a direct transcriptional target of Osa

To analyze Ham protein expression, we generated a specific antibody (see Methods). In the central larval brain, Ham is exclusively detected in type II lineages (Fig. 19A). Ham protein is not found in type II NBs and Ase$^-$ imINPs. Expression is activated during INP maturation before the re-expression of Dpn at around the same time as Ase expression (Fig. 19B, top panels). As expected from the transcriptome data, Ham protein is absent from all cells in *osa* mutant clones, even though the expression of Ase was successfully activated (Fig. 19B, lower panels). Thus, Osa activates Ham expression in imINPs.

To assess whether the regulation of Ham by the BAP complex is direct, we performed ChIP-qPCR analysis from third instar larval brains using a specific antibody we generated to Osa (see Methods, Fig. 20A). While Osa does not bind to the Ham coding region, we observed significant and reproducible binding upstream of the first and third transcription start sites (TSSs) of the *ham* locus (Fig. 20B). Binding of the SWI/SNF complex to these regions is further supported by the ChIP-chip data available for Brm from modENCODE that predict similar binding sites (Nègre et al., 2012).

Surprisingly, Osa expression itself is not INP specific and is ubiquitous in the larval brain, including type I and type II NBs (Fig. 20C). The specific activation of Ham in the INPs led us to speculate that the BAP complex might be absent from its target loci in the NBs, but recruited in the INPs. Since it is not possible to get sufficient amounts of pure type II NBs or INPs for the ChIP-qPCR analysis, we used *brat* mutant brains, where tumors consisting entirely of type II NBs are formed (Bowman et al., 2008; T. D. Carney et al., 2012). Although Osa expression was not affected in the *brat* mutant brains, binding to the target loci was reduced to background levels (Fig. 20D-E). Thus, although the BAP complex is expressed throughout type II lineages, it is specifically recruited to its target loci only in the INPs (Fig. 20F).

Using similar ChIP-qPCR assays, we found that Osa also binds near the TSSs of the *erm*, *opa*, *oaz* and *D* loci (Fig. 21A, see below). However, Osa does not bind upstream of the *dpn*, *HLHmγ* or *ase* loci (Fig. 21A, data not shown), consistent with the observation that expression of these genes is not dependent on Osa. By analyzing the DNA sequence of the

identified binding sites and the promoter regions of up and downregulated genes we observed an enrichment for a GA-rich motif in Osa target genes that are downregulated upon loss of Osa function (see methods, Fig. 21C-D). Thus, our results indicate that Osa binding initiates a transcriptional program that prevents reversion to NBs when expression of self-renewal genes is re-initiated in transit amplifying INPs.

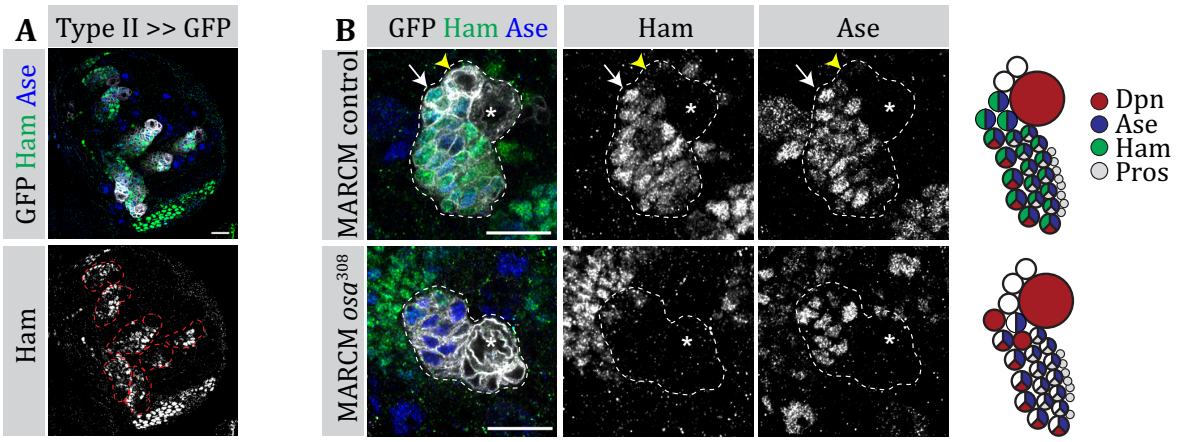

Figure 19. Ham is absent in the NB and in osa mutant clones.

(A) *Ham is expressed exclusively in the type II lineages. Overview image of a central brain lobe stained for Ham and Ase. Type II lineages are marked with membrane-bound GFP driven by wor-Gal4 ase-Gal80. Scale bars: 20 μm.* ***(B)*** *Ham is absent in osa mutant clones. Control and osa^{308} MARCM clones stained for Ham and Ase 75 hrs after clone induction. Control clones (upper panel) contain a Ham^{-} NB (indicated by an asterisk) and imINPs (marked with a yellow arrowhead). Ham and Ase are co-expressed during INP maturation (marked with an arrow). osa^{308} mutant clones (lower panel) have Ase^{+} INPs, but lack Ham^{+} cells. Schematic representation of various markers in control vs. osa^{308} clones is shown to the right. Scale bars: 15 μm.*

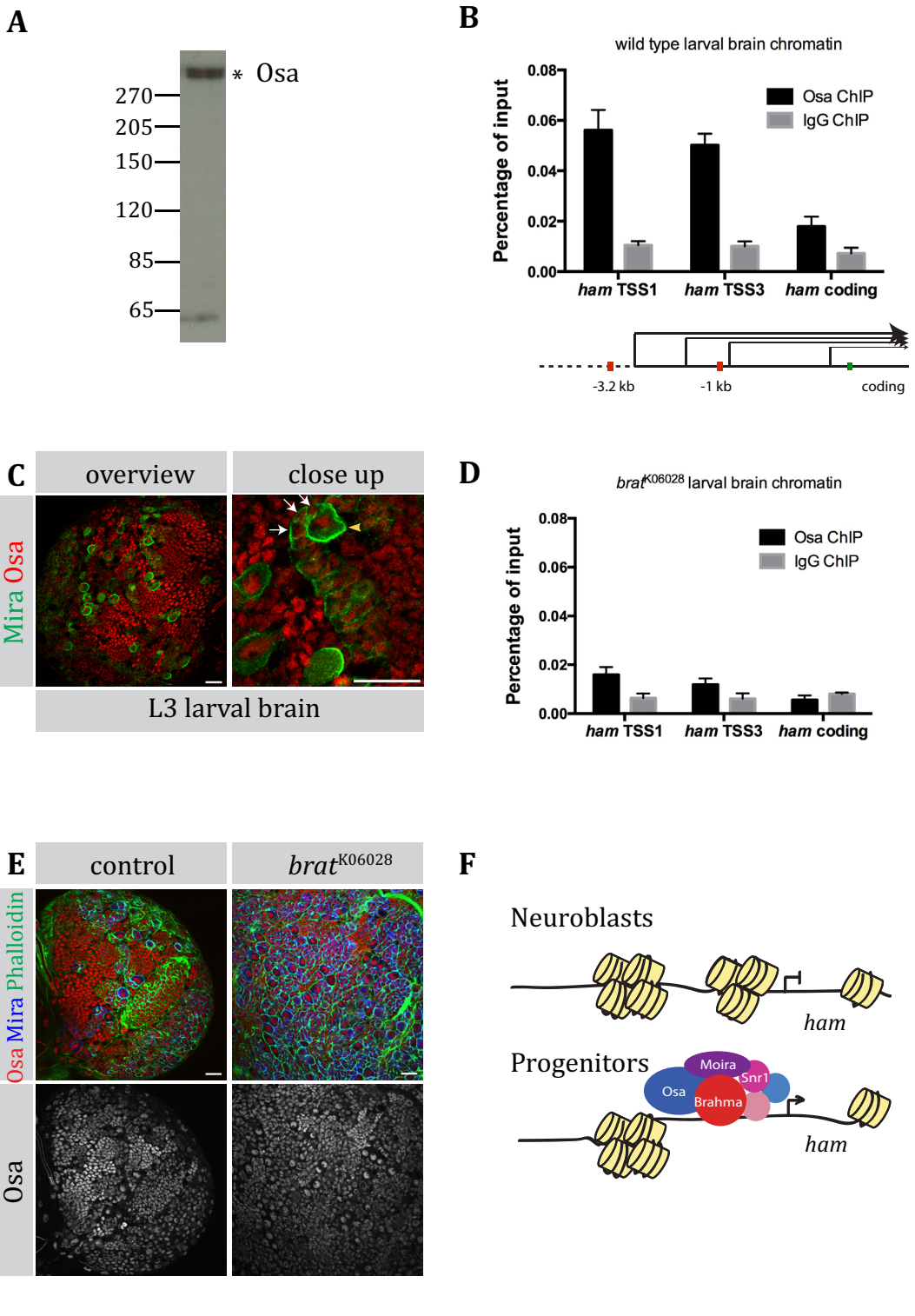
A
* Osa
270
205
150
120
85
65
B
wild type larval brain chromatin
Percentage of input
0.08
0.06
0.04
0.02
0.00
Osa ChIP
IgG ChIP
ham TSS1
ham TSS3
ham coding
-3.2 kb
-1 kb
coding
C
overview
close up
Mira Osa
L3 larval brain
D
brat K06028 larval brain chromatin
Percentage of input
0.08
0.06
0.04
0.02
0.00
Osa ChIP
IgG ChIP
ham TSS1
ham TSS3
ham coding
E
control
brat K06028
Osa Mira Phalloidin
Osa
F
Neuroblasts
ham
Progenitors
Moira
Snr1
Osa
Brahma
ham

Figure 20. Ham expression is directly activated by Osa in INPs.

(A) *Western blot of third instar larval brain extract. Osa antibody generated in this study recognizes the Osa protein (marked with an asterisk) above 270 kDa and a weak unspecific band below 65 kDa.* ***(B)*** *ChIP analysis at ham locus in wild type larval brain tissue for Osa and control IgG. ChIP signals are represented as percentage of input chromatin. Distances from the closest TSS are indicated in kilobases in the scheme of ham locus below. A region in the ham coding sequence was selected as negative control region. Error bars represent the s.e.m of three independent ChIP experiments.* ***(C)*** *Larval brain stained for Osa and Mira. Osa is ubiquitously expressed in the larval brain. Type II NB (yellow arrowhead) and most recently born INPs (white arrows) have similar Osa levels. Scale bars: 20 μm.* ***(D)*** *ChIP analysis at the ham locus in brat mutant (brat^{K06028}) larval brain tissue for Osa and control IgG. ChIP signals are represented as percentage of input chromatin. Error bars represent the s.e.m of three independent ChIP experiments.* ***(E)*** *Control vs. brat mutant larval brains stained for Osa and Mira show similar Osa levels (shown as single channel in lower panels).* ***(F)*** *Cartoon showing the binding of Osa to ham locus in progenitors but not in NBs.*

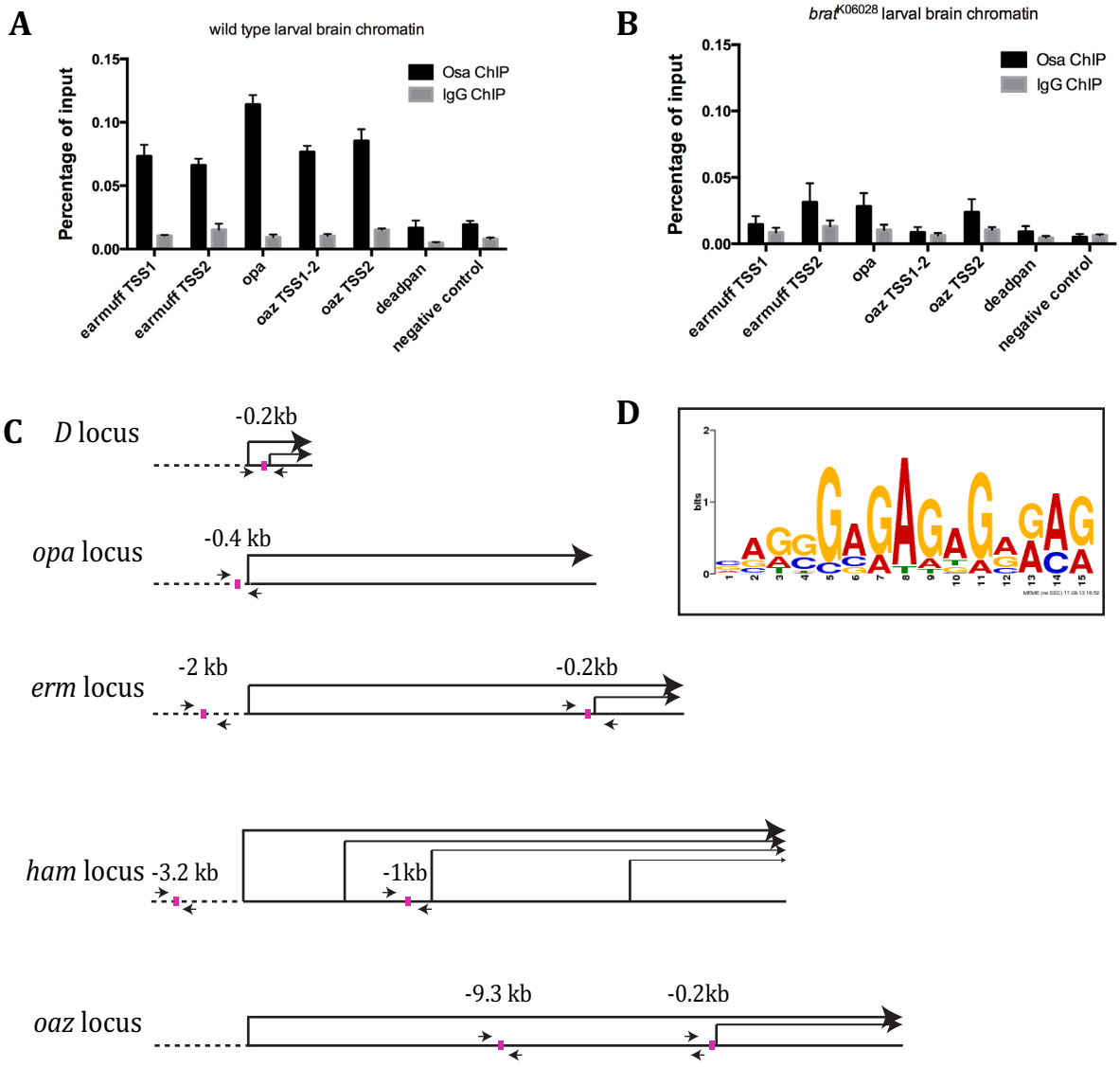

Figure 21. Osa binds to INP-specific gene loci.

(A) *ChIP-qPCR analysis of erm, opa and oaz loci in wild type larval brain tissue for Osa and control IgG. ChIP signals are represented as percentage of input chromatin. dpn is used as a control gene that is present in both NBs and INPs. A region in the ham coding sequence was selected as negative control. Error bars represent the s.e.m of 3 independent ChIP experiments.* ***(B)*** *Binding of Osa to the erm, opa and oaz loci are lost in brat mutant brains. ChIP-qPCR analysis in brat^{K06028} larval brain tissue for Osa and control IgG. ChIP signals are represented as percentage of input chromatin. Error bars represent the s.e.m of 3 independent ChIP experiments.* ***(C)*** *Osa binds to promoter regions of its target genes. Map of Osa target gene loci and identified binding sites (indicated by magenta squares) relative to the closest transcription start sites.* ***(D)*** *GA-rich sequence motif enriched in Osa bound regions identified in this study. E value= 2.8e^{-006}.*

4.1.5 Ham can inhibit self-renewal in NBs

To test whether the upregulation of Ham is an essential component of the Osa induced transcriptional program we performed rescue experiments (Fig. 22A-D'). Indeed, tumor formation upon *osa* shmiR was completely prevented upon co-expression of Ham (Fig. 22C-C').

We wanted to test the effect of Ham on NBs. When Ham was overexpressed in type II NBs, most lineages disappeared and only 1-2 type II lineages per brain lobe remained (Fig. 22D-D'). This could be due to apoptosis but could also arise from premature differentiation, as differentiated neurons are not labeled by GFP in the line used for the experiment. As co-expressing the apoptosis inhibitor *p35* did not prevent the NB loss caused by Ham expression in the type II NBs (0 type II NBs detected, n=7 brains) (Fig. 22E), we conclude that Ham can induce premature differentiation in type II NBs.

To investigate the early stages of the Ham induced underproliferation phenotype we utilized the temporal and regional gene expression targeting (TARGET) system to regulate Ham expression in type II NBs by *PntP1*-Gal4 (McGuire, Mao, & Davis, 2004; S. Zhu et al., 2011). After 24 hrs of Ham expression, 64% of type II NBs activated Ase (n=14 type II NBs, Fig. 22F, lower panels) and the average NB diameter decreased by 22% (control 11.5 ± 0.5 μm s.e.m, n=10 type II NBs, UAS-*ham* 8.9 ± 0.2 μm s.e.m, n=10 type II NBs, Student's t test $P<0.001$). While Pros was never nuclear in the most recently born wild type NB progeny, Ham expressing type II NBs were surrounded by $Pros^{+}$ cells (Fig. 22F, right panel). Additionally, GFP levels driven by *PntP1*-Gal4 were decreased (Fig. 22F), supporting the loss of NB identity. Thus, ectopic Ham expression in type II NBs limits their ability to undergo self-renewing divisions and causes their premature differentiation.

The differentiation phenotype could indicate a type II lineage specific effect or a more general role in limiting stem cell self-renewal. To distinguish these, we expressed Ham in type I NBs. Ham expression in type I NBs for 48 hrs by *ase*-Gal4 reduced the total number of type I NBs per brain lobe by 80% (control n=5 brains, UAS-*ham* n=4 brains) (Fig. 23A-B). Additionally, NB diameter was reduced by 15% (control n=25 type I NBs, UAS-*ham* n=25 type I NBs) (Fig. 23C). Furthermore, 11% of $Mira^{+}$ type I NBs showed nuclear Pros

staining after 15 hrs of Ham expression, indicating that they were prematurely differentiating (n= 5 brains, Fig. 23D). To follow the effect of Ham in real time, we performed live imaging of Ham expressing type I NBs in culture. NBs expressing Ham reproducibly generated fewer progeny due to increased cell cycle times, exemplified by a 2.53-fold increase in the period between the first and the second divisions of control vs. Ham expressing NBs (Fig. 24A-C). Thus, Ham is a potent inhibitor of self-renewing divisions and cellular growth that can act in various kinds of *Drosophila* neural stem cells.

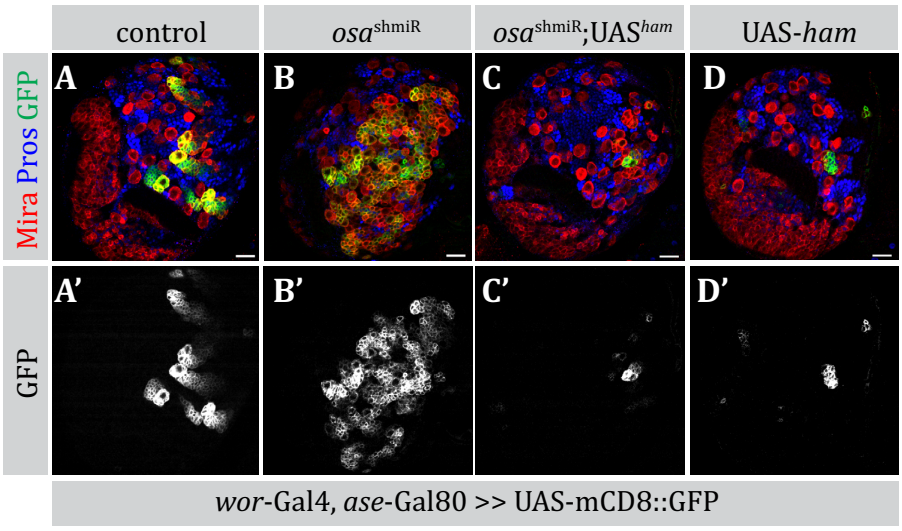
control
osa shmiR
osa shmiR;UAS ham
UAS-ham
Mira Pros GFP
GFP
A
B
C
D
A'
B'
C'
D'
wor-Gal4, ase-Gal80 >> UAS-mCD8::GFP

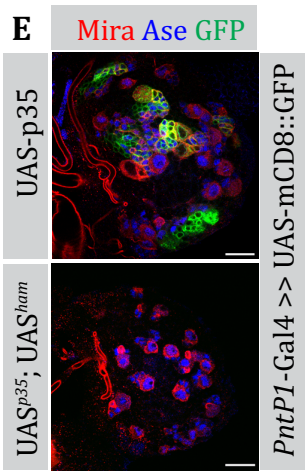
E
Mira Ase GFP
UAS-p35
UAS p35; UAS ham
PntP1-Gal4 >> UAS-mCD8::GFP

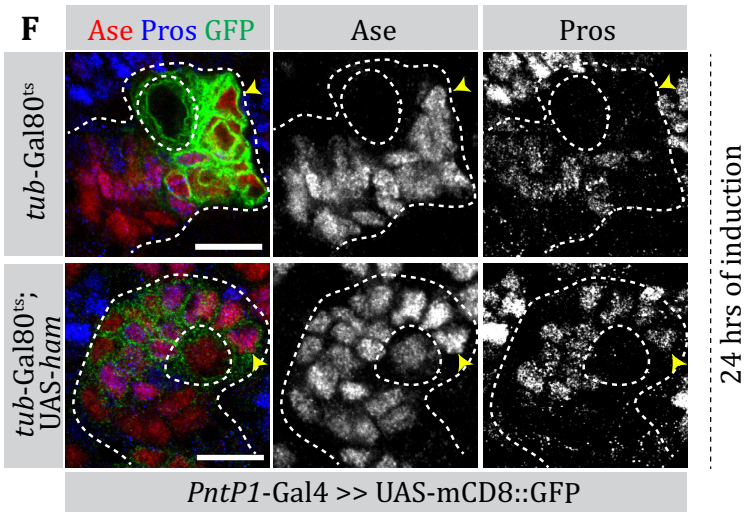
F
Ase Pros GFP
Ase
Pros
tub-Gal80ts
tub-Gal80ts; UAS-ham
24 hrs of induction
PntP1-Gal4 >> UAS-mCD8::GFP

Figure 22. Ham overexpression is sufficient to limit type II NB self-renewal

(A-D') *Larval brains expressing osa shmiR, UAS-ham or both in the type II lineages by wor-Gal4, ase-Gal80, stained for Mira and Pros.* ***(A-A')*** *Control larval brains contain 8 type II lineages (B-B') Expression of osa shmiR in type II lineages causes overproliferation seen as increase in* GFP^+ *cells* ***(C-C')*** *Simultaneous induction of osa shmiR and Ham expression prevents tumor formation.* ***(D-D')*** *Overexpression of Ham causes loss of* GFP^+ *type II lineages.* ***(E)*** *Overexpression of apoptosis inhibitor p35 in type II lineages by PntP1-Gal4 is not sufficient to prevent type II lineage loss upon Ham overexpression.* ***(F)*** *Expression of Ham in type II NBs for 24 hrs by PntP1-Gal4 causes premature differentiation. Control type II NB is* Ase^- *(upper panel). Ham expressing type II NB is* Ase^+ *(lower panel). Most recently born daughter cells do not show nuclear Pros staining in the control lineage (upper panel).* $Pros^+$ *progeny surround Ham expressing NB (lower panel). Scale bars: 20 μm (A-E), 10 μm (F).*

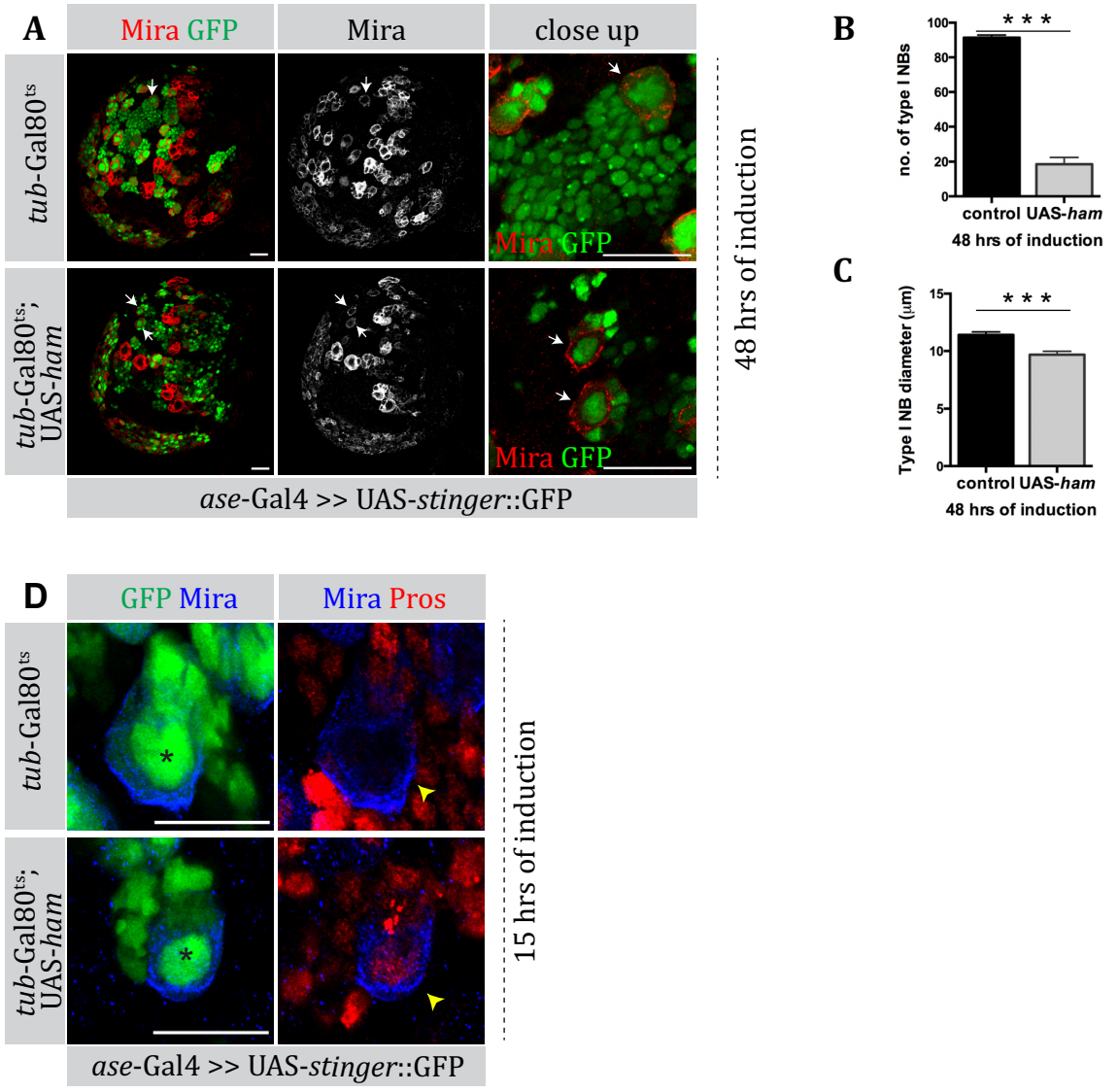

Figure 23. Ham overexpression is sufficient to limit type I NB self-renewal.

(A) *Larval brains expressing Ham in the type I NBs for 48 hrs by ase-Gal4 have reduced numbers of Type I NBs seen as a reduction in the number of GFP⁺ progeny and Mira⁺ cells. Scale bars: 20 µm.* ***(B)*** *Graph showing the decrease in the number of Type I NBs upon Ham expression for 48 hrs (control n=5 brains, UAS-ham, n=4 brains, Student's t test P<0.001) Error bars represent s.e.m.* ***(C)*** *Graph showing the decrease in the NB diameter upon Ham expression for 48 hrs (control n=25 type I NBs, UAS-ham n=25 type I NBs, Student's t test P<0.001). Error bars represent s.e.m.* ***(D)*** *Ham overexpression in Type I NBs causes premature differentiation. Type I NBs (indicated by an asterisk in the panels to the left and by yellow arrowheads in the panels to the right) expressing Ham for 15 hrs show nuclear Pros staining (lower right panel), indicative of premature differentiation. Scale bars: 15 µm.*

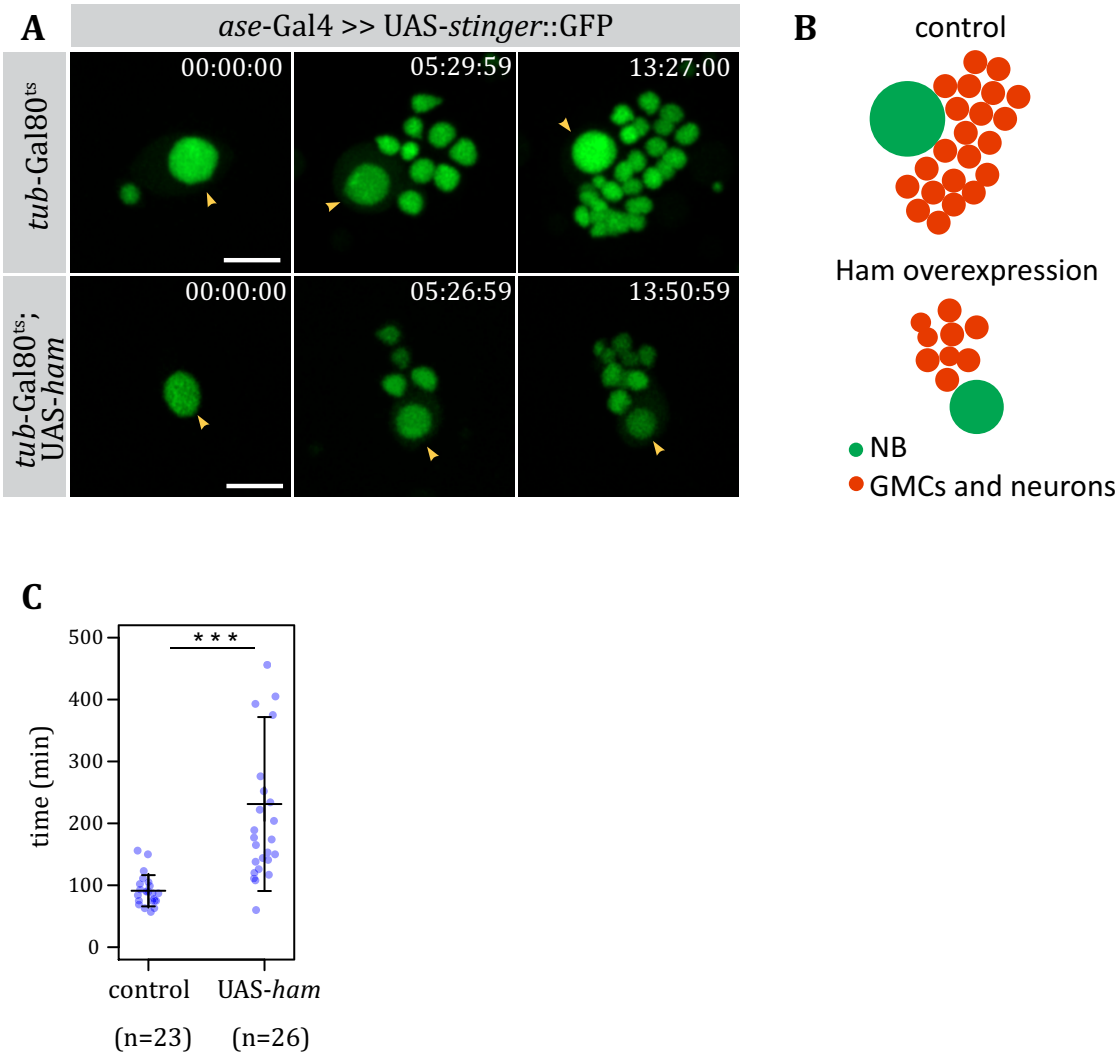

Figure 24. Live imaging of Ham expressing Type I NBs.

(A) *Stills from live imaging movies of a control type I NB or a Ham expressing type I NB. Ham expression was induced for 29 hrs, larval brains were dissected and cultured as dissociated cells. Yellow arrowheads indicate type I NBs. Scale bars: 10 μm.* ***(B)*** *Cartoon showing the lineages generated by control and Ham expressing type I NBs.* ***(C)*** *Cell cycle times are extended upon Ham expression. Scatter plot showing the time span between the first and the second NB divisions (control n=23, UAS-ham n=26 NBs). Error bars represent SD. P value=2.23x10^{-5}, Student's t-test.*

4.1.6 Ham is required to limit self-renewal in INPs

To test whether Ham is required for limiting self-renewal in INPs, we expressed *ham* shmiR using *erm*-Gal4 (III). This resulted in the formation of ectopic Mira^{+}, Ase^{+} cells (Fig. 25A), indicating that Ham is required in mINPs to prevent overproliferation. We used the TARGET system to investigate the early stages of this phenotype. *ham* shmiR expression by *insc*-Gal4 for 48 hrs increased the average number of mINPs (Ase^{+}, Dpn^{+}) by 56% (Fig. 25B-C) and the average number of GMCs (Ase^{+}, Pros^{+}, Dpn^{-}) by 38% (Fig. 25D). The average number of pH3^{+} dividing INPs increased by 2.27-fold, while the average number of pH3^{+} dividing GMCs was unchanged (control n=18, *ham* shmiR n=17 type II lineages), suggesting that the increase in GMC numbers arises from increased INP divisions.

To exclude off-target effects we analyzed *ham* mutant clones. 123 hrs after clone induction, mINP numbers in *ham* mutant clones increased by 52% (control 32.33 ± 1.76 s.e.m, n=9, ham^{1} 49.11 ± 3.65 s.e.m, n=9, Fig. 26A-B), confirming the shmiR phenotype. aPKC and Mira localized asymmetrically in the dividing *ham* mutant INPs (Fig. 26C). Thus, loss of Ham function leads to the formation of supernumerary mINPs that generate extra GMCs. Furthermore, staining of *ham* mutant clones for H3K9me1 did not reveal any global change at the level of this histone mark (Fig. 26D), indicating that Ham function in type II lineages of *Drosophila* is not to initiate global heterochromatin formation as demonstrated for its mammalian homologs (Pinheiro et al., 2012).

Surprisingly, transplantation of ectopic INPs generated upon *ham* loss of function into the abdomen of adult host flies did not cause tumors (*ham* shmiR expressed in Dpn^{-}, Ase^{-} imINPs by *erm*-Gal4 (II) or or in Dpn^{-}, Ase^{+} imINPs by *erm*-Gal4 (III), 0 flies out of 58 for each genotype, 5 weeks), indicating that NB-like cell reversion is crucial for tumorigenesis.

The excessive mINPs resulting from loss of Ham could arise from symmetric divisions, from GMC to INP reversion, from lack of cell death in INPs or from prolonged INP divisions due to extended INP life span. We used live imaging of INPs in dissociated cell culture to distinguish between these different possibilities. We utilized *erm*-Gal4 (III) to label INPs with membrane-bound GFP and analyzed the division patterns of INPs and their

daughter cells. Control INP divisions generated one daughter cell that went through 3-4 self-renewing divisions and a daughter cell that divided only once more into two terminally differentiating neurons (Fig. 27A-E). INPs expressing *ham* shmiR were indistinguishable from the control INPs, reproducibly generating a GMC that divides once more into two differentiating neurons (Fig. 27F-J) (control, n=24 INPs, *ham* shmiR n=29 INPs followed for 3-4 divisions). Thus, excessive INPs upon Ham loss are not due to symmetric INP divisions or GMC to INP reversion. Moreover, the time span between the first and the second INP divisions showed no significant difference upon *ham* shmiR (Fig. 27K), ruling out slower cell cycle that might extend INP life span. To determine whether wild type INPs disappear through apoptosis, we performed TUNEL staining and identified that only 0.16 % of Dpn^+ mINPs were TUNEL positive (n=23 lineages, Fig. 27L), suggesting that cell death is not a common mechanism for INPs to exit cell cycle. Thus, we conclude that Ham must control the number of INP self-renewal divisions, rather than asymmetric daughter fate, cell cycle length or apoptosis. Taken together, our data suggest that activation of Ham by the BAP complex in the INPs is key to establishing the self-renewal capacity difference between the NBs and the progenitors.

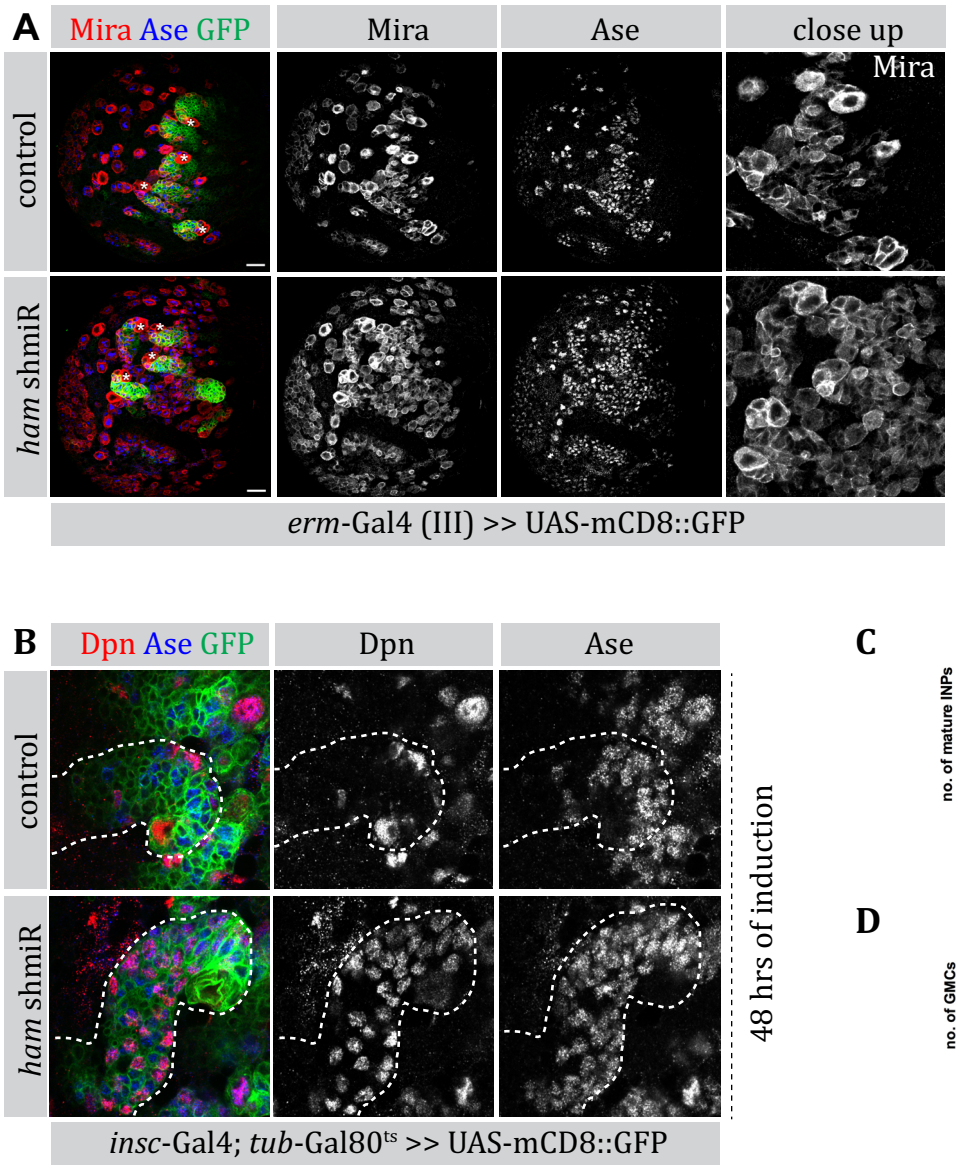

Figure 25. Knockdown of Ham causes overproliferation.

(A) *Larval brains expressing ham shmiR by erm-Gal4 (III) stained for Mira and Ase. There is an increase in the number of Mira⁺ Ase⁺ cells upon ham shmiR. Type II NBs are indicated by asterisks. Scale bars: 20 μm.* ***(C)*** *Type II lineages expressing ham shmiR for 48 hrs by insc-Gal4; tub-Gal80^{ts} stained for Dpn and Ase. Note that Dpn staining in ham shmiR expressing NB is faint due to cell division.* ***(D-E)*** *Number of mINPs and GMCs increase upon ham shmiR. Quantification of mINP (Dpn⁺ Ase⁺) and GMC (Ase⁺ Pros⁺) numbers 48 hrs after ham shmiR induction by insc-Gal4; tub-Gal80^{ts}. Error bars represent s.e.m; P value<0.001 Student's t test. n denotes the number of type II lineages analyzed.*

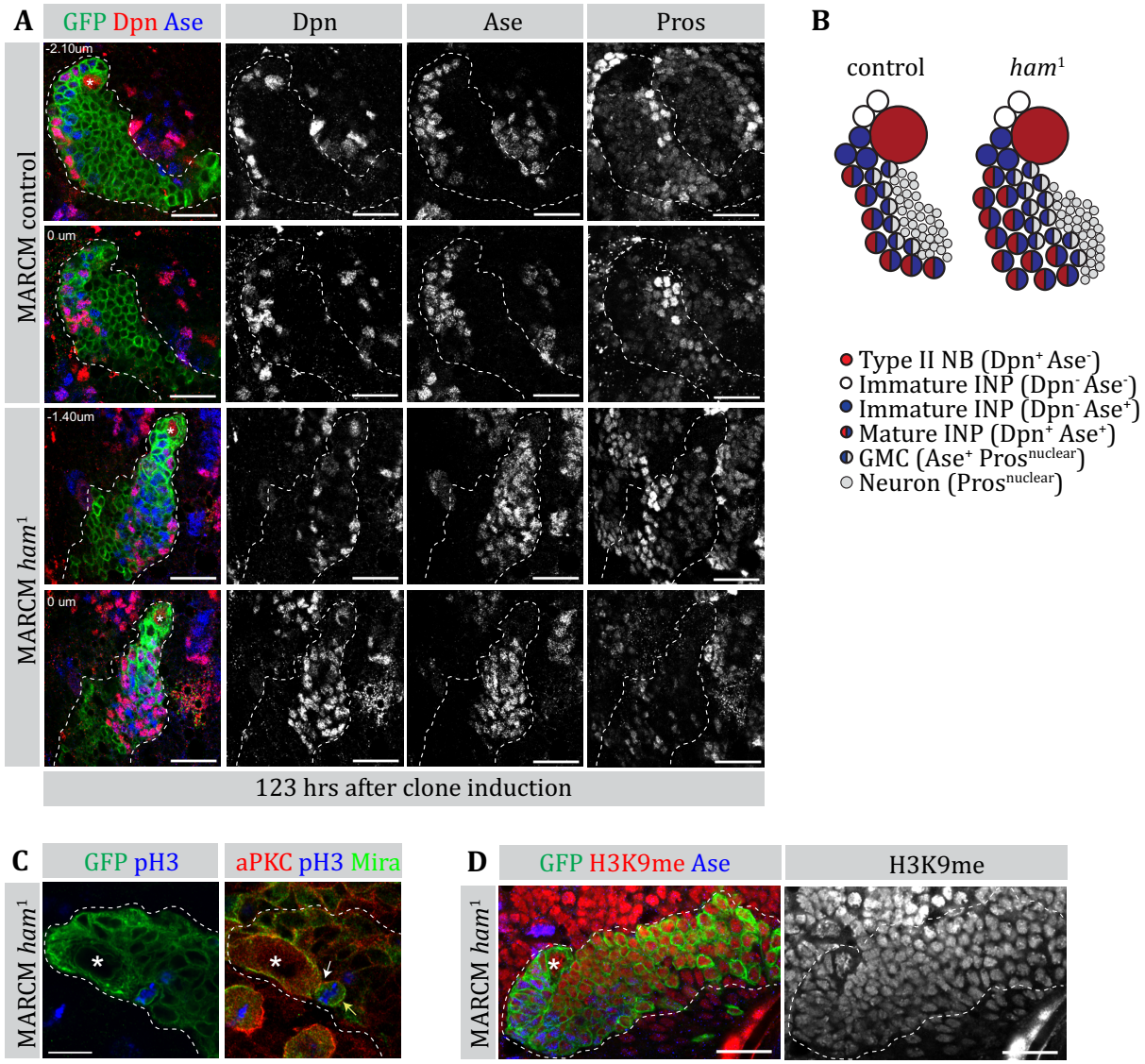

Figure 26. Ham is required in the mINPs to limit self-renewal

(A) *ham¹ MARCM clones confirm the shmiR phenotype. MARCM clones marked with membrane-bound GFP, stained for Dpn, Ase and Pros 123 hrs after clone induction. Two separate Z-stacks are shown for each genotype. ham¹ clones have increased number of Ase⁺ cells.* ***(B)*** *Cartoon summarizing the ham loss of function phenotype.* ***(C)*** *ham mutant INPs segregate cell fate determinants aPKC and Mira asymmetrically. ham mutant clone (right panel, outlined with dashed line), stained for pH3, aPKC and Mira. Type II NB is indicated by an asterisk. aPKC crescent is indicated by a white arrow, Mira crescent is indicated by a yellow arrow.* ***(D)*** *There is no global change in H3K9me1 levels in ham mutants. ham mutant clone (outlined) stained for the heterochromatin mark, H3K9me1, 120 hrs after clone induction. Heterozygous cells surrounding the homozygous clone serve as control. Scale bars: 20 μm (A, D), 10 μm (C).*

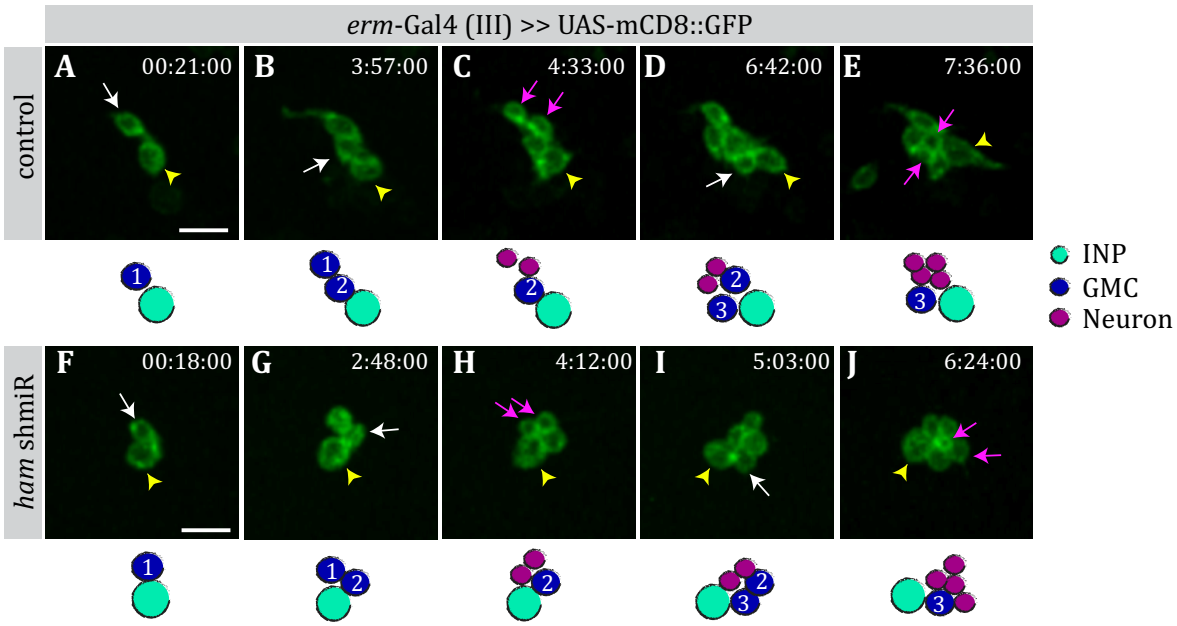
erm-Gal4 (III) >> UAS-mCD8::GFP
control
A 00:21:00
B 3:57:00
C 4:33:00
D 6:42:00
E 7:36:00
ham shmiR
F 00:18:00
G 2:48:00
H 4:12:00
I 5:03:00
J 6:24:00
INP
GMC
Neuron

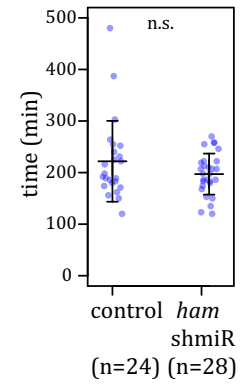
K
n.s.
time (min)
500
400
300
200
100
0
control
ham shmiR
(n=24) (n=28)

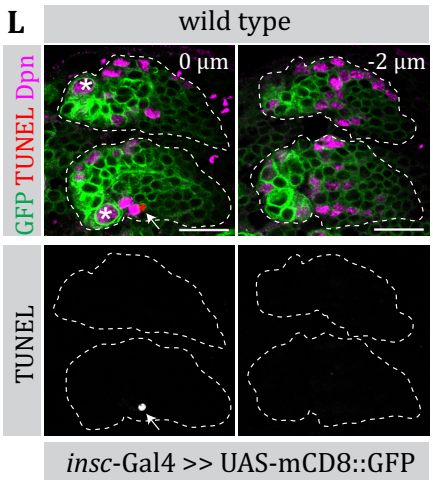
L
wild type
GFP TUNEL Dpn
0 µm
-2 µm
TUNEL
insc-Gal4 >> UAS-mCD8::GFP

Figure 27. Ham loss of function does not alter INP/GMC cell cycle times or daughter cell fate.

(A-J) *INPs expressing ham shmiR generate lineages indistinguishable from control INPs. Stills from live imaging movies of a control INP* ***(A-E)*** *or a ham shmiR expressing INP* ***(F-J)****. erm-Gal4 (III) was used to drive expression of a membrane-tethered GFP and shmiR. INPs (indicated by yellow arrowheads) are followed for 3 divisions and their daughter GMCs (indicated by white arrows) are followed for 2 divisions. Magenta arrows indicate neurons generated from GMC divisions. Lineages are shown as cartoons below the stills, where daughter GMCs are numbered according to their birth order. Scale bars: 10 μm.* ***(K)*** *Scatter plot showing the time span between the first and the second INP divisions (control n=24, ham shmiR n=28 INPs). Error bars represent SD. No significant difference was observed between control and ham shmiR (P value=0.15, Student's t-test).* ***(L)*** *INPs do not exit cell cycle through apoptosis. Type II lineages marked by membrane-bound GFP driven by insc-Gal4, stained for TUNEL and mINP marker Dpn. Two separate Z-stacks are shown. NBs are indicated by asterisks. Arrow indicates a* $Dpn^{-}TUNEL^{+}$ *(bottom panels, shown as a single channel) cell. Scale bars: 15 μm.*

4.1.7 Ham and Osa are required for temporal patterning of INPs

How does Ham control INP cell division numbers? Recent experiments have demonstrated that INPs sequentially express the TFs D, Grh and Ey to determine temporal identity and ensure timely cell cycle exit (Bayraktar & Doe, 2013). To test the expression of the temporal TFs upon *ham* knockdown, we performed immunostainings 48 hrs after induction of *ham* shmiR by *insc*-Gal4. While D and Grh were successfully activated in mINPs upon *ham* knockdown, repression of Grh in middle-aged INPs failed (Fig. 28A-C). Unexpectedly, even though the percentage of Ey^+ INPs was significantly reduced, Ey expression was not completely blocked (Fig. 28D-E), suggesting that these INPs fail to transit from the Grh^+, Ey^+ to Grh^-, Ey^+ stage.

As *D* was among the differentially expressed genes upon *osa* knockdown, we checked whether Osa might be acting upstream of Ham to initiate the temporal patterning of INPs. *osa* mutant clones failed to activate *D* expression 72 hrs after clone induction (Fig. 28F). Furthermore, we detected Osa binding upstream of the second TSS of *D* (Fig. 28G), suggesting that Osa initiates temporal patterning of INPs, while Ham is required for its progression (Fig. 28H).

To investigate whether incorrect temporal patterning of INPs upon loss of Ham function extends their life span, we stained pupal brains for Mira, D and Grh 25 hrs after puparium formation (APF). As type II NBs disappear at early stages of pupal life (~0-16 hrs APF at 29°C) (Homem & Knoblich, 2012; Maurange et al., 2008; Truman & Bate, 1988), data not shown), generation of INPs ceases, which is followed by disappearance of INPs at the end of their proliferative stage. Wild type pupal brains contained few Grh^+ INPs 25 hrs APF (Fig. 29A). 50 hrs APF, there were no more INPs detectable (Fig. 29B). In contrast, *ham* shmiR expressing pupal brains contained numerous Grh^+ INPs 25 hrs APF (Fig. 29A), some of which perdured to 50 hrs APF (Fig. 29B), indicating that INP life span is extended upon *ham* knockdown (Fig. 29C).

It has been shown that INPs generate different neuronal progeny based on their temporal patterning. For example, loss of Ey results in loss of late INP progeny (Bayraktar & Doe, 2013). To determine the consequence of incorrect temporal patterning upon *ham*

knockdown on the specification of neuronal progeny, we analyzed *ham* shmiR clones 96 hrs after clone induction and stained for Toy, a marker for late INP progeny (Bayraktar & Doe, 2013). While wild type clones contained several Toy^+ neurons (34.67 ± 3.32, n=9 clones), *ham* shmiR clones lacked Toy^+ neurons (2.91 ± 1.44, n=11 clones, Fig. 30A-B), consistent with the absence of Grh^-, Ey^+ INPs.

Taken together, our data indicate that SWI/SNF activates a "transit-amplifying" program in imINPs that induces temporal patterning, restricts self-renewal capacity and prevents reversion to NBs. Ham is a key component of this program that limits the number of ensuing self-renewal divisions by ensuring progression of temporal patterning initiated by SWI/SNF. (Fig. 31).

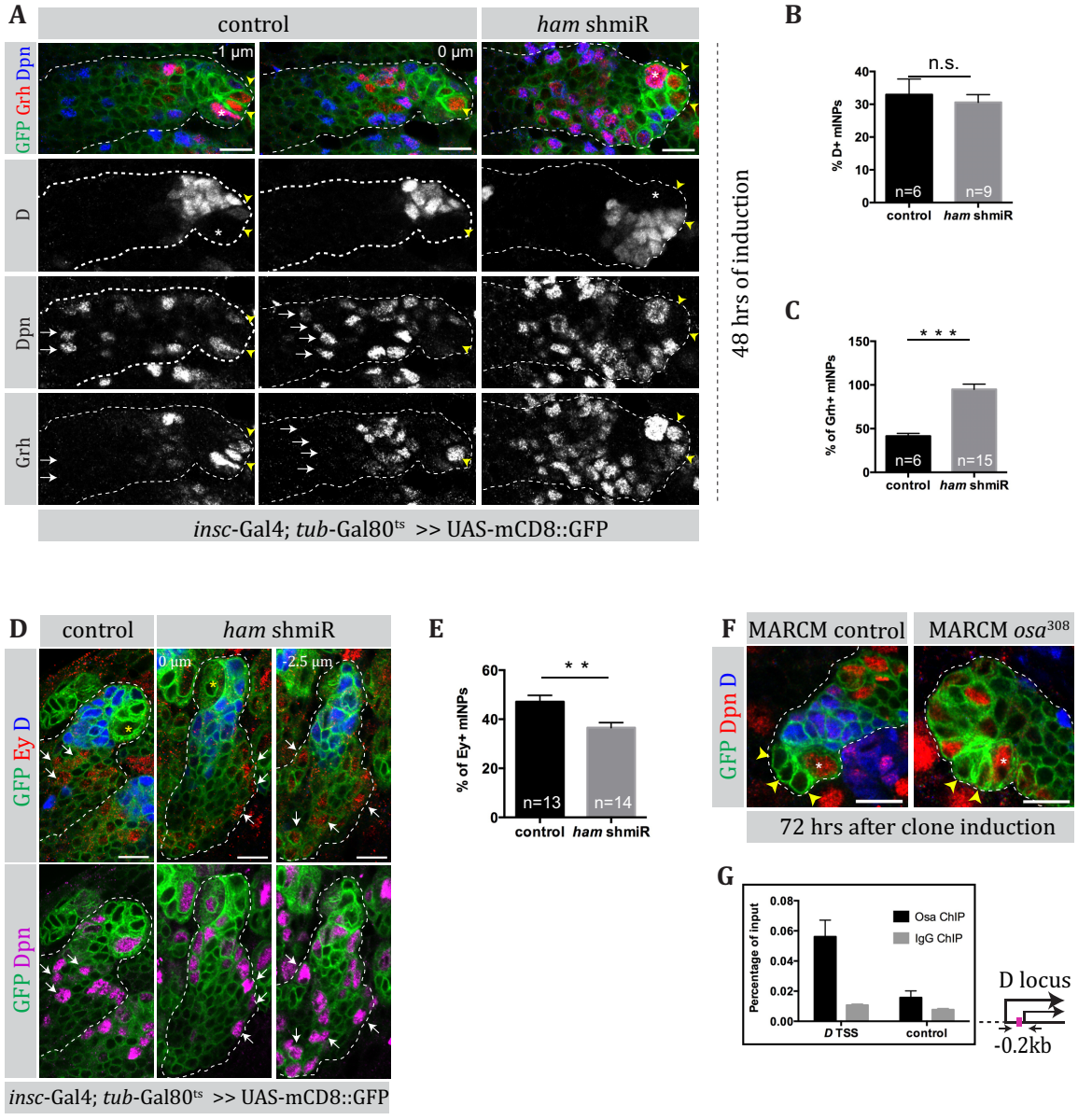
A
control
ham shmiR
GFP Grh Dpn
1 µm
0 µm
D
Dpn
Grh
48 hrs of induction
insc-Gal4; tub-Gal80ts >> UAS-mCD8::GFP
B
n.s.
% D+ miNPs
n=6
n=9
control
ham shmiR
C
* * *
% of Grh+ miNPs
n=6
n=15
control
ham shmiR
D
control
ham shmiR
GFP Ey D
GFP Dpn
0 µm
-2.5 µm
insc-Gal4; tub-Gal80ts >> UAS-mCD8::GFP
E
* *
% of Ey+ miNPs
n=13
n=14
control
ham shmiR
F
MARCM control
MARCM osa308
GFP Dpn D
72 hrs after clone induction
G
Percentage of input
Osa ChIP
IgG ChIP
D TSS
control
D locus
-0.2kb
H
wild type
mINP
ham LOF
mINP
osa LOF
D
Grh
Ey
D
Grh
Ey
Ham
Osa

Figure 28. Expression of temporal transcription factors is altered in INPs upon ham or osa loss of function

(A) *mINPs expressing ham shmiR fail to turn off Grh expression. Close up images of larval brains expressing ham shmiR for 48 hrs by insc-Gal4; tub-Gal80^{ts}, stained for temporal TFs D, Grh and mINP marker Dpn. In the control type II lineage (dorsomedial 2 - DM2) (two separate Z-stacks are shown), type II NB (indicated by an asterisk) and imINPs (yellow arrowheads) stain positive for Grh. Grh is initially downregulated during INP maturation and D is upregulated. Middle-aged INPs resume Grh expression. As INPs transit from middle-aged to old, Grh expression is shut down (Dpn$^+$ cells marked with white arrows further away from the parental NB). Upon ham knockdown middle-aged INPs fail to shut down Grh expression. Scale bars: 10 μm.* ***(B-C)*** *Graphs showing the percentage of D$^+$* ***(B)*** *or Grh$^+$* ***(C)*** *mINPs in control and ham shmiR expressing type II (dorsomedial 2 - DM2) lineages 48 hrs after shmiR induction by insc-Gal4.* ***(B)*** *There is no significant difference in the percentage of D$^+$ mINPs upon ham knockdown (control n=6, ham shmiR n=9 lineages, P value > 0.05, Student's t-test) Error bars represent s.e.m.* ***(C)*** *Percentage of Grh$^+$ mINPs increase upon ham knockdown (control n=6, ham shmiR n=15 lineages, Student's t test P<0.001) Error bars represent s.e.m.* ***(D)*** *Ey expression is not blocked upon ham knockdown. Control and ham shmiR expressing brains stained for mINP marker Dpn, first INP temporal TF D and last INP temporal TF Ey, 48 hrs after shmiR induction by insc-Gal4 line. Two separate Z-stacks are shown for ham shmiR. As in control type II (DM2) lineages, ham shmiR expressing mINPs turn on the expression of Ey as they age (indicated by white arrows). Note that young INPs stain positive for D (top panels). Scale bars: 15 μm.* ***(E)*** *Graph showing the percentage of Ey$^+$ mINPs upon ham knockdown (control n=13, ham shmiR n=14 lineages, P value < 0.01, Student's t-test). Error bars represent s.e.m.* ***(F)*** *osa mutant INPs fail to initiate expression of mINP temporal TFs. Control and osa mutant MARCM clones stained for D and mINP marker Dpn 72 hrs after clone induction. osa mutant INPs fail to activate D. Scale bars: 10 μm.* ***(G)*** *Osa binds to D locus. ChIP analysis at D locus in wild type larval brain tissue for Osa and control IgG. ChIP signals are represented as percentage of input chromatin. Distance from the closest TSS is indicated in kilobases in the scheme of D locus. Error bars represent the s.e.m of three independent ChIP experiments.* ***(H)*** *Cartoon summarizing the defects in INP temporal TF progression upon ham or osa loss of function (LOF). While osa loss of function (LOF) results in failure of initiation of temporal patterning, ham LOF results in failure of progression of the temporal patterning in INPs.*

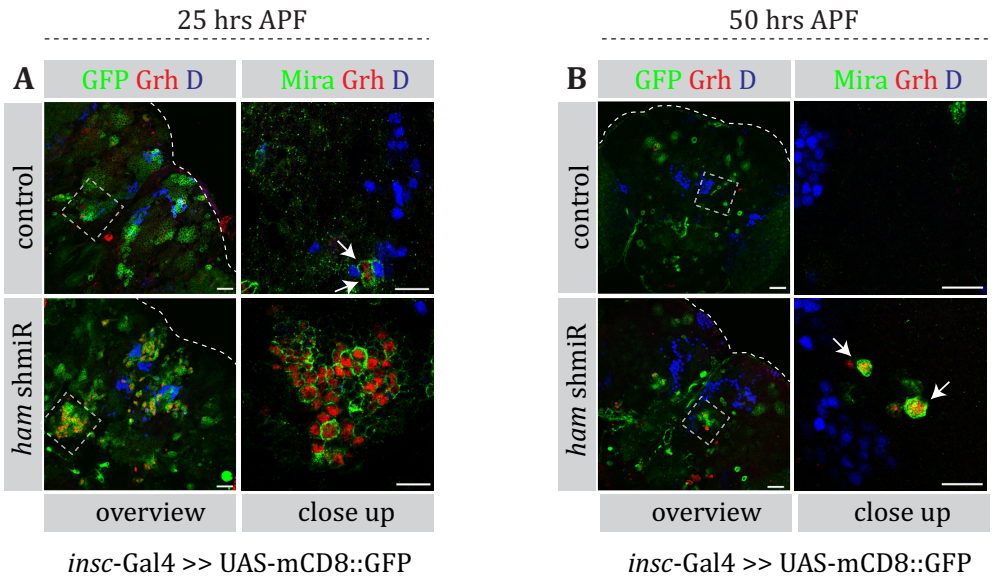
25 hrs APF
50 hrs APF
A
B
GFP Grh D
Mira Grh D
control
ham shmiR
overview
close up
insc-Gal4 >> UAS-mCD8::GFP

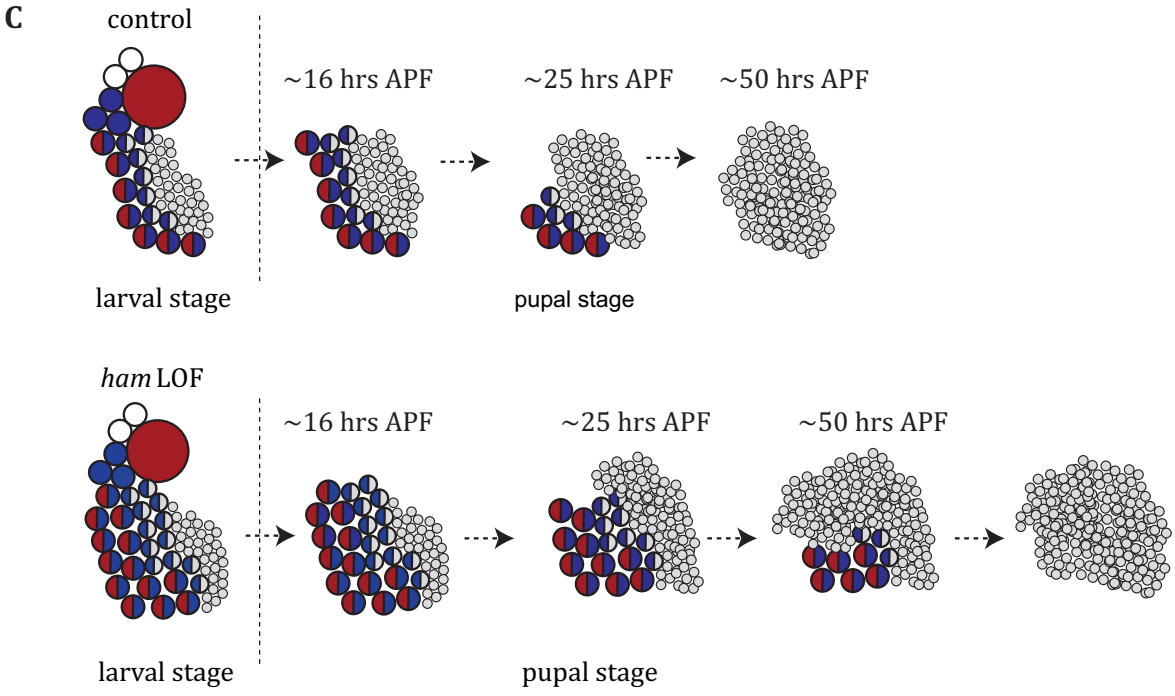
C
control
~16 hrs APF
~25 hrs APF
~50 hrs APF
larval stage
pupal stage
ham LOF

Figure 29. INPs expressing ham shmiR live longer than their wild type counterparts.

(A-B) *Overview and close up images of pupal brains expressing ham shmiR by insc-Gal4 stained for Mira, Grh and D 25 hrs* ***(A)*** *or 50 hrs* ***(B)*** *after puparium formation (APF) at 29°C.* ***(A)*** *Control brain contains few Mira⁺, Grh⁺ INPs (indicated by white arrows in close up images, top right panel), while ham shmiR expressing brain contains several (bottom right panel).* ***(B)*** *50 hrs APF (at 29°C) no Mira⁺, Grh⁺ INPs are detected in the control brain (top right panel). ham shmiR expressing brain contains few Mira⁺, Grh⁺ INPs (indicated by white arrows, bottom right panel). Scale bars: 30 μm overview images, 15 μm close up images.* ***(C)*** *Cartoon showing the progressive loss of NBs and INPs during pupal stages. INPs expressing ham shmiR live longer.*

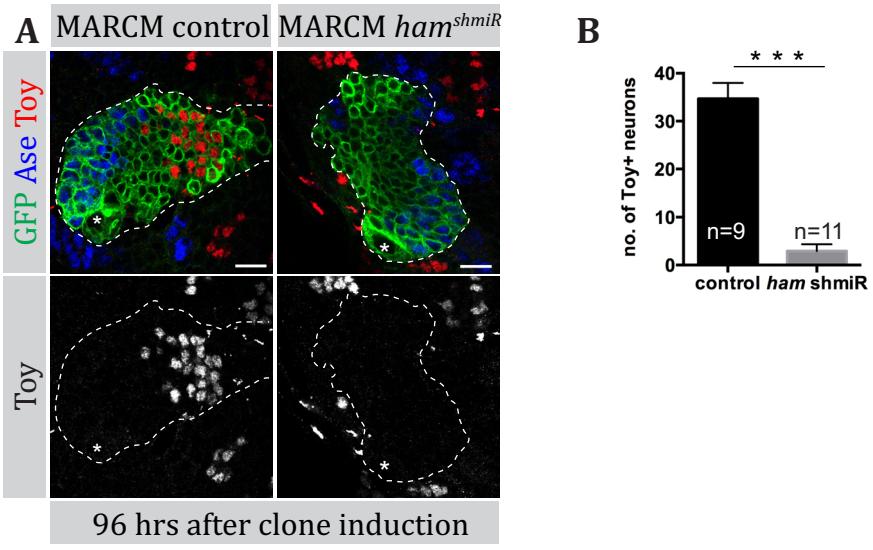

Figure 30. ham shmiR expressing lineages fail to generate Toy-expressing late INP progeny

(A) *Control and ham shmiR MARCM clones stained for Ase (marks INPs and GMCs) and Toy (neuronal marker for late INP progeny) 96 hrs after clone induction. ham shmiR clones lack Toy⁺ neurons. Scale bars: 10 μm.* ***(B)*** *Graph showing the decrease in the number of Toy⁺ neurons upon ham knockdown. (control n=9, ham shmiR n=11, P value < 0.001, Student's t-test). Error bars represent s.e.m.*

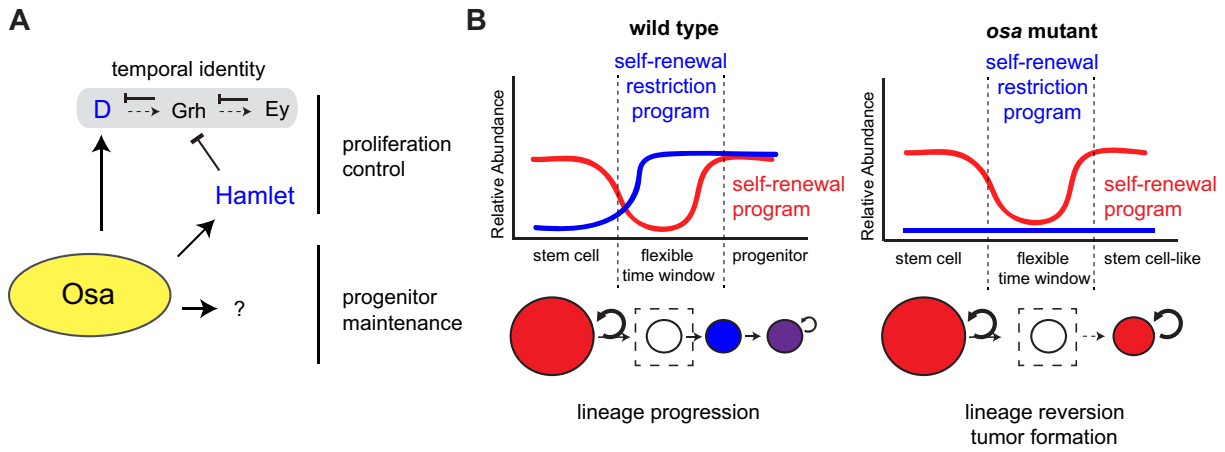

Figure 31. Graphical model.

(A) *Osa directly activates D and Ham to ensure proliferation control in progenitors.* ***(B)*** *Even though self-renewal program is not affected in osa mutants, self-renewal restriction program fails to turn on and progenitors revert to NB-like cells.*

DISCUSSION

Our data reveal an essential function for the chromatin remodeling SWI/SNF complex in ensuring directionality in stem cell lineages. When neural stem cells/NBs progress towards the transit-amplifying/INP fate, the SWI/SNF complex activates a transcriptional program that limits self-renewal and initiates a TF cascade to confer temporal identity. Failure to do so results in lineage reversion and tumor formation. We identify the temporal TF D and the Prdm domain protein Ham as direct SWI/SNF targets and show that induction of Ham limits the number of transit amplifying divisions by ensuring the progression of temporal patterning (Fig. 31A). Members of the SWI/SNF complex, particularly the Osa homologs ARID1A/B, are among the most frequently mutated genes in human cancer and our findings provide a potential mechanism for their tumor suppressing activity.

Osa-containing SWI/SNF complex provides lineage directionality

osa mutant progenitors revert to NB-like cells. 50 hrs after clone induction we observe correctly specified Dpn^-, Ase^- imINPs in *osa* mutant clones, suggesting that the asymmetric NB division generates a daughter cell that successfully turns off the self-renewal program. 75 hrs after clone induction, however, ectopic Dpn^+, Ase^- NB-like cells appear. Thus, *osa* mutant imINPs fail to undergo maturation and re-gain NB-like self-renewal capacity. This phenotype is different from the previously described *erm* mutant phenotype, where fully matured INPs fail to maintain their progenitor identity (Weng et al., 2010). We propose a model, where two transcriptional programs act in concert in the type II lineages to prevent progenitors from acquiring aberrant proliferation capabilities (Fig. 31B). The "self-renewal" program includes the transcription factors Dpn, Klu and HLHmγ. It is active in NBs and is terminated by Numb and Brat in the imINPs immediately after asymmetric division. As INPs undergo maturation, the program is re-initiated when Brat and Numb disappear, allowing self-renewal to resume (Berger et al., 2012; San-Juán & Baonza, 2011; Song & Lu, 2011; Xiao et al., 2012; Zacharioudaki et al., 2012; S. Zhu et al., 2011). Our data indicate that Osa function is crucial to ensure the activation of a second "self-renewal restriction" program before this re-initiation occurs to ensure that INPs,

unlike NBs, only complete around five rounds of asymmetric cell division before they differentiate. In *osa* mutants, the restriction program is not activated (Fig. 19, Supplemental Table 1). The self-renewal program, however, is unaffected and therefore, INPs regain NB-like properties resulting in unlimited self-renewal and brain tumor formation.

Ham is a self-renewal restrictor

We identify Ham as a key component of the self-renewal restriction program. Ham expression is activated in INPs in an Osa-dependent manner and its co-expression with *osa* shmiR can prevent tumor formation (Fig.20, 22). Nevertheless the *ham* mutant phenotype is different from *osa* mutants. While *osa* mutant INPs revert to NBs, *ham* mutant INPs maintain their progenitor identity but lose proliferation control (Fig.13, 26), indicating that Ham is responsible for executing a subset of Osa functions. Indeed, our results suggest a tight functional connection between the SWI/SNF complex and the temporal TF cascade that confers temporal identity to INPs. SWI/SNF directly induces transcription of D, the first member of this cascade. In addition, it induces Ham, a chromatin regulator that can limit self-renewal capacity in INPs, but also when ectopically expressed in NBs. In INPs, Ham is specifically required for the transition from Grh^{+}, Ey^{+} middle-aged INPs to Grh^{-}, Ey^{+} old INPs. As transition to the terminal transcriptional state is important for timely cell cycle exit in mINPs (Bayraktar and Doe, 2013), this explains the overproliferation phenotype observed in *ham* mutants.

How could Ham mediate temporal progression of INPs? It has been previously shown that recruitment of the earliest component of the NB "transcriptional clock" to the nuclear periphery permanently silences its expression and limits NB competence (Kohwi et al., 2013). Evi1 and Prdm16, the mammalian homologs of Ham have been postulated to initiate heterochromatin formation by methylating H3K9 (Pinheiro et al., 2012). As H3K9 methylation is crucial for recruiting gene loci to the nuclear periphery, it is interesting to speculate that Ham acts in INPs by driving the transition to the next transcriptional state and ultimately, to differentiation (Gonzalez, 2013; Towbin et al., 2012; Yuzyuk, Fakhouri, Kiefer, & Mango, 2009).

SWI/SNF complex subunits are frequently mutated in human tumors

Mutations in the mammalian SWI/SNF complex subunits are potential drivers of tumorigenesis in a wide variety of tissues including the brain (Kadoch et al., 2013; Shain & Pollack, 2013; Wilson & Roberts, 2011). The Brm homolog SMARCA4 and the Osa homologs ARID1A/B are among the chromatin modifiers that are recurrently mutated in medullablastoma, the most common malignant childhood brain tumor (Northcott et al., 2012; Parsons et al., 2011). Identifying the cell of origin in brain tumors is crucial in designing effective therapeutic strategies (Liu & Zong, 2012). Stem cells could acquire oncogenic mutations that initiate tumor formation (Alcantara Llaguno et al., 2009). On the other hand, tumors could also originate from more restricted progenitors that inherit these mutations and become malignant (Liu et al., 2011; Schüller et al., 2008; Z.-J. Yang et al., 2008). Our study offers an alternative explanation: Provided that the function of SWI/SNF is conserved in humans, mutations occurring in restricted progenitors could affect lineage directionality causing progenitors to revert into stem cells. In this case, the cell of origin would be a progenitor despite the fact that tumors are made up of stem cells. In fact, this possibility has been proposed for other tumor suppressors (Schwitalla et al., 2013) and could be tested rigorously for SWI/SNF mutations given the recent significant advances in cell lineage tracing in tumors (J. Chen et al., 2012; Driessens, Beck, Caauwe, Simons, & Blanpain, 2012; Schepers et al., 2012).

4.2 EXPERIMENTAL PROCEDURES

4.2.1 *Drosophila* strains, RNAi, and clonal analysis

Drosophila stocks used in this study were: *brm* RNAi (TID: 37720, 37721, VDRC), *mor* RNAi (TID: 6969, 110712, VDRC), *osa* RNAi (TID: 7810, VDRC), *ham* shmiR (BL32420), *osa* shmiR (generated in this study), *snr1* RNAi (TID: 108599, VDRC), *snr1* shmiR (BL32372), *mCherry* shmiR (BL35785), $brat^{K06028}$ (Arama et al., 2000), UAS-ham (Moore et al., 2002), UAS-p35, E(spl)mγ-GFP (Almeida & Bray, 2005), E(spl)mγ-GFP; *osa* RNAi. Mutant fly strains used for clonal analysis were: ham^{1}, FRT40A (Moore et al., 2002), FRT40A; *ham* shmiR, FRT82B, osa^{308} (Treisman, Luk, Rubin, & Heberlein, 1997) (BL5949), FRT82B, $snr1^{R3}$ (Zeng, Lin, & Hou, 2013). Gal4-driver lines used: UAS-*dicer2*; MZ1407 (*insc*)-Gal4, UAS-mCD8::GFP; *tub*-$Gal80^{ts}$, *ase*-Gal4, UAS-*stinger*::GFP (S. Zhu et al., 2006), UAS-mCD8::GFP;;*PointedP1*-Gal4 (S. Zhu et al., 2011), *erm*-Gal4 (II) (Xiao et al., 2012), *erm*-Gal4 (III) (Pfeiffer et al., 2008; Weng et al., 2010), UAS-*dicer2*; *wor*-Gal4, *ase*-Gal80; UAS-mCD8::GFP (Neumüller et al., 2011), UAS-*dicer2*; *wor*-Gal4, *ase*-Gal80; UAS-*stinger*::RFP. Clones of NBs homozygous for osa^{308}, $snr1^{R3}$ or ham^{1} were generated by FLP/FRT mediated mitotic recombination, using the *elav*-Gal4 (C155) (T. Lee & Luo, 1999). Larvae were heat-shocked for 1 hr at 38°C and dissected as third instar wandering larvae. RNAi crosses were set up and reared at 29°C and wandering third instar larvae were dissected 5 days after. For analysis of INP perdurance white prepupa were collected and staged at 29°C for 25 or 50 hrs.

4.2.2 Antibodies and immunohistochemistry

Antibodies generated in this study: guinea pig anti-Osa (maltose-binding protein (MBP) fusion of aa 2123-2717, affinity purified IgGs, 7.5 ug/ChIP), rabbit anti-Ham (against the peptide DAFFKDRAQAEHILQEWVRRREPVC, affinity purified, 1:50), guinea pig anti-Deadpan (against full-length MBP fusion protein, serum, 1:1000), rat anti-Asense (Bhalerao, Berdnik, Török, & Knoblich, 2005), rabbit anti-Prospero (serum, 1:1000, (Vaessin et al., 1991). Other antibodies used are: mouse anti-Osa (Developmental Studies Hybridoma Bank [DSHB]), guinea pig anti-Asense (1:100, (Bhalerao et al., 2005), rabbit anti-Miranda (1:100, (Betschinger et al., 2006)), guinea pig anti-Miranda (1:100), chicken

GFP (1:500, abcam), mouse anti-Prospero (1:100, DSHB), mouse anti-pH3 (1:1000, Cell Signaling Technology), rat anti-Elav (1:100, DSHB, 7E8A10), rabbit anti-aPKC (1:500, Santa Cruz Biotechnology), rabbit anti-Numb (1:100, (Schober et al., 1999)), rabbit anti-Brat (1:100, (Betschinger et al., 2006)), rat anti-Grainy head (1:1000, (Baumgardt, Karlsson, Terriente, Díaz-Benjumea, & Thor, 2009)), rabbit anti-Dichaete (1:1000, (Ma et al., 1998)), mouse anti-Eyeless (1:10, DSHB), guinea pig anti-Toy, rabbit anti-H3K9me1 (abcam9045), Alexa Fluor 488 phalloidin (Invitrogen), normal guinea pig IgG (Santa Cruz Biotechnology). In situ cell death detection kit, TMR red by Roche (12156792910) was used for TUNEL staining.

Larval brains were dissected in PBS, fixed for 20 min in 5% paraformaldehyde in PBS with 0.1% TritonX-100 (PBST), blocked in 2% normal goat serum (NGS) in PBST (blocking solution), antibodies were diluted in blocking solution. Brains were mounted in Vectashield (Vector Laboratories). TritonX-100 concentration in PBST was increased to 0.3% for Ham stainings. FACS sorted cell staining: cells were allowed to attach to the poly-D-lysine-hydrobromide-coated glass-bottom dishes (MatTek) for 1 hr at RT, fixed in 8% paraformaldehyde in PEM for 15 min, rinsed with PBST, blocked with 2% NGS in PBS, incubated with primary antibodies overnight, and rinsed 3 times with PBS afterwards. Secondary antibodies were incubated for 1 hr at RT, rinsed 3 times with PBS and cells were preserved in Vectashield mounting media.

4.2.3 Cell dissociation, FACS, sample preparation, and RNA sequencing

Cell dissociation, FACS sorting and bioinformatic analysis were done as previously described with minor modifications (Berger et al., 2012; Harzer, Berger, Conder, Schmauss, & Knoblich, 2013). UAS-dicer2; *wor*-Gal4, *ase*-Gal80; UAS-mCD8::GFP line was used to induce the expression of membrane-bound GFP and *osa* RNAi. 200-300 larval brains were dissected to obtain sufficient wild type type II NBs and INPs per each replicate of the qPCR experiment. 76-bp Illumina paired-end sequencing of Poly-A-mRNA libraries was performed on GAIIx. Experiment lacked biological replicates due to difficulties in getting sufficient material to prepare the sequencing library. For the analysis, DESeq was instructed to ignore the condition labels and estimate the variance by treating all the

samples as if they were replicates of the same condition (method="blind") (Anders & Huber, 2010).

4.2.4 Chromatin immunoprecipitation

Chromatin immunoprecipitation (ChIP) experiments were performed as described before (T. I. Lee, Johnstone, & Young, 2006c; Richter, Oktaba, Steinmann, Müller, & Knoblich, 2011) with minor modifications. Briefly, 100 wild-type (w^{1118}) third instar larval brains were dissected in ice-cold PBS and fixed in crosslinking solution (50 mM HEPES, 1 mM EDTA, 0.5 mM EGTA, 100 mM NaCl) containing 1.8% formaldehyde (Thermo scientific, formaldehyde ampules, methanol free) for 20 min. Fixed brains were homogenized in lysis buffer 1 and nuclei were isolated as described previously (T. I. Lee, Johnstone, & Young, 2006c). The nuclei were resuspended in 2 mL lysis buffer 3 and sonicated with a microtip sonicator (Omni-Ruptor 250, Omni International; microtip, power output: 20) for 18 cycles, 20 seconds on, 60 seconds off on ice-water bath. This resulted in 200-500 bp fragments. After centrifugation (4°C, 10 min, 16000*g*) and addition of Triton X-100 to a final concentration of 1%, the soluble chromatin was used directly for ChIP. 1000 µl chromatin was pre-cleared with 30 µl Protein A Sepharose beads. 100 µl pre-cleared chromatin was reserved as the input sample. Remaining chromatin was incubated with 7.5 µg antibody overnight at 4°C. Antibody-protein complexes were incubated with 30 µl Protein A Sepharose beads and washed 5 times, 3 minutes each with LiCl buffer (250 mM LiCl, 10 mM Tris-HCl pH 8.0, 1 mM EDTA, 0.5 % NP-40, 0.5 % sodium deoxycholate), followed by a TE with 50 mM NaCl wash. Elution of the material from the beads and crosslinking reversal were performed as previously described (T. I. Lee, Johnstone, & Young, 2006c). After DNA purification, IP pellets were resuspended in 360 µl H_2O, input pellet was resuspended in 720 µl H_2O. 10 µl suspension was used per qPCR reaction. See extended experimental procedures for qPCR primer sequences.

4.2.5 qPCR analysis of FACS sorted cells

First strand cDNA was generated using random primers on Trizol extracted total FACS sorted cell RNA. qPCR was done using BioRad IQ SYBR Green Super Mix on a BioRad CFX96 cycler. Expression of each gene was normalized to RpS8, and relative levels were

calculated using the $2^{-\Delta\Delta C_T}$ method (Livak & Schmittgen, 2001). See extended experimental procedures for qPCR primer sequences.

4.2.6 Microscopy and live cell imaging

Confocal images were acquired on LSM780 microscopes (Carl Zeiss GmbH). Long-term culturing of dissociated cells and live imaging was performed as described previously (Homem, Reichardt, Berger, Lendl, & Knoblich, 2013). Briefly, live imaging of cells was performed with a Perkin Elmer Ultra*VIEW* VoX spinning disc confocal system installed on an AxioObserver Z1 microscope (Carl Zeiss GmbH). Images were captured with a Hamamatsu EMCDD 9100-13 (Hamamatsu Photonics GmbH) camera in 8Bit mode, using 40x/1.3 EC plan-neofluar lens (Carl Zeiss GmbH). Volocity 3D Image Acquisition and Analysis suite was used for image acquisition. The interval for picture recording was set to 3 min and multiple positions were monitored. Laser power and exposure settings were adjusted to minimize phototoxicity. Cells of different genotypes were kept in Schneider's medium in separate chambers of a 4-chamber glass-bottom petri dish coated with Poly-D-lysine and left to settle for 30-60 minutes after dissociation. Cell-cycle lengths were measured from the cell-membrane or nuclear membrane breakdown of INPs/GMCs or type I/II NBs respectively, until the next cell-/nuclear membrane breakdown.

4.2.7 Generation of *osa* shmiR

Efficient shRNA prediction was made by implementing an algorithm described previously (Vert, Foveau, Lajaunie, & Vandenbrouck, 2006) and modified for 22-bp shmiRs. An off-target algorithm was designed to exclude potential off-targets (Brennecke, Stark, Russell, & Cohen, 2005; Haley, Foys, & Levine, 2010). The synthesized oligos were annealed and cloned into the Walium20 vector according to the protocols of The Transgenic RNAi Project (flyrnai.org). The following oligos were used:

CTAGCAGTTCGGAGATTGTTAACATTCCATAGTTATATTCAAGCATATGGAATGTTAACAATCT
CCGAGCG

AATTCGCTCGGAGATTGTTAACATTCCATATGCTTGAATATAACTATGGAATGTTAACAATCTCC
GAACTG

4.2.8 Transplantation of larval brains

For the results displayed in Fig.1B, UAS-*dicer2*; MZ1407(*insc*)-Gal4,UAS-mCD8::GFP was used to drive the expression of control or UAS-RNAi lines against *osa* (TID: 7810, VDRC), *mor* (TID: 6969,VDRC)*, brm* (TID: 37721, VDRC) or *snr1* (TID: 108599) at 29°C. For all the other transplantations, *erm*-Gal4; UAS-mCD8::GFP and UAS-mCD8::GFP; *erm*-Gal4 were used to drive the expression of *osa* shmiR (generated in this study) or *ham* shmiR (BL32420). GFP^+ larval brain pieces were transplanted into the abdomen of adult host flies as previously described (Caussinus & Gonzalez, 2005). Flies were observed under a fluorescent scope twice a week to assay tumor formation. Due to the weakness of GFP signal with *erm*-Gal4 driver transplanted flies were dissected to analyze tumor formation.

4.2.9 Motif analysis

Transcription start sites (TSS) of the 50 up- and downregulated genes respective to their primary transcripts were manually curated. For the genes with known binding sites (ChIP-qPCR) amplified sequences were taken into account. For all the other genes, promoter regions were assigned to be -1500bp to +200bp relative to the TSS. MEME was used to identify a common motif of up- and downregulated sequences separately (-dna -nmotifs 10 -maxw 15) (Bailey, 2005).

Table 1 List of primers for ChIP followed by qPCR

Gene	Sequence
erm TSS 1 fwd	GCGAAAAGATGGATGCTAGAGC
erm TSS 1 rev	GTGTGCAGTATGTGTTCGCG
erm TSS 2 fwd	CAATCCATCTCGCTCTGTCG
erm TSS 2 rev	GCGAGTGCTGGGGTGAATC
opa fwd	TCGGCCCACCACCCAATG
opa rev	CTCCTCGCATGCTCCAGA
ham TSS 1 fwd	CAAGCAGAGAGAGAGATAATG
ham TSS 1 rev	CGCACTAATACAGCCAAACG
ham TSS 2 fwd	TGTCTGGTCTGGGCCAAC
ham TSS 2 rev	CTCCGATGCAGCTGTAGATA
oaz TSS 1-2 fwd	GCAGCTCTTACGGGAAACATG
oaz TSS 1-2 rev	CCATAATTCCATACCCCCTC
oaz TSS 2 fwd	CACACGAAGCTTTCTCACTC
oaz TSS 2 rev	CGTGCCTTTTGGGATTCTCG
D TSS2 fwd	GAACAAAGCCAGTGGAACAATG
D TSS2 rev	GCAACCCTCGCACCATTAC
dpn fwd	GACTTGGCTTAACCGAATGTTG
dpn rev	GAGTAGGTATTCCCAGGCAGGC
ham coding fwd	GACTCATCCCACCTTCCATC
ham coding rev	GATCCTTCGTCTTGAGTCCC

Table 2 List of primers for qPCR analysis of FACS sorted samples

Gene	Sequence
dpn fwd	CATCATGCCGAACACAGGTT
dpn rev	GAAGATTGGCCGGAACTGAG
HLHmγ fwd	AAGGTGATGAAGCCCATGCT
HLHmγ rev	GCTTTCTCCAAACGGGTGAC
klu fwd	CAACAATAATGAGACCCACTCC
klu rev	GATCTTCATCCTGTTCGGCATC
mira fwd	CCCAATTGGAGCTGGACAACA
mira rev	GGTGTTCCCAGCAGAGAGG
erm fwd	GGGACTTGAGCGCATTTTTC
erm rev	TTCTTGTCGTTGTGCGTGTG
ase fwd	AGCCCGTGAGCTTCTACGAC
ase rev	GCATCGATCATGCTCTCGTC
ham fwd	ATAGATCCTTTGGCCAGCAGAC
ham rev	AGTACTCCTCCCTTTCGGCAAT
opa fwd	CTGAACCATTTCGGACACCATC
opa rev	CCAGTTCTCCCACTCTCAATAC
oaz fwd	GGAAGTCTGCAGGAGCCAGT
oaz rev	TCAGAGTGCTTGCCACGTTT
fer2 fwd	TGCGTCCAGCTACAAAATGC
fer2 rev	ACGGAAAGGTGGGTACATGG
tap fwd	CCTCTTGCACAGCACCAG
tap rev	CATGCTGCCTGTAAAGTCG
optix fwd	GACTCGGACATCTCACTGG
optix rev	GTCCACGCTCAAGCTCTCC
CG13897 fwd	CGCCCTTCCAGAATGTCTTC
CG13897 rev	TCGTTGCTCAGGTTGCTGTT
run fwd	CTGAGGAACTGCACCACGAC

Table 2 List of primers for qPCR analysis of FACS sorted samples

Gene	Sequence
run rev	GTGATGGTCAGCGTGAAGGA
ap fwd	ACCAAACGAATGCGAACCTC
ap rev	GACCCTCTTTGGTAAACCAGT
hbn fwd	CCCAAGCTAGTGCCTCATCC
hbn rev	GAGATCAGTCCGCCCGTTAG
nerfin-1 fwd	GAACCTACAACGAAAGCCAAAG
nerfin-1 rev	GTAGGAGCAAAGGAGTAGATG
oli fwd	CACGGACACATGCCAATACC
oli rev	GGGCATAGAAACCACCCAGA
rps8 fwd	CTTGGTGAAGAACAGCATCGTG
rps8 rev	GTCGTTCTCGTCCTCTTTCTGG

5. CHAPTER II: IDENTIFICATION OF SWI/SNF COMPLEX COMPOSITION IN THE LARVAL BRAIN

5.1 INTRODUCTION

As discussed in the previous chapter, subunits of the SWI/SNF complex are ubiquitously expressed in the *Drosophila* larval brain. However the phenotype arising from *osa* loss of function specifically comes from immature INPs. How does this cell type specific function arise? In *Drosophila*, there are two evolutionarily conserved subclasses of the SWI/SNF complex. These two subclasses, BAP (Brahma-associated proteins) and PBAP (Polybromo-associated BAP), share seven core subunits. While BAP complex is defined by the presence of a signature subunit called Osa, PBAP complex is defined by the presence of Polybromo (PB), BAP170 and e(y)3 (Chalkley et al., 2008; Mohrmann et al., 2004). Even though the core components of the complex are sufficient for chromatin remodeling *in vitro*, RNAi knockdown of signature subunits in *Drosophila* S2 cells followed by transcriptome profiling shows that such assemblies are defective in controlling transcription (Moshkin, Mohrmann, van Ijcken, & Verrijzer, 2007). Therefore, core subunits of the complex are required for the enzymatic and architectural functions, but the signature subunits are necessary to give the complex functional specificity. Both BAP and PBAP complexes are required for the viability of the flies (Moshkin et al., 2007). However, Osa and PB localize differentially on larval salivary gland polytene chromosomes, suggesting that they control distinct sets of target genes (Mohrmann et al., 2004). Genome-wide expression profiling of BAP and PBAP target genes in S2 cells suggest that they regulate distinct biological processes. GO-term analysis shows that BAP complex is involved in cell cycle regulation, while PBAP complex is involved in signal transduction cascades (Moshkin et al., 2007). Furthermore, a recent study shows that the PBAP complex, but not the BAP complex associates with GAGA-factor and mediates H3.3 replacement at chromatin boundaries, confirming the differential roles of BAP and PBAP complexes (Nakayama, Shimojima, & Hirose, 2012).

Signature subunits of BAP and PBAP complexes are conserved in mammals, forming BAF and PBAF complexes respectively. However, in contrast to the dimorphic *Drosophila*

complexes, expansion of gene families encoding the complex subunits and combinatorial assembly give rise to polymorphic mammalian SWI/SNF (mSWI/SNF) complexes (Fig. 32A). This was initially discovered during the course of neurogenesis, where the transition from self-renewing neural progenitors to post-mitotic neurons was accompanied by a switch between the subunits BAF45a, BAF53a, SS18 and BAF45b, BAF45c, BAF53b, CREST (Lessard et al., 2007; Staahl et al., 2013; J. I. Wu, Lessard, & Crabtree, 2009) (Fig. 32B). This switch is functionally relevant as BAF45a expression is sufficient to enhance neural stem cell (NSC) proliferation phase (Lessard et al., 2007). Similarly, knockdown of SS18 in NSCs greatly reduces self-renewal capacity. On the contrary, overexpression of SS18 in primary cortical neurons compromises dendritic growth (Staahl et al., 2013). Another nBAF complex specific subunit, BAF53b has been shown to be required for dendritic development and npBAF specific subunit BAF53a cannot replace its function (J. I. Wu et al., 2007). Moreover, forcing the formation of nBAF complex in fibroblasts results in their conversion to neurons underlining the importance of cell-type specific functions of combinatorial assemblies (Yoo et al., 2011). Further examples of combinatorial assemblies of mSWI/SNF complexes appear in cardiac progenitors where BAF60c, but not BAF60a or b has crucial functions in heart morphogenesis (Lickert et al., 2004). Similarly mouse embryonic stem cells require a specific assembly of the mSWI/SNF complexes consisting of Brg, BAF155 and BAF60a, excluding Brm, BAF170 and BAF60c, for the maintenance of pluripotency (Ho et al., 2009). Taken together, combinatorial assembly of mSWI/SNF complexes is crucial to achieve cell type specific functions of the complex.

So far such a diverse assembly for the *Drosophila* SWI/SNF complexes has not been shown. Furthermore, it is not clear whether there is a preferential requirement for BAP vs. PBAP complex in the *Drosophila* larval brain. In order to test whether subunit composition of the *Drosophila* SWI/SNF complex is dynamic in the larval brain we performed affinity purification followed by mass spectrometry analysis to characterize the complex in detail.

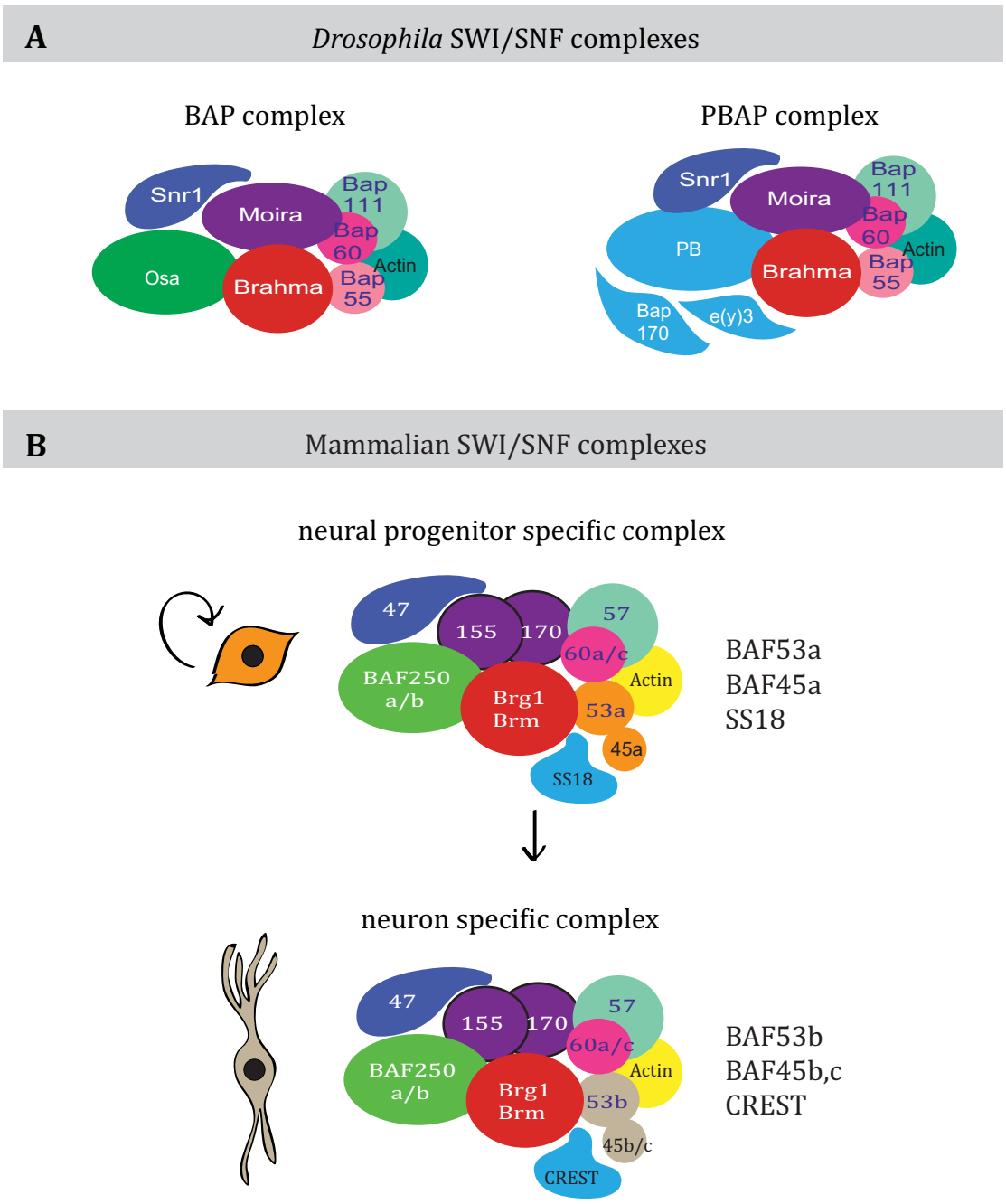

Figure 32: Combinatorial assembly of the mammalian SWI/SNF complexes

(A) *Cartoon showing BAP and PBAP complexes, which share 7 core subunits. Osa is the signature subunit for the BAP complex and Polybromo (PB), Bap170 and e(y)3 are signature subunits of PBAP.* ***(B)*** *Cartoon showing the combinatorial assembly of the SWI/SNF complex in the mammalian nervous system development. The neural progenitor cell specific complex consists of BAF53a, BAF45a and SS18. As cells exit mitosis BAF53b, BAF45b/c and CREST replace these subunits.*

5.2 RESULTS AND DISCUSSION

5.2.1 Signature subunits are differentially expressed in NBs vs. neurons

Currently it is not clear whether there is a preferential requirement for BAP vs. PBAP complex in the *Drosophila* larval brain. To check whether signature subunits of these complexes are differentially expressed in self-renewing NBs vs. differentiating neurons, we analyzed expression levels of *e(y)3*, *Bap170*, *PB* and *osa* taking advantage of the existing transcriptome data generated in our laboratory from pure FACS sorted NBs and neurons (Berger et al., 2012). While *e(y)3* and *Bap170* were expressed at similar levels in NBs and neurons, *PB* was upregulated 0.99 fold (log2) in NBs (Fig. 33A). Conversely, *osa* expression was upregulated 1.8 fold (log2) in neurons (Fig. 33A). Furthermore, immunostainings of larval brains for PB and Osa confirmed the differential expression (Fig. 33B-C). PB staining was enriched in Mira-positive NBs (Fig. 33B). Osa staining was ubiquitous across the larval brain. However it was enriched in some neural clusters (Fig. 33C). Taking together, we conclude that the signature subunits of BAP and PBAP complexes, Osa and PB, are differentially expressed, raising the possibility that there might be a switch from PBAP to BAP complex during neural differentiation.

In order to test whether this switch has functional consequences we performed RNAi knockdown and overexpression analysis of the PBAP complex signature subunits. Surprisingly, neither the RNAi knockdown nor the overexpression of PBAP signature subunits caused a phenotype in NB lineages, suggesting that PBAP complex activity in the larval brain is dispensable for achieving the balance between self-renewal and differentiation of *Drosophila* NB lineages (Neumüller et al., 2011) (data not shown).

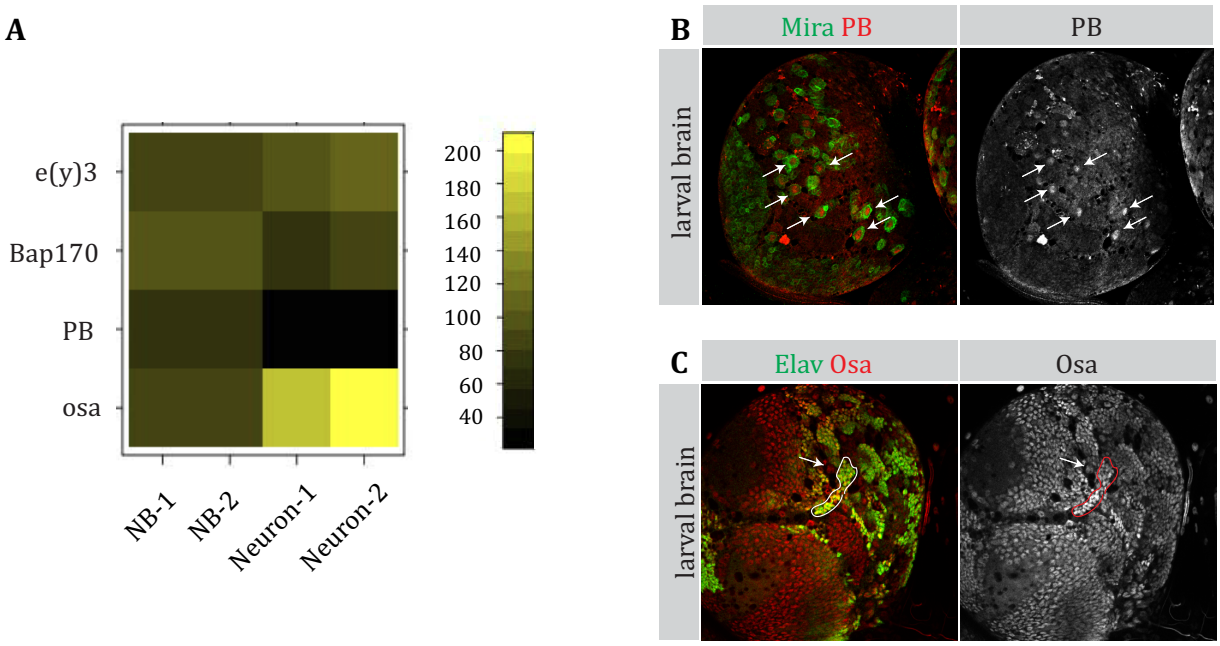

Figure 33: Signature subunits of BAP and PBAP complexes are differentially expressed in NBs vs. neurons.

(A) *Expression of signature subunits in self-renewing NBs vs. differentiating neurons. Heat map showing the FPKM values for e(y)3, Bap170, PB and osa in NBs and neurons. PB expression is upregulated in NBs and Osa expression is upregulated in neurons.* ***(B)*** *Wild type larval brain stained for the NB marker Mira and PB. PB staining is stronger in NBs (indicated by arrows).* ***(C)*** *Wild type larval brain stained for neural marker Elav and Osa. Osa staining is stronger in neurons. A representative NB is indicated by an arrow. A representative cluster of neurons is outlined.*

5.2.2 Purification of *Drosophila* SWI/SNF complex from larval brain identifies novel subunits

To identify novel components of the BAP complex that might be required for cell type specific functions, we affinity purified the complex from L3 stage larval brain extract utilizing various antibodies and protein digestion methods (Fig. 34A). Affinity purification of the SWI/SNF complex using an antibody generated against the core subunit Brahma (Brm) (see Methods) demonstrated a specific pattern of co-purifying proteins (Fig. 34B). These proteins were subjected to in gel tryptic digestion, followed by nanoscale liquid chromatography coupled to tandem mass spectrometry (nano LC-MS/MS) and identified using the Thermo Proteome Discoverer software. Purification based on the Brm antibody yielded identification of 40 proteins (over 95% probability, minimum 3 peptides, % coverage ≥ 4, Supplemental Table 3). Among these were all known SWI/SNF complex subunits confirming the successful purification of the complex (Fig. 34B, in red). Moreover, novel binding partners such as Sbf, CG8108, Cdc5, d4, CG12333 were identified (Fig. 34B). Sbf is a SET domain binding protein and a component of trithorax (Trx) acetylation complex (TAC1) (Cui et al., 1998; Petruk et al., 2001). Even though an interaction between Sbf and Brm has not been shown before, Trx binds to Snr1, implicating a potential interaction between TAC1 and SWI/SNF complex. CG8108 is an uncharacterized protein that contains a C2H2-like zinc finger domain (flybase). Cdc5 (CG6905) is a Myb DNA-binding domain containing protein that has been identified as a potential component of the Hedgehog signaling (Nybakken, Vokes, Lin, McMahon, & Perrimon, 2005). CG12333 is an uncharacterized protein with a role in lateral inhibition (Mummery-Widmer et al., 2009). d4 is a transcription factor (Nabirochkina et al., 2002). Its mammalian homolog DPF1/2 has been identified as a specific subunit of the mammalian neural BAF complex (Lessard et al., 2007). However, it has not been previously identified in *Drosophila* SWI/SNF complex. Taken together, these are potentially interesting novel binding partners of Brm.

Since Brm is a component of both BAP and PBAP complexes, these novel subunits might belong to either assembly. To determine which one of these novel components belong to the BAP complex, we affinity purified the BAP complex signature subunit Osa. A

protein trap line that tags endogenous Osa protein with GFP was utilized for the affinity purification (Fig. 35A). Mutations in *osa* gene cause early embryonic lethality (Treisman et al., 1997). Transgenic flies expressing endogenously tagged Osa protein were homozygous viable, suggesting that GFP tagged Osa protein is fully functional. Western blot analysis detected a shift in the size Osa protein tagged with GFP (Fig. 35B). Furthermore, immunofluorescence showed complete overlap of Osa staining with the GFP signal (Fig. 35C). Taken together, we conclude that GFP tagged Osa protein is functional and can be used to determine binding partners of Osa.

Affinity purification of Osa utilizing a GFP-binding protein coupled to agarose beads (GFP-trap) under stringent conditions revealed a specific pattern of co-purifying proteins (Fig. 35D). In gel tryptic digestion followed by mass spectrometry analysis detected 22 unambiguously identified proteins (over 95% probability, minimum 3 peptides, % coverage ≥ 4, Supplemental Table 4). 2 of these were CG8108 and Cdc5, which were also co-purified with Brm, suggesting that they might be true novel components of the BAP complex (Fig. 35E).

Even though in gel digestion of proteins isolated by gel electrophoresis increases the depth of analysis, alternative methods such as on-bead tryptic proteolysis might increase sensitivity (Fukuyama et al., 2012; Shevchenko, Tomas, Havlis, Olsen, & Mann, 2006). As a complimentary approach we performed on bead tryptic digestion of proteins that co-purify with Osa and repeated the mass spectrometry. Using this method we identified 16 proteins (over 95% probability, minimum 2 peptides, % coverage ≥ 6.5, Supplemental Table 5). To exclude identification of false positives we affinity purified Osa-containing SWI/SNF complex using an antibody we generated (see Methods in Chapter I) and performed on bead-tryptic digestion followed by mass spectrometry analysis. Comparison of proteins identified using GFP-trap and an antibody against Osa revealed 3 novel binding partners (Table 3, in red). These were d4, Toothrin (Tth) and BCL7-like. A recent study identifies d4 and Tth as novel signature subunits of the BAP complex, confirming our findings (Moshkin et al., 2012). Moreover, mammalian homologs of *Drosophila* Bcl7-like, BCL7A, BCL7B and BCL7C have recently been identified as novel

subunits of the mammalian BAF complex, further supporting our results and indicating the conservation of complex composition in higher species (Kadoch et al., 2013).

Using a combination of different antibodies and elution methods we were able to identify 5 novel components of the BAP complex (Fig. 36). While RNAi knockdown of *d4*, *tth*, *CG8108* and *BCL7-like* did not cause a phenotype, loss of *cdc5* function resulted in underproliferation of NB lineages (data not shown)(Neumüller et al., 2011), suggesting that there might be various BAP complexes responsible for different aspects of self-renewal vs. differentiation control.

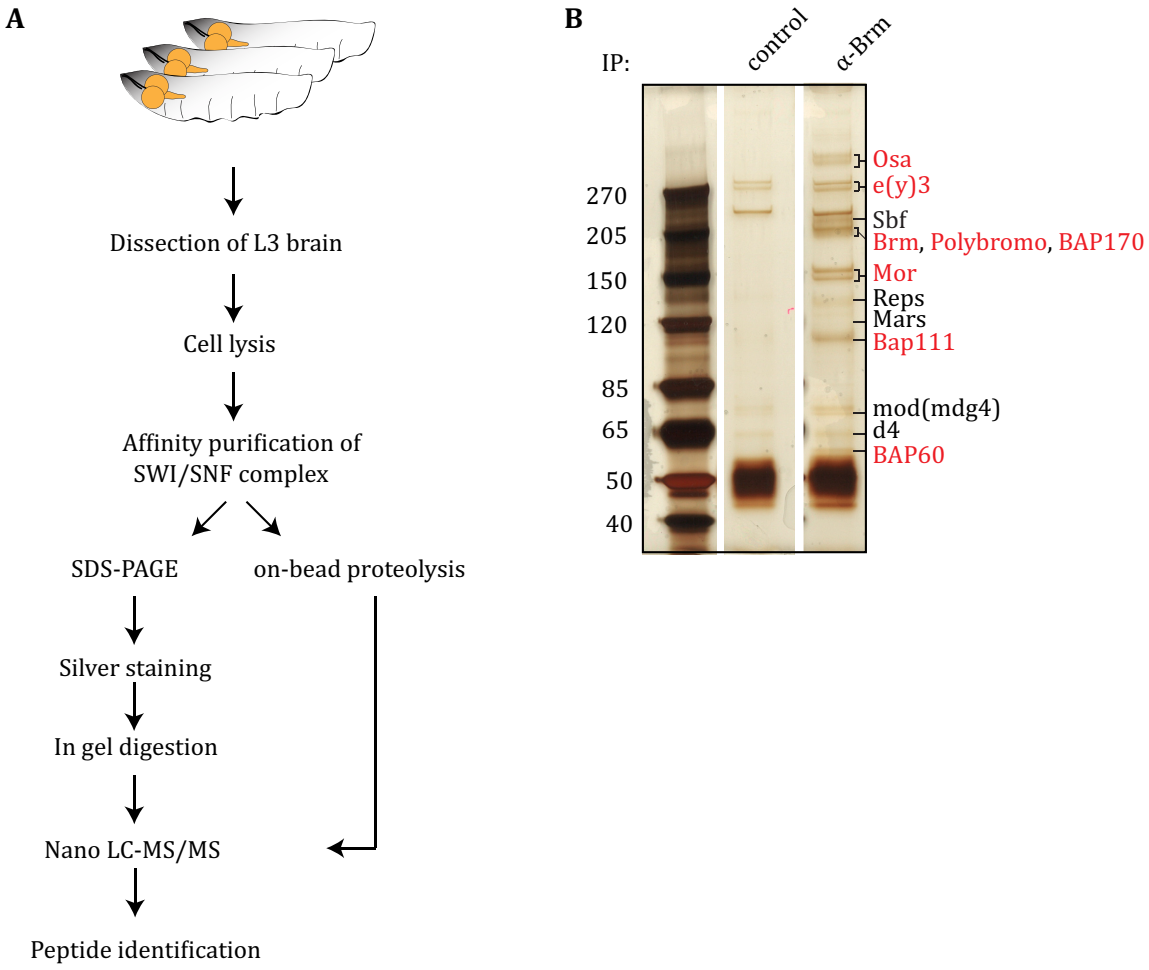

Figure 34: Affinity purification of the SWI/SNF complex from Drosophila larval brain tissue.

(A) *Strategy for purification of the SWI/SNF complexes from L3 stage larval brain.* ***(B)*** *Silver stain analysis of affinity purified endogenous SWI/SNF complexes from Drosophila larval brain extracts. An antibody against Brm was used for immunopurification. Core components of the complex are shown in red. Signature subunit of the BAP complex, Osa, is shown in green. Signature subunits of the PBAP complex, Polybromo, e(y)3 and Bap170 are shown in blue. Novel binding partners are shown in black. Peptide block was used as a negative control. Refer to Table X for complete list of identified binding partners.*

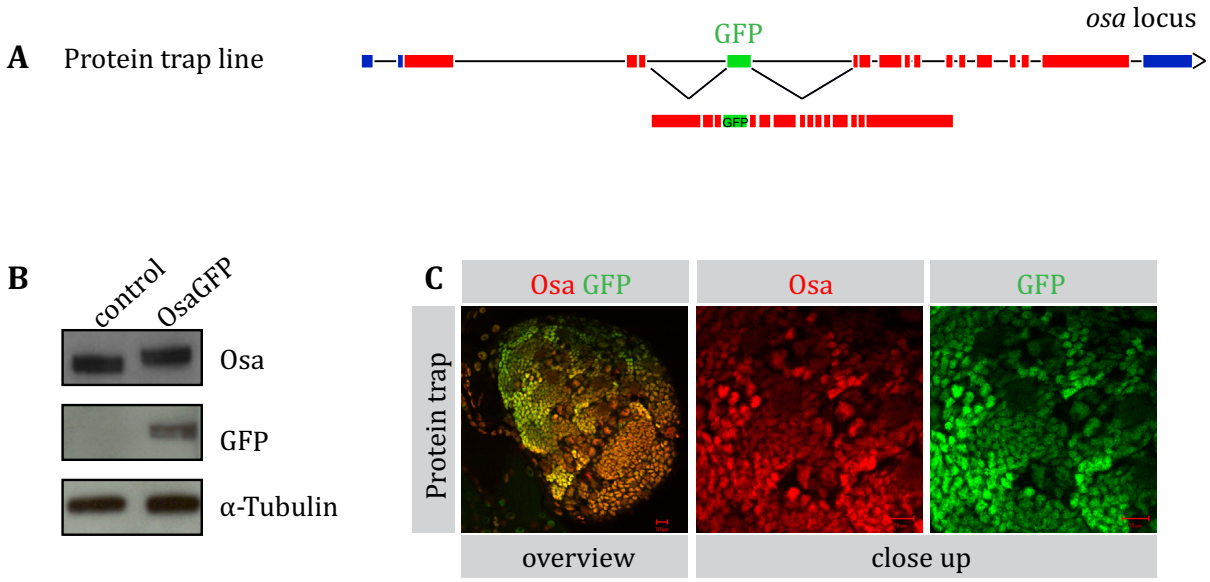
A
Protein trap line
GFP
osa locus
B
control
OsaGFP
Osa
GFP
α-Tubulin
C
Osa GFP
Osa
GFP
Protein trap
overview
close up
D
control IP
GFP trap IP
270
205
150
120
85
65
50
40
Osa
Brm
Mor
CG8108
Bap111, Cdc5
Bap55
Snr1
larval brain
E
Osa IP
Brm IP
30
7
53
Mor
Osa
Brm
Bap111
Bap55
Cdc5
CG8108

Figure 35: GFP-tagged endogenous Osa is functional and can be used to purify BAP complex.

(A) *Modified Osa locus. A GFP exon is inserted in an intron in osa genomic locus. Resulting protein is tagged with GFP.* ***(B)*** *Western blot analysis of wild type and OsaGFP larval brain extracts. An antibody against Osa recognizes the GFP-tagged Osa shifted to higher molecular weight compared to endogenous protein. An antibody against GFP recognizes a specific band. α-tubulin was used as loading control.* ***(C)*** *Larval brains of the protein trap line stained for Osa and GFP. Overview image of the right lobe shows overlapping Osa and GFP immunofluorescence.* ***(D)*** *Silver stain analysis of affinity purified endogenous BAP complex from Drosophila larval brain extracts. GFP-trap (see methods) was used for immunopurification. Complex members are denoted in black. Novel binding partners are denoted in red.* ***(E)*** *Venn diagram showing the overlap of binding partners that co-purify with Osa and Brm. Cdc5 and CG8108 are potential novel BAP subunits. Wild type larval brain extract was used as negative control. Refer to Table X for complete list of binding partners.*

	Osa antibody IP		GFP-trap IP	
Protein	% coverage	# peptides	% coverage	# peptides
Osa	19	37	17	40
Moira	39	42	37	41
Brahma	28	39	27	29
Bap60	44	21	34	18
Bap55	49	15	37	12
Bap111	32	19	34	20
Snr1	35	11	30	8
BCL7-like	27	4	27	6
d4	15	9	18	12
Tth	5.4	2	6.8	2

Table 3: Mass spectrometry analysis identifies potential novel BAP complex subunits.

Proteins identified as Osa binding partners using the on-bead digestion method followed by nano LC-MS/MS. Osa-containing BAP complex was affinity purified either using an antibody against endogenous Osa or an antibody against GFP-tagged Osa. Bcl7-like, d4 and Tth are reproducibly identified novel BAP complex subunits.

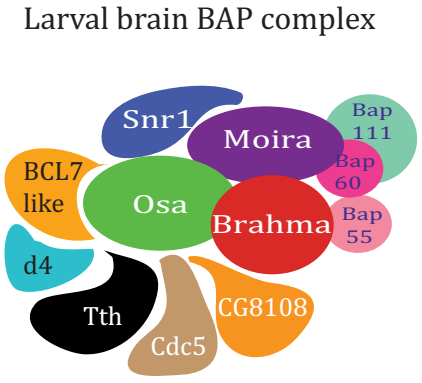

Figure 36: *Cartoon showing the updated BAP complex composition identified in the Drosophila larval brain. BCL7-like, d4, Tth, Cdc5 and CG8108 are novel BAP complex subunits identified using various antibodies and protein digestion protocols.*

5.2.3 Purification of the complex from *brat* mutant larval brains

To determine whether there are uncharacterized BAP complex subunits that are differentially required in self-renewing vs. differentiating cells, we utilized *brat* mutant brains that are enriched for type II NBs in contrast to wild type brains that are enriched for neurons. Osa was affinity purified from wild type and *brat* mutant ($brat^{K06028}$) larval brains and co-purifying proteins were analyzed by on bead tryptic digestion followed by mass spectrometry. We identified similar number of unique peptides for the core components of the complex (Brm, Mor, Bap60, Bap55, Bap111, Snr1) in wild type and *brat* mutant brains (Table 4, Supplemental Table 6). Similarly, number of peptides identified for Osa and for the novel BAP subunits identified in this study (BCL7-like, d4, Tth) did not vary between neuron enriched wild type brains and type II NB enriched *brat* mutant brains. Surprisingly, we identified only one protein (Wee) that showed increased % coverage in *brat* mutant brains. Wee is a tyrosine kinase involved in cell cycle regulation (Campbell, Sprenger, Edgar, & O'Farrell, 1995) and it has been shown to phosphorylate and deactivate Cdk1 (Price, Rabinovitch, O'Farrell, & Campbell, 2000). Analysis of *wee* expression showed 1.9-fold (log2) upregulation of *wee* in NBs (Fig. 37), suggesting that it might be a NB-specific SWI/SNF complex member. Surprisingly, four proteins were detected only in wild type larval brains. These were CG2519, Rapgap1, Argk, and CG2950 (PD isoform). CG2519, Rapgap1 and CG2950 showed higher expression levels in neurons compared to NBs (Fig. 37), raising the possibility that these could be complex components of the differentiated cell types. RNAi knockdown of these genes in NB lineages did not reveal any phenotype (data not shown), suggesting that there might be functional redundancy between subunits of the complex.

	wild type		*brat*^{K06028}	
Protein	% coverage	# peptides	% coverage	# peptides
Osa	19	37	22	38
Mor	39	42	37	37
Brm	28	39	27	38
Bap60	44	21	38	17
Bap55	49	15	42	13
Bap111	32	19	39	21
Snr1	35	11	22	7
BCL7-like	27	4	27	4
d4	15	9	21	11
Tth	5.4	2	5.4	2
Wee	13	6	30	13
CG2519	15	17	0	0
Rapgap1	12	7	0	0
Argk	10	5	0	0
CG2950-PD	23	3	0	0

Table 4: Mass spectrometry analysis identifies Osa co-purifying proteins that are differentially detected in wild type and brat mutant larval brain extracts.

Table showing the proteins co-purified with Osa from wild type and brat mutant larval brains. Percent coverage based on unique peptides identified with over 95% probability and number of unique peptides are shown. Wee is a potential NB specific binding partner whose % coverage is increased in the brat mutant brain extract. CG2519, Rapgap1, Argk and CD2950 are potential neuronal complex subunits that are not detected in brat mutant brains.

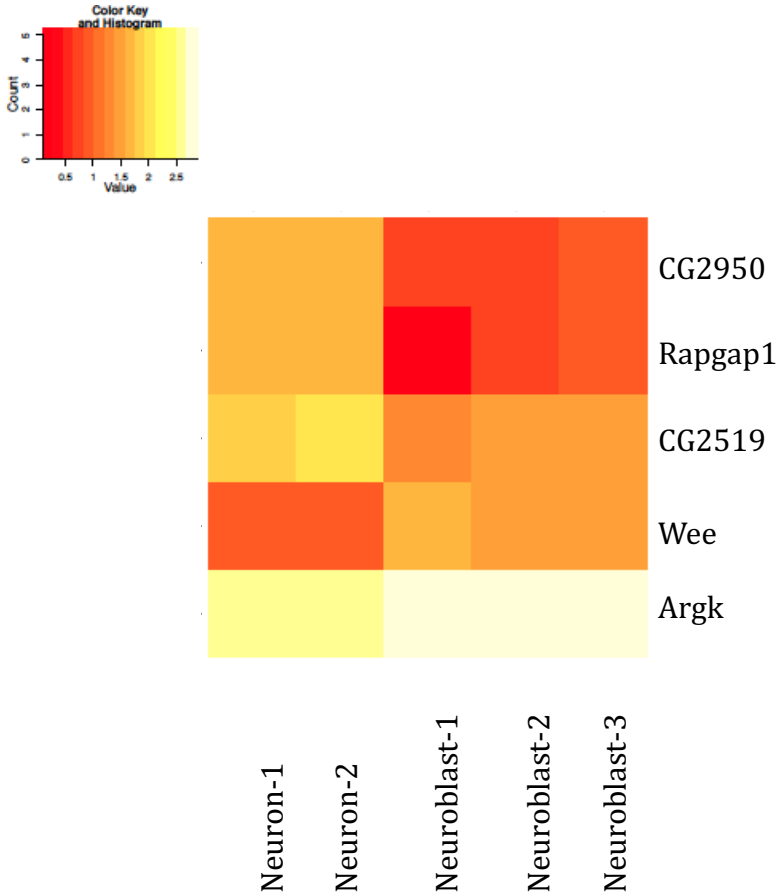

Figure 37: Expression analysis of differentially bound proteins.

Heat map showing the FPKM values (log10) for genes identified in mass spectrometric analysis. CG2950, Rapgap1 and CG2519 are upregulated in neurons, while Wee is upregulated in NBs. Red color indicates low expression and yellow color indicates high expression.

5.2.4 Temporal control of Notch signaling in cell culture

Since a major difference between self-renewing and differentiated cells of the larval brain is their Notch activity, we tested whether the complex composition changes in response to Notch signaling. In order to do this, we established a cell culture method where Notch receptor activation can be temporally controlled. It has been reported that calcium depletion leads to dissociation and activation of the Notch receptor (Rand et al., 2000). Previously it has been shown that treatment of *Drosophila* S2 cells by divalent cation chelator EDTA is sufficient to activate Notch target genes (Krejcí & Bray, 2007). We utilized BG3 cells that are derived from third instar larval central nervous system to stay as close to the *in vivo* state as possible. To test whether Notch signaling can be activated in BG3 cells, we optimized the culture conditions and assessed the response of BG3 cells to EDTA treatment by monitoring the expression levels of selected genes in the E(spl) complex that are direct targets of Notch activation (Fig. 38A) (Campos-Ortega, 1994; Delidakis & Artavanis-Tsakonas, 1992; Krejcí & Bray, 2007). All the tested E(spl) complex genes showed rapid increase in expression levels upon 30 minutes of EDTA treatment (Fig. 38B). On the contrary, treatment of the cells with the Notch signaling inhibitor DAPT for 17 hours resulted in repression of E(spl) complex genes (Fig. 38C). Taken together, we conclude that there is already a basal level of Notch activity in untreated BG3 cells and it is greatly enhanced upon EDTA treatment.

5.2.5 Composition of SWI/SNF complex does not change in response to Notch activation

In order to test whether a conserved larval brain SWI/SNF complex can be purified from BG3 cells, we immunoprecipitated Brm and performed on bead tryptic digestion followed by mass spectrometric analysis. Both BAP and PBAP complex subunits were successfully purified (Table 5). Additionally some of the novel subunits identified in the larval brain, such as CG12333, d4, BCL7-like were also identified in BG3 cells suggesting conservation of the complex purified from the larval brain tissue. Interestingly, analysis of the complex composition from mock treated and EDTA treated cell lysates revealed a slight increase in the % coverage of peptides in PBAP complex subunits such as

Polybromo, Mars and l(3)j2D3, while BAP complex subunits, Osa, d4 and BCL7-like were either detected at similar levels or slightly decreased (Table 5). However, overall there were no major changes in the complex composition. This was further supported by immunoprecipitation of Osa. Potential novel NB vs. neuron subunits identified to be differentially bound in wild type and *brat* mutant brains (CG2950, Rapgap1, Wee) did not show a significant change upon Notch activation (Table 6). CG2519 and Argk were not identified as Osa binding partners in BG3 cells. Taken together, our results suggest that there are NB vs. neuron specific BAP complex assemblies, however Notch signaling is not responsible for triggering the change in complex composition.

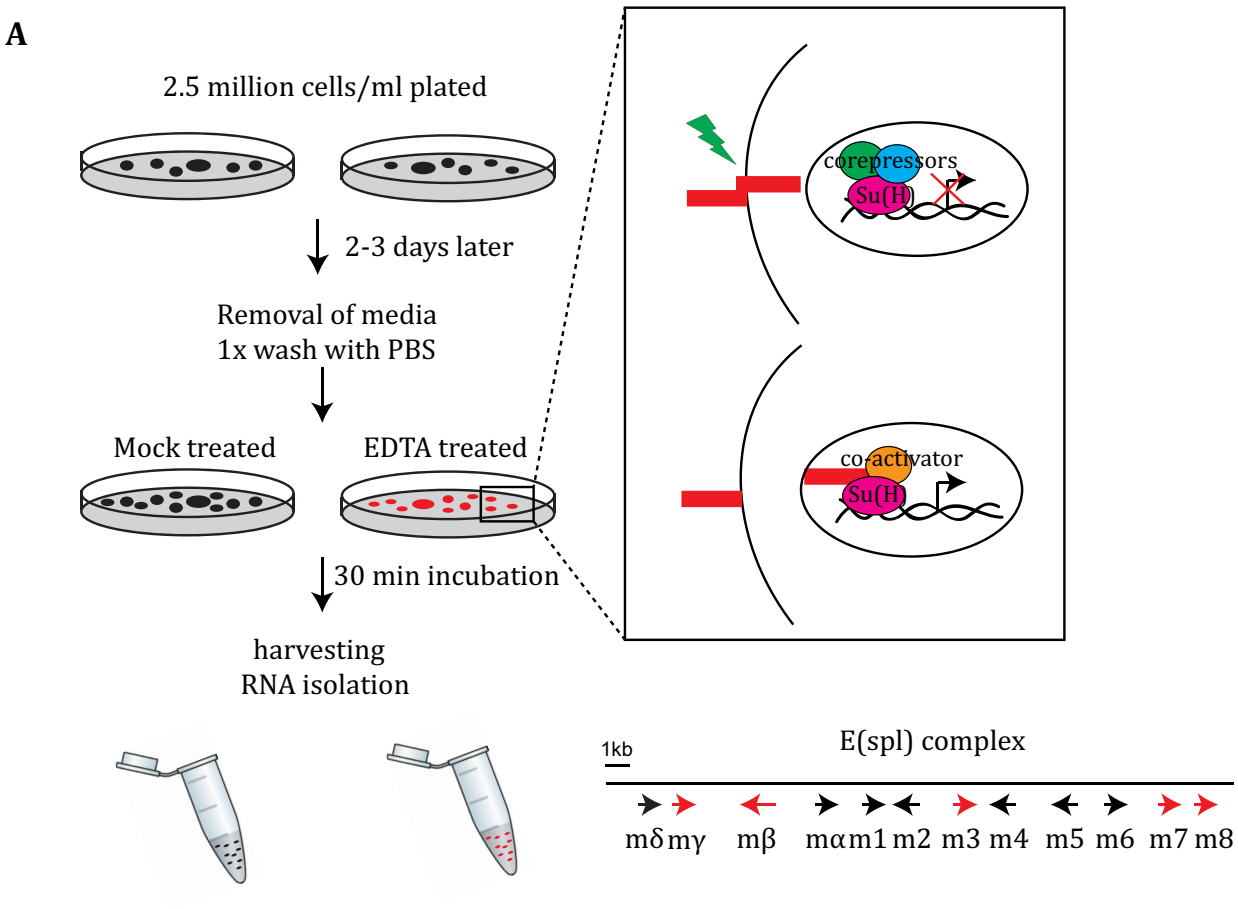
A
2.5 million cells/ml plated
2-3 days later
Removal of media
1x wash with PBS
Mock treated
EDTA treated
30 min incubation
harvesting
RNA isolation
corepressors
Su(H)
co-activator
Su(H)
1kb
E(spl) complex
mδ mγ mβ mα m1 m2 m3 m4 m5 m6 m7 m8

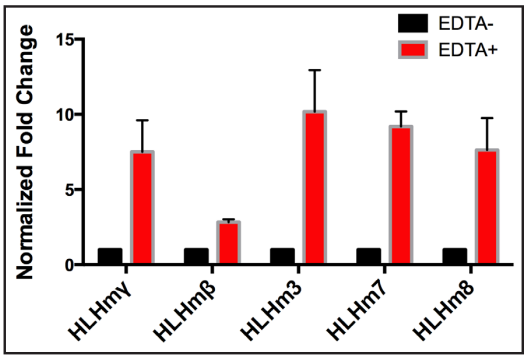
B
Normalized Fold Change
EDTA-
EDTA+
HLHmγ
HLHmβ
HLHm3
HLHm7
HLHm8

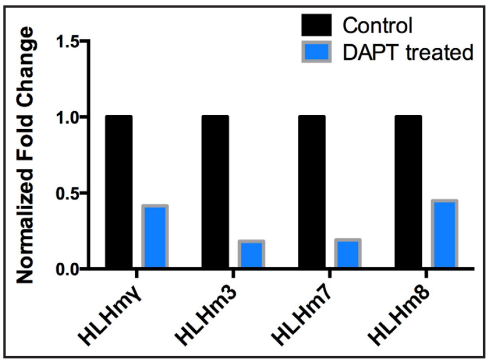
C
Normalized Fold Change
Control
DAPT treated
HLHmγ
HLHm3
HLHm7
HLHm8

Figure 38: Temporal control of Notch signaling in BG3 cells.

(A) *Flow chart of the experiment. BG3 cells are plated at 2.5-million/ml density. 2-3 days after, cells are washed with PBS and incubated with either PBS (mock treated) or PBS with 2 mM EDTA for 30 min. EDTA treatment triggers ectodomain shedding of the Notch receptor and the Notch intracellular domain translocates into the nucleus to activate target genes. Activation of the pathway can be monitored by expression analysis of E(spl) complex loci genes which are well-characterized Notch targets.* ***(B)*** *qRT-PCR result showing the upregulation of selected E(spl) genes upon EDTA treatment. Experiment was performed 3 independent times. Error bars represent s.e.m.* ***(C)*** *DAPT treatment inhibits Notch signaling. qRT-PCR result showing the downregulation of Notch target genes upon 17 hrs of DAPT treatment.*

	Mock treated		EDTA treated	
Protein	% coverage	# peptides	% coverage	# peptides
Brm	16	23	19	26
Mor	29	24	26	26
Osa	9.4	18	9.6	19
Bap111	23	13	28	14
CG12333	38	12	38	12
Bap55	32	10	40	12
Bap60	21	11	26	13
Snr1	24	6	24	6
Reps	13	10	14	11
e(y)3	4.2	7	4.3	7
Polybromo	3.1	5	5.4	9
Bap170	7.4	7	6.8	7
Mars	4.8	4	13	8
l(3)j2D3	7.9	2	13	4
d4	11	5	6.6	4
BCL7-like	19	3	19	3
mod(mdg4)	11	4	11	4
CG7154	7.1	4	7.3	4
KrT95D	3.2	2	4.9	4
ssp	8.7	2	11	3

Table 5: Activation of Notch signaling does not change the composition of SWI/SNF complex in BG3 cells.

Table showing the proteins co-purified with Brm from mock or EDTA treated BG3 cells. Percent coverage based on unique peptides identified with over 95% probability and number of unique peptides are shown.

	Mock treated		EDTA treated	
Protein	% coverage	# peptides	% coverage	# peptides
Mor	36	35	36	35
Brm	23	34	23	34
Osa	17	34	16	32
Bap111	31	20	34	19
Bap60	41	20	33	16
CG2950	24	15	26	16
Bap55	42	13	42	13
Wee	34	13	27	11
d4	17	9	15	9
Snr1	26	7	26	7
Rapgap1	9	6	13	7
BCL7-like	21	4	27	5
Tth	5.4	2	5.4	2

Table 6: Activation of Notch signaling does not change the composition of BAP complex in BG3 cells.

Table showing the proteins co-purified with Osa from mock or EDTA treated BG3 cells. Percent coverage based on unique peptides identified with over 95% probability and number of unique peptides are shown.

DISCUSSION

As demonstrated in the previous Chapter, Osa is ubiquitously expressed in the brain and its expression is not restricted to INPs (Fig.20C). Surprisingly, Osa is not bound to its target loci in the NBs as ChIP-qPCR from *brat* mutant brains that are consisted entirely of type II NBs showed loss of binding (Fig.20D) (Bowman et al., 2008). How then is the imINP specific function of the complex achieved? As a subunit switch in the SWI/SNF complex is thought to trigger the switch from self-renewal to differentiation in mammalian neural stem cell lineages (Lessard et al., 2007; J. I. Wu et al., 2007; 2009; Yoo & Crabtree, 2009) we analyzed the composition of *Drosophila* larval brain SWI/SNF complex to determine whether a similar subunit switch could explain INP specific SWI/SNF complex activity. Our analysis did not identify any binding partner that recapitulates the overproliferation phenotype observed upon loss of SWI/SNF complex function in type II lineages. Since INPs are extremely rare in the larval brain, our analysis might not be sensitive enough to detect a key-binding partner in imINPs. However, it is not possible to perform biochemical studies from purified INPs due to difficulties in obtaining enough starting material. Alternatively, there might be no functional change in the composition of SWI/SNF complex during the transition from the NBs to imINPs. Instead, lack of complex binding in NBs might be a consequence of target loci being occupied in this cell type. Components of the self-renewal program; Dpn, Klu and HLHmγ might simply compete with SWI/SNF for binding sites. This possibility is supported by the known transcriptional repressor activity of these three factors (Bier et al., 1992; Jennings et al., 1994; Klein & Campos-Ortega, 1997) and by the fact that another key Osa target, *opa* is a direct Dpn target in the embryonic CNS (Southall & Brand, 2009). Nevertheless, we identify novel SWI/SNF complex subunits in the *Drosophila* larval brain. As RNAi knockdown of these subunits does not recapitulate the *osa*, *brm*, *mor* and *snr1* RNAi phenotypes, role of these subunits for the complex function remains to be determined.

5.3 EXPERIMENTAL PROCEDURES

5.3.1 *Drosophila* strains

w^{1118}, flytrap line CC00445 (Buszczak et al., 2007), $brat^{K06028}$ (Arama, Dickman, Kimchie, Shearn, & Lev, 2000) were used for affinity purifications.

5.3.2 Co-immunoprecipitation

For the mass spectrometry analysis from the larval brain tissue roughly 180 larval brains were dissected per IP condition. During the dissection brains were kept in ice-cold Rinaldini Solution (KCl 20mg, NaH_2PO_4 5 mg, $NaHCO_3$ 100 mg, Glucose 100mg, NaCl 800 mg). Brains were lysed in 50 µl Low Salt CoIP Buffer (Tris-HCl 50 mM, NaCl 100 mM, MgCl2 10 mM, EDTA 1 mM, DTT, Glycerol 10%, NP-40 0.5%, PMSF, protease inhibitor coctail) with the help of a pestle for homogenization. 200 µl more Low Salt CoIP Buffer was added and the tubes were kept on ice for 10 min. 1 µl Benzonase (Novagen, 70664-3) was added to the lysate to digest nucleases. After the lysis protein concentration was measured using the BCA Protein Assay (Thermo Scientific, 23225) and 1 mg protein extract was used per IP condition. The lysate volume was increased to 1000 µl and the lysate was pre-cleared with 30 µl Protein A Sepharose CL-48 (GE Healthcare, 17-0780-01) (for guinea pig anti-Brm IPs) or 30 µl Protein A Agarose (Roche, 11719408001) beads, rotating for 1 hr at 4^0C. After the pre-clearing samples were centrifuged 1 min at 2000 rpm and the supernatant was transferred to fresh tubes. For Brm pull-down, lysate was incubated with gp Brm (3 µg) overnight at 4°C. Brm antibody blocked with the peptide used to raise the antibody was used as control. Lysates were incubated with 30 µl Protein A Sepharose beads for 1 hr at 4°C and washed 3 times 10 min each with High Salt CoIP buffer (Tris-HCl 50 mM, NaCl 200 mM, MgCl2 10 mM, EDTA 1 mM, DTT, Glycerol 10%, NP-40 0.5%, PMSF, protease inhibitor coctail). For GFP pull-down, lysate was incubated with 20 µl GFP-trap® (Chromotek, gta-20) for 30 min at 4°C. Lysate prepared from w^{1118} flies lacking GFP was used as a control. Samples were washed as described above (NaCl concentration was increased to 300 mM). After the washes, samples were kept at 70°C for 10 min with 30 µl

Laemmli buffer. Samples were run on 3-8% Tris-Acetate Gels (NuPAGE, Invitrogen EA0378) and Silver staining was performed using the Pierce Silver Stain kit.

5.3.3 On bead digestion

Beads were resuspended with 2X bead volume 100 mM NH_4HCO_3. Proteins were predigested with 200ng endoproteinase lys-C (Wako Chemicals, USA) at 37°C for 2 hrs. Elution was performed by addition of 3X bead volume 100 mM glycine, pH 2. Glycine was neutralized with 1M Tris pH 8. To reduce the disulfide bonds samples were incubated with 6.25 mM TCEP-HCl for 30 min at 60°C. Samples were spun and cooled down to room temperature. Alkylation was performed by incubating the samples with 40 mM MMTS for 30 min avoiding light. Peptides were digested with 200 ng trypsin (Trypsin Gold, Promega) overnight at 37°C. Digestion was stopped by 10% TFE.

5.3.4 Nano LC-MS analysis following on bead proteolysis of proteins

The nano HPLC system used was an UltiMate 3000 HPLC RSLC nano system (Thermo Fisher Scientific, Bremen, Germany) coupled to a QExactive mass spectrometer (Thermo Fisher Scientific, Bremen, Germany), equipped with a Proxeon nanospray source (Proxeon, Odense, Denmark). Peptides were loaded onto a trap column (Thermo Fisher Scientific, Bremen, Germany, PepMap C18, 5 mm × 300 μm ID, 5 μm particles, 100 Å pore size) at a flow rate of 25 μL min^{-1} using 0.1% TFA as mobile phase. After 10 min, the trap column was switched in line with the analytical column (Thermo Fisher Scientific, Bremen, Germany, PepMap C18, 500 mm × 75 μm ID, 3 μm, 100 Å). Peptides were eluted using a flow rate of 230 nl min^{-1}, and a binary 3hour gradient, respectively 225 minutes.

The gradient starts with the mobile phases: 98% A (water/formic acid, 99.9/0.1, v/v) and 2% B (water/acetonitrile/formic acid, 19.92/80/0.08, v/v/v) increases to 35%B over the next 180min, followed by a gradient in 5 min to 90%B, stays there for 5 min and decreases in 2 min back to the gradient 98%A and 2%B for equilibration at 30°C for 20 min. The Q Exactive mass spectrometer was operated in data-dependent mode, using a full scan (m/z range 350-1650, nominal resolution of 70 000, target value 1E6) followed by MS/MS scans of the 12 most abundant ions. MS/MS spectra were acquired using normalized collision

energy 30%, isolation width of 2 and the target value was set to 5E4. Precursor ions selected for fragmentation (charge state 2 and higher) were put on a dynamic exclusion list for 10 s. Additionally, the underfill ratio was set to 20% resulting in an intensity threshold of 2e4. The peptide match feature and the exclude isotopes feature were enabled.

5.3.5 Nano LC-MS analysis following in gel digestion of proteins

The nano HPLC system used was an UltiMate 3000 HPLC system (Dionex, Amsterdam, The Netherlands coupled to an LTQ Orbitrap XL mass spectrometer (Thermo Fisher Scientific, Bremen, Germany), equipped with a Proxeon nanospray source (Proxeon, Odense, Denmark). Peptides were loaded onto a trap column (Dionex PepMap C18, 5 mm × 300 μm ID, 5 μm particles, 100 Å pore size) at a flow rate of 25 μL min-1 using 0.1% TFA as mobile phase. After 15 min, the trap column was switched in line with the analytical column (Dionex PepMap C18, 250 mm × 75 μm ID, 3 μm, 100 Å). Peptides were eluted using a flow rate of 275 nl min-1, and a ternary 50 min gradient, with the following mobile phases: A (water/acetonitrile/formic acid, 95/5/0.1, v/v/v), B (water/acetonitrile/formic acid, 70/30/0.08, v/v/v), and C (water/acetonitrile/trifluoroethanol/formic acid, 10/80/10/0.08, v/v/v/v) at 30°C. The LTQ Orbitrap XL was operated in data-dependent mode, using a full scan in the Orbitrap (m/z range 400-1800, nominal resolution of 60 000 at m/z 400, target value 1E6) followed by MS/ MS scans of the five most abundant ions in the linear ion trap. MS/MS spectra (normalized collision energy, 35%; activation value q, 0.25; activation time, 30 ms; isolation width, 3 m/z units, target value 5E4) were acquired and subsequent activation was performed on fragment ions through multistage activation. The neutral loss mass list was therefore set to -98, -49, and -32.6 m/z. Precursor ions selected for fragmentation (charge state 2 and higher) were put on a dynamic exclusion list for 180 s. Additionally, singly-charged parent ions were excluded from selection for MS/MS experiments and the monoisotopic precursor selection feature was enabled.

5.3.6 Data analysis

For peptide identification, the .RAW-files were loaded into Proteome Discoverer (version 1.4.0.288, Thermo Scientific). All hereby created MS/MS spectra were searched using Mascot 2.2.07 (Matrix Science, London, UK) against the flybase sequence database

(28399 sequences; 18526190 residues). The following search parameters were used: Beta-methylthiolation on cysteine was set as a fixed modification and oxidation on methionine was set as variable modification. Monoisotopic masses were searched within unrestricted protein masses for tryptic peptides. The peptide mass tolerance was set to ±5 ppm and the fragment mass tolerance to ±30 mmu. The maximal number of missed cleavages was set to 2. The result was filtered to 1% FDR using Percolator algorithm integrated in Thermo Proteome Discoverer.

5.3.7 Culturing of the BG3 cells and EDTA treatment

ML-DmBG3-c2 cells (stock number 68) were obtained from the Drosophila Genomics Resource Center (DGRC) and cultured in Shields and Sang M3 insect medium (Sigma Aldrich, S3652) supplemented with select yeast extract (Sigma, Y1000), bacto-peptone (Fischer Scientific W1654E), 10% Fetal Calf Serum (PAA Laboratories, A15-104) and 10 µg/ml insulin (Sigma Aldrich, I9278). Cells were passaged every 3-4 days. Media was aspirated and 10 ml fresh media was added onto the cells. Clumps were broken and single cell suspension was achieved by rigorous pipetting. 2-2.5x10^6 cells/ml were transferred in fresh media to a T-75 flask. For the EDTA treatment, 2mM EDTA in PBS was prepared. Old media was aspirated and cells were rinsed with 1X PBS. Cells were incubated at room temperature (RT) with mock or 2mM EDTA for 30 minutes. Afterwards, cells were resuspended and transferred into an eppendorf tube. Cells were spun for 2 min at 2000 rpm and rinsed with 1X PBS (performed twice). RNA was isolated following previously described methods.

6. CHAPTER III: EPIGENETIC PROFILING OF FACS SORTED NEUROBLASTS AND NEURONS

6.1 INTRODUCTION

Growing evidence suggests that changes at the level of chromatin accompany cell fate transitions. Moreover, with the discovery of induced pluripotency it became evident that it is possible to drive cell fate transitions upon expression of key transcription factors (TFs) (Takahashi & Yamanaka, 2006). However, reprogramming of the epigenome is crucial for the efficient binding of these TFs and induction of pluripotent stem cells (Koche et al., 2011; Papp & Plath, 2013), underlining the importance of understanding chromatin states. In the course of lineage progression, lineage-specific genes that are poised and silenced in stem cells are activated, while self-renewal genes are stably silenced to prevent cell fate reversions. In addition to transcriptional networks, an intricate epigenetic network of DNA methylation/demetylation, chromatin remodeling and histone modifications are required to balance self-renewal and differentiation (reviewed in (Coskun, Tsoa, & Sun, 2012)). Polycomb group (PcG) proteins are instrumental for gene silencing in stem cell lineages (Boyer et al., 2006; Coskun et al., 2012; Endoh et al., 2008; T. I. Lee, Jenner, Boyer, Guenther, et al., 2006b). Differentiation genes are trimethylated at histone H3 lysine 27 (H3K27me3) by Polycomb repressive complexes (PRCs) in embryonic stem cells. Loss of PcG proteins causes derepression of their target genes and ESC differentiation (Boyer et al., 2006; Coskun et al., 2012; Endoh et al., 2008; T. I. Lee, Jenner, Boyer, Guenther, et al., 2006b). On the other hand, H3K4me3 mark, catalyzed by trithorax-group proteins is associated with active promoters (Byrd & Shearn, 2003; Wysocka, Myers, Laherty, Eisenman, & Herr, 2003). Interestingly, it was shown that key developmental gene loci in ESCs harbor both H3K4me3 and H3K27me3 mark and denoted as "bivalent domains" (Bernstein et al., 2006). These genes are transcriptionally silenced and are thought to be poised for activation or repression, as they resolve into monovalent markings upon differentiation (Mikkelsen et al., 2007). Surprisingly, such bivalent domains have not been observed in *Drosophila* so far, even though PcG and TrxG proteins exist (Schuettengruber et al., 2009; Voigt, Tee, & Reinberg, 2013). Chromatin state profiling of

adult *Drosophila* male germline stem cells shows that most differentiation genes are either monovalent (marked with H3K4me3 or H3K27me3), or not marked (Gan et al., 2010).

Most of our current knowledge on the epigenetic landscape of stem cells is based on studies in embryonic stem cell cultures. Observing chromatin dynamics in a cell-type specific manner in complex tissues have been challenging due to the need for pure cell population of interest in sufficient quantitites for downstream applications such as chromatin immunoprecipitation or DNA adenine methyltransferase identification (DamID). However, methodologies based on FACS sorting or affinity-based isolation of nuclei have been developed in recent years to overcome these issues.

Neural stem cell lineages of *Drosophila* represent an attractive model system to investigate the chromatin state changes during lineage progression. As described in the first chapter of this thesis, several transcription factors have been identified to maintain self-renewal or induce differentiation in NB lineages. However, chromatin state changes have been elusive due to difficulties in obtaining sufficient material to perform such analysis. Here we describe establishment of a fast and robust methodology to map histone modifications in pure NB and neuron populations.

6.2 RESULTS AND DISCUSSION

6.2.1 ChIP-Seq was successfully performed from limited number of FACS sorted cells

Recently, a FACS sorting protocol was established in our laboratory to isolate pure populations of NBs and neurons. Transcriptional profiles of these cell populations have been determined by RNA-sequencing (Berger et al., 2012; Harzer et al., 2013). However, chromatin states have not been determined. In order to profile the epigenetic landscape of NBs and neurons, a protocol was established to obtain solubilized fragmented chromatin from dissociated larval brains (Fig. 39A). Parameters such as crosslinking of DNA-protein complexes and fragmentation of the chromatin were optimized with 10^5 cells from dissociated larval brains. Fixing the cells with 1% formaldehyde (FA) for 5 minutes followed by micrococcal nuclease (MNase) digestion and brief sonication resulted in efficient fragmentation of the chromatin (Fig. 39B). Additionally, digestion of the chromatin with 5 Units (U) of MNase yielded the best fragment size (Fig. 39C).

To obtain pure populations of NBs and neurons, *ase*-Gal4 line was used to induce the expression of nuclear GFP in type I NBs and their progeny (Fig. 40A). 50,000 NBs and neurons were sorted based on GFP intensity and cell size (Fig. 40B). Conditions described above were employed to prepare fragmented soluble chromatin (Fig. 40C). ChIP was performed using antibodies against H3K4me3 and H3K27me3 and enrichment was tested by qPCR analysis before proceeding with library preparation (Fig. 40D, Fig. 41). Primers were designed for constitutively active genes, intergenic regions and a silenced gene to test whether H3K4me3 and H3K27me3 ChIPs were specific. H3K4me3 ChIP-qPCR detected 3-8% of input in actively transcribed gene loci such as Actin5C and RpL32, while there was no enrichment in intergenic regions, suggesting specific H3K4me3 pull down (Fig. 41A). Similarly, H3K27me3 ChIP-qPCR detected 20-60% of input in silenced AbdB locus, and no signal at actively transcribed Actin5C locus (Fig. 41B). Thus, we conclude that ChIP from limited number of FACS sorted cells successfully enriches for H3K4me3 and H3K27me3 marked loci.

We prepared Illumina sequencing libraries utilizing a protocol adjusted for picogram quantities of DNA (Bowman et al., 2013) and performed single end sequencing.

60-80% of the reads aligned with the *Drosophila* genome. Strand cross correlation analysis revealed the expected fragment size for all the sequencing libraries (Fig. 42). Similarly, analysis of signal enrichment relative to transcription start site showed expected distribution patterns for H3K4me3 and H3K27me3 modifications (Fig. 43), indicating that sequencing was successfully done from limited number of FACS sorted NBs and neurons.

6.2.2 A subset of neural genes is poised for expression in the NBs

As H3K4me3 and H3K27me3 marks correlate well with transcription, we first checked the enrichment of these marks in known NB and neural gene loci. As expected, self-renewal gene loci, such as *grainyhead* (*grh*) showed enrichment for the H3K4me3 modification in NBs, but not in neurons (Fig. 44A). Additionally, these loci are marked with the H3K27me3 modification in neurons, reflecting their transcriptional status (Fig. 44A). Surprisingly, we noticed that enrichment for the H3K4me3 and H3K27me3 marks in neural gene loci did not always fit the expected pattern, as we observed presence of both H3K4me3 and H3K27me3 mark in NBs samples (Fig. 44B). Global analysis revealed 98 genes in NBs that contained both H3K4me3 and H3K27me3 modifications (Supplemental Table 7). A gene ontology (GO) term analysis revealed enrichment for processes such as axon guidance, neuron development and neuron projection morphogenesis (Supplemental Table 8). Indeed 39 out of 98 genes were expressed higher in neurons compared to NBs (log2 fold change > 1.5, false discovery rate < 0.05) (exemplified in Fig. 45A-C, Supplemental Table 9) (Berger et al., 2012), suggesting that there might be a subset of neural genes that are poised in the NBs similar to bivalent domains in mammalian cells.

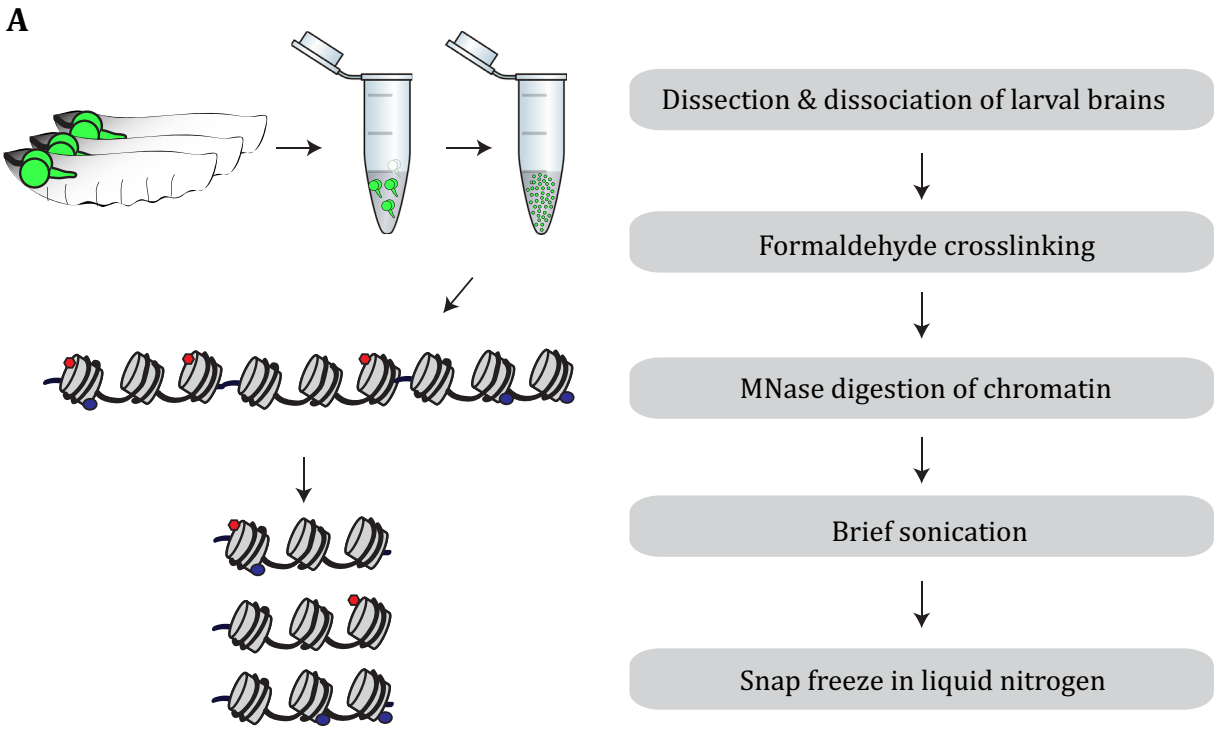
A
Dissection & dissociation of larval brains
Formaldehyde crosslinking
MNase digestion of chromatin
Brief sonication
Snap freeze in liquid nitrogen
B
Duration of crosslinking
1 min
1 min
5 min
5 min
10 min
10 min
seconds
*
110
100
90
80
70
60
50
40
Tip sonication:
+
-
+
-
+
-
C
MNase concentration
0.5 U
1 U
5 U
10 U
20 U
bp
*
7000
2000
1000
600
500
400
300
200
150
100
35

Figure 39: Optimization of chromatin preparation from dissociated larval brain tissue.

(A) *Cartoon illustrating the key steps of chromatin preparation from limited number of cells obtained from dissociated larval brain tissue. Larval brains are dissected and enzymatically dissociated. 10^5 cells are crosslinked with formaldehyde and chromatin is enzymatically digested by MNase treatment. A short pulse of tip sonication is applied to break the nuclear membrane. Chromatin is snap frozen in liquid nitrogen.* ***(B)*** *Electrophoresis image showing the fragment size of DNA resulting from a ranging concentration of MNase treatment. 5U of MNase treatment yields an optimal fragment size around 150 base-pairs (marked with an asterisk).* ***(C)*** *Electrophoresis image showing the fragment size of DNA upon various fixation conditions in the presence or absence of tip sonication. Note that formaldehyde concentration was 1% for each condition and DNA was fragmented with 5U of MNase after fixation. 5 minutes of fixation yielded optimal fragment size (marked with an asterisk). Tip sonication was required to obtain soluble chromatin.*

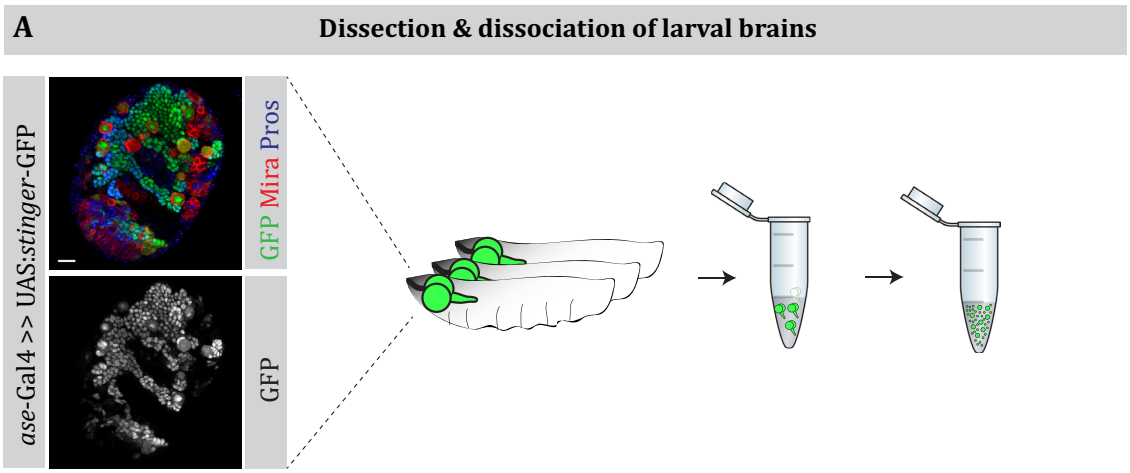
A
Dissection & dissociation of larval brains
ase-Gal4 >> UAS:stinger-GFP
GFP Mira Pros
GFP
B
FACS sort of NBs and neurons
fluorescence
size
NB
neuron
NBs
Neurons
C
Preparation of fragmented chromatin
Formaldehyde crosslinking
MNase digestion of chromatin
Brief sonication
D
ChIP-Seq
Histone mark ChIP
Library preparation
Illumina sequencing

Figure 40: Flow chart showing the steps of ChIP-Seq of histone marks from FACS sorted NBs and neurons.

(A) *Larval brain expressing nuclear GFP in the type I lineages by ase-Gal4 stained for the NB marker Mira and neuronal marker Pros. Larval brains are dissected and enzymatically dissociated.* ***(B)*** *GFP intensity (vertical axis) vs. size (horizontal axis) plot shows a large, highly GFP-positive population that represents NBs and a smaller, less GFP-positive population that represents neurons.* ***(C)*** *50000 FACS sorted NBs or neurons are fixed with formaldehyde. Chromatin is fragmented by micrococcal nuclease treatment, followed by brief sonication.* ***(D)*** *Antibodies against histone marks are used to perform ChIP, followed by library preparation and Illumina sequencing.*

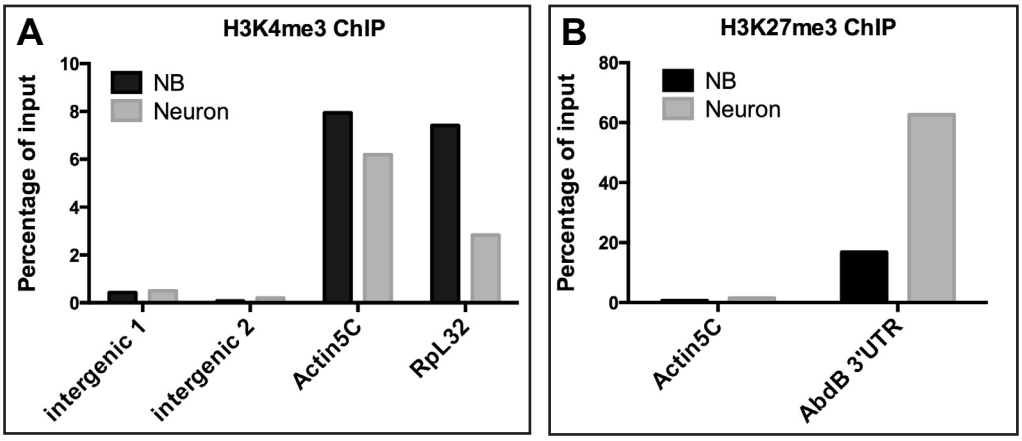

Figure 41: H3K4me3 and H3K27me3 enrichment can be detected in FACS sorted NB/neuron chromatin

(A-B) *ChIP-qPCR analysis of H3K4me3 and H3K27me3 modifications at representative loci.* ***(A)*** *H3K4me3 enrichment at actively transcribed gene loci is presented as percentage of input chromatin. Intergenic regions are used as negative controls.* ***(B)*** *H3K27me3 enrichment can be detected at the 3'UTR of AbdB. Note that AbdB is not expressed in NBs and neurons. Housekeeping gene Act5C is included as a negative control.*

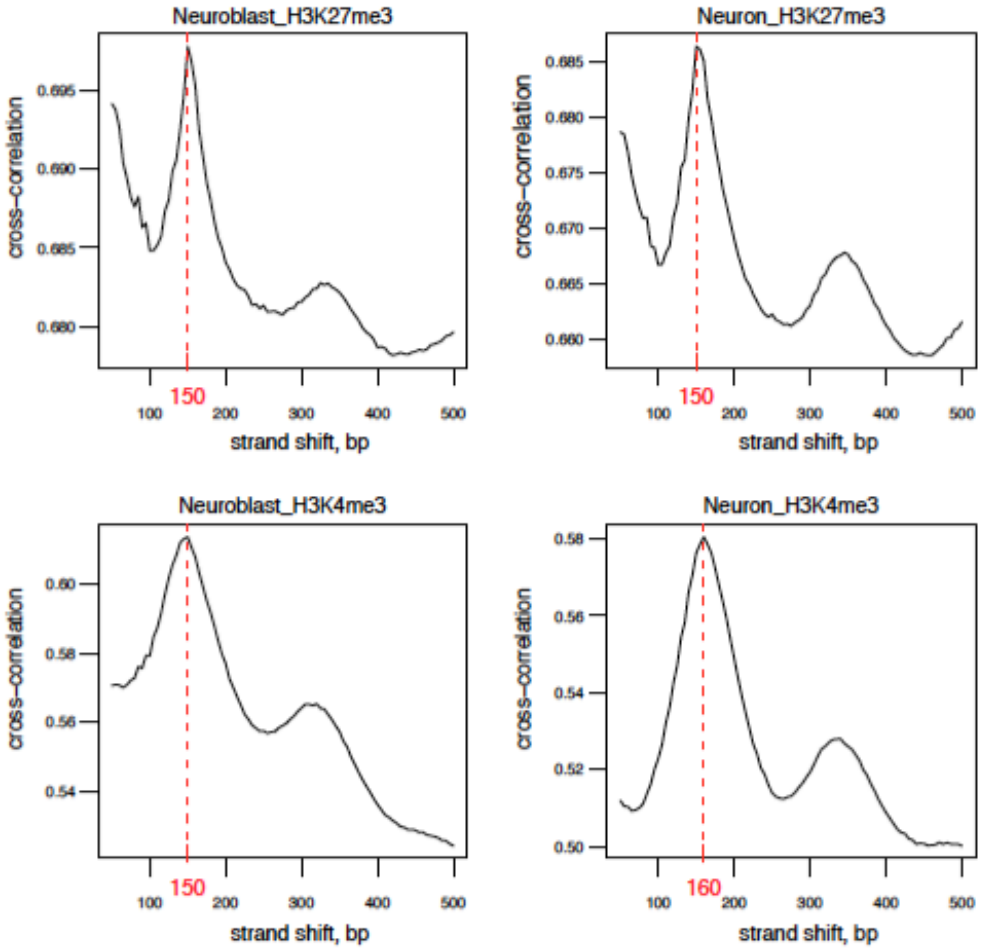

Figure 42: *Strand cross correlation plots show the estimated average length of the sequenced DNA fragments. Highest cross correlation value is observed around 150 base-pairs (indicated by a red dashed line).*

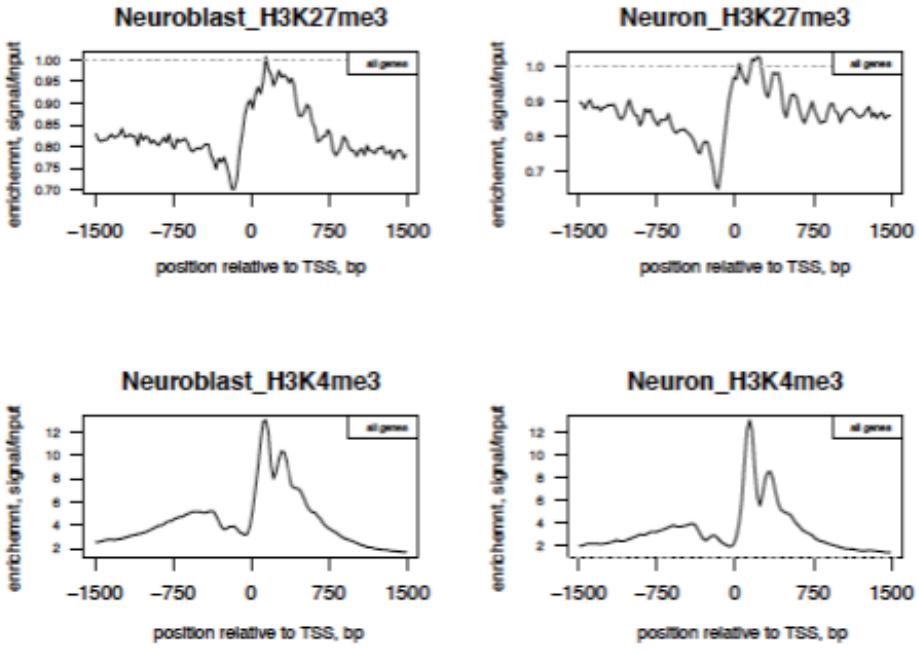

Figure 43: *Plots showing the enrichment of H3K27me3 and H3K4me3 signals relative to the transcription start site (TSS). While the enrichment for the H3K27me3 signal spreads downstream of the TSS, enrichment for the H3K4me3 signal shows bimodal pattern around the TSS for both the NB and neuron samples.*

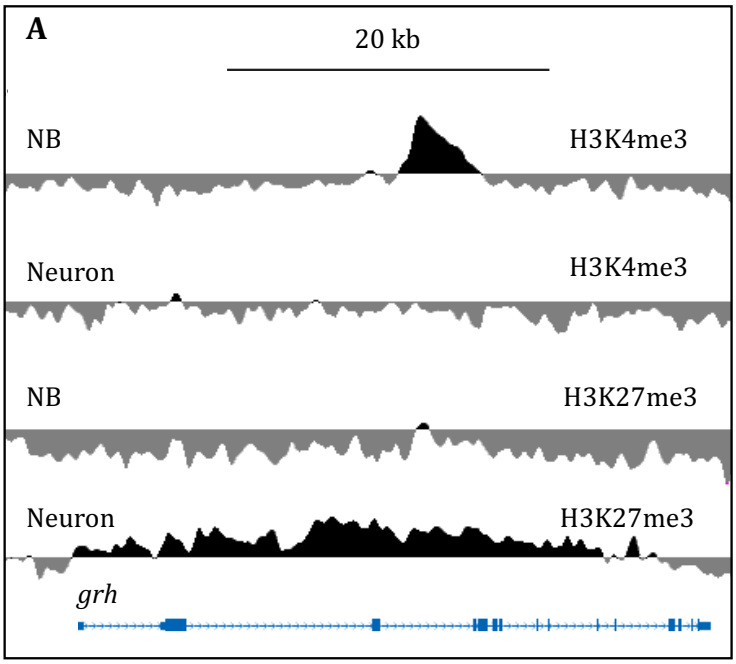

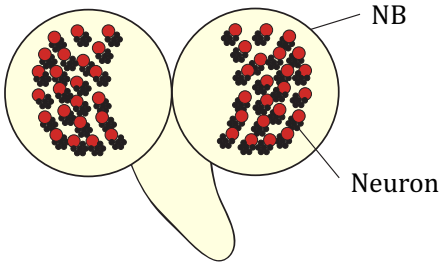

low expression
high expression

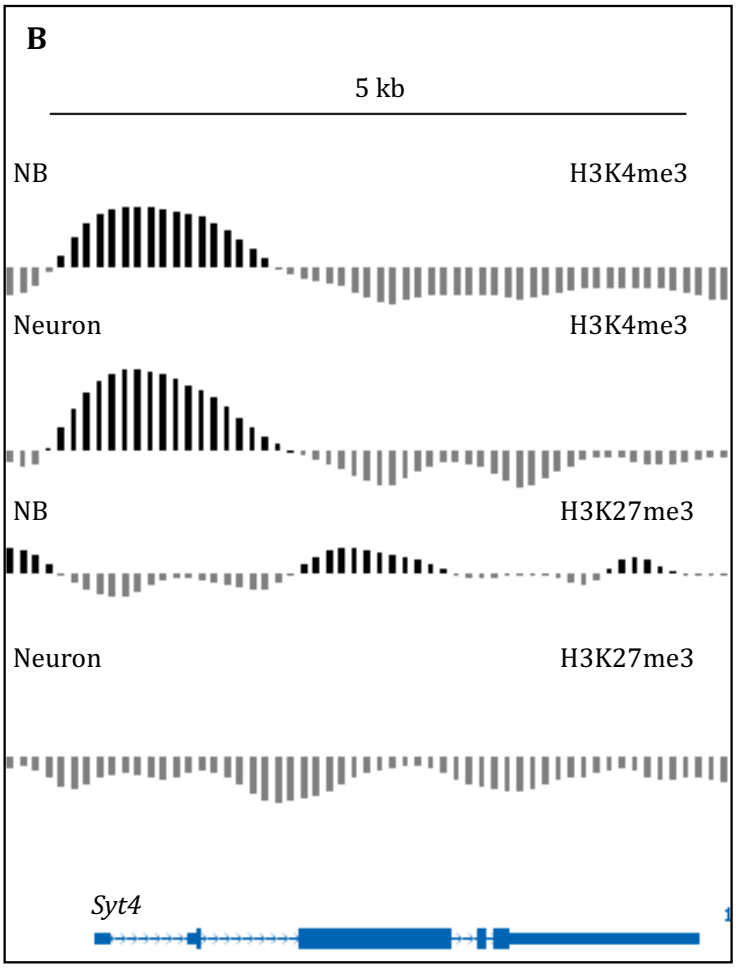

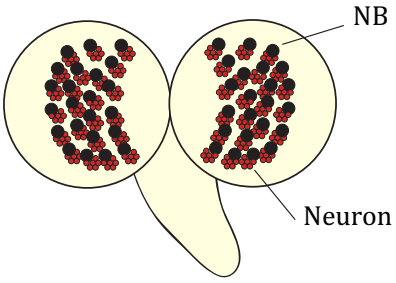

low expression
high expression

Figure 44: Normalized ChIP-Seq reads from H3K4me3 and H3K27me3 pull down (log2 enrichment over input).

(A-B) *grainyhead (grh) locus was selected as a representative NB gene. synaptotagmin IV (sytIV) locus was selected as a representative neural gene.* ***(A)*** *There is H3K4me3 enrichment at the TSS of grh in NBs but not in neurons. H3K27me3 enrichment can be detected over the gene body in neurons but not in NBs. All tracks are set to the same scale (-4 to 5)* ***(B)*** *There is H3K4me3 enrichment at the TSS of the neural gene sytIV both in NBs and neurons. NBs have the repressive mark H3K27me3, while neurons do not.*

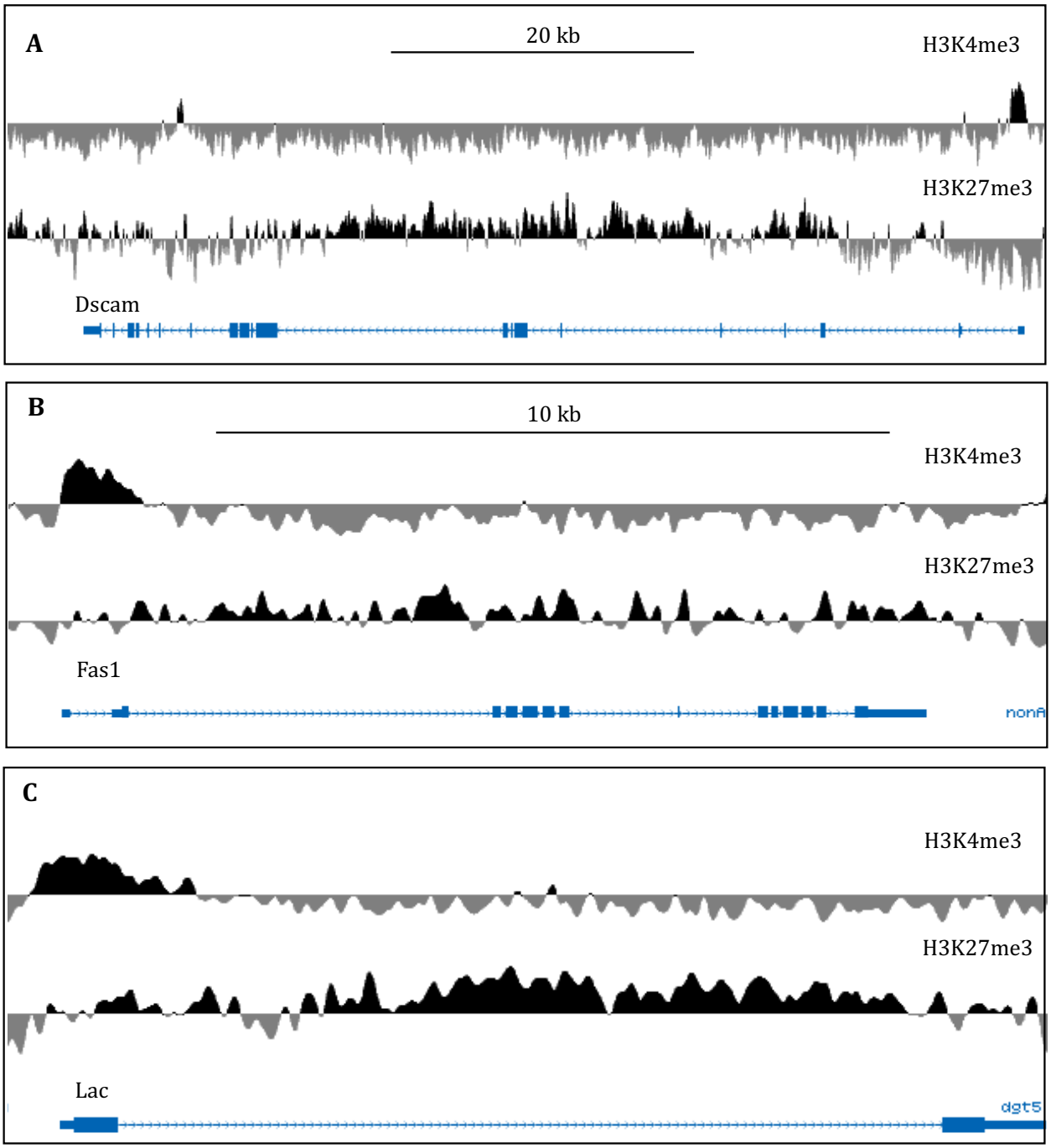

Figure 45: Subset of neural genes is poised in the NBs

(A-C) *Examples of neural genes that show enrichment for both H3K4me3 and H3K27me3 marks in the NBs. Note that only one transcript is shown per gene for simplicity.*

DISCUSSION

Here we describe the successful establishment of a ChIP-Seq protocol from limited number of FACS sorted NBs and neurons. Changes in the chromatin states during the transition from self-renewal to differentiation have been studied in embryonic stem cell cultures (Mikkelsen et al., 2007) (reviewed in (Armstrong, 2012)). However, given the fact that this differentiation event is highly dependent on *in vitro* cues, whether the same principles hold true *in vivo* has been elusive. In fact, a recent paper describes macroscale chromatin state aberrations in cells differentiated *in vitro* compared to the differentiated cells *in vivo* (J. Zhu et al., 2013). FACS sorting of NBs and neurons from dissociated larval brains provide well-defined cell populations to investigate *in vivo* chromatin changes that accompany differentiation. Moreover, this technique can be used to investigate the epigenetic changes in tumor samples, upon loss of the cell fate determinants *brat*, *prospero* or *numb*.

Alternative methods have been described to obtain cell-type specific chromatin profiles (Bonn et al., 2012; Deal & Henikoff, 2011; Henry, Davis, Picard, & Eddy, 2012; Schauer et al., 2013; Southall et al., 2013). A recently described methodology, called targeted DamID (TaDa) was used to analyze the binding pattern of RNA Polymerase II in optic lobe NBs and neuroepithelial cells (Southall et al., 2013). While this technique has the advantage of requiring as few as 10,000 cells, it depends on the expression of a Dam-fusion protein by specific Gal4 lines. Expression of Gal4 protein can perdure in the progeny of the cell of interest, reducing the purity of the sample. Furthermore, DamID has limited resolution due to spreading of targeted methylation. Similarly, a methodology based on isolation of nuclei tagged in a specific cell type (INTACT) has been used to analyze the genome-wide distribution of the H3K4me3, H3K27me3 and H3K27ac marks in kenyon cells and octopaminergic neurons of the adult brain (Henry et al., 2012). However, this technique is so far not applicable at larval stages, as it requires freezing of the animals (Henry et al., 2012). Evidently, majority of the existing protocols require generation of transgenic flies, which can be time consuming.

Preliminary analysis of the genome-wide H3K4me3 and H3K27me3 distributions in NBs reveals presence of domains that show enrichment for both marks (Fig. 46). Surprisingly, expression of 40% of these genes is upregulated in neurons, suggesting that some of the neural genes might be poised in the NBs for rapid activation upon differentiation. Further experiments, such as profiling of RNA Polymerase II binding, will be required to see whether these gene loci are truly poised for transcription. But, what would be the functional relevance of such a phenomenon? So far it has not been possible to specifically ablate binding of the PcG and TrxG proteins at a subset of their target loci to analyze the effect of losing these marks only at bivalent/balanced domains. PcG proteins have been shown to be necessary for the survival of *Drosophila* NBs, as their mutations cause dramatic reduction of proliferation capacity (Bello, Holbro, & Reichert, 2007). Interestingly, we observe loss of poising in *brat* mutant NBs that have a differentiation block (data not shown), suggesting that priming of neural genes might be important for lineage progression. Future experiments will be required to understand the details of such a mechanism.

6.3 EXPERIMENTAL PROCEDURES

6.3.1 Larval brain dissociation and FACS sorting

100 larval brains were dissected in ice-cold PBS and collected in 1 ml cold Rinaldini's solution. Once the dissection was completed, Rinaldini's solution was carefully removed, without disturbing the brains that sunk to the bottom of the low-retention tubes. Brains were dissociated in 500 uL dissociation buffer (50 uL collagenase I (20 mg/ml stock), 50 uL papain (20 mg/ml stock) and 400 uL Rinaldini's solution) for 1 hr at 30C. At the end of the incubation period, brains were washed three times with 500 uL Rinaldini's solution and two times with complete Schneider's media and dissociated by rigorous pipetting in 200 uL complete Schneider's media. The dissociated cell suspension was filtered through a 30 um mesh 5 ml FACS tube and further diluted with Schneider's media up to 500 ul. Cell solution was kept on ice until the FACS sort was started. Cell types of interest were sorted in 2 mL low-retention tubes containing 1400 uL complete Schneider's medium and the temperature was maintained at 4°C.

6.3.2 Preparation of soluble chromatin

Once 50000 cells of interest were sorted, cells were pelleted by centrifuging at 3000 rpm for 10 min. Media was removed without disturbing the pellet and cells were resuspended in 150 uL complete media. 10 uL 16% formaldehyde (FA) was added to fix the cells in a final concentration of 1% FA for 5 min at room temperature. Fixation was ended by adding 25 uL 1 M glycine and 15 uL complete media (final concentration: 125 mM) and incubated for 3 min at room temperature. Cells were centrifuged at 3000 rpm for 10 min and the supernatant was discarded. Cells were resuspended in 100 uL 1X PBS, 0.1 uL $CaCl_2$ (final concentration: 1mM) and 1 uL 10% TritonX-100 (final concentration: 0.1%) and incubated with 5 Units micrococal nuclease (MNase, Worthington Biochemical, LS004798) at 37°C for 3 min. Tube was transferred rapidly on ice and 2.5 uL 0.5 M EDTA, 6.25 uL 0.2 M EGTA and 1.25 uL 1X PBS were added to stop the reaction. The sample volume was adjusted to 300 uL with 1X PBS and the sample was sonicated with a microtip sonicator (Omni-Ruptor 250, Omni International; microtip, power output: 20) for 20 seconds in a

pre-chilled metal holder to prevent overheating of the sample. Following the sonication, the sample was snap frozen in liquid nitrogen.

For the optimization of the conditions, the protocol described above was employed to prepare chromatin from 10^5 dissociated (unsorted) cells. Crosslinking was reversed following the previously described methods and the fragment size was assessed using the Agilent High Sensitivity DNA Assay.

6.3.3 Chromatin immunoprecipitation

Chromatin aliquots were thawed and sample volume was adjusted to 500 uL with 50 uL 10X lysis buffer (1 mM EDTA, 10 mM Tris-HCl pH8, 0.1% Na-Deoxycholate, 0.5% N-lauroylsarcosine, 1% TritonX-100), 140 uL water and 10 uL of 50X complete protease inhibitor. The sample was gently mixed and incubated on ice for 5 min, followed by a centrifuge at maximum speed for 10 min at 4°C. Supernatant was transferred to fresh tubes and 5 uL was saved as input sample (1%) at 4°C. Chromatin was incubated with primary antibodies overnight at 4°C. The sample was incubated with 10 uL Dynabeads Protein A (Invitrogen) for 1 hour at 4°C. The supernatant was removed and sample was washed 6 times with lysis buffer containing 100 mM NaCl and 1% TritonX-100. ChIP DNA was eluted twice with 125 uL fresh elution buffer (0.2% SDS, 0.1M $NaHCO_3$), 5 mM DTT) at 65C for 10 min. The input DNA volume was adjusted to 250 uL with elution buffer. For reversal of crosslinking, samples were supplemented with 1 M Tris-HCl (10 mM final concentration) and 500 mM EDTA (2 mM final concentration). Antibodies used for ChIP were: H3K27me3 (Active Motif, 39155) and H3K4me3 (Millipore 07-473).

6.3.4 Picogram-scale library construction

Library construction was performed as previously described (Bowman et al., 2013). Briefly, ChIP sample volume was adjusted to 37.5 uL and end polishing reaction (50 uL) was performed by incubating the sample with 1X T4 ligase buffer (NEB, Ipswich, MA, USA), 0.4 mM dNTPs, 7.5U T4 Polymerase (NEB), 2.5U Klenow polymerase (NEB), 25U polynucleotide kinase for 30 min at 20°C in a thermocycler. Solid Phase Reversible Immobilization (SPRI) beads (Agencourt AMPure XP, Beckman Coulter) were used at a 1.8X

beads ratio to cleanup the sample. DNA was eluted with 16.5 uL water. A-tailing reaction (25 uL) was performed by incubating 16 uL sample with 1X NEB buffer 2, 0.2 mM dATP, 7.5U Klenow 3'-5' exo minus (NEB) for 30 min at 37°C. SPRI cleanup was performed with 1.8X beads ratio and DNA was eluted with 9.5 uL of water. Adapter ligation reaction (25 uL) was performed by incubating 9 uL of sample with 1X rapid T4 ligase buffer (Enzymatics, Beverly, MA, USA), 0.01 uM annealed universal adapter, 150 U T4 rapid ligase (Enzymatics) for 15 min at room temperature. SPRI cleanup was performed with 1.6X beads ratio and DNA was eluted with 10.5 uL water.

Library amplification was performed by setting up a PCR reaction (50 uL) consisting of 1X Phusion HF master mix (NEB), 0.2 uM universal primer, 0.2 uM barcoded primer, 1X SYBR Green I (Invitrogen), and 0.5 uL Rox (USB). PCR reaction was performed using an Applied Biosystems 7500 Fast Real-Time PCR System. Program used for the thermocycling consisted of an initial denaturing for 30 seconds at 98°C, followed by multiple cycles of 10 seconds denaturation at 98°C, 20 seconds annealing at 64°C, and 45 seconds extension at 72°C. Reactions were terminated at the end of the extension phase, after SYBR green reported reaction kinetics in the log phase for several cycles.

Table 7 List of primers for ChIP-qPCR analysis

Gene	Sequence
intergenic 1 fwd	ACACTGCGAGCGCCTCACACGC
intergenic 1 rev	CCTAGGTGAATGTGCGGCACAC
intergenic 2 fwd	TCAAGCCGAACCCTCTAAAAT
intergenic 2 rev	AACGCCAACAAACAGAAAATG
Actin5C fwd	CGAAGAAGTTGCTGCTCTGGTTGTCG
Actin5C rev	GGACGTCCCACAATCGATGGGAAG
AbdB fwd	AAACTGCATTTGCATCAACG
AbdB rev	GATGAGCAACTGCCCAGAAG
RpL32 fwd	CCACCAGCTTTTTCTTTTCG
RpL32 rev	CACGGACTAACGCAGTTCAA

7. REFERENCES

Abrams, J. M., White, K., Fessler, L. I., & Steller, H. (1993). Programmed cell death during Drosophila embryogenesis. *Development (Cambridge, England)*, *117*(1), 29–43.

Alcantara Llaguno, S., Chen, J., Kwon, C.-H., Jackson, E. L., Li, Y., Burns, D. K., et al. (2009). Malignant astrocytomas originate from neural stem/progenitor cells in a somatic tumor suppressor mouse model. *Cancer Cell*, *15*(1), 45–56. doi:10.1016/j.ccr.2008.12.006

Almeida, M. S., & Bray, S. J. (2005). Regulation of post-embryonic neuroblasts by Drosophila Grainyhead. *Mechanisms of Development*, *122*(12), 1282–1293. doi:10.1016/j.mod.2005.08.004

Anders, S., & Huber, W. (2010). Differential expression analysis for sequence count data. *Genome Biology*, *11*(10), R106. doi:10.1186/gb-2010-11-10-r106

Arama, E., Dickman, D., Kimchie, Z., Shearn, A., & Lev, Z. (2000). Mutations in the beta-propeller domain of the Drosophila brain tumor (brat) protein induce neoplasm in the larval brain. *Oncogene*, *19*(33), 3706–3716. doi:10.1038/sj.onc.1203706

Armstrong, L. (2012). Epigenetic control of embryonic stem cell differentiation. *Stem Cell Reviews*, *8*(1), 67–77. doi:10.1007/s12015-011-9300-4

Atwood, S. X., & Prehoda, K. E. (2009). aPKC phosphorylates Miranda to polarize fate determinants during neuroblast asymmetric cell division. *Current Biology : CB*, *19*(9), 723–729. doi:10.1016/j.cub.2009.03.056

Bailey, T. L. (2005). FITTING A MIXTURE MODEL BY EXPECTATION MAXIMIZATIONTO DISCOVER MOTIFS IN BIOPOLYMERS, 1–33.

Basto, R., Brunk, K., Vinadogrova, T., Peel, N., Franz, A., Khodjakov, A., & Raff, J. W. (2008). Centrosome amplification can initiate tumorigenesis in flies. *Cell*, *133*(6), 1032–1042. doi:10.1016/j.cell.2008.05.039

Baumgardt, M., Karlsson, D., Terriente, J., Díaz-Benjumea, F. J., & Thor, S. (2009). Neuronal subtype specification within a lineage by opposing temporal feed-forward loops. *Cell*, *139*(5), 969–982. doi:10.1016/j.cell.2009.10.032

Bayraktar, O. A., & Doe, C. Q. (2013). Combinatorial temporal patterning in progenitors expands neural diversity. *Nature*, 1–8. doi:10.1038/nature12266

Bello, B. C., Izergina, N., Caussinus, E., & Reichert, H. (2008). Amplification of neural stem cell proliferation by intermediate progenitor cells in Drosophila brain development. *Neural Development*, *3*, 5. doi:10.1186/1749-8104-3-5

Bello, B., Holbro, N., & Reichert, H. (2007). Polycomb group genes are required for neural stem cell survival in postembryonic neurogenesis of Drosophila. *Development (Cambridge, England)*, *134*(6), 1091–1099. doi:10.1242/dev.02793

Bello, B., Reichert, H., & Hirth, F. (2006). The brain tumor gene negatively regulates neural progenitor cell proliferation in the larval central brain of Drosophila. *Development (Cambridge, England)*, *133*(14), 2639–2648. doi:10.1242/dev.02429

Berdnik, D., Török, T., González-Gaitán, M., & Knoblich, J. A. (2002). The endocytic protein alpha-Adaptin is required for numb-mediated asymmetric cell division in Drosophila. *Developmental Cell*, *3*(2), 221–231.

Berger, C., Harzer, H., Burkard, T. R., Steinmann, J., van der Horst, S., Laurenson, A.-S., et al. (2012). FACS purification and transcriptome analysis of drosophila neural stem cells reveals a role for Klumpfuss in self-renewal. *Cell Reports*, *2*(2), 407–418. doi:10.1016/j.celrep.2012.07.008

Bernstein, B. E., Mikkelsen, T. S., Xie, X., Kamal, M., Huebert, D. J., Cuff, J., et al. (2006). A bivalent chromatin structure marks key developmental genes in embryonic stem cells. *Cell*, *125*(2), 315–326. doi:10.1016/j.cell.2006.02.041

Betschinger, J., Mechtler, K., & Knoblich, J. A. (2006). Asymmetric segregation of the tumor

suppressor brat regulates self-renewal in Drosophila neural stem cells. *Cell*, *124*(6), 1241–1253. doi:10.1016/j.cell.2006.01.038

Bhalerao, S., Berdnik, D., Török, T., & Knoblich, J. A. (2005). Localization-dependent and -independent roles of numb contribute to cell-fate specification in Drosophila. *Current Biology : CB*, *15*(17), 1583–1590. doi:10.1016/j.cub.2005.07.061

Bhat, K. M. (1999). Segment polarity genes in neuroblast formation and identity specification during Drosophila neurogenesis. *BioEssays : News and Reviews in Molecular, Cellular and Developmental Biology*, *21*(6), 472–485. doi:10.1002/(SICI)1521-1878(199906)21:6<472::AID-BIES4>3.0.CO;2-W

Bier, E., Vaessin, H., Younger-Shepherd, S., Jan, L. Y., & Jan, Y. N. (1992). deadpan, an essential pan-neural gene in Drosophila, encodes a helix-loop-helix protein similar to the hairy gene product. *Genes & Development*, *6*(11), 2137–2151.

Bonn, S., Zinzen, R. P., Perez-Gonzalez, A., Riddell, A., Gavin, A.-C., & Furlong, E. E. M. (2012). Cell type-specific chromatin immunoprecipitation from multicellular complex samples using BiTS-ChIP. *Nature Protocols*, *7*(5), 978–994. doi:10.1038/nprot.2012.049

Boone, J. Q., & Doe, C. Q. (2008). Identification of Drosophila type II neuroblast lineages containing transit amplifying ganglion mother cells. *Developmental Neurobiology*, *68*(9), 1185–1195. doi:10.1002/dneu.20648

Bork, P., & Margolis, B. (1995). A phosphotyrosine interaction domain. *Cell*, *80*(5), 693–694.

Bowman, S. K., Rolland, V., Betschinger, J., Kinsey, K. A., Emery, G., & Knoblich, J. A. (2008). The tumor suppressors Brat and Numb regulate transit-amplifying neuroblast lineages in Drosophila. *Developmental Cell*, *14*(4), 535–546. doi:10.1016/j.devcel.2008.03.004

Bowman, S. K., Simon, M. D., Deaton, A. M., Tolstorukov, M., Borowsky, M. L., & Kingston, R. E. (2013). Multiplexed Illumina sequencing libraries from picogram quantities of DNA. *BMC Genomics*, *14*, 466. doi:10.1186/1471-2164-14-466

Boyer, L. A., Plath, K., Zeitlinger, J., Brambrink, T., Medeiros, L. A., Lee, T. I., et al. (2006). Polycomb complexes repress developmental regulators in murine embryonic stem cells. *Nature*, *441*(7091), 349–353. doi:10.1038/nature04733

Brand, A. H., & Livesey, F. J. (2011). Neural stem cell biology in vertebrates and invertebrates: more alike than different? *Neuron*, *70*(4), 719–729. doi:10.1016/j.neuron.2011.05.016

Brand, A. H., & Perrimon, N. (1993). Targeted gene expression as a means of altering cell fates and generating dominant phenotypes. *Development (Cambridge, England)*, *118*(2), 401–415.

Brennecke, J., Stark, A., Russell, R. B., & Cohen, S. M. (2005). Principles of microRNA-target recognition. *PLoS Biology*, *3*(3), e85. doi:10.1371/journal.pbio.0030085

Britton, J. S., & Edgar, B. A. (1998). Environmental control of the cell cycle in Drosophila: nutrition activates mitotic and endoreplicative cells by distinct mechanisms. *Development (Cambridge, England)*, *125*(11), 2149–2158.

Bush, A., Hiromi, Y., & Cole, M. (1996). Biparous: a novel bHLH gene expressed in neuronal and glial precursors in Drosophila. *Developmental Biology*, *180*(2), 759–772. doi:10.1006/dbio.1996.0344

Buszczak, M., Paterno, S., Lighthouse, D., Bachman, J., Planck, J., Owen, S., et al. (2007). The carnegie protein trap library: a versatile tool for Drosophila developmental studies. *Genetics*, *175*(3), 1505–1531. doi:10.1534/genetics.106.065961

Byrd, K. N., & Shearn, A. (2003). ASH1, a Drosophila trithorax group protein, is required for methylation of lysine 4 residues on histone H3. *Proceedings of the National Academy of Sciences of the United States of America*, *100*(20), 11535–11540. doi:10.1073/pnas.1933593100

Campbell, S. D., Sprenger, F., Edgar, B. A., & O'Farrell, P. H. (1995). Drosophila Wee1 kinase rescues fission yeast from mitotic catastrophe and phosphorylates Drosophila Cdc2 in vitro. *Molecular Biology of the Cell*, *6*(10), 1333–1347.

Campos-Ortega, J. A. (1994). Genetic mechanisms of early neurogenesis in Drosophila

melanogaster. *Journal of Physiology, Paris*, *88*(2), 111–122.
Carney, T. D., Miller, M. R., Robinson, K. J., Bayraktar, O. A., Osterhout, J. A., & Doe, C. Q. (2012). Functional genomics identifies neural stem cell sub-type expression profiles and genes regulating neuroblast homeostasis. *Developmental Biology*, *361*(1), 137–146. doi:10.1016/j.ydbio.2011.10.020
Castellanos, E., Dominguez, P., & Gonzalez, C. (2008). Centrosome dysfunction in Drosophila neural stem cells causes tumors that are not due to genome instability. *Current Biology : CB*, *18*(16), 1209–1214. doi:10.1016/j.cub.2008.07.029
Caussinus, E., & Gonzalez, C. (2005). Induction of tumor growth by altered stem-cell asymmetric division in Drosophila melanogaster. *Nature Genetics*, *37*(10), 1125–1129. doi:10.1038/ng1632
Cayouette, M., Mattar, P., & Harris, W. A. (2013). Progenitor competence: genes switching places. *Cell*, *152*(1-2), 13–14. doi:10.1016/j.cell.2012.12.038
Ceron, J., Tejedor, F. J., & Moya, F. (2006). A primary cell culture of Drosophila postembryonic larval neuroblasts to study cell cycle and asymmetric division. *European Journal of Cell Biology*, *85*(6), 567–575. doi:10.1016/j.ejcb.2006.02.006
Chabu, C., & Doe, C. Q. (2009). Developmental Biology. *Developmental Biology*, *330*(2), 399–405. doi:10.1016/j.ydbio.2009.04.014
Chalkley, G. E., Moshkin, Y. M., Langenberg, K., Bezstarosti, K., Blastyak, A., Gyurkovics, H., et al. (2008). The transcriptional coactivator SAYP is a trithorax group signature subunit of the PBAP chromatin remodeling complex. *Molecular and Cellular Biology*, *28*(9), 2920–2929. doi:10.1128/MCB.02217-07
Chell, J. M., & Brand, A. H. (2010). Nutrition-responsive glia control exit of neural stem cells from quiescence. *Cell*, *143*(7), 1161–1173. doi:10.1016/j.cell.2010.12.007
Chen, J., Li, Y., Yu, T.-S., McKay, R. M., Burns, D. K., Kernie, S. G., & Parada, L. F. (2012). A restricted cell population propagates glioblastoma growth after chemotherapy. *Nature*, *488*(7412), 522–526. doi:10.1038/nature11287
Chen, S., Wang, S., & Xie, T. (2011). Restricting self-renewal signals within the stem cell niche: multiple levels of control. *Current Opinion in Genetics & Development*, *21*(6), 684–689. doi:10.1016/j.gde.2011.07.008
Choksi, S. P., Southall, T. D., Bossing, T., Edoff, K., de Wit, E., Fischer, B. E., et al. (2006). Prospero acts as a binary switch between self-renewal and differentiation in Drosophila neural stem cells. *Developmental Cell*, *11*(6), 775–789. doi:10.1016/j.devcel.2006.09.015
Chu-LaGraff, Q., Wright, D. M., McNeil, L. K., & Doe, C. Q. (1991). The prospero gene encodes a divergent homeodomain protein that controls neuronal identity in Drosophila. *Development (Cambridge, England)*, *Suppl 2*, 79–85.
Chuikov, S., Levi, B. P., Smith, M. L., & Morrison, S. J. (2010). Prdm16 promotes stem cell maintenance in multiple tissues, partly by regulating oxidative stress. *Nature Cell Biology*, *12*(10), 999–1006. doi:10.1038/ncb2101
Collins, R. T., Furukawa, T., Tanese, N., & Treisman, J. E. (1999). Osa associates with the Brahma chromatin remodeling complex and promotes the activation of some target genes. *The EMBO Journal*, *18*(24), 7029–7040. doi:10.1093/emboj/18.24.7029
Colombani, J., Raisin, S., Pantalacci, S., Radimerski, T., Montagne, J., & Léopold, P. (2003). A nutrient sensor mechanism controls Drosophila growth. *Cell*, *114*(6), 739–749.
Coskun, V., Tsoa, R., & Sun, Y. E. (2012). Epigenetic regulation of stem cells differentiating along the neural lineage. *Current Opinion in Neurobiology*, *22*(5), 762–767. doi:10.1016/j.conb.2012.07.001
Cotton, M., Benhra, N., & Le Borgne, R. (2013). Numb inhibits the recycling of Sanpodo in Drosophila sensory organ precursor. *Current Biology : CB*, *23*(7), 581–587. doi:10.1016/j.cub.2013.02.020
Couturier, L., Mazouni, K., & Schweisguth, F. (2013). Numb localizes at endosomes and controls the endosomal sorting of notch after asymmetric division in Drosophila. *Current Biology : CB*, *23*(7),

588–593. doi:10.1016/j.cub.2013.03.002
Crosby, M. A., Miller, C., Alon, T., Watson, K. L., Verrijzer, C. P., Goldman-Levi, R., & Zak, N. B. (1999). The trithorax group gene moira encodes a brahma-associated putative chromatin-remodeling factor in Drosophila melanogaster. *Molecular and Cellular Biology*, *19*(2), 1159–1170.
Cui, X., De Vivo, I., Slany, R., Miyamoto, A., Firestein, R., & Cleary, M. L. (1998). Association of SET domain and myotubularin-related proteins modulates growth control. *Nature Genetics*, *18*(4), 331–337. doi:10.1038/ng0498-331
Deal, R. B., & Henikoff, S. (2011). The INTACT method for cell type-specific gene expression and chromatin profiling in Arabidopsis thaliana. *Nature Protocols*, *6*(1), 56–68. doi:10.1038/nprot.2010.175
Delidakis, C., & Artavanis-Tsakonas, S. (1992). The Enhancer of split [E(spl)] locus of Drosophila encodes seven independent helix-loop-helix proteins. *Proceedings of the National Academy of Sciences of the United States of America*, *89*(18), 8731–8735.
Dessaud, E., McMahon, A. P., & Briscoe, J. (2008). Pattern formation in the vertebrate neural tube: a sonic hedgehog morphogen-regulated transcriptional network. *Development (Cambridge, England)*, *135*(15), 2489–2503. doi:10.1242/dev.009324
Doe, C. Q., Chu-LaGraff, Q., Wright, D. M., & Scott, M. P. (1991). The prospero gene specifies cell fates in the Drosophila central nervous system. *Cell*, *65*(3), 451–464.
Driessens, G., Beck, B., Caauwe, A., Simons, B. D., & Blanpain, C. (2012). Defining the mode of tumour growth by clonal analysis. *Nature*, *488*(7412), 527–530. doi:10.1038/nature11344
Endo, K., Karim, M. R., Taniguchi, H., Krejcí, A., Kinameri, E., Siebert, M., et al. (2012). Chromatin modification of Notch targets in olfactory receptor neuron diversification. *Nature Neuroscience*, *15*(2), 224–233. doi:10.1038/nn.2998
Endoh, M., Endo, T. A., Endoh, T., Fujimura, Y.-I., Ohara, O., Toyoda, T., et al. (2008). Polycomb group proteins Ring1A/B are functionally linked to the core transcriptional regulatory circuitry to maintain ES cell identity. *Development (Cambridge, England)*, *135*(8), 1513–1524. doi:10.1242/dev.014340
Fukuyama, H., Ndiaye, S., Hoffmann, J., Rossier, J., Liuu, S., Vinh, J., & Verdier, Y. (2012). On-bead tryptic proteolysis: an attractive procedure for LC-MS/MS analysis of the Drosophila caspase 8 protein complex during immune response against bacteria. *Journal of Proteomics*, *75*(15), 4610–4619. doi:10.1016/j.jprot.2012.03.003
Gan, Q., Schones, D. E., Ho Eun, S., Wei, G., Cui, K., Zhao, K., & Chen, X. (2010). Monovalent and unpoised status of most genes in undifferentiated cell-enriched Drosophila testis. *Genome Biology*, *11*(4), R42. doi:10.1186/gb-2010-11-4-r42
Gao, X., Tate, P., Hu, P., Tjian, R., Skarnes, W. C., & Wang, Z. (2008). ES cell pluripotency and germ-layer formation require the SWI/SNF chromatin remodeling component BAF250a. *Proceedings of the National Academy of Sciences of the United States of America*, *105*(18), 6656–6661. doi:10.1073/pnas.0801802105
Gaspard, N., Bouschet, T., Hourez, R., Dimidschstein, J., Naeije, G., van den Ameele, J., et al. (2008). An intrinsic mechanism of corticogenesis from embryonic stem cells. *Nature*, *455*(7211), 351–357. doi:10.1038/nature07287
Gateff, E. (1978). Malignant neoplasms of genetic origin in Drosophila melanogaster. *Science (New York, N.Y.)*, *200*(4349), 1448–1459.
Gonzalez, C. (2013). Drosophila melanogaster: a model and a tool to investigate malignancy and identify new therapeutics. *Nature Reviews. Cancer*, *13*(3), 172–183. doi:10.1038/nrc3461
Grosskortenhaus, R., Robinson, K. J., & Doe, C. Q. (2006). Pdm and Castor specify late-born motor neuron identity in the NB7-1 lineage. *Genes & Development*, *20*(18), 2618–2627. doi:10.1101/gad.1445306
Guidi, C. J., Sands, A. T., Zambrowicz, B. P., Turner, T. K., Demers, D. A., Webster, W., et al. (2001). Disruption of Ini1 leads to peri-implantation lethality and tumorigenesis in mice. *Molecular and*

Cellular Biology, *21*(10), 3598–3603. doi:10.1128/MCB.21.10.3598-3603.2001
Haenfler, J. M., Kuang, C., & Lee, C.-Y. (2012). Cortical aPKC kinase activity distinguishes neural stem cells from progenitor cells by ensuring asymmetric segregation of Numb. *Developmental Biology*, *365*(1), 219–228. doi:10.1016/j.ydbio.2012.02.027
Haley, B., Foys, B., & Levine, M. (2010). Vectors and parameters that enhance the efficacy of RNAi-mediated gene disruption in transgenic Drosophila. *Proceedings of the National Academy of Sciences of the United States of America*, *107*(25), 11435–11440. doi:10.1073/pnas.1006689107
Hargreaves, D. C., & Crabtree, G. R. (2011). ATP-dependent chromatin remodeling: genetics, genomics and mechanisms. *Cell Research*, *21*(3), 396–420. doi:10.1038/cr.2011.32
Harris, R. E., Pargett, M., Sutcliffe, C., Umulis, D., & Ashe, H. L. (2011). Brat Promotes Stem Cell Differentiation via Control of a Bistable Switch that Restricts BMP Signaling. *Developmental Cell*, *20*(1), 72–83. doi:10.1016/j.devcel.2010.11.019
Hartenstein, V., Spindler, S., Pereanu, W., & Fung, S. (2008). The development of the Drosophila larval brain. *Advances in Experimental Medicine and Biology*, *628*, 1–31. doi:10.1007/978-0-387-78261-4_1
Harzer, H., Berger, C., Conder, R., Schmauss, G., & Knoblich, J. A. (2013). FACS purification of Drosophila larval neuroblasts for next-generation sequencing. *Nature Protocols*, *8*(6), 1088–1099. doi:10.1038/nprot.2013.062
Henry, G. L., Davis, F. P., Picard, S., & Eddy, S. R. (2012). Cell type-specific genomics of Drosophila neurons. *Nucleic Acids Research*, *40*(19), 9691–9704. doi:10.1093/nar/gks671
Hirschhorn, J. N., Brown, S. A., Clark, C. D., & Winston, F. (1992). Evidence that SNF2/SWI2 and SNF5 activate transcription in yeast by altering chromatin structure. *Genes & Development*, *6*(12A), 2288–2298.
Ho, L., Miller, E. L., Ronan, J. L., Ho, W. Q., Jothi, R., & Crabtree, G. R. (2011). esBAF facilitates pluripotency by conditioning the genome for LIF/STAT3 signalling and by regulating polycomb function. *Nature Cell Biology*, *13*(8), 903–913. doi:10.1038/ncb2285
Ho, L., Ronan, J. L., Wu, J., Staahl, B. T., Chen, L., Kuo, A., et al. (2009). An embryonic stem cell chromatin remodeling complex, esBAF, is essential for embryonic stem cell self-renewal and pluripotency. *Proceedings of the National Academy of Sciences of the United States of America*, *106*(13), 5181–5186. doi:10.1073/pnas.0812889106
Hohenauer, T., & Moore, A. W. (2012). The Prdm family: expanding roles in stem cells and development. *Development (Cambridge, England)*, *139*(13), 2267–2282. doi:10.1242/dev.070110
Homem, C. C. F., & Knoblich, J. A. (2012). Drosophila neuroblasts: a model for stem cell biology. *Development (Cambridge, England)*, *139*(23), 4297–4310. doi:10.1242/dev.080515
Homem, C. C. F., Reichardt, I., Berger, C., Lendl, T., & Knoblich, J. A. (2013). Long-Term Live Cell Imaging and Automated 4D Analysis of Drosophila Neuroblast Lineages. *PloS One*, *8*(11), e79588. doi:10.1371/journal.pone.0079588
Imbalzano, A. N., Kwon, H., Green, M. R., & Kingston, R. E. (1994). Facilitated binding of TATA-binding protein to nucleosomal DNA. *Nature*, *370*(6489), 481–485. doi:10.1038/370481a0
Isshiki, T., & Doe, C. Q. (2004). Maintaining youth in Drosophila neural progenitors. *Cell Cycle (Georgetown, Tex.)*, *3*(3), 296–299.
Isshiki, T., Pearson, B., Holbrook, S., & Doe, C. Q. (2001). Drosophila neuroblasts sequentially express transcription factors which specify the temporal identity of their neuronal progeny. *Cell*, *106*(4), 511–521.
Jacob, J., Maurange, C., & Gould, A. P. (2008). Temporal control of neuronal diversity: common regulatory principles in insects and vertebrates? *Development (Cambridge, England)*, *135*(21), 3481–3489. doi:10.1242/dev.016931
Jennings, B., Preiss, A., Delidakis, C., & Bray, S. (1994). The Notch signalling pathway is required for Enhancer of split bHLH protein expression during neurogenesis in the Drosophila embryo.

Development (Cambridge, England), *120*(12), 3537–3548.
Johnston, C. A., Hirono, K., Prehoda, K. E., & Doe, C. Q. (2009). Identification of an Aurora-A/PinsLINKER/Dlg spindle orientation pathway using induced cell polarity in S2 cells. *Cell*, *138*(6), 1150–1163. doi:10.1016/j.cell.2009.07.041
Jones, D. T. W., Jäger, N., Kool, M., Zichner, T., Hutter, B., Sultan, M., et al. (2012). Dissecting the genomic complexity underlying medulloblastoma. *Nature*, *488*(7409), 100–105. doi:10.1038/nature11284
Jones, S., Wang, T.-L., Shih, I.-M., Mao, T.-L., Nakayama, K., Roden, R., et al. (2010). Frequent mutations of chromatin remodeling gene ARID1A in ovarian clear cell carcinoma. *Science (New York, N.Y.)*, *330*(6001), 228–231. doi:10.1126/science.1196333
Kadoch, C., Hargreaves, D. C., Hodges, C., Elias, L., Ho, L., Ranish, J., & Crabtree, G. R. (2013). Proteomic and bioinformatic analysis of mammalian SWI/SNF complexes identifies extensive roles in human malignancy. *Nature Genetics*. doi:10.1038/ng.2628
Kambadur, R., Koizumi, K., Stivers, C., Nagle, J., Poole, S. J., & Odenwald, W. F. (1998). Regulation of POU genes by castor and hunchback establishes layered compartments in the Drosophila CNS. *Genes & Development*, *12*(2), 246–260.
Kennison, J. A., & Tamkun, J. W. (1988). Dosage-dependent modifiers of polycomb and antennapedia mutations in Drosophila. *Proceedings of the National Academy of Sciences of the United States of America*, *85*(21), 8136–8140.
Kia, S. K., Gorski, M. M., Giannakopoulos, S., & Verrijzer, C. P. (2008). SWI/SNF mediates polycomb eviction and epigenetic reprogramming of the INK4b-ARF-INK4a locus. *Molecular and Cellular Biology*, *28*(10), 3457–3464. doi:10.1128/MCB.02019-07
Kidder, B. L., Palmer, S., & Knott, J. G. (2009). SWI/SNF-Brg1 regulates self-renewal and occupies core pluripotency-related genes in embryonic stem cells. *Stem Cells (Dayton, Ohio)*, *27*(2), 317–328. doi:10.1634/stemcells.2008-0710
Kim, J. K., Huh, S. O., Choi, H., Lee, K. S., Shin, D., Lee, C., et al. (2001). Srg3, a mouse homolog of yeast SWI3, is essential for early embryogenesis and involved in brain development. *Molecular and Cellular Biology*, *21*(22), 7787–7795. doi:10.1128/MCB.21.22.7787-7795.2001
Klein, T., & Campos-Ortega, J. A. (1997). klumpfuss, a Drosophila gene encoding a member of the EGR family of transcription factors, is involved in bristle and leg development. *Development (Cambridge, England)*, *124*(16), 3123–3134.
Klochendler-Yeivin, A., Fiette, L., Barra, J., Muchardt, C., Babinet, C., & Yaniv, M. (2000). The murine SNF5/INI1 chromatin remodeling factor is essential for embryonic development and tumor suppression. *EMBO Reports*, *1*(6), 500–506. doi:10.1093/embo-reports/kvd129
Knoblich, J. A. (2008). Mechanisms of asymmetric stem cell division. *Cell*, *132*(4), 583–597. doi:10.1016/j.cell.2008.02.007
Knoblich, J. A. (2010). Asymmetric cell division: recent developments and their implications for tumour biology. *Nature Reviews. Molecular Cell Biology*, *11*(12), 849–860. doi:10.1038/nrm3010
Knoblich, J. A., Jan, L. Y., & Jan, Y. N. (1997). The N terminus of the Drosophila Numb protein directs membrane association and actin-dependent asymmetric localization. *Proceedings of the National Academy of Sciences of the United States of America*, *94*(24), 13005–13010.
Knust, E., Schrons, H., Grawe, F., & Campos-Ortega, J. A. (1992). Seven genes of the Enhancer of split complex of Drosophila melanogaster encode helix-loop-helix proteins. *Genetics*, *132*(2), 505–518.
Koche, R. P., Smith, Z. D., Adli, M., Gu, H., Ku, M., Gnirke, A., et al. (2011). Reprogramming factor expression initiates widespread targeted chromatin remodeling. *Cell Stem Cell*, *8*(1), 96–105. doi:10.1016/j.stem.2010.12.001
Kohwi, M., & Doe, C. Q. (2013). Temporal fate specification and neural progenitor competence during development. *Nature Reviews. Neuroscience*, *14*(12), 823–838. doi:10.1038/nrn3618

Kohwi, M., Lupton, J. R., Lai, S.-L., Miller, M. R., & Doe, C. Q. (2013). Developmentally Regulated Subnuclear Genome Reorganization Restricts NeuralProgenitor Competence in Drosophila. *Cell*, *152*(1-2), 97–108. doi:10.1016/j.cell.2012.11.049

Komori, H., Xiao, Q., McCartney, B. M., & Lee, C.-Y. (2013). Brain tumor specifies intermediate progenitor cell identity by attenuating β-catenin/Armadillo activity. *Development (Cambridge, England)*. doi:10.1242/dev.099382

Kraut, R., Chia, W., Jan, L. Y., Jan, Y. N., & Knoblich, J. A. (1996). Role of inscuteable in orienting asymmetric cell divisions in Drosophila. *Nature*, *383*(6595), 50–55. doi:10.1038/383050a0

Krejcí, A., & Bray, S. (2007). Notch activation stimulates transient and selective binding of Su(H)/CSL to target enhancers. *Genes & Development*, *21*(11), 1322–1327. doi:10.1101/gad.424607

Kruger, W., Peterson, C. L., Sil, A., Coburn, C., Arents, G., Moudrianakis, E. N., & Herskowitz, I. (1995). Amino acid substitutions in the structured domains of histones H3 and H4 partially relieve the requirement of the yeast SWI/SNF complex for transcription. *Genes & Development*, *9*(22), 2770–2779.

Kuchinke, U., Grawe, F., & Knust, E. (1998). Control of spindle orientation in Drosophila by the Par-3-related PDZ-domain protein Bazooka. *Current Biology*, *8*(25), 1357–1365.

Kwon, H., Imbalzano, A. N., Khavari, P. A., Kingston, R. E., & Green, M. R. (1994). Nucleosome disruption and enhancement of activator binding by a human SW1/SNF complex. *Nature*, *370*(6489), 477–481. doi:10.1038/370477a0

la Serna, de, I. L., Ohkawa, Y., & Imbalzano, A. N. (2006). Chromatin remodelling in mammalian differentiation: lessons from ATP-dependent remodellers. *Nature Reviews. Genetics*, *7*(6), 461–473. doi:10.1038/nrg1882

Le Borgne, R., Bardin, A., & Schweisguth, F. (2005). The roles of receptor and ligand endocytosis in regulating Notch signaling. *Development (Cambridge, England)*, *132*(8), 1751–1762. doi:10.1242/dev.01789

Lee, C.-Y., Wilkinson, B. D., Siegrist, S. E., Wharton, R. P., & Doe, C. Q. (2006a). Brat is a Miranda cargo protein that promotes neuronal differentiation and inhibits neuroblast self-renewal. *Developmental Cell*, *10*(4), 441–449. doi:10.1016/j.devcel.2006.01.017

Lee, T. I., Jenner, R. G., Boyer, L. A., Guenther, M. G., Levine, S. S., Kumar, R. M., et al. (2006b). Control of developmental regulators by Polycomb in human embryonic stem cells. *Cell*, *125*(2), 301–313. doi:10.1016/j.cell.2006.02.043

Lee, T. I., Johnstone, S. E., & Young, R. A. (2006c). Chromatin immunoprecipitation and microarray-based analysis of protein location. *Nature Protocols*, *1*(2), 729–748. doi:10.1038/nprot.2006.98

Lee, T., & Luo, L. (1999). Mosaic analysis with a repressible cell marker for studies of gene function in neuronal morphogenesis. *Neuron*, *22*(3), 451–461.

Lessard, J. A., & Crabtree, G. R. (2010). Chromatin regulatory mechanisms in pluripotency. *Annual Review of Cell and Developmental Biology*, *26*, 503–532. doi:10.1146/annurev-cellbio-051809-102012

Lessard, J., Wu, J. I., Ranish, J. A., Wan, M., Winslow, M. M., Staahl, B. T., et al. (2007). An essential switch in subunit composition of a chromatin remodeling complex during neural development. *Neuron*, *55*(2), 201–215. doi:10.1016/j.neuron.2007.06.019

Li, L., & Vaessin, H. (2000). Pan-neural Prospero terminates cell proliferation during Drosophila neurogenesis. *Genes & Development*, *14*(2), 147–151.

Li, X., Chen, Z., & Desplan, C. (2013). Temporal patterning of neural progenitors in Drosophila. *Current Topics in Developmental Biology*, *105*, 69–96. doi:10.1016/B978-0-12-396968-2.00003-8

Lickert, H., Takeuchi, J. K., Both, Von, I., Walls, J. R., McAuliffe, F., Adamson, S. L., et al. (2004). Baf60c is essential for function of BAF chromatin remodelling complexes in heart development. *Nature*, *432*(7013), 107–112. doi:10.1038/nature03071

Lin, S., & Lee, T. (2012). Generating neuronal diversity in the Drosophila central nervous system. *Developmental Dynamics : an Official Publication of the American Association of Anatomists*, *241*(1), 57–68. doi:10.1002/dvdy.22739

Liu, C., & Zong, H. (2012). Developmental origins of brain tumors. *Current Opinion in Neurobiology*, *22*(5), 844–849. doi:10.1016/j.conb.2012.04.012

Liu, C., Sage, J. C., Miller, M. R., Verhaak, R. G. W., Hippenmeyer, S., Vogel, H., et al. (2011). Mosaic analysis with double markers reveals tumor cell of origin in glioma. *Cell*, *146*(2), 209–221. doi:10.1016/j.cell.2011.06.014

Livak, K. J., & Schmittgen, T. D. (2001). Analysis of Relative Gene Expression Data Using Real-Time Quantitative PCR and the 2−ΔΔCT Method. *Methods*, *25*(4), 402–408. doi:10.1006/meth.2001.1262

Logie, C., & Peterson, C. L. (1997). Catalytic activity of the yeast SWI/SNF complex on reconstituted nucleosome arrays. *The EMBO Journal*, *16*(22), 6772–6782. doi:10.1093/emboj/16.22.6772

Ma, Y., Niemitz, E. L., Nambu, P. A., Shan, X., Sackerson, C., Fujioka, M., et al. (1998). Gene regulatory functions of Drosophila fish-hook, a high mobility group domain Sox protein. *Mechanisms of Development*, *73*(2), 169–182.

Maurange, C., Cheng, L., & Gould, A. P. (2008). Temporal transcription factors and their targets schedule the end of neural proliferation in Drosophila. *Cell*, *133*(5), 891–902. doi:10.1016/j.cell.2008.03.034

McGuire, S. E., Mao, Z., & Davis, R. L. (2004). Spatiotemporal gene expression targeting with the TARGET and gene-switch systems in Drosophila. *Science's STKE : Signal Transduction Knowledge Environment*, *2004*(220), pl6. doi:10.1126/stke.2202004pl6

Mikkelsen, T. S., Ku, M., Jaffe, D. B., Issac, B., Lieberman, E., Giannoukos, G., et al. (2007). Genome-wide maps of chromatin state in pluripotent and lineage-committed cells. *Nature*, *448*(7153), 553–560. doi:10.1038/nature06008

Mohrmann, L., Langenberg, K., Krijgsveld, J., Kal, A. J., Heck, A. J. R., & Verrijzer, C. P. (2004). Differential targeting of two distinct SWI/SNF-related Drosophila chromatin-remodeling complexes. *Molecular and Cellular Biology*, *24*(8), 3077–3088.

Moore, A. W., Barbel, S., Jan, L. Y., & Jan, Y. N. (2000). A genomewide survey of basic helix-loop-helix factors in Drosophila. *Proceedings of the National Academy of Sciences of the United States of America*, *97*(19), 10436–10441. doi:10.1073/pnas.170301897

Moore, A. W., Jan, L. Y., & Jan, Y.-N. (2002). hamlet, a binary genetic switch between single- and multiple- dendrite neuron morphology. *Science (New York, N.Y.)*, *297*(5585), 1355–1358. doi:10.1126/science.1072387

Moore, A. W., Roegiers, F., Jan, L. Y., & Jan, Y.-N. (2004). Conversion of neurons and glia to external-cell fates in the external sensory organs of Drosophila hamlet mutants by a cousin-cousin cell-type respecification. *Genes & Development*, *18*(6), 623–628. doi:10.1101/gad.1170904

Moshkin, Y. M., Chalkley, G. E., Kan, T. W., Reddy, B. A., Ozgur, Z., van Ijcken, W. F. J., et al. (2012). Remodelers Organize Cellular Chromatin by Counteracting Intrinsic Histone-DNA Sequence Preferences in a Class-Specific Manner. *Molecular and Cellular Biology*, *32*(3), 675–688. doi:10.1128/MCB.06365-11

Moshkin, Y. M., Mohrmann, L., van Ijcken, W. F. J., & Verrijzer, C. P. (2007). Functional differentiation of SWI/SNF remodelers in transcription and cell cycle control. *Molecular and Cellular Biology*, *27*(2), 651–661. doi:10.1128/MCB.01257-06

Mummery-Widmer, J. L., Yamazaki, M., Stoeger, T., Novatchkova, M., Bhalerao, S., Chen, D., et al. (2009). Genome-wide analysis of Notch signalling in Drosophila by transgenic RNAi. *Nature*, *458*(7241), 987–992. doi:10.1038/nature07936

Muraro, N. I., Weston, A. J., Gerber, A. P., Luschnig, S., Moffat, K. G., & Baines, R. A. (2008). Pumilio binds para mRNA and requires Nanos and Brat to regulate sodium current in Drosophila motoneurons. *The Journal of Neuroscience : the Official Journal of the Society for Neuroscience*,

28(9), 2099–2109. doi:10.1523/JNEUROSCI.5092-07.2008
Nabirochkina, E., Simonova, O. B., Mertsalov, I. B., Kulikova, D. A., Ladigina, N. G., Korochkin, L. I., & Buchman, V. L. (2002). Expression pattern of dd4, a sole member of the d4 family of transcription factors in Drosophila melanogaster. *Mechanisms of Development*, *114*(1-2), 119–123.
Naka, H., Nakamura, S., Shimazaki, T., & Okano, H. (2008). Requirement for COUP-TFI and II in the temporal specification of neural stem cells in CNS development. *Nature Neuroscience*, *11*(9), 1014–1023. doi:10.1038/nn.2168
Nakayama, T., Shimojima, T., & Hirose, S. (2012). The PBAP remodeling complex is required for histone H3.3 replacement at chromatin boundaries and for boundary functions. *Development (Cambridge, England)*, *139*(24), 4582–4590. doi:10.1242/dev.083246
Neigeborn, L., & Carlson, M. (1984). Genes affecting the regulation of SUC2 gene expression by glucose repression in Saccharomyces cerevisiae. *Genetics*, *108*(4), 845–858.
Neumüller, R. A., Richter, C., Fischer, A., Novatchkova, M., Neumüller, K. G., & Knoblich, J. A. (2011). Genome-wide analysis of self-renewal in Drosophila neural stem cells by transgenic RNAi. *Cell Stem Cell*, *8*(5), 580–593. doi:10.1016/j.stem.2011.02.022
Nègre, N., Brown, C. D., Ma, L., Bristow, C. A., Miller, S. W., Wagner, U., et al. (2012). A cis-regulatory map of the Drosophila genome. *Nature*, *471*(7339), 527–531. doi:10.1038/nature09990
Northcott, P. A., Jones, D. T. W., Kool, M., Robinson, G. W., Gilbertson, R. J., Cho, Y.-J., et al. (2012). Medulloblastomics: the end of the beginning. *Nature Reviews. Cancer*, *12*(12), 818–834. doi:10.1038/nrc3410
Nybakken, K., Vokes, S. A., Lin, T.-Y., McMahon, A. P., & Perrimon, N. (2005). A genome-wide RNA interference screen in Drosophila melanogaster cells for new components of the Hh signaling pathway. *Nature Genetics*, *37*(12), 1323–1332. doi:10.1038/ng1682
Ogawa, H., Ohta, N., Moon, W., & Matsuzaki, F. (2009). Protein phosphatase 2A negatively regulates aPKC signaling by modulating phosphorylation of Par-6 in Drosophila neuroblast asymmetric divisions. *Journal of Cell Science*, *122*(Pt 18), 3242–3249. doi:10.1242/jcs.050955
Owen-Hughes, T., Utley, R. T., Côté, J., Peterson, C. L., & Workman, J. L. (1996). Persistent site-specific remodeling of a nucleosome array by transient action of the SWI/SNF complex. *Science (New York, N.Y.)*, *273*(5274), 513–516.
Papp, B., & Plath, K. (2013). Epigenetics of reprogramming to induced pluripotency. *Cell*, *152*(6), 1324–1343. doi:10.1016/j.cell.2013.02.043
Parsons, D. W., Li, M., Zhang, X., Jones, S., Leary, R. J., Lin, J. C.-H., et al. (2011). The genetic landscape of the childhood cancer medulloblastoma. *Science (New York, N.Y.)*, *331*(6016), 435–439. doi:10.1126/science.1198056
Peterson, C., Carney, G. E., Taylor, B. J., & White, K. (2002). reaper is required for neuroblast apoptosis during Drosophila development. *Development (Cambridge, England)*, *129*(6), 1467–1476.
Petronczki, M., & Knoblich, J. A. (2001). DmPAR-6 directs epithelial polarity and asymmetric cell division of neuroblasts in Drosophila. *Nature Cell Biology*, *3*(1), 43–49. doi:10.1038/35050550
Petruk, S., Sedkov, Y., Smith, S., Tillib, S., Kraevski, V., Nakamura, T., et al. (2001). Trithorax and dCBP acting in a complex to maintain expression of a homeotic gene. *Science (New York, N.Y.)*, *294*(5545), 1331–1334. doi:10.1126/science.1065683
Pfeiffer, B. D., Jenett, A., Hammonds, A. S., Ngo, T.-T. B., Misra, S., Murphy, C., et al. (2008). Tools for neuroanatomy and neurogenetics in Drosophila. *Proceedings of the National Academy of Sciences of the United States of America*, *105*(28), 9715–9720. doi:10.1073/pnas.0803697105
Phelan, M. L., Sif, S., Narlikar, G. J., & Kingston, R. E. (1999). Reconstitution of a core chromatin remodeling complex from SWI/SNF subunits. *Molecular Cell*, *3*(2), 247–253.
Pinheiro, I., Margueron, R., Shukeir, N., Eisold, M., Fritzsch, C., Richter, F. M., et al. (2012). Prdm3 and Prdm16 are H3K9me1 methyltransferases required for mammalian heterochromatin integrity.

Cell, *150*(5), 948–960. doi:10.1016/j.cell.2012.06.048
Price, D., Rabinovitch, S., O'Farrell, P. H., & Campbell, S. D. (2000). Drosophila wee1 has an essential role in the nuclear divisions of early embryogenesis. *Genetics*, *155*(1), 159–166.
Rand, M. D., Grimm, L. M., Artavanis-Tsakonas, S., Patriub, V., Blacklow, S. C., Sklar, J., & Aster, J. C. (2000). Calcium depletion dissociates and activates heterodimeric notch receptors. *Molecular and Cellular Biology*, *20*(5), 1825–1835.
Rebollo, E., Roldán, M., & Gonzalez, C. (2009). Spindle alignment is achieved without rotation after the first cell cycle in Drosophila embryonic neuroblasts. *Development (Cambridge, England)*, *136*(20), 3393–3397. doi:10.1242/dev.041822
Reichert, H. (2011). Drosophila neural stem cells: cell cycle control of self-renewal, differentiation, and termination in brain development. *Results and Problems in Cell Differentiation*, *53*, 529–546. doi:10.1007/978-3-642-19065-0_21
Rhyu, M. S., Jan, L. Y., & Jan, Y. N. (1994). Asymmetric distribution of numb protein during division of the sensory organ precursor cell confers distinct fates to daughter cells. *Cell*, *76*(3), 477–491.
Richter, C., Oktaba, K., Steinmann, J., Müller, J., & Knoblich, J. A. (2011). The tumour suppressor L(3)mbt inhibits neuroepithelial proliferation and acts on insulator elements. *Nature Cell Biology*, *13*(9), 1029–1039. doi:10.1038/ncb2306
Roberts, C. W. M., & Orkin, S. H. (2004). The SWI/SNF complex--chromatin and cancer. *Nature Reviews. Cancer*, *4*(2), 133–142. doi:10.1038/nrc1273
Ronan, J. L., Wu, W., & Crabtree, G. R. (2013). From neural development to cognition: unexpected roles for chromatin. *Nature Reviews. Genetics*, *14*(5), 347–359. doi:10.1038/nrg3413
San-Juán, B. P., & Baonza, A. (2011). The bHLH factor deadpan is a direct target of Notch signaling and regulates neuroblast self-renewal in Drosophila. *Developmental Biology*, *352*(1), 70–82. doi:10.1016/j.ydbio.2011.01.019
Schaefer, M., Shevchenko, A., Shevchenko, A., & Knoblich, J. A. (2000). A protein complex containing Inscuteable and the Galpha-binding protein Pins orients asymmetric cell divisions in Drosophila. *Current Biology*, *10*(7), 353–362.
Schauer, T., Schwalie, P. C., Handley, A., Margulies, C. E., Flicek, P., & Ladurner, A. G. (2013). CAST-ChIP Maps Cell-Type-Specific Chromatin States in the Drosophila Central Nervous System. *Cell Reports*, *5*(1), 271–282. doi:10.1016/j.celrep.2013.09.001
Schepers, A. G., Snippert, H. J., Stange, D. E., van den Born, M., van Es, J. H., van de Wetering, M., & Clevers, H. (2012). Lineage tracing reveals Lgr5+ stem cell activity in mouse intestinal adenomas. *Science (New York, N.Y.)*, *337*(6095), 730–735. doi:10.1126/science.1224676
SCHNITZLER, G. R., Sif, S., & Kingston, R. E. (1998). A Model for Chromatin Remodeling by the SWI/SNF Family. *Cold Spring Harbor Symposia on Quantitative Biology*, *63*(0), 535–544. doi:10.1101/sqb.1998.63.535
Schober, M., Schaefer, M., & Knoblich, J. A. (1999). Bazooka recruits Inscuteable to orient asymmetric cell divisions in Drosophila neuroblasts. *Nature*, *402*(6761), 548–551. doi:10.1038/990135
Schuettengruber, B., Ganapathi, M., Leblanc, B., Portoso, M., Jaschek, R., Tolhuis, B., et al. (2009). Functional anatomy of polycomb and trithorax chromatin landscapes in Drosophila embryos. *PLoS Biology*, *7*(1), e13. doi:10.1371/journal.pbio.1000013
Schüller, U., Heine, V. M., Mao, J., Kho, A. T., Dillon, A. K., Han, Y.-G., et al. (2008). Acquisition of granule neuron precursor identity is a critical determinant of progenitor cell competence to form Shh-induced medulloblastoma. *Cancer Cell*, *14*(2), 123–134. doi:10.1016/j.ccr.2008.07.005
Schwitalla, S., Fingerle, A. A., Cammareri, P., Nebelsiek, T., Göktuna, S. I., Ziegler, P. K., et al. (2013). Intestinal tumorigenesis initiated by dedifferentiation and acquisition of stem-cell-like properties. *Cell*, *152*(1-2), 25–38. doi:10.1016/j.cell.2012.12.012
Shain, A. H., & Pollack, J. R. (2013). The spectrum of SWI/SNF mutations, ubiquitous in human

cancers. *PloS One*, *8*(1), e55119. doi:10.1371/journal.pone.0055119
Shen, Q., Wang, Y., Dimos, J. T., Fasano, C. A., Phoenix, T. N., Lemischka, I. R., et al. (2006). The timing of cortical neurogenesis is encoded within lineages of individual progenitor cells. *Nature Neuroscience*, *9*(6), 743–751. doi:10.1038/nn1694
Shevchenko, A., Tomas, H., Havlis, J., Olsen, J. V., & Mann, M. (2006). In-gel digestion for mass spectrometric characterization of proteins and proteomes. *Nature Protocols*, *1*(6), 2856–2860. doi:10.1038/nprot.2006.468
Siegrist, S. E., & Doe, C. Q. (2005). Microtubule-induced Pins/Galphai cortical polarity in Drosophila neuroblasts. *Cell*, *123*(7), 1323–1335. doi:10.1016/j.cell.2005.09.043
Siller, K. H., & Doe, C. Q. (2008). Lis1/dynactin regulates metaphase spindle orientation in Drosophila neuroblasts. *Developmental Biology*, *319*(1), 1–9. doi:10.1016/j.ydbio.2008.03.018
Siller, K. H., Cabernard, C., & Doe, C. Q. (2006). The NuMA-related Mud protein binds Pins and regulates spindle orientation in Drosophila neuroblasts. *Nature Cell Biology*, *8*(6), 594–600. doi:10.1038/ncb1412
Simons, B. D., & Clevers, H. (2011). Strategies for homeostatic stem cell self-renewal in adult tissues. *Cell*, *145*(6), 851–862. doi:10.1016/j.cell.2011.05.033
Slack, F. J., & Ruvkun, G. (1998). A novel repeat domain that is often associated with RING finger and B-box motifs. *Trends in Biochemical Sciences*, *23*(12), 474–475.
Smith, C. A., Lau, K. M., Rahmani, Z., Dho, S. E., Brothers, G., She, Y. M., et al. (2007). aPKC-mediated phosphorylation regulates asymmetric membrane localization of the cell fate determinant Numb. *The EMBO Journal*, *26*(2), 468–480. doi:10.1038/sj.emboj.7601495
Song, Y., & Lu, B. (2011). Regulation of cell growth by Notch signaling and its differential requirement in normal vs. tumor-forming stem cells in Drosophila. *Genes & Development*, *25*(24), 2644–2658. doi:10.1101/gad.171959.111
Song, Y., & Lu, B. (2012). Interaction of Notch signaling modulator Numb with α-Adaptin regulates endocytosis of Notch pathway components and cell fate determination of neural stem cells. *Journal of Biological Chemistry*, *287*(21), 17716–17728. doi:10.1074/jbc.M112.360719
Sonoda, J., & Wharton, R. P. (2001). Drosophila Brain Tumor is a translational repressor. *Genes & Development*, *15*(6), 762–773. doi:10.1101/gad.870801
Sousa-Nunes, R., & Somers, W. G. (2010). Phosphorylation and dephosphorylation events allow for rapid segregation of fate determinants during Drosophila neuroblast asymmetric divisions. *Communicative & Integrative Biology*, *3*(1), 46–49.
Sousa-Nunes, R., Chia, W., & Somers, W. G. (2009). Protein phosphatase 4 mediates localization of the Miranda complex during Drosophila neuroblast asymmetric divisions. *Genes & Development*, *23*(3), 359–372. doi:10.1101/gad.1723609
Sousa-Nunes, R., Yee, L. L., & Gould, A. P. (2011). Fat cells reactivate quiescent neuroblasts via TOR and glial insulin relays in Drosophila. *Nature*, *471*(7339), 508–512. doi:10.1038/nature09867
Southall, T. D., & Brand, A. H. (2009). Neural stem cell transcriptional networks highlight genes essential for nervous system development. *The EMBO Journal*, *28*(24), 3799–3807. doi:10.1038/emboj.2009.309
Southall, T. D., Gold, K. S., Egger, B., Davidson, C. M., Caygill, E. E., Marshall, O. J., & Brand, A. H. (2013). Cell-Type-Specific Profiling of Gene Expression and Chromatin Binding without Cell Isolation: Assaying RNA Pol II Occupancy in Neural Stem Cells. *Developmental Cell*. doi:10.1016/j.devcel.2013.05.020
Sprang, S. R. (1997). G protein mechanisms: insights from structural analysis. *Annual Review of Biochemistry*, *66*, 639–678. doi:10.1146/annurev.biochem.66.1.639
Staahl, B. T., Tang, J., Wu, W., Sun, A., Gitler, A. D., Yoo, A. S., & Crabtree, G. R. (2013). Kinetic Analysis of npBAF to nBAF Switching Reveals Exchange of SS18 with CREST and Integration with Neural Developmental Pathways. *The Journal of Neuroscience : the Official Journal of the Society for Neuroscience*, *33*(25), 10348–10361. doi:10.1523/JNEUROSCI.1258-13.2013

Stern, M., Jensen, R., & Herskowitz, I. (1984). Five SWI genes are required for expression of the HO gene in yeast. *Journal of Molecular Biology*, *178*(4), 853–868.

Sudarsanam, P., Iyer, V. R., Brown, P. O., & Winston, F. (2000). Whole-genome expression analysis of snf/swi mutants of Saccharomyces cerevisiae. *Proceedings of the National Academy of Sciences of the United States of America*, *97*(7), 3364–3369. doi:10.1073/pnas.050407197

Suzuki, A., & Ohno, S. (2006). The PAR-aPKC system: lessons in polarity. *Journal of Cell Science*, *119*(Pt 6), 979–987. doi:10.1242/jcs.02898

Takahashi, K., & Yamanaka, S. (2006). Induction of pluripotent stem cells from mouse embryonic and adult fibroblast cultures by defined factors. *Cell*, *126*(4), 663–676. doi:10.1016/j.cell.2006.07.024

Tamkun, J. W., Deuring, R., Scott, M. P., Kissinger, M., Pattatucci, A. M., Kaufman, T. C., & Kennison, J. A. (1992). brahma: a regulator of Drosophila homeotic genes structurally related to the yeast transcriptional activator SNF2/SWI2. *Cell*, *68*(3), 561–572.

Tio, M., Udolph, G., Yang, X., & Chia, W. (2001). cdc2 links the Drosophila cell cycle and asymmetric division machineries. *Nature*, *409*(6823), 1063–1067. doi:10.1038/35059124

Touma, J. J., Weckerle, F. F., & Cleary, M. D. (2012). Drosophila Polycomb complexes restrict neuroblast competence to generate motoneurons. *Development (Cambridge, England)*, *139*(4), 657–666. doi:10.1242/dev.071589

Towbin, B. D., González-Aguilera, C., Sack, R., Gaidatzis, D., Kalck, V., Meister, P., et al. (2012). Step-wise methylation of histone H3K9 positions heterochromatin at the nuclear periphery. *Cell*, *150*(5), 934–947. doi:10.1016/j.cell.2012.06.051

Treisman, J. E., Luk, A., Rubin, G. M., & Heberlein, U. (1997). eyelid antagonizes wingless signaling during Drosophila development and has homology to the Bright family of DNA-binding proteins. *Genes & Development*, *11*(15), 1949–1962.

Truman, J. W., & Bate, M. (1988). Spatial and temporal patterns of neurogenesis in the central nervous system of Drosophila melanogaster. *Developmental Biology*, *125*(1), 145–157.

Tsuji, T., Hasegawa, E., & Isshiki, T. (2008). Neuroblast entry into quiescence is regulated intrinsically by the combined action of spatial Hox proteins and temporal identity factors. *Development (Cambridge, England)*, *135*(23), 3859–3869. doi:10.1242/dev.025189

Tulina, N., & Matunis, E. (2001). Control of stem cell self-renewal in Drosophila spermatogenesis by JAK-STAT signaling. *Science (New York, N.Y.)*, *294*(5551), 2546–2549. doi:10.1126/science.1066700

Tuoc, T. C., Boretius, S., Sansom, S. N., Pitulescu, M.-E., Frahm, J., Livesey, F. J., & Stoykova, A. (2013). Chromatin Regulation by BAF170 Controls Cerebral Cortical Size and Thickness. *Developmental Cell*, *25*(3), 256–269. doi:10.1016/j.devcel.2013.04.005

Udolph, G. (2012). Notch signaling and the generation of cell diversity in Drosophila neuroblast lineages. *Advances in Experimental Medicine and Biology*, *727*, 47–60. doi:10.1007/978-1-4614-0899-4_4

Uemura, T., Shepherd, S., Ackerman, L., Jan, L. Y., & Jan, Y. N. (1989). numb, a gene required in determination of cell fate during sensory organ formation in Drosophila embryos. *Cell*, *58*(2), 349–360.

Vaessin, H., Grell, E., Wolff, E., Bier, E., Jan, L. Y., & Jan, Y. N. (1991). prospero is expressed in neuronal precursors and encodes a nuclear protein that is involved in the control of axonal outgrowth in Drosophila. *Cell*, *67*(5), 941–953.

Versteege, I., Sévenet, N., Lange, J., Rousseau-Merck, M. F., Ambros, P., Handgretinger, R., et al. (1998). Truncating mutations of hSNF5/INI1 in aggressive paediatric cancer. *Nature*, *394*(6689), 203–206. doi:10.1038/28212

Vert, J.-P., Foveau, N., Lajaunie, C., & Vandenbrouck, Y. (2006). An accurate and interpretable model for siRNA efficacy prediction. *BMC Bioinformatics*, *7*, 520. doi:10.1186/1471-2105-7-520

Visvader, J. E. (2011). Cells of origin in cancer. *Nature*, *469*(7330), 314–322.

doi:10.1038/nature09781
Voigt, P., Tee, W.-W., & Reinberg, D. (2013). A double take on bivalent promoters. *Genes & Development*, *27*(12), 1318–1338. doi:10.1101/gad.219626.113
Wang, C., Chang, K. C., Somers, G., Virshup, D., Ang, B. T., Tang, C., et al. (2009). Protein phosphatase 2A regulates self-renewal of Drosophila neural stem cells. *Development (Cambridge, England)*, *136*(13), 2287–2296. doi:10.1242/dev.035758
Wang, H., Ouyang, Y., Somers, W. G., Chia, W., & Lu, B. (2007). Polo inhibits progenitor self-renewal and regulates Numb asymmetry by phosphorylating Pon. *Nature*, *449*(7158), 96–100. doi:10.1038/nature06056
Wang, H., Somers, G. W., Bashirullah, A., Heberlein, U., Yu, F., & Chia, W. (2006). Aurora-A acts as a tumor suppressor and regulates self-renewal of Drosophila neuroblasts. *Genes & Development*, *20*(24), 3453–3463. doi:10.1101/gad.1487506
Wang, X., Nagl, N. G., Flowers, S., Zweitzig, D., Dallas, P. B., & Moran, E. (2004). Expression of p270 (ARID1A), a component of human SWI/SNF complexes, in human tumors. *International Journal of Cancer. Journal International Du Cancer*, *112*(4), 636. doi:10.1002/ijc.20450
Weng, M., & Lee, C.-Y. (2011). Keeping neural progenitor cells on a short leash during Drosophila neurogenesis. *Current Opinion in Neurobiology*, *21*(1), 36–42. doi:10.1016/j.conb.2010.09.005
Weng, M., Golden, K. L., & Lee, C.-Y. (2010). dFezf/Earmuff Maintains the Restricted Developmental Potential of Intermediate Neural Progenitors in Drosophila. *Developmental Cell*, *18*(1), 126–135. doi:10.1016/j.devcel.2009.12.007
White, K., & Kankel, D. R. (1978). Patterns of cell division and cell movement in the formation of the imaginal nervous system in Drosophila melanogaster. *Developmental Biology*, *65*(2), 296–321.
White, K., Grether, M. E., Abrams, J. M., Young, L., Farrell, K., & Steller, H. (1994). Genetic control of programmed cell death in Drosophila. *Science (New York, N.Y.)*, *264*(5159), 677–683.
Wilson, B. G., & Roberts, C. W. M. (2011). SWI/SNF nucleosome remodellers and cancer. *Nature Reviews. Cancer*, *11*(7), 481–492. doi:10.1038/nrc3068
Wirtz-Peitz, F., Nishimura, T., & Knoblich, J. A. (2008). Linking cell cycle to asymmetric division: Aurora-A phosphorylates the Par complex to regulate Numb localization. *Cell*, *135*(1), 161–173. doi:10.1016/j.cell.2008.07.049
Wodarz, A., Ramrath, A., Grimm, A., & Knust, E. (2000). Drosophila atypical protein kinase C associates with Bazooka and controls polarity of epithelia and neuroblasts. *The Journal of Cell Biology*, *150*(6), 1361–1374.
Wu, J. I., Lessard, J., & Crabtree, G. R. (2009). Understanding the words of chromatin regulation. *Cell*, *136*(2), 200–206. doi:10.1016/j.cell.2009.01.009
Wu, J. I., Lessard, J., Olave, I. A., Qiu, Z., Ghosh, A., Graef, I. A., & Crabtree, G. R. (2007). Regulation of dendritic development by neuron-specific chromatin remodeling complexes. *Neuron*, *56*(1), 94–108. doi:10.1016/j.neuron.2007.08.021
Wu, P.-S., Egger, B., & Brand, A. H. (2008). Asymmetric stem cell division: lessons from Drosophila. *Seminars in Cell & Developmental Biology*, *19*(3), 283–293. doi:10.1016/j.semcdb.2008.01.007
Wysocka, J., Myers, M. P., Laherty, C. D., Eisenman, R. N., & Herr, W. (2003). Human Sin3 deacetylase and trithorax-related Set1/Ash2 histone H3-K4 methyltransferase are tethered together selectively by the cell-proliferation factor HCF-1. *Genes & Development*, *17*(7), 896–911. doi:10.1101/gad.252103
Xiao, Q., Komori, H., & Lee, C.-Y. (2012). klumpfuss distinguishes stem cells from progenitor cells during asymmetric neuroblast division. *Development (Cambridge, England)*, *139*(15), 2670–2680. doi:10.1242/dev.081687
Yan, Z., Wang, Z., Sharova, L., Sharov, A. A., Ling, C., Piao, Y., et al. (2008). BAF250B-associated SWI/SNF chromatin-remodeling complex is required to maintain undifferentiated mouse embryonic stem cells. *Stem Cells (Dayton, Ohio)*, *26*(5), 1155–1165. doi:10.1634/stemcells.2007-0846

Yang, Z.-J., Ellis, T., Markant, S. L., Read, T.-A., Kessler, J. D., Bourboulas, M., et al. (2008). Medulloblastoma can be initiated by deletion of Patched in lineage-restricted progenitors or stem cells. *Cancer Cell*, *14*(2), 135–145. doi:10.1016/j.ccr.2008.07.003

Yoo, A. S., & Crabtree, G. R. (2009). ATP-dependent chromatin remodeling in neural development. *Current Opinion in Neurobiology*, *19*(2), 120–126. doi:10.1016/j.conb.2009.04.006

Yoo, A. S., Sun, A. X., Li, L., Shcheglovitov, A., Portmann, T., Li, Y., et al. (2011). MicroRNA-mediated conversion of human fibroblasts to neurons. *Nature*, *476*(7359), 228–231. doi:10.1038/nature10323

Yuzyuk, T., Fakhouri, T. H. I., Kiefer, J., & Mango, S. E. (2009). The polycomb complex protein mes-2/E(z) promotes the transition from developmental plasticity to differentiation in C. elegans embryos. *Developmental Cell*, *16*(5), 699–710. doi:10.1016/j.devcel.2009.03.008

Zacharioudaki, E., Magadi, S. S., & Delidakis, C. (2012). bHLH-O proteins are crucial for Drosophila neuroblast self-renewal and mediate Notch-induced overproliferation. *Development (Cambridge, England)*, *139*(7), 1258–1269. doi:10.1242/dev.071779

Zeng, X., Lin, X., & Hou, S. X. (2013). The Osa-containing SWI/SNF chromatin-remodeling complex regulates stem cell commitment in the adult Drosophila intestine. *Development (Cambridge, England)*, *140*(17), 3532–3540. doi:10.1242/dev.096891

Zhu, J., Adli, M., Zou, J. Y., Verstappen, G., Coyne, M., Zhang, X., et al. (2013). Genome-wide chromatin state transitions associated with developmental and environmental cues. *Cell*, *152*(3), 642–654. doi:10.1016/j.cell.2012.12.033

Zhu, S., Barshow, S., Wildonger, J., Jan, L. Y., & Jan, Y.-N. (2011). Ets transcription factor Pointed promotes the generation of intermediate neural progenitors in Drosophila larval brains. *Proceedings of the National Academy of Sciences of the United States of America*, *108*(51), 20615–20620. doi:10.1073/pnas.1118595109

Zhu, S., Lin, S., Kao, C.-F., Awasaki, T., Chiang, A.-S., & Lee, T. (2006). Gradients of the Drosophila Chinmo BTB-zinc finger protein govern neuronal temporal identity. *Cell*, *127*(2), 409–422. doi:10.1016/j.cell.2006.08.045

Abrams, J. M., White, K., Fessler, L. I., & Steller, H. (1993). Programmed cell death during Drosophila embryogenesis. *Development (Cambridge, England)*, *117*(1), 29–43.

Alcantara Llaguno, S., Chen, J., Kwon, C.-H., Jackson, E. L., Li, Y., Burns, D. K., et al. (2009). Malignant astrocytomas originate from neural stem/progenitor cells in a somatic tumor suppressor mouse model. *Cancer Cell*, *15*(1), 45–56. doi:10.1016/j.ccr.2008.12.006

Almeida, M. S., & Bray, S. J. (2005). Regulation of post-embryonic neuroblasts by Drosophila Grainyhead. *Mechanisms of Development*, *122*(12), 1282–1293. doi:10.1016/j.mod.2005.08.004

Anders, S., & Huber, W. (2010). Differential expression analysis for sequence count data. *Genome Biology*, *11*(10), R106. doi:10.1186/gb-2010-11-10-r106

Arama, E., Dickman, D., Kimchie, Z., Shearn, A., & Lev, Z. (2000). Mutations in the beta-propeller domain of the Drosophila brain tumor (brat) protein induce neoplasm in the larval brain. *Oncogene*, *19*(33), 3706–3716. doi:10.1038/sj.onc.1203706

Armstrong, L. (2012). Epigenetic control of embryonic stem cell differentiation. *Stem Cell Reviews*, *8*(1), 67–77. doi:10.1007/s12015-011-9300-4

Atwood, S. X., & Prehoda, K. E. (2009). aPKC phosphorylates Miranda to polarize fate determinants during neuroblast asymmetric cell division. *Current Biology : CB*, *19*(9), 723–729. doi:10.1016/j.cub.2009.03.056

Bailey, T. L. (2005). FITTING A MIXTURE MODEL BY EXPECTATION MAXIMIZATIONTO DISCOVER MOTIFS IN BIOPOLYMERS, 1–33.

Basto, R., Brunk, K., Vinadogrova, T., Peel, N., Franz, A., Khodjakov, A., & Raff, J. W. (2008). Centrosome amplification can initiate tumorigenesis in flies. *Cell*, *133*(6), 1032–1042. doi:10.1016/j.cell.2008.05.039

Baumgardt, M., Karlsson, D., Terriente, J., Díaz-Benjumea, F. J., & Thor, S. (2009). Neuronal subtype specification within a lineage by opposing temporal feed-forward loops. *Cell*, *139*(5), 969–982. doi:10.1016/j.cell.2009.10.032

Bayraktar, O. A., & Doe, C. Q. (2013). Combinatorial temporal patterning in progenitors expands neural diversity. *Nature*, 1–8. doi:10.1038/nature12266

Bello, B. C., Izergina, N., Caussinus, E., & Reichert, H. (2008). Amplification of neural stem cell proliferation by intermediate progenitor cells in Drosophila brain development. *Neural Development*, *3*, 5. doi:10.1186/1749-8104-3-5

Bello, B., Reichert, H., & Hirth, F. (2006). The brain tumor gene negatively regulates neural progenitor cell proliferation in the larval central brain of Drosophila. *Development (Cambridge, England)*, *133*(14), 2639–2648. doi:10.1242/dev.02429

Berdnik, D., Török, T., González-Gaitán, M., & Knoblich, J. A. (2002). The endocytic protein alpha-Adaptin is required for numb-mediated asymmetric cell division in Drosophila. *Developmental Cell*, *3*(2), 221–231.

Berger, C., Harzer, H., Burkard, T. R., Steinmann, J., van der Horst, S., Laurenson, A.-S., et al. (2012). FACS purification and transcriptome analysis of drosophila neural stem cells reveals a role for Klumpfuss in self-renewal. *Cell Reports*, *2*(2), 407–418. doi:10.1016/j.celrep.2012.07.008

Bernstein, B. E., Mikkelsen, T. S., Xie, X., Kamal, M., Huebert, D. J., Cuff, J., et al. (2006). A bivalent chromatin structure marks key developmental genes in embryonic stem cells. *Cell*, *125*(2), 315–326. doi:10.1016/j.cell.2006.02.041

Betschinger, J., Mechtler, K., & Knoblich, J. A. (2006). Asymmetric segregation of the tumor suppressor brat regulates self-renewal in Drosophila neural stem cells. *Cell*, *124*(6), 1241–1253. doi:10.1016/j.cell.2006.01.038

Bhalerao, S., Berdnik, D., Török, T., & Knoblich, J. A. (2005). Localization-dependent and -independent roles of numb contribute to cell-fate specification in Drosophila. *Current Biology : CB*, *15*(17), 1583–1590. doi:10.1016/j.cub.2005.07.061

Bhat, K. M. (1999). Segment polarity genes in neuroblast formation and identity specification during Drosophila neurogenesis. *BioEssays : News and Reviews in Molecular, Cellular and*

Developmental Biology, *21*(6), 472–485. doi:10.1002/(SICI)1521-1878(199906)21:6<472::AID-BIES4>3.0.CO;2-W

Bier, E., Vaessin, H., Younger-Shepherd, S., Jan, L. Y., & Jan, Y. N. (1992). deadpan, an essential pan-neural gene in Drosophila, encodes a helix-loop-helix protein similar to the hairy gene product. *Genes & Development*, *6*(11), 2137–2151.

Bonn, S., Zinzen, R. P., Perez-Gonzalez, A., Riddell, A., Gavin, A.-C., & Furlong, E. E. M. (2012). Cell type-specific chromatin immunoprecipitation from multicellular complex samples using BiTS-ChIP. *Nature Protocols*, *7*(5), 978–994. doi:10.1038/nprot.2012.049

Boone, J. Q., & Doe, C. Q. (2008). Identification of Drosophila type II neuroblast lineages containing transit amplifying ganglion mother cells. *Developmental Neurobiology*, *68*(9), 1185–1195. doi:10.1002/dneu.20648

Bork, P., & Margolis, B. (1995). A phosphotyrosine interaction domain. *Cell*, *80*(5), 693–694.

Bowman, S. K., Rolland, V., Betschinger, J., Kinsey, K. A., Emery, G., & Knoblich, J. A. (2008). The tumor suppressors Brat and Numb regulate transit-amplifying neuroblast lineages in Drosophila. *Developmental Cell*, *14*(4), 535–546. doi:10.1016/j.devcel.2008.03.004

Bowman, S. K., Simon, M. D., Deaton, A. M., Tolstorukov, M., Borowsky, M. L., & Kingston, R. E. (2013). Multiplexed Illumina sequencing libraries from picogram quantities of DNA. *BMC Genomics*, *14*, 466. doi:10.1186/1471-2164-14-466

Boyer, L. A., Plath, K., Zeitlinger, J., Brambrink, T., Medeiros, L. A., Lee, T. I., et al. (2006). Polycomb complexes repress developmental regulators in murine embryonic stem cells. *Nature*, *441*(7091), 349–353. doi:10.1038/nature04733

Brand, A. H., & Livesey, F. J. (2011). Neural stem cell biology in vertebrates and invertebrates: more alike than different? *Neuron*, *70*(4), 719–729. doi:10.1016/j.neuron.2011.05.016

Brennecke, J., Stark, A., Russell, R. B., & Cohen, S. M. (2005). Principles of microRNA-target recognition. *PLoS Biology*, *3*(3), e85. doi:10.1371/journal.pbio.0030085

Britton, J. S., & Edgar, B. A. (1998). Environmental control of the cell cycle in Drosophila: nutrition activates mitotic and endoreplicative cells by distinct mechanisms. *Development (Cambridge, England)*, *125*(11), 2149–2158.

Bush, A., Hiromi, Y., & Cole, M. (1996). Biparous: a novel bHLH gene expressed in neuronal and glial precursors in Drosophila. *Developmental Biology*, *180*(2), 759–772. doi:10.1006/dbio.1996.0344

Buszczak, M., Paterno, S., Lighthouse, D., Bachman, J., Planck, J., Owen, S., et al. (2007). The carnegie protein trap library: a versatile tool for Drosophila developmental studies. *Genetics*, *175*(3), 1505–1531. doi:10.1534/genetics.106.065961

Byrd, K. N., & Shearn, A. (2003). ASH1, a Drosophila trithorax group protein, is required for methylation of lysine 4 residues on histone H3. *Proceedings of the National Academy of Sciences of the United States of America*, *100*(20), 11535–11540. doi:10.1073/pnas.1933593100

Campbell, S. D., Sprenger, F., Edgar, B. A., & O'Farrell, P. H. (1995). Drosophila Wee1 kinase rescues fission yeast from mitotic catastrophe and phosphorylates Drosophila Cdc2 in vitro. *Molecular Biology of the Cell*, *6*(10), 1333–1347.

Campos-Ortega, J. A. (1994). Genetic mechanisms of early neurogenesis in Drosophila melanogaster. *Journal of Physiology, Paris*, *88*(2), 111–122.

Carney, T. D., Miller, M. R., Robinson, K. J., Bayraktar, O. A., Osterhout, J. A., & Doe, C. Q. (2012). Functional genomics identifies neural stem cell sub-type expression profiles and genes regulating neuroblast homeostasis. *Developmental Biology*, *361*(1), 137–146. doi:10.1016/j.ydbio.2011.10.020

Castellanos, E., Dominguez, P., & Gonzalez, C. (2008). Centrosome dysfunction in Drosophila neural stem cells causes tumors that are not due to genome instability. *Current Biology : CB*, *18*(16), 1209–1214. doi:10.1016/j.cub.2008.07.029

Caussinus, E., & Gonzalez, C. (2005). Induction of tumor growth by altered stem-cell asymmetric

division in Drosophila melanogaster. *Nature Genetics*, *37*(10), 1125–1129. doi:10.1038/ng1632
Cayouette, M., Mattar, P., & Harris, W. A. (2013). Progenitor competence: genes switching places. *Cell*, *152*(1-2), 13–14. doi:10.1016/j.cell.2012.12.038
Ceron, J., Tejedor, F. J., & Moya, F. (2006). A primary cell culture of Drosophila postembryonic larval neuroblasts to study cell cycle and asymmetric division. *European Journal of Cell Biology*, *85*(6), 567–575. doi:10.1016/j.ejcb.2006.02.006
Chabu, C., & Doe, C. Q. (2009). Developmental Biology. *Developmental Biology*, *330*(2), 399–405. doi:10.1016/j.ydbio.2009.04.014
Chalkley, G. E., Moshkin, Y. M., Langenberg, K., Bezstarosti, K., Blastyak, A., Gyurkovics, H., et al. (2008). The transcriptional coactivator SAYP is a trithorax group signature subunit of the PBAP chromatin remodeling complex. *Molecular and Cellular Biology*, *28*(9), 2920–2929. doi:10.1128/MCB.02217-07
Chell, J. M., & Brand, A. H. (2010). Nutrition-responsive glia control exit of neural stem cells from quiescence. *Cell*, *143*(7), 1161–1173. doi:10.1016/j.cell.2010.12.007
Chen, J., Li, Y., Yu, T.-S., McKay, R. M., Burns, D. K., Kernie, S. G., & Parada, L. F. (2012). A restricted cell population propagates glioblastoma growth after chemotherapy. *Nature*, *488*(7412), 522–526. doi:10.1038/nature11287
Chen, S., Wang, S., & Xie, T. (2011). Restricting self-renewal signals within the stem cell niche: multiple levels of control. *Current Opinion in Genetics & Development*, *21*(6), 684–689. doi:10.1016/j.gde.2011.07.008
Choksi, S. P., Southall, T. D., Bossing, T., Edoff, K., de Wit, E., Fischer, B. E., et al. (2006). Prospero acts as a binary switch between self-renewal and differentiation in Drosophila neural stem cells. *Developmental Cell*, *11*(6), 775–789. doi:10.1016/j.devcel.2006.09.015
Chu-LaGraff, Q., Wright, D. M., McNeil, L. K., & Doe, C. Q. (1991). The prospero gene encodes a divergent homeodomain protein that controls neuronal identity in Drosophila. *Development (Cambridge, England)*, *Suppl 2*, 79–85.
Chuikov, S., Levi, B. P., Smith, M. L., & Morrison, S. J. (2010). Prdm16 promotes stem cell maintenance in multiple tissues, partly by regulating oxidative stress. *Nature Cell Biology*, *12*(10), 999–1006. doi:10.1038/ncb2101
Collins, R. T., Furukawa, T., Tanese, N., & Treisman, J. E. (1999). Osa associates with the Brahma chromatin remodeling complex and promotes the activation of some target genes. *The EMBO Journal*, *18*(24), 7029–7040. doi:10.1093/emboj/18.24.7029
Colombani, J., Raisin, S., Pantalacci, S., Radimerski, T., Montagne, J., & Léopold, P. (2003). A nutrient sensor mechanism controls Drosophila growth. *Cell*, *114*(6), 739–749.
Coskun, V., Tsoa, R., & Sun, Y. E. (2012). Epigenetic regulation of stem cells differentiating along the neural lineage. *Current Opinion in Neurobiology*, *22*(5), 762–767. doi:10.1016/j.conb.2012.07.001
Cotton, M., Benhra, N., & Le Borgne, R. (2013). Numb inhibits the recycling of Sanpodo in Drosophila sensory organ precursor. *Current Biology : CB*, *23*(7), 581–587. doi:10.1016/j.cub.2013.02.020
Couturier, L., Mazouni, K., & Schweisguth, F. (2013). Numb localizes at endosomes and controls the endosomal sorting of notch after asymmetric division in Drosophila. *Current Biology : CB*, *23*(7), 588–593. doi:10.1016/j.cub.2013.03.002
Crosby, M. A., Miller, C., Alon, T., Watson, K. L., Verrijzer, C. P., Goldman-Levi, R., & Zak, N. B. (1999). The trithorax group gene moira encodes a brahma-associated putative chromatin-remodeling factor in Drosophila melanogaster. *Molecular and Cellular Biology*, *19*(2), 1159–1170.
Cui, X., De Vivo, I., Slany, R., Miyamoto, A., Firestein, R., & Cleary, M. L. (1998). Association of SET domain and myotubularin-related proteins modulates growth control. *Nature Genetics*, *18*(4), 331–337. doi:10.1038/ng0498-331
Deal, R. B., & Henikoff, S. (2011). The INTACT method for cell type-specific gene expression and chromatin profiling in Arabidopsis thaliana. *Nature Protocols*, *6*(1), 56–68.

doi:10.1038/nprot.2010.175
Delidakis, C., & Artavanis-Tsakonas, S. (1992). The Enhancer of split [E(spl)] locus of Drosophila encodes seven independent helix-loop-helix proteins. *Proceedings of the National Academy of Sciences of the United States of America*, *89*(18), 8731–8735.
Dessaud, E., McMahon, A. P., & Briscoe, J. (2008). Pattern formation in the vertebrate neural tube: a sonic hedgehog morphogen-regulated transcriptional network. *Development (Cambridge, England)*, *135*(15), 2489–2503. doi:10.1242/dev.009324
Doe, C. Q., Chu-LaGraff, Q., Wright, D. M., & Scott, M. P. (1991). The prospero gene specifies cell fates in the Drosophila central nervous system. *Cell*, *65*(3), 451–464.
Driessens, G., Beck, B., Caauwe, A., Simons, B. D., & Blanpain, C. (2012). Defining the mode of tumour growth by clonal analysis. *Nature*, *488*(7412), 527–530. doi:10.1038/nature11344
Endo, K., Karim, M. R., Taniguchi, H., Krejcí, A., Kinameri, E., Siebert, M., et al. (2012). Chromatin modification of Notch targets in olfactory receptor neuron diversification. *Nature Neuroscience*, *15*(2), 224–233. doi:10.1038/nn.2998
Endoh, M., Endo, T. A., Endoh, T., Fujimura, Y.-I., Ohara, O., Toyoda, T., et al. (2008). Polycomb group proteins Ring1A/B are functionally linked to the core transcriptional regulatory circuitry to maintain ES cell identity. *Development (Cambridge, England)*, *135*(8), 1513–1524. doi:10.1242/dev.014340
Fukuyama, H., Ndiaye, S., Hoffmann, J., Rossier, J., Liuu, S., Vinh, J., & Verdier, Y. (2012). On-bead tryptic proteolysis: an attractive procedure for LC-MS/MS analysis of the Drosophila caspase 8 protein complex during immune response against bacteria. *Journal of Proteomics*, *75*(15), 4610–4619. doi:10.1016/j.jprot.2012.03.003
Gan, Q., Schones, D. E., Ho Eun, S., Wei, G., Cui, K., Zhao, K., & Chen, X. (2010). Monovalent and unpoised status of most genes in undifferentiated cell-enriched Drosophila testis. *Genome Biology*, *11*(4), R42. doi:10.1186/gb-2010-11-4-r42
Gaspard, N., Bouschet, T., Hourez, R., Dimidschstein, J., Naeije, G., van den Ameele, J., et al. (2008). An intrinsic mechanism of corticogenesis from embryonic stem cells. *Nature*, *455*(7211), 351–357. doi:10.1038/nature07287
Gateff, E. (1978). Malignant neoplasms of genetic origin in Drosophila melanogaster. *Science (New York, N.Y.)*, *200*(4349), 1448–1459.
Gonzalez, C. (2013). Drosophila melanogaster: a model and a tool to investigate malignancy and identify new therapeutics. *Nature Reviews. Cancer*, *13*(3), 172–183. doi:10.1038/nrc3461
Grosskortenhaus, R., Robinson, K. J., & Doe, C. Q. (2006). Pdm and Castor specify late-born motor neuron identity in the NB7-1 lineage. *Genes & Development*, *20*(18), 2618–2627. doi:10.1101/gad.1445306
Haenfler, J. M., Kuang, C., & Lee, C.-Y. (2012). Cortical aPKC kinase activity distinguishes neural stem cells from progenitor cells by ensuring asymmetric segregation of Numb. *Developmental Biology*, *365*(1), 219–228. doi:10.1016/j.ydbio.2012.02.027
Haley, B., Foys, B., & Levine, M. (2010). Vectors and parameters that enhance the efficacy of RNAi-mediated gene disruption in transgenic Drosophila. *Proceedings of the National Academy of Sciences of the United States of America*, *107*(25), 11435–11440. doi:10.1073/pnas.1006689107
Hargreaves, D. C., & Crabtree, G. R. (2011). ATP-dependent chromatin remodeling: genetics, genomics and mechanisms. *Cell Research*, *21*(3), 396–420. doi:10.1038/cr.2011.32
Harris, R. E., Pargett, M., Sutcliffe, C., Umulis, D., & Ashe, H. L. (2011). Brat Promotes Stem Cell Differentiation via Control of a Bistable Switch that Restricts BMP Signaling. *Developmental Cell*, *20*(1), 72–83. doi:10.1016/j.devcel.2010.11.019
Hartenstein, V., Spindler, S., Pereanu, W., & Fung, S. (2008). The development of the Drosophila larval brain. *Advances in Experimental Medicine and Biology*, *628*, 1–31. doi:10.1007/978-0-387-78261-4_1
Harzer, H., Berger, C., Conder, R., Schmauss, G., & Knoblich, J. A. (2013). FACS purification of

Drosophila larval neuroblasts for next-generation sequencing. *Nature Protocols*, *8*(6), 1088–1099. doi:10.1038/nprot.2013.062

Henry, G. L., Davis, F. P., Picard, S., & Eddy, S. R. (2012). Cell type-specific genomics of Drosophila neurons. *Nucleic Acids Research*, *40*(19), 9691–9704. doi:10.1093/nar/gks671

Hirschhorn, J. N., Brown, S. A., Clark, C. D., & Winston, F. (1992). Evidence that SNF2/SWI2 and SNF5 activate transcription in yeast by altering chromatin structure. *Genes & Development*, *6*(12A), 2288–2298.

Ho, L., Miller, E. L., Ronan, J. L., Ho, W. Q., Jothi, R., & Crabtree, G. R. (2011). esBAF facilitates pluripotency by conditioning the genome for LIF/STAT3 signalling and by regulating polycomb function. *Nature Cell Biology*, *13*(8), 903–913. doi:10.1038/ncb2285

Ho, L., Ronan, J. L., Wu, J., Staahl, B. T., Chen, L., Kuo, A., et al. (2009). An embryonic stem cell chromatin remodeling complex, esBAF, is essential for embryonic stem cell self-renewal and pluripotency. *Proceedings of the National Academy of Sciences of the United States of America*, *106*(13), 5181–5186. doi:10.1073/pnas.0812889106

Hohenauer, T., & Moore, A. W. (2012). The Prdm family: expanding roles in stem cells and development. *Development (Cambridge, England)*, *139*(13), 2267–2282. doi:10.1242/dev.070110

Homem, C. C. F., & Knoblich, J. A. (2012). Drosophila neuroblasts: a model for stem cell biology. *Development (Cambridge, England)*, *139*(23), 4297–4310. doi:10.1242/dev.080515

Imbalzano, A. N., Kwon, H., Green, M. R., & Kingston, R. E. (1994). Facilitated binding of TATA-binding protein to nucleosomal DNA. *Nature*, *370*(6489), 481–485. doi:10.1038/370481a0

Isshiki, T., & Doe, C. Q. (2004). Maintaining youth in Drosophila neural progenitors. *Cell Cycle (Georgetown, Tex.)*, *3*(3), 296–299.

Isshiki, T., Pearson, B., Holbrook, S., & Doe, C. Q. (2001). Drosophila neuroblasts sequentially express transcription factors which specify the temporal identity of their neuronal progeny. *Cell*, *106*(4), 511–521.

Jacob, J., Maurange, C., & Gould, A. P. (2008). Temporal control of neuronal diversity: common regulatory principles in insects and vertebrates? *Development (Cambridge, England)*, *135*(21), 3481–3489. doi:10.1242/dev.016931

Jennings, B., Preiss, A., Delidakis, C., & Bray, S. (1994). The Notch signalling pathway is required for Enhancer of split bHLH protein expression during neurogenesis in the Drosophila embryo. *Development (Cambridge, England)*, *120*(12), 3537–3548.

Johnston, C. A., Hirono, K., Prehoda, K. E., & Doe, C. Q. (2009). Identification of an Aurora-A/PinsLINKER/Dlg spindle orientation pathway using induced cell polarity in S2 cells. *Cell*, *138*(6), 1150–1163. doi:10.1016/j.cell.2009.07.041

Jones, D. T. W., Jäger, N., Kool, M., Zichner, T., Hutter, B., Sultan, M., et al. (2012). Dissecting the genomic complexity underlying medulloblastoma. *Nature*, *488*(7409), 100–105. doi:10.1038/nature11284

Jones, S., Wang, T.-L., Shih, I.-M., Mao, T.-L., Nakayama, K., Roden, R., et al. (2010). Frequent mutations of chromatin remodeling gene ARID1A in ovarian clear cell carcinoma. *Science (New York, N.Y.)*, *330*(6001), 228–231. doi:10.1126/science.1196333

Kadoch, C., Hargreaves, D. C., Hodges, C., Elias, L., Ho, L., Ranish, J., & Crabtree, G. R. (2013). Proteomic and bioinformatic analysis of mammalian SWI/SNF complexes identifies extensive roles in human malignancy. *Nature Genetics*. doi:10.1038/ng.2628

Kambadur, R., Koizumi, K., Stivers, C., Nagle, J., Poole, S. J., & Odenwald, W. F. (1998). Regulation of POU genes by castor and hunchback establishes layered compartments in the Drosophila CNS. *Genes & Development*, *12*(2), 246–260.

Kennison, J. A., & Tamkun, J. W. (1988). Dosage-dependent modifiers of polycomb and antennapedia mutations in Drosophila. *Proceedings of the National Academy of Sciences of the United States of America*, *85*(21), 8136–8140.

Kia, S. K., Gorski, M. M., Giannakopoulos, S., & Verrijzer, C. P. (2008). SWI/SNF mediates polycomb eviction and epigenetic reprogramming of the INK4b-ARF-INK4a locus. *Molecular and Cellular Biology*, *28*(10), 3457–3464. doi:10.1128/MCB.02019-07

Klein, T., & Campos-Ortega, J. A. (1997). klumpfuss, a Drosophila gene encoding a member of the EGR family of transcription factors, is involved in bristle and leg development. *Development (Cambridge, England)*, *124*(16), 3123–3134.

Knoblich, J. A. (2008). Mechanisms of asymmetric stem cell division. *Cell*, *132*(4), 583–597. doi:10.1016/j.cell.2008.02.007

Knoblich, J. A. (2010). Asymmetric cell division: recent developments and their implications for tumour biology. *Nature Reviews. Molecular Cell Biology*, *11*(12), 849–860. doi:10.1038/nrm3010

Knoblich, J. A., Jan, L. Y., & Jan, Y. N. (1997). The N terminus of the Drosophila Numb protein directs membrane association and actin-dependent asymmetric localization. *Proceedings of the National Academy of Sciences of the United States of America*, *94*(24), 13005–13010.

Knust, E., Schrons, H., Grawe, F., & Campos-Ortega, J. A. (1992). Seven genes of the Enhancer of split complex of Drosophila melanogaster encode helix-loop-helix proteins. *Genetics*, *132*(2), 505–518.

Koche, R. P., Smith, Z. D., Adli, M., Gu, H., Ku, M., Gnirke, A., et al. (2011). Reprogramming factor expression initiates widespread targeted chromatin remodeling. *Cell Stem Cell*, *8*(1), 96–105. doi:10.1016/j.stem.2010.12.001

Kohwi, M., & Doe, C. Q. (2013). Temporal fate specification and neural progenitor competence during development. *Nature Reviews. Neuroscience*, *14*(12), 823–838. doi:10.1038/nrn3618

Kohwi, M., Lupton, J. R., Lai, S.-L., Miller, M. R., & Doe, C. Q. (2013). Developmentally Regulated Subnuclear Genome Reorganization Restricts NeuralProgenitor Competence in Drosophila. *Cell*, *152*(1-2), 97–108. doi:10.1016/j.cell.2012.11.049

Komori, H., Xiao, Q., McCartney, B. M., & Lee, C.-Y. (2013). Brain tumor specifies intermediate progenitor cell identity by attenuating β-catenin/Armadillo activity. *Development (Cambridge, England)*. doi:10.1242/dev.099382

Kraut, R., Chia, W., Jan, L. Y., Jan, Y. N., & Knoblich, J. A. (1996). Role of inscuteable in orienting asymmetric cell divisions in Drosophila. *Nature*, *383*(6595), 50–55. doi:10.1038/383050a0

Krejcí, A., & Bray, S. (2007). Notch activation stimulates transient and selective binding of Su(H)/CSL to target enhancers. *Genes & Development*, *21*(11), 1322–1327. doi:10.1101/gad.424607

Kruger, W., Peterson, C. L., Sil, A., Coburn, C., Arents, G., Moudrianakis, E. N., & Herskowitz, I. (1995). Amino acid substitutions in the structured domains of histones H3 and H4 partially relieve the requirement of the yeast SWI/SNF complex for transcription. *Genes & Development*, *9*(22), 2770–2779.

Kuchinke, U., Grawe, F., & Knust, E. (1998). Control of spindle orientation in Drosophila by the Par-3-related PDZ-domain protein Bazooka. *Current Biology*, *8*(25), 1357–1365.

Kwon, H., Imbalzano, A. N., Khavari, P. A., Kingston, R. E., & Green, M. R. (1994). Nucleosome disruption and enhancement of activator binding by a human SW1/SNF complex. *Nature*, *370*(6489), 477–481. doi:10.1038/370477a0

Le Borgne, R., Bardin, A., & Schweisguth, F. (2005). The roles of receptor and ligand endocytosis in regulating Notch signaling. *Development (Cambridge, England)*, *132*(8), 1751–1762. doi:10.1242/dev.01789

Lee, C.-Y., Wilkinson, B. D., Siegrist, S. E., Wharton, R. P., & Doe, C. Q. (2006a). Brat is a Miranda cargo protein that promotes neuronal differentiation and inhibits neuroblast self-renewal. *Developmental Cell*, *10*(4), 441–449. doi:10.1016/j.devcel.2006.01.017

Lee, T. I., Jenner, R. G., Boyer, L. A., Guenther, M. G., Levine, S. S., Kumar, R. M., et al. (2006b). Control of developmental regulators by Polycomb in human embryonic stem cells. *Cell*, *125*(2), 301–

313. doi:10.1016/j.cell.2006.02.043
Lee, T. I., Johnstone, S. E., & Young, R. A. (2006c). Chromatin immunoprecipitation and microarray-based analysis of protein location. *Nature Protocols*, *1*(2), 729–748. doi:10.1038/nprot.2006.98
Lee, T., & Luo, L. (1999). Mosaic analysis with a repressible cell marker for studies of gene function in neuronal morphogenesis. *Neuron*, *22*(3), 451–461.
Lessard, J., Wu, J. I., Ranish, J. A., Wan, M., Winslow, M. M., Staahl, B. T., et al. (2007). An essential switch in subunit composition of a chromatin remodeling complex during neural development. *Neuron*, *55*(2), 201–215. doi:10.1016/j.neuron.2007.06.019
Li, L., & Vaessin, H. (2000). Pan-neural Prospero terminates cell proliferation during Drosophila neurogenesis. *Genes & Development*, *14*(2), 147–151.
Li, X., Chen, Z., & Desplan, C. (2013). Temporal patterning of neural progenitors in Drosophila. *Current Topics in Developmental Biology*, *105*, 69–96. doi:10.1016/B978-0-12-396968-2.00003-8
Lickert, H., Takeuchi, J. K., Both, Von, I., Walls, J. R., McAuliffe, F., Adamson, S. L., et al. (2004). Baf60c is essential for function of BAF chromatin remodelling complexes in heart development. *Nature*, *432*(7013), 107–112. doi:10.1038/nature03071
Lin, S., & Lee, T. (2012). Generating neuronal diversity in the Drosophila central nervous system. *Developmental Dynamics : an Official Publication of the American Association of Anatomists*, *241*(1), 57–68. doi:10.1002/dvdy.22739
Liu, C., & Zong, H. (2012). Developmental origins of brain tumors. *Current Opinion in Neurobiology*, *22*(5), 844–849. doi:10.1016/j.conb.2012.04.012
Liu, C., Sage, J. C., Miller, M. R., Verhaak, R. G. W., Hippenmeyer, S., Vogel, H., et al. (2011). Mosaic analysis with double markers reveals tumor cell of origin in glioma. *Cell*, *146*(2), 209–221. doi:10.1016/j.cell.2011.06.014
Livak, K. J., & Schmittgen, T. D. (2001). Analysis of Relative Gene Expression Data Using Real-Time Quantitative PCR and the 2−ΔΔCT Method. *Methods*, *25*(4), 402–408. doi:10.1006/meth.2001.1262
Logie, C., & Peterson, C. L. (1997). Catalytic activity of the yeast SWI/SNF complex on reconstituted nucleosome arrays. *The EMBO Journal*, *16*(22), 6772–6782. doi:10.1093/emboj/16.22.6772
Ma, Y., Niemitz, E. L., Nambu, P. A., Shan, X., Sackerson, C., Fujioka, M., et al. (1998). Gene regulatory functions of Drosophila fish-hook, a high mobility group domain Sox protein. *Mechanisms of Development*, *73*(2), 169–182.
Maurange, C., Cheng, L., & Gould, A. P. (2008). Temporal transcription factors and their targets schedule the end of neural proliferation in Drosophila. *Cell*, *133*(5), 891–902. doi:10.1016/j.cell.2008.03.034
McGuire, S. E., Mao, Z., & Davis, R. L. (2004). Spatiotemporal gene expression targeting with the TARGET and gene-switch systems in Drosophila. *Science's STKE : Signal Transduction Knowledge Environment*, *2004*(220), pl6. doi:10.1126/stke.2202004pl6
Mikkelsen, T. S., Ku, M., Jaffe, D. B., Issac, B., Lieberman, E., Giannoukos, G., et al. (2007). Genome-wide maps of chromatin state in pluripotent and lineage-committed cells. *Nature*, *448*(7153), 553–560. doi:10.1038/nature06008
Mohrmann, L., Langenberg, K., Krijgsveld, J., Kal, A. J., Heck, A. J. R., & Verrijzer, C. P. (2004). Differential targeting of two distinct SWI/SNF-related Drosophila chromatin-remodeling complexes. *Molecular and Cellular Biology*, *24*(8), 3077–3088.
Moore, A. W., Barbel, S., Jan, L. Y., & Jan, Y. N. (2000). A genomewide survey of basic helix-loop-helix factors in Drosophila. *Proceedings of the National Academy of Sciences of the United States of America*, *97*(19), 10436–10441. doi:10.1073/pnas.170301897
Moore, A. W., Jan, L. Y., & Jan, Y.-N. (2002). hamlet, a binary genetic switch between single- and multiple- dendrite neuron morphology. *Science (New York, N.Y.)*, *297*(5585), 1355–1358. doi:10.1126/science.1072387

Moore, A. W., Roegiers, F., Jan, L. Y., & Jan, Y.-N. (2004). Conversion of neurons and glia to external-cell fates in the external sensory organs of Drosophila hamlet mutants by a cousin-cousin cell-type respecification. *Genes & Development*, *18*(6), 623–628. doi:10.1101/gad.1170904

Moshkin, Y. M., Chalkley, G. E., Kan, T. W., Reddy, B. A., Ozgur, Z., van Ijcken, W. F. J., et al. (2012). Remodelers Organize Cellular Chromatin by Counteracting Intrinsic Histone-DNA Sequence Preferences in a Class-Specific Manner. *Molecular and Cellular Biology*, *32*(3), 675–688. doi:10.1128/MCB.06365-11

Moshkin, Y. M., Mohrmann, L., van Ijcken, W. F. J., & Verrijzer, C. P. (2007). Functional differentiation of SWI/SNF remodelers in transcription and cell cycle control. *Molecular and Cellular Biology*, *27*(2), 651–661. doi:10.1128/MCB.01257-06

Mummery-Widmer, J. L., Yamazaki, M., Stoeger, T., Novatchkova, M., Bhalerao, S., Chen, D., et al. (2009). Genome-wide analysis of Notch signalling in Drosophila by transgenic RNAi. *Nature*, *458*(7241), 987–992. doi:10.1038/nature07936

Muraro, N. I., Weston, A. J., Gerber, A. P., Luschnig, S., Moffat, K. G., & Baines, R. A. (2008). Pumilio binds para mRNA and requires Nanos and Brat to regulate sodium current in Drosophila motoneurons. *The Journal of Neuroscience : the Official Journal of the Society for Neuroscience*, *28*(9), 2099–2109. doi:10.1523/JNEUROSCI.5092-07.2008

Nabirochkina, E., Simonova, O. B., Mertsalov, I. B., Kulikova, D. A., Ladigina, N. G., Korochkin, L. I., & Buchman, V. L. (2002). Expression pattern of dd4, a sole member of the d4 family of transcription factors in Drosophila melanogaster. *Mechanisms of Development*, *114*(1-2), 119–123.

Naka, H., Nakamura, S., Shimazaki, T., & Okano, H. (2008). Requirement for COUP-TFI and II in the temporal specification of neural stem cells in CNS development. *Nature Neuroscience*, *11*(9), 1014–1023. doi:10.1038/nn.2168

Nakayama, T., Shimojima, T., & Hirose, S. (2012). The PBAP remodeling complex is required for histone H3.3 replacement at chromatin boundaries and for boundary functions. *Development (Cambridge, England)*, *139*(24), 4582–4590. doi:10.1242/dev.083246

Neigeborn, L., & Carlson, M. (1984). Genes affecting the regulation of SUC2 gene expression by glucose repression in Saccharomyces cerevisiae. *Genetics*, *108*(4), 845–858.

Neumüller, R. A., Richter, C., Fischer, A., Novatchkova, M., Neumüller, K. G., & Knoblich, J. A. (2011). Genome-wide analysis of self-renewal in Drosophila neural stem cells by transgenic RNAi. *Cell Stem Cell*, *8*(5), 580–593. doi:10.1016/j.stem.2011.02.022

Nègre, N., Brown, C. D., Ma, L., Bristow, C. A., Miller, S. W., Wagner, U., et al. (2012). A cis-regulatory map of the Drosophila genome. *Nature*, *471*(7339), 527–531. doi:10.1038/nature09990

Northcott, P. A., Jones, D. T. W., Kool, M., Robinson, G. W., Gilbertson, R. J., Cho, Y.-J., et al. (2012). Medulloblastomics: the end of the beginning. *Nature Reviews. Cancer*, *12*(12), 818–834. doi:10.1038/nrc3410

Nybakken, K., Vokes, S. A., Lin, T.-Y., McMahon, A. P., & Perrimon, N. (2005). A genome-wide RNA interference screen in Drosophila melanogaster cells for new components of the Hh signaling pathway. *Nature Genetics*, *37*(12), 1323–1332. doi:10.1038/ng1682

Ogawa, H., Ohta, N., Moon, W., & Matsuzaki, F. (2009). Protein phosphatase 2A negatively regulates aPKC signaling by modulating phosphorylation of Par-6 in Drosophila neuroblast asymmetric divisions. *Journal of Cell Science*, *122*(Pt 18), 3242–3249. doi:10.1242/jcs.050955

Owen-Hughes, T., Utley, R. T., Côté, J., Peterson, C. L., & Workman, J. L. (1996). Persistent site-specific remodeling of a nucleosome array by transient action of the SWI/SNF complex. *Science (New York, N.Y.)*, *273*(5274), 513–516.

Parsons, D. W., Li, M., Zhang, X., Jones, S., Leary, R. J., Lin, J. C.-H., et al. (2011). The genetic landscape of the childhood cancer medulloblastoma. *Science (New York, N.Y.)*, *331*(6016), 435–439. doi:10.1126/science.1198056

Peterson, C., Carney, G. E., Taylor, B. J., & White, K. (2002). reaper is required for neuroblast

apoptosis during Drosophila development. *Development (Cambridge, England)*, *129*(6), 1467–1476.
Petronczki, M., & Knoblich, J. A. (2001). DmPAR-6 directs epithelial polarity and asymmetric cell division of neuroblasts in Drosophila. *Nature Cell Biology*, *3*(1), 43–49. doi:10.1038/35050550
Petruk, S., Sedkov, Y., Smith, S., Tillib, S., Kraevski, V., Nakamura, T., et al. (2001). Trithorax and dCBP acting in a complex to maintain expression of a homeotic gene. *Science (New York, N.Y.)*, *294*(5545), 1331–1334. doi:10.1126/science.1065683
Pfeiffer, B. D., Jenett, A., Hammonds, A. S., Ngo, T.-T. B., Misra, S., Murphy, C., et al. (2008). Tools for neuroanatomy and neurogenetics in Drosophila. *Proceedings of the National Academy of Sciences of the United States of America*, *105*(28), 9715–9720. doi:10.1073/pnas.0803697105
Phelan, M. L., Sif, S., Narlikar, G. J., & Kingston, R. E. (1999). Reconstitution of a core chromatin remodeling complex from SWI/SNF subunits. *Molecular Cell*, *3*(2), 247–253.
Pinheiro, I., Margueron, R., Shukeir, N., Eisold, M., Fritzsch, C., Richter, F. M., et al. (2012). Prdm3 and Prdm16 are H3K9me1 methyltransferases required for mammalian heterochromatin integrity. *Cell*, *150*(5), 948–960. doi:10.1016/j.cell.2012.06.048
Price, D., Rabinovitch, S., O'Farrell, P. H., & Campbell, S. D. (2000). Drosophila wee1 has an essential role in the nuclear divisions of early embryogenesis. *Genetics*, *155*(1), 159–166.
Rand, M. D., Grimm, L. M., Artavanis-Tsakonas, S., Patriub, V., Blacklow, S. C., Sklar, J., & Aster, J. C. (2000). Calcium depletion dissociates and activates heterodimeric notch receptors. *Molecular and Cellular Biology*, *20*(5), 1825–1835.
Rebollo, E., Roldán, M., & Gonzalez, C. (2009). Spindle alignment is achieved without rotation after the first cell cycle in Drosophila embryonic neuroblasts. *Development (Cambridge, England)*, *136*(20), 3393–3397. doi:10.1242/dev.041822
Reichert, H. (2011). Drosophila neural stem cells: cell cycle control of self-renewal, differentiation, and termination in brain development. *Results and Problems in Cell Differentiation*, *53*, 529–546. doi:10.1007/978-3-642-19065-0_21
Rhyu, M. S., Jan, L. Y., & Jan, Y. N. (1994). Asymmetric distribution of numb protein during division of the sensory organ precursor cell confers distinct fates to daughter cells. *Cell*, *76*(3), 477–491.
Richter, C., Oktaba, K., Steinmann, J., Müller, J., & Knoblich, J. A. (2011). The tumour suppressor L(3)mbt inhibits neuroepithelial proliferation and acts on insulator elements. *Nature Cell Biology*, *13*(9), 1029–1039. doi:10.1038/ncb2306
Roberts, C. W. M., & Orkin, S. H. (2004). The SWI/SNF complex--chromatin and cancer. *Nature Reviews. Cancer*, *4*(2), 133–142. doi:10.1038/nrc1273
San-Juán, B. P., & Baonza, A. (2011). The bHLH factor deadpan is a direct target of Notch signaling and regulates neuroblast self-renewal in Drosophila. *Developmental Biology*, *352*(1), 70–82. doi:10.1016/j.ydbio.2011.01.019
Schaefer, M., Shevchenko, A., Shevchenko, A., & Knoblich, J. A. (2000). A protein complex containing Inscuteable and the Galpha-binding protein Pins orients asymmetric cell divisions in Drosophila. *Current Biology*, *10*(7), 353–362.
Schauer, T., Schwalie, P. C., Handley, A., Margulies, C. E., Flicek, P., & Ladurner, A. G. (2013). CAST-ChIP Maps Cell-Type-Specific Chromatin States in the Drosophila Central Nervous System. *Cell Reports*, *5*(1), 271–282. doi:10.1016/j.celrep.2013.09.001
Schepers, A. G., Snippert, H. J., Stange, D. E., van den Born, M., van Es, J. H., van de Wetering, M., & Clevers, H. (2012). Lineage tracing reveals Lgr5+ stem cell activity in mouse intestinal adenomas. *Science (New York, N.Y.)*, *337*(6095), 730–735. doi:10.1126/science.1224676
SCHNITZLER, G. R., Sif, S., & Kingston, R. E. (1998). A Model for Chromatin Remodeling by the SWI/SNF Family. *Cold Spring Harbor Symposia on Quantitative Biology*, *63*(0), 535–544. doi:10.1101/sqb.1998.63.535
Schober, M., Schaefer, M., & Knoblich, J. A. (1999). Bazooka recruits Inscuteable to orient asymmetric cell divisions in Drosophila neuroblasts. *Nature*, *402*(6761), 548–551.

doi:10.1038/990135
Schuettengruber, B., Ganapathi, M., Leblanc, B., Portoso, M., Jaschek, R., Tolhuis, B., et al. (2009). Functional anatomy of polycomb and trithorax chromatin landscapes in Drosophila embryos. *PLoS Biology*, *7*(1), e13. doi:10.1371/journal.pbio.1000013
Schüller, U., Heine, V. M., Mao, J., Kho, A. T., Dillon, A. K., Han, Y.-G., et al. (2008). Acquisition of granule neuron precursor identity is a critical determinant of progenitor cell competence to form Shh-induced medulloblastoma. *Cancer Cell*, *14*(2), 123–134. doi:10.1016/j.ccr.2008.07.005
Schwitalla, S., Fingerle, A. A., Cammareri, P., Nebelsiek, T., Göktuna, S. I., Ziegler, P. K., et al. (2013). Intestinal tumorigenesis initiated by dedifferentiation and acquisition of stem-cell-like properties. *Cell*, *152*(1-2), 25–38. doi:10.1016/j.cell.2012.12.012
Shain, A. H., & Pollack, J. R. (2013). The spectrum of SWI/SNF mutations, ubiquitous in human cancers. *PloS One*, *8*(1), e55119. doi:10.1371/journal.pone.0055119
Shen, Q., Wang, Y., Dimos, J. T., Fasano, C. A., Phoenix, T. N., Lemischka, I. R., et al. (2006). The timing of cortical neurogenesis is encoded within lineages of individual progenitor cells. *Nature Neuroscience*, *9*(6), 743–751. doi:10.1038/nn1694
Shevchenko, A., Tomas, H., Havlis, J., Olsen, J. V., & Mann, M. (2006). In-gel digestion for mass spectrometric characterization of proteins and proteomes. *Nature Protocols*, *1*(6), 2856–2860. doi:10.1038/nprot.2006.468
Siegrist, S. E., & Doe, C. Q. (2005). Microtubule-induced Pins/Galphai cortical polarity in Drosophila neuroblasts. *Cell*, *123*(7), 1323–1335. doi:10.1016/j.cell.2005.09.043
Siller, K. H., & Doe, C. Q. (2008). Lis1/dynactin regulates metaphase spindle orientation in Drosophila neuroblasts. *Developmental Biology*, *319*(1), 1–9. doi:10.1016/j.ydbio.2008.03.018
Siller, K. H., Cabernard, C., & Doe, C. Q. (2006). The NuMA-related Mud protein binds Pins and regulates spindle orientation in Drosophila neuroblasts. *Nature Cell Biology*, *8*(6), 594–600. doi:10.1038/ncb1412
Simons, B. D., & Clevers, H. (2011). Strategies for homeostatic stem cell self-renewal in adult tissues. *Cell*, *145*(6), 851–862. doi:10.1016/j.cell.2011.05.033
Slack, F. J., & Ruvkun, G. (1998). A novel repeat domain that is often associated with RING finger and B-box motifs. *Trends in Biochemical Sciences*, *23*(12), 474–475.
Smith, C. A., Lau, K. M., Rahmani, Z., Dho, S. E., Brothers, G., She, Y. M., et al. (2007). aPKC-mediated phosphorylation regulates asymmetric membrane localization of the cell fate determinant Numb. *The EMBO Journal*, *26*(2), 468–480. doi:10.1038/sj.emboj.7601495
Song, Y., & Lu, B. (2011). Regulation of cell growth by Notch signaling and its differential requirement in normal vs. tumor-forming stem cells in Drosophila. *Genes & Development*, *25*(24), 2644–2658. doi:10.1101/gad.171959.111
Song, Y., & Lu, B. (2012). Interaction of Notch signaling modulator Numb with α-Adaptin regulates endocytosis of Notch pathway components and cell fate determination of neural stem cells. *Journal of Biological Chemistry*, *287*(21), 17716–17728. doi:10.1074/jbc.M112.360719
Sonoda, J., & Wharton, R. P. (2001). Drosophila Brain Tumor is a translational repressor. *Genes & Development*, *15*(6), 762–773. doi:10.1101/gad.870801
Sousa-Nunes, R., & Somers, W. G. (2010). Phosphorylation and dephosphorylation events allow for rapid segregation of fate determinants during Drosophila neuroblast asymmetric divisions. *Communicative & Integrative Biology*, *3*(1), 46–49.
Sousa-Nunes, R., Chia, W., & Somers, W. G. (2009). Protein phosphatase 4 mediates localization of the Miranda complex during Drosophila neuroblast asymmetric divisions. *Genes & Development*, *23*(3), 359–372. doi:10.1101/gad.1723609
Sousa-Nunes, R., Yee, L. L., & Gould, A. P. (2011). Fat cells reactivate quiescent neuroblasts via TOR and glial insulin relays in Drosophila. *Nature*, *471*(7339), 508–512. doi:10.1038/nature09867
Southall, T. D., & Brand, A. H. (2009). Neural stem cell transcriptional networks highlight genes

essential for nervous system development. *The EMBO Journal*, *28*(24), 3799–3807. doi:10.1038/emboj.2009.309

Southall, T. D., Gold, K. S., Egger, B., Davidson, C. M., Caygill, E. E., Marshall, O. J., & Brand, A. H. (2013). Cell-Type-Specific Profiling of Gene Expression and Chromatin Binding without Cell Isolation: Assaying RNA Pol II Occupancy in Neural Stem Cells. *Developmental Cell*. doi:10.1016/j.devcel.2013.05.020

Sprang, S. R. (1997). G protein mechanisms: insights from structural analysis. *Annual Review of Biochemistry*, *66*, 639–678. doi:10.1146/annurev.biochem.66.1.639

Staahl, B. T., Tang, J., Wu, W., Sun, A., Gitler, A. D., Yoo, A. S., & Crabtree, G. R. (2013). Kinetic Analysis of npBAF to nBAF Switching Reveals Exchange of SS18 with CREST and Integration with Neural Developmental Pathways. *The Journal of Neuroscience : the Official Journal of the Society for Neuroscience*, *33*(25), 10348–10361. doi:10.1523/JNEUROSCI.1258-13.2013

Stern, M., Jensen, R., & Herskowitz, I. (1984). Five SWI genes are required for expression of the HO gene in yeast. *Journal of Molecular Biology*, *178*(4), 853–868.

Sudarsanam, P., Iyer, V. R., Brown, P. O., & Winston, F. (2000). Whole-genome expression analysis of snf/swi mutants of Saccharomyces cerevisiae. *Proceedings of the National Academy of Sciences of the United States of America*, *97*(7), 3364–3369. doi:10.1073/pnas.050407197

Suzuki, A., & Ohno, S. (2006). The PAR-aPKC system: lessons in polarity. *Journal of Cell Science*, *119*(Pt 6), 979–987. doi:10.1242/jcs.02898

Tamkun, J. W., Deuring, R., Scott, M. P., Kissinger, M., Pattatucci, A. M., Kaufman, T. C., & Kennison, J. A. (1992). brahma: a regulator of Drosophila homeotic genes structurally related to the yeast transcriptional activator SNF2/SWI2. *Cell*, *68*(3), 561–572.

Tio, M., Udolph, G., Yang, X., & Chia, W. (2001). cdc2 links the Drosophila cell cycle and asymmetric division machineries. *Nature*, *409*(6823), 1063–1067. doi:10.1038/35059124

Touma, J. J., Weckerle, F. F., & Cleary, M. D. (2012). Drosophila Polycomb complexes restrict neuroblast competence to generate motoneurons. *Development (Cambridge, England)*, *139*(4), 657–666. doi:10.1242/dev.071589

Towbin, B. D., González-Aguilera, C., Sack, R., Gaidatzis, D., Kalck, V., Meister, P., et al. (2012). Step-wise methylation of histone H3K9 positions heterochromatin at the nuclear periphery. *Cell*, *150*(5), 934–947. doi:10.1016/j.cell.2012.06.051

Treisman, J. E., Luk, A., Rubin, G. M., & Heberlein, U. (1997). eyelid antagonizes wingless signaling during Drosophila development and has homology to the Bright family of DNA-binding proteins. *Genes & Development*, *11*(15), 1949–1962.

Truman, J. W., & Bate, M. (1988). Spatial and temporal patterns of neurogenesis in the central nervous system of Drosophila melanogaster. *Developmental Biology*, *125*(1), 145–157.

Tsuji, T., Hasegawa, E., & Isshiki, T. (2008). Neuroblast entry into quiescence is regulated intrinsically by the combined action of spatial Hox proteins and temporal identity factors. *Development (Cambridge, England)*, *135*(23), 3859–3869. doi:10.1242/dev.025189

Tulina, N., & Matunis, E. (2001). Control of stem cell self-renewal in Drosophila spermatogenesis by JAK-STAT signaling. *Science (New York, N.Y.)*, *294*(5551), 2546–2549. doi:10.1126/science.1066700

Udolph, G. (2012). Notch signaling and the generation of cell diversity in Drosophila neuroblast lineages. *Advances in Experimental Medicine and Biology*, *727*, 47–60. doi:10.1007/978-1-4614-0899-4_4

Uemura, T., Shepherd, S., Ackerman, L., Jan, L. Y., & Jan, Y. N. (1989). numb, a gene required in determination of cell fate during sensory organ formation in Drosophila embryos. *Cell*, *58*(2), 349–360.

Vaessin, H., Grell, E., Wolff, E., Bier, E., Jan, L. Y., & Jan, Y. N. (1991). prospero is expressed in neuronal precursors and encodes a nuclear protein that is involved in the control of axonal outgrowth in Drosophila. *Cell*, *67*(5), 941–953.

Versteege, I., Sévenet, N., Lange, J., Rousseau-Merck, M. F., Ambros, P., Handgretinger, R., et al. (1998). Truncating mutations of hSNF5/INI1 in aggressive paediatric cancer. *Nature*, *394*(6689), 203–206. doi:10.1038/28212

Vert, J.-P., Foveau, N., Lajaunie, C., & Vandenbrouck, Y. (2006). An accurate and interpretable model for siRNA efficacy prediction. *BMC Bioinformatics*, *7*, 520. doi:10.1186/1471-2105-7-520

Visvader, J. E. (2011). Cells of origin in cancer. *Nature*, *469*(7330), 314–322. doi:10.1038/nature09781

Voigt, P., Tee, W.-W., & Reinberg, D. (2013). A double take on bivalent promoters. *Genes & Development*, *27*(12), 1318–1338. doi:10.1101/gad.219626.113

Wang, C., Chang, K. C., Somers, G., Virshup, D., Ang, B. T., Tang, C., et al. (2009). Protein phosphatase 2A regulates self-renewal of Drosophila neural stem cells. *Development (Cambridge, England)*, *136*(13), 2287–2296. doi:10.1242/dev.035758

Wang, H., Ouyang, Y., Somers, W. G., Chia, W., & Lu, B. (2007). Polo inhibits progenitor self-renewal and regulates Numb asymmetry by phosphorylating Pon. *Nature*, *449*(7158), 96–100. doi:10.1038/nature06056

Wang, H., Somers, G. W., Bashirullah, A., Heberlein, U., Yu, F., & Chia, W. (2006). Aurora-A acts as a tumor suppressor and regulates self-renewal of Drosophila neuroblasts. *Genes & Development*, *20*(24), 3453–3463. doi:10.1101/gad.1487506

Wang, X., Nagl, N. G., Flowers, S., Zweitzig, D., Dallas, P. B., & Moran, E. (2004). Expression of p270 (ARID1A), a component of human SWI/SNF complexes, in human tumors. *International Journal of Cancer. Journal International Du Cancer*, *112*(4), 636. doi:10.1002/ijc.20450

Weng, M., & Lee, C.-Y. (2011). Keeping neural progenitor cells on a short leash during Drosophila neurogenesis. *Current Opinion in Neurobiology*, *21*(1), 36–42. doi:10.1016/j.conb.2010.09.005

Weng, M., Golden, K. L., & Lee, C.-Y. (2010). dFezf/Earmuff Maintains the Restricted Developmental Potential of Intermediate Neural Progenitors in Drosophila. *Developmental Cell*, *18*(1), 126–135. doi:10.1016/j.devcel.2009.12.007

White, K., & Kankel, D. R. (1978). Patterns of cell division and cell movement in the formation of the imaginal nervous system in Drosophila melanogaster. *Developmental Biology*, *65*(2), 296–321.

White, K., Grether, M. E., Abrams, J. M., Young, L., Farrell, K., & Steller, H. (1994). Genetic control of programmed cell death in Drosophila. *Science (New York, N.Y.)*, *264*(5159), 677–683.

Wilson, B. G., & Roberts, C. W. M. (2011). SWI/SNF nucleosome remodellers and cancer. *Nature Reviews. Cancer*, *11*(7), 481–492. doi:10.1038/nrc3068

Wirtz-Peitz, F., Nishimura, T., & Knoblich, J. A. (2008). Linking cell cycle to asymmetric division: Aurora-A phosphorylates the Par complex to regulate Numb localization. *Cell*, *135*(1), 161–173. doi:10.1016/j.cell.2008.07.049

Wodarz, A., Ramrath, A., Grimm, A., & Knust, E. (2000). Drosophila atypical protein kinase C associates with Bazooka and controls polarity of epithelia and neuroblasts. *The Journal of Cell Biology*, *150*(6), 1361–1374.

Wu, J. I., Lessard, J., & Crabtree, G. R. (2009). Understanding the words of chromatin regulation. *Cell*, *136*(2), 200–206. doi:10.1016/j.cell.2009.01.009

Wu, J. I., Lessard, J., Olave, I. A., Qiu, Z., Ghosh, A., Graef, I. A., & Crabtree, G. R. (2007). Regulation of dendritic development by neuron-specific chromatin remodeling complexes. *Neuron*, *56*(1), 94–108. doi:10.1016/j.neuron.2007.08.021

Wu, P.-S., Egger, B., & Brand, A. H. (2008). Asymmetric stem cell division: lessons from Drosophila. *Seminars in Cell & Developmental Biology*, *19*(3), 283–293. doi:10.1016/j.semcdb.2008.01.007

Wysocka, J., Myers, M. P., Laherty, C. D., Eisenman, R. N., & Herr, W. (2003). Human Sin3 deacetylase and trithorax-related Set1/Ash2 histone H3-K4 methyltransferase are tethered together selectively by the cell-proliferation factor HCF-1. *Genes & Development*, *17*(7), 896–911. doi:10.1101/gad.252103

Xiao, Q., Komori, H., & Lee, C.-Y. (2012). klumpfuss distinguishes stem cells from progenitor cells

during asymmetric neuroblast division. *Development (Cambridge, England)*, *139*(15), 2670–2680. doi:10.1242/dev.081687

Yang, Z.-J., Ellis, T., Markant, S. L., Read, T.-A., Kessler, J. D., Bourboulas, M., et al. (2008). Medulloblastoma can be initiated by deletion of Patched in lineage-restricted progenitors or stem cells. *Cancer Cell*, *14*(2), 135–145. doi:10.1016/j.ccr.2008.07.003

Yoo, A. S., & Crabtree, G. R. (2009). ATP-dependent chromatin remodeling in neural development. *Current Opinion in Neurobiology*, *19*(2), 120–126. doi:10.1016/j.conb.2009.04.006

Yoo, A. S., Sun, A. X., Li, L., Shcheglovitov, A., Portmann, T., Li, Y., et al. (2011). MicroRNA-mediated conversion of human fibroblasts to neurons. *Nature*, *476*(7359), 228–231. doi:10.1038/nature10323

Yuzyuk, T., Fakhouri, T. H. I., Kiefer, J., & Mango, S. E. (2009). The polycomb complex protein mes-2/E(z) promotes the transition from developmental plasticity to differentiation in C. elegans embryos. *Developmental Cell*, *16*(5), 699–710. doi:10.1016/j.devcel.2009.03.008

Zacharioudaki, E., Magadi, S. S., & Delidakis, C. (2012). bHLH-O proteins are crucial for Drosophila neuroblast self-renewal and mediate Notch-induced overproliferation. *Development (Cambridge, England)*, *139*(7), 1258–1269. doi:10.1242/dev.071779

Zeng, X., Lin, X., & Hou, S. X. (2013). The Osa-containing SWI/SNF chromatin-remodeling complex regulates stem cell commitment in the adult Drosophila intestine. *Development (Cambridge, England)*, *140*(17), 3532–3540. doi:10.1242/dev.096891

Zhu, S., Barshow, S., Wildonger, J., Jan, L. Y., & Jan, Y.-N. (2011). Ets transcription factor Pointed promotes the generation of intermediate neural progenitors in Drosophila larval brains. *Proceedings of the National Academy of Sciences of the United States of America*, *108*(51), 20615–20620. doi:10.1073/pnas.1118595109

Zhu, S., Lin, S., Kao, C.-F., Awasaki, T., Chiang, A.-S., & Lee, T. (2006). Gradients of the Drosophila Chinmo BTB-zinc finger protein govern neuronal temporal identity. *Cell*, *127*(2), 409–422. doi:10.1016/j.cell.2006.08.045

8. CONTRIBUTIONS

Chapter I of this thesis is partially from the manuscript "The SWI/SNF complex ensures lineage progression and induces temporal patterning in *Drosophila* neural stem cell lineages" that is currently under review in Cell.

The genome-wide RNAi screen that identified the subunits of the SWI/SNF complex in self-renewal control was performed by Ralph Neumueller, Constance Richter, Anja Fischer, Maria Novatchkova, Klaus Neumueller and Juergen Knoblich. The subunit Snr1, was found to cause overproliferation by Catarina Homem. Bioinformatic analysis of the mRNA sequencing was performed by Thomas R. Burkard. Transplantation experiments were performed by Yanrui Jiang and Nidhi Saini in Dr. Heinrich Reichert's Laboratory. Mass spectrometry and analysis of the data were performed by the Protein Chemistry Department. Protocol for the chromatin preparation from FACS sorted cells was established in collaboration with Sarah K. Bowman in Robert Kingston's Laboratory. Dissection of the larval brains and FACS sorting for the ChIP-Seq experiments were done together with Lisa Landskron. Sequencing libraries were prepared by Sarah K. Bowman. Bioinformatic analysis of these data was performed by Michael Tolstorukov and Jakub Mieczkowski. The transcriptome analysis of neuroblasts and neurons were performed by Christian Berger and Heike Harzer. Rest of the work was contributed by the author of this thesis.

9. ACKNOWLEDGMENTS

I would like to express my gratitude to my supervisor Juergen Knoblich for reminding me the big picture whenever I got lost in details and his support during the preparation of the manuscript.

I would like to thank all the past and current members of the Lab for their passion in science, sports and success.

With no particular order I would like to thank:

Anja Fischer for her support in the first year of my PhD, for her friendship and for her sincerity.

Catarina Homem for being a fun neighbor in the 2. District, lab and flyroom!

Heike Harzer and Lilly Sommer for being my gym buddies and reminding me to have some fun.

Christoph Jueschke and Madeline Lancaster for their support during my paper and thesis writing times in the Postdoc office.

Ilka Reichardt for truly fruitful scientific discussions, sushi and movie nights.

Suzanne van der Horst for being my running partner and never leaving me behind.

Birgit Ritschka and Lisa Landskron for being great friends and all the Tapas in Spain.

Ailem: Annem ve babam, yaptığınız tüm fedekarlıklar için minnettarım. Sizin desteğiniz olmadan çılgın kariyer hayallerimi takip etmem mümkün değildi! Her şey için teşekkür ederim.

And finally a big thank you to my best-friend, my husband Mikael Andersson who has been through every step of this work supporting me and believing in me even when I had doubts.

CURRICULUM VITAE

ELIF EROGLU
IMBA, Dr. Bohr-Gasse 3, 1030 Vienna, Austria
0043 676 390 72 96
elif.eroglu@imba.oeaw.ac.at

EDUCATION

University of Vienna 2009 – present
Pre-doctoral student, Molecular Biology

Stanford University 2007 – 2009
Master of Science, Biological Sciences

Istanbul Technical University 2002 – 2007
Bachelor of Science, Molecular Biology and Genetics

RESEARCH EXPERIENCE

Dr. Juergen Knoblich's Laboratory September 2009 – present
IMBA – Institute of Molecular Biotechnology of the Austrian Academy of Sciences

Title: Role of the chromatin-remodeling SWI/SNF complex in *Drosophila* neural stem cell self-renewal control

Dr. Roel Nusse's Laboratory October 2007 – June 2009
Stanford University

Title: Investigating the role of Wnt proteins on the embryonic stem cell self-renewal.

Dr. Arzu Karabay's Laboratory January - August 2007
Istanbul Technical University

Title: Katanin and Spastin specific riboprobe design for expression analysis in chicken neural tissue

Dr. Harvey Lodish's Laboratory June - September 2006
Massachusetts Institute of Technology

Title: Signal transduction mediated by integrins in erythropoiesis.

SCHOLARSHIPS & AWARDS

Fulbright Scholarship for a Master of Science Degree 2007 – 2009
The Delta Kappa Gamma Society International, World Fellowship 2007 – 2009
Summa cum laude in Molecular Biology and Genetics 2007
Istanbul Technical University

Dr. Yuk. Muh. Orhan Ocalgiray High Honor Award, 2007
For graduating with the highest GPA among the Science and Letters Faculty

Istanbul Technical University - Massachusetts Institute of Technology 2005
Freshman Scholarship for high achievement in biology course
(Ranked 1st) Visited MIT for one week

SCIENTIFIC PUBLICATIONS

Berge D., Kurek D., Blauwkamp T., Koole W., Mass A., **Eroglu E.**, Siu R., Nusse R., Embryonic Stem cells require Wnt proteins to prevent differentiation to epiblast stem cells. *Nature Cell Biology*, 2011 Sep Vol.13, No.9: 1070-1075.

Berge D., Koole W., Fuerer C., Fish M., **Eroglu E.**, Nusse R. Wnt Signaling Mediates Self-Organization in Embryoid Bodies. *Cell Stem Cell*, 2008 Nov 6;3(5):508-18.

SCIENTIFIC PRESENTATIONS

Eroglu E., Burkard T.R., Saini N., Reichert H., Knoblich J.A., The SWI/SNF complex regulates the Prdm protein Hamlet to ensure lineage directionality in *Drosophila* neural stem cells., Poster Presentation, Cancer Epigenomics, Cell Symposia, October 6 – October 8, 2013.

Eroglu E., Neumuller R., Richter C., Fischer A., Novatchkova M., Knoblich J., Role of the SWI/SNF complex in the control of *Drosophila* neural stem cell self-renewal., Poster Presentation, Mechanisms of Eukaryotic Transcription, Cold Spring Harbor, August 30 – September 3, 2011.

APPENDIX

Supplemental Table 1: Differentially expressed genes in Osa tumor

FBgn_r5.44	gene_symbol	log2FoldChange	padj	FPKM-osa RNAi	FPKM-wild type
FBgn0003002	opa	Inf	3.01E-17	0	22.53
FBgn0002567	ltd		5.24E-13	25.01	0
FBgn0041087	wun2	Inf	2.85E-06	0	14.94
FBgn0003996	w	-2.134470523	6.14E-06	239.53	47.21
FBgn0003300	run	5.142620179	0.000288584	0.8	13.48
FBgn0000099	ap	Inf	0.000370831	0.03	7.61
FBgn0262735	Imp	-2.686104099	0.000524723	15.62	3.71
FBgn0028999	nerfin-1	3.044269021	0.001569106	3.24	24.3
FBgn0082585	sprt	2.835542001	0.001803727	3.1	26.93
FBgn0040348	CG3703	3.890822018	0.001872006	0.8	14.03
FBgn0003118	pnt	-2.199839324	0.002798845	53.28	13.83
FBgn0000411	D	1.863426939	0.003563098	23.77	82.31
FBgn0031401	papi	-4.238979692	0.003563098	15.21	3.06
FBgn0039972	CG17018		0.004748382	4.52	0
FBgn0000116	Argk	1.455016931	0.007406006	138.53	390.58
FBgn0035770	pst		0.018574805	7.4	0.67
FBgn0015625	CycB3	-1.487834934	0.019122336	163.76	54.38
FBgn0035656	CG10479	Inf	0.019122336	0	8.24
FBgn0051386	CR31386	-1.478855131	0.019122336	210.39	88.69
FBgn0010238	Lac	1.726686397	0.02168181	28.41	87.99
FBgn0021895	ytr	-1.345575987	0.022269928	402.96	154.18
FBgn0261613	Oaz	3.779816036	0.022269928	0.29	7.04
FBgn0008636	hbn	3.71282805	0.025118915	1.49	22.5
FBgn0033741	CG8545	-1.687449317	0.030929302	53.35	16.5
FBgn0034075	Asph		0.030929302	4.14	0
FBgn0003748	Treh	-1.806274258	0.034233105	47.11	12.65
FBgn0025360	Optix	1.730509741	0.035174867	19.6	54.12
FBgn0037845	CG14694	Inf	0.035174867	0	1.69
FBgn0035160	CG13897	2.176611367	0.037290723	13.61	47.6
FBgn0035989	CG3967	-1.957109886	0.037290723	53.49	13.67
FBgn0051144	CR31144	1.506438357	0.040567374	45.67	78.26
FBgn0037057	CG10512	-3.093234503	0.045404694	24.45	2.42
FBgn0003159	ptr	-3.643320865	0.061075092	5.79	0.49
FBgn0034908	CG5543	2.782839691	0.061075092	2.46	17.11
FBgn0038402	Fer2	Inf	0.061075092	0	7.31
FBgn0012036	Aldh	-1.543252633	0.065898184	84.94	30.18
FBgn0034724	CG3624	1.927498063	0.065898184	18.45	72.99
FBgn0045852	ham	1.48101961	0.065898184	18.05	50
FBgn0003719	tld		0.066285568	3.46	0.05
FBgn0003888	betaTub60D	-1.457236537	0.066285568	83.54	27.92
FBgn0062928	pncr009:3L	1.834606263	0.066285568	39.44	118.82
FBgn0259211	grh	-1.407131301	0.066285568	92.19	33.59

Supplemental Table 1: Differentially expressed genes in Osa tumor

FBgn_r5.44	gene_symbol	log2FoldChange	padj	FPKM-osa RNAi	FPKM-wild type
FBgn0001098	Gdh	-1.616424734	0.068960882	65.89	19.41
FBgn0015550	tap	1.594821491	0.068960882	27.17	81.39
FBgn0032651	Oli	1.705238499	0.068960882	29.42	94.98
FBgn0004875	enc	-1.354866186	0.084278156	40.11	15.57
FBgn0034013	unc-5	1.698195191	0.095637795	7.32	21.82
FBgn0053207	pxb		0.095637795	4.74	0
FBgn0010114	hig	2.210131997	0.099728985	2.79	12.96

Supplemental Table 2: Enriched GO terms in Osa tumor

GO-ID	corr p-value	Description
2001141	4.44E-04	regulation of RNA biosynthetic process
6355	4.44E-04	regulation of transcription, DNA-dependent
48513	4.44E-04	organ development
48731	4.44E-04	system development
51252	4.44E-04	regulation of RNA metabolic process
2000112	4.44E-04	regulation of cellular macromolecule biosynthetic process
10556	4.44E-04	regulation of macromolecule biosynthetic process
60255	4.44E-04	regulation of macromolecule metabolic process
10468	4.50E-04	regulation of gene expression
32501	4.50E-04	multicellular organismal process
31326	4.50E-04	regulation of cellular biosynthetic process
48699	4.50E-04	generation of neurons
9889	4.50E-04	regulation of biosynthetic process
19219	4.50E-04	regulation of nucleobase-containing compound metabolic process
51171	4.50E-04	regulation of nitrogen compound metabolic process
7275	5.07E-04	multicellular organismal development
32502	5.07E-04	developmental process
48856	5.07E-04	anatomical structure development
30182	5.07E-04	neuron differentiation
6357	5.36E-04	regulation of transcription from RNA polymerase II promoter
80090	5.36E-04	regulation of primary metabolic process
31323	7.10E-04	regulation of cellular metabolic process
19222	7.10E-04	regulation of metabolic process
7399	8.61E-04	nervous system development
48468	9.11E-04	cell development
904	2.04E-03	cell morphogenesis involved in differentiation
42221	2.08E-03	response to chemical stimulus
6935	2.08E-03	chemotaxis
30154	2.40E-03	cell differentiation
10628	2.44E-03	positive regulation of gene expression
48869	3.12E-03	cellular developmental process
9953	3.15E-03	dorsal/ventral pattern formation
45944	4.06E-03	positive regulation of transcription from RNA polymerase II promoter
48666	4.06E-03	neuron development
9653	4.29E-03	anatomical structure morphogenesis
902	5.06E-03	cell morphogenesis
42330	5.06E-03	taxis
10604	5.34E-03	positive regulation of macromolecule metabolic process
48812	5.73E-03	neuron projection morphogenesis
3002	5.73E-03	regionalization
7409	5.73E-03	axonogenesis

Supplemental Table 2: Enriched GO terms in Osa tumor

GO-ID	corr p-value	Description
31175	5.73E-03	neuron projection development
48667	5.86E-03	cell morphogenesis involved in neuron differentiation
40011	6.69E-03	locomotion
50794	7.29E-03	regulation of cellular process
22008	7.29E-03	neurogenesis
35282	7.32E-03	segmentation
7389	7.37E-03	pattern specification process
48858	8.04E-03	cell projection morphogenesis
32990	8.04E-03	cell part morphogenesis
7411	8.58E-03	axon guidance
9893	8.58E-03	positive regulation of metabolic process

Supplemenatl Table 3: Number of unique peptides identified in Brahma IP-mass spectrometry (over 95% probability, min 3 peptides, % coverage ≥4)

Identified Proteins	Accession Number	MW	Control 1	Sample 1	Control 2	Sample 2	Control 3	Sample 3	Control 4	Sample 4
brm-PC	FBpp0075278	185 kDa	0	0	0	0	0	5	0	7
mor-PB	FBpp0291706	125 kDa	0	0	0	0	0	0	0	0
osa-PB	FBpp0088543	284 kDa	0	3	0	0	0	28	0	4
mars-PA	FBpp0086788	102 kDa	0	0	0	0	0	0	0	0
Bap60-PA	FBpp0073572	58 kDa	0	0	0	0	0	0	0	0
dalao-PA	FBpp0071235	79 kDa	0	0	0	0	0	0	0	0
Sbf-PB	FBpp0082004	223 kDa	0	0	0	0	0	0	0	0
polybromo-PA	FBpp0084115	190 kDa	0	0	0	0	0	0	0	0
Reps-PA	FBpp0079817	96 kDa	0	0	0	0	0	0	0	0
Bap170-PA	FBpp0085442	183 kDa	0	0	0	0	0	0	0	0
d4-PA	FBpp0085418	55 kDa	0	0	0	0	0	0	0	0
e(y)3-PA	FBpp0074531	213 kDa	0	0	0	0	0	5	0	11
mtm-PA	FBpp0078854	70 kDa	0	0	0	0	0	0	0	0
CG7154-PA	FBpp0079111	96 kDa	0	0	0	0	0	0	0	0
Ubi-p5E-PA	FBpp0070894	60 kDa	0	0	0	0	0	0	0	0
l(3)j2D3-PA	FBpp0075723	45 kDa	0	0	0	0	0	0	0	0
mod(mdg4)-PF	FBpp0083464	59 kDa	0	0	0	0	0	0	0	0
KrT95D-PB	FBpp0083894	125 kDa	0	0	0	0	0	0	0	0
CG12333-PA	FBpp0083070	53 kDa	0	0	0	0	0	0	0	0
Glt-PC	FBpp0079329	119 kDa	0	0	0	0	0	0	0	0
LBR-PB	FBpp0071628	80 kDa	0	0	0	0	0	0	0	0
CG5726-PA	FBpp0085951	87 kDa	0	0	0	0	0	0	0	0
betaTub56D-PB	FBpp0085720	50 kDa	0	0	0	0	0	0	0	0
CG10732-PA	FBpp0075586	184 kDa	0	0	0	0	0	0	0	0
Gnf1-PA	FBpp0078478	109 kDa	0	0	0	0	0	0	0	0
CG8478-PB	FBpp0081611	62 kDa	0	0	0	0	0	0	0	0

Supplemenatl Table 3: Number of unique peptides identified in Brahma IP-mass spectrometry (over 95% probability, min 3 peptides, % coverage ≥4)

Identified Proteins	Accession Number	MW	Control 1	Sample 1	Control 2	Sample 2	Control 3	Sample 3	Control 4	Sample 4
CG17838-PA	FBpp0083365	63 kDa	0	0	0	0	0	0	0	0
Bap55-PA	FBpp0086115	47 kDa	0	0	0	0	0	0	0	0
uzip-PA	FBpp0072304	54 kDa	0	0	0	0	0	0	0	0
CG18259-PA	FBpp0074432	53 kDa	0	0	0	0	0	0	0	0
CG6455-PC	FBpp0288710	82 kDa	0	0	0	0	0	0	0	0
CG8798-PC	FBpp0271918	115 kDa	0	0	0	0	0	0	0	0
Rpd3-PA	FBpp0073173	58 kDa	0	0	0	0	0	0	0	0
CG8108-PA	FBpp0076068	103 kDa	0	0	0	0	0	0	0	0
bor-PA	FBpp0082728	68 kDa	0	0	0	0	0	0	0	0
pUf68-PA	FBpp0072593	68 kDa	0	0	0	0	0	0	0	0
CG6905-PA	FBpp0072468	93 kDa	0	0	0	0	0	0	0	0
Sas-4-PA	FBpp0081088	103 kDa	0	0	0	0	0	0	0	0
PH4alphaEFB-PA	FBpp0085012	63 kDa	0	0	0	0	0	0	0	0
lost-PA	FBpp0078561	60 kDa	0	0	0	0	0	0	0	0

Supplemenatl Table 3: Number of unique peptides identified in Brahma IP-mass spectrometry (over 95% probability, min 3 peptides, % coverage ≥4)

Identified Proteins	Accession Number	MW	Control 5	Sample 5	Control 6	Sample 6	Control 7	Sample 7	Control 8	Sample 8
brm-PC	FBpp0075278	185 kDa	0	16	0	58	0	6	0	0
mor-PB	FBpp0291706	125 kDa	0	0	0	0	0	45	0	5
osa-PB	FBpp0088543	284 kDa	0	0	0	0	0	0	0	0
mars-PA	FBpp0086788	102 kDa	0	0	0	0	0	0	0	14
Bap60-PA	FBpp0073572	58 kDa	0	0	0	0	0	0	0	0
dalao-PA	FBpp0071235	79 kDa	0	0	0	0	0	0	0	0
Sbf-PB	FBpp0082004	223 kDa	0	14	0	20	0	0	0	0
polybromo-PA	FBpp0084115	190 kDa	0	0	0	25	0	0	0	0
Reps-PA	FBpp0079817	96 kDa	0	0	0	0	0	5	0	15
Bap170-PA	FBpp0085442	183 kDa	0	0	0	23	0	0	0	0
d4-PA	FBpp0085418	55 kDa	0	0	0	0	0	0	0	0
e(y)3-PA	FBpp0074531	213 kDa	0	0	0	0	0	0	0	0
mtm-PA	FBpp0078854	70 kDa	0	0	0	0	0	0	0	0
CG7154-PA	FBpp0079111	96 kDa	0	0	0	0	0	0	0	3
Ubi-p5E-PA	FBpp0070894	60 kDa	0	0	0	0	0	0	0	4
l(3)j2D3-PA	FBpp0075723	45 kDa	0	0	0	0	0	0	0	0
mod(mdg4)-PF	FBpp0083464	59 kDa	0	0	0	0	0	0	0	0
KrT95D-PB	FBpp0083894	125 kDa	0	0	0	0	0	0	0	13
CG12333-PA	FBpp0083070	53 kDa	0	0	0	0	0	0	0	0
Glt-PC	FBpp0079329	119 kDa	0	0	0	0	0	12	0	0
LBR-PB	FBpp0071628	80 kDa	0	0	0	0	0	0	0	0
CG5726-PA	FBpp0085951	87 kDa	0	0	0	0	0	0	0	0
betaTub56D-PB	FBpp0085720	50 kDa	0	0	0	0	0	0	0	0
CG10732-PA	FBpp0075586	184 kDa	0	8	0	3	0	0	0	0
Gnf1-PA	FBpp0078478	109 kDa	0	0	0	0	0	0	0	0
CG8478-PB	FBpp0081611	62 kDa	0	0	0	0	0	0	0	0

Supplemenatl Table 3: Number of unique peptides identified in Brahma IP-mass spectrometry (over 95% probability, min 3 peptides, % coverage ≥4)

Identified Proteins	Accession Number	MW	Control 5	Sample 5	Control 6	Sample 6	Control 7	Sample 7	Control 8	Sample 8
CG17838-PA	FBpp0083365	63 kDa	0	0	0	0	0	0	0	0
Bap55-PA	FBpp0086115	47 kDa	0	0	0	0	0	0	0	0
uzip-PA	FBpp0072304	54 kDa	0	0	0	0	0	0	0	0
CG18259-PA	FBpp0074432	53 kDa	0	0	0	0	0	0	0	0
CG6455-PC	FBpp0288710	82 kDa	0	0	0	0	0	0	0	0
CG8798-PC	FBpp0271918	115 kDa	0	0	0	0	0	0	0	0
Rpd3-PA	FBpp0073173	58 kDa	0	0	0	0	0	0	0	0
CG8108-PA	FBpp0076068	103 kDa	0	0	0	0	0	0	0	3
bor-PA	FBpp0082728	68 kDa	0	0	0	0	0	0	0	0
pUf68-PA	FBpp0072593	68 kDa	0	0	0	0	0	0	0	0
CG6905-PA	FBpp0072468	93 kDa	0	0	0	0	0	0	0	0
Sas-4-PA	FBpp0081088	103 kDa	0	0	0	0	0	0	0	0
PH4alphaEFB-PA	FBpp0085012	63 kDa	0	0	0	0	0	0	0	0
lost-PA	FBpp0078561	60 kDa	0	0	0	0	0	0	0	0

Supplemenatl Table 3: Number of unique peptides identified in Brahma IP-mass spectrometry (over 95% probability, min 3 peptides, % coverage ≥4)

Identified Proteins	Accession Number	MW	Control 9	Sample 9	Control 10	Sample 10	Control 11	Sample 11	Control 12	Sample 12
brm-PC	FBpp0075278	185 kDa	0	0	0	0	0	0	0	0
mor-PB	FBpp0291706	125 kDa	0	3	0	0	0	0	0	0
osa-PB	FBpp0088543	284 kDa	0	0	0	0	0	0	0	0
mars-PA	FBpp0086788	102 kDa	0	34	0	7	0	0	0	0
Bap60-PA	FBpp0073572	58 kDa	0	0	0	0	0	6	0	11
dalao-PA	FBpp0071235	79 kDa	0	6	0	10	0	0	0	0
Sbf-PB	FBpp0082004	223 kDa	0	0	0	0	0	0	0	0
polybromo-PA	FBpp0084115	190 kDa	0	0	0	0	0	0	0	0
Reps-PA	FBpp0079817	96 kDa	0	9	0	0	0	0	0	0
Bap170-PA	FBpp0085442	183 kDa	0	0	0	0	0	0	0	0
d4-PA	FBpp0085418	55 kDa	0	0	0	0	0	0	0	9
e(y)3-PA	FBpp0074531	213 kDa	0	0	0	0	0	0	0	0
mtm-PA	FBpp0078854	70 kDa	0	0	0	0	0	0	0	12
CG7154-PA	FBpp0079111	96 kDa	0	6	0	0	0	0	0	0
Ubi-p5E-PA	FBpp0070894	60 kDa	0	0	0	0	0	0	0	0
l(3)j2D3-PA	FBpp0075723	45 kDa	0	0	0	0	0	0	0	0
mod(mdg4)-PF	FBpp0083464	59 kDa	0	0	0	0	0	10	0	0
KrT95D-PB	FBpp0083894	125 kDa	0	0	0	0	0	0	0	0
CG12333-PA	FBpp0083070	53 kDa	0	0	0	0	0	0	0	0
Glt-PC	FBpp0079329	119 kDa	0	0	0	0	0	0	0	0
LBR-PB	FBpp0071628	80 kDa	0	0	0	0	0	5	0	7
CG5726-PA	FBpp0085951	87 kDa	0	3	0	4	0	0	0	3
betaTub56D-PB	FBpp0085720	50 kDa	0	0	0	0	0	0	0	3
CG10732-PA	FBpp0075586	184 kDa	0	0	0	0	0	0	0	0
Gnf1-PA	FBpp0078478	109 kDa	0	4	0	0	0	0	0	0
CG8478-PB	FBpp0081611	62 kDa	0	0	0	0	0	0	0	5

Supplemenatl Table 3: Number of unique peptides identified in Brahma IP-mass spectrometry (over 95% probability, min 3 peptides, % coverage ≥4)

Identified Proteins	Accession Number	MW	Control 9	Sample 9	Control 10	Sample 10	Control 11	Sample 11	Control 12	Sample 12
CG17838-PA	FBpp0083365	63 kDa	0	0	0	0	0	0	0	5
Bap55-PA	FBpp0086115	47 kDa	0	0	0	0	0	3	0	0
uzip-PA	FBpp0072304	54 kDa	0	0	0	0	0	3	0	0
CG18259-PA	FBpp0074432	53 kDa	0	0	0	0	0	0	0	0
CG6455-PC	FBpp0288710	82 kDa	0	0	0	0	0	4	0	0
CG8798-PC	FBpp0271918	115 kDa	0	0	0	5	0	0	0	0
Rpd3-PA	FBpp0073173	58 kDa	0	0	0	0	0	0	0	5
CG8108-PA	FBpp0076068	103 kDa	0	0	0	0	0	0	0	0
bor-PA	FBpp0082728	68 kDa	0	0	0	0	0	0	0	4
pUf68-PA	FBpp0072593	68 kDa	0	0	0	0	0	4	0	0
CG6905-PA	FBpp0072468	93 kDa	0	0	0	3	0	0	0	0
Sas-4-PA	FBpp0081088	103 kDa	0	3	0	0	0	0	0	0
PH4alphaEFB-PA	FBpp0085012	63 kDa	0	0	0	0	0	0	0	4
lost-PA	FBpp0078561	60 kDa	0	0	0	0	0	3	0	0

Supplemenatl Table 3: Number of unique peptides identified in Brahma IP-mass spectrometry (over 95% probability, min 3 peptides, % coverage ≥4)

Identified Proteins	Accession Number	MW	Control 13	Sample 13
brm-PC	FBpp0075278	185 kDa	0	0
mor-PB	FBpp0291706	125 kDa	0	0
osa-PB	FBpp0088543	284 kDa	0	0
mars-PA	FBpp0086788	102 kDa	0	0
Bap60-PA	FBpp0073572	58 kDa	0	25
dalao-PA	FBpp0071235	79 kDa	0	0
Sbf-PB	FBpp0082004	223 kDa	0	0
polybromo-PA	FBpp0084115	190 kDa	0	0
Reps-PA	FBpp0079817	96 kDa	0	0
Bap170-PA	FBpp0085442	183 kDa	0	0
d4-PA	FBpp0085418	55 kDa	0	6
e(y)3-PA	FBpp0074531	213 kDa	0	0
mtm-PA	FBpp0078854	70 kDa	0	0
CG7154-PA	FBpp0079111	96 kDa	0	0
Ubi-p5E-PA	FBpp0070894	60 kDa	0	0
l(3)j2D3-PA	FBpp0075723	45 kDa	0	7
mod(mdg4)-PF	FBpp0083464	59 kDa	0	0
KrT95D-PB	FBpp0083894	125 kDa	0	0
CG12333-PA	FBpp0083070	53 kDa	0	8
Glt-PC	FBpp0079329	119 kDa	0	0
LBR-PB	FBpp0071628	80 kDa	0	0
CG5726-PA	FBpp0085951	87 kDa	0	0
betaTub56D-PB	FBpp0085720	50 kDa	0	6
CG10732-PA	FBpp0075586	184 kDa	0	0
Gnf1-PA	FBpp0078478	109 kDa	0	0
CG8478-PB	FBpp0081611	62 kDa	0	0

Supplemenatl Table 3: Number of unique peptides identified in Brahma IP-mass spectrometry (over 95% probability, min 3 peptides, % coverage ≥4)

Identified Proteins	Accession Number	MW	Control 13	Sample 13
CG17838-PA	FBpp0083365	63 kDa	0	0
Bap55-PA	FBpp0086115	47 kDa	0	0
uzip-PA	FBpp0072304	54 kDa	0	0
CG18259-PA	FBpp0074432	53 kDa	0	5
CG6455-PC	FBpp0288710	82 kDa	0	0
CG8798-PC	FBpp0271918	115 kDa	0	0
Rpd3-PA	FBpp0073173	58 kDa	0	0
CG8108-PA	FBpp0076068	103 kDa	0	0
bor-PA	FBpp0082728	68 kDa	0	0
pUf68-PA	FBpp0072593	68 kDa	0	0
CG6905-PA	FBpp0072468	93 kDa	0	0
Sas-4-PA	FBpp0081088	103 kDa	0	0
PH4alphaEFB-PA	FBpp0085012	63 kDa	0	0
lost-PA	FBpp0078561	60 kDa	0	0

Supplemental Table 4: Number of unique peptides identified in Osa-GFP IP-mass spectrometry (over 95% probability, min. 3 peptides, % coverage ≥4)

Identified Proteins	Accession Number	MW	Control 1	Sample 1	Control 2	Sample 2	Control 3	Sample 3	Control 4	Sample 4
mor-PB	FBpp0291706	125 kDa	0	0	0	0	0	3	0	26
osa-PB	FBpp0088543	284 kDa	0	32	0	10	0	4	0	0
brm-PC	FBpp0075278	185 kDa	0	0	0	3	0	50	0	0
dalao-PA	FBpp0071235	79 kDa	0	0	0	0	0	0	0	0
Bap55-PA	FBpp0086115	47 kDa	0	0	0	0	0	0	0	0
CG5033-PA	FBpp0088519	90 kDa	0	0	0	0	0	0	0	0
koi-PB	FBpp0292403	64 kDa	0	0	0	0	0	0	0	0
Ef1gamma-PB	FBpp0084761	49 kDa	0	0	0	0	0	0	0	0
rhea-PA	FBpp0076353	307 kDa	0	0	0	9	0	0	0	0
Snr1-PA	FBpp0078331	42 kDa	0	0	0	0	0	0	0	0
RpL3-PA	FBpp0081822	47 kDa	0	0	0	0	0	0	0	0
eIF4AIII-PA	FBpp0081324	46 kDa	0	0	0	0	0	0	0	0
Ald-PB	FBpp0084367	39 kDa	0	0	0	0	0	0	0	0
l(1)G0020-PA	FBpp0071217	113 kDa	0	0	0	0	0	0	0	0
CG12050-PB	FBpp0113107	120 kDa	0	0	0	0	0	0	0	0
pav-PA	FBpp0073083	101 kDa	0	0	0	0	0	0	0	0
CG17838-PA	FBpp0083365	63 kDa	0	0	0	0	0	0	0	0
CG3287-PB	FBpp0085490	52 kDa	0	0	0	0	0	0	0	0
CG6905-PA	FBpp0072468	93 kDa	0	0	0	0	0	0	0	0
CG8108-PA	FBpp0076068	103 kDa	0	0	0	0	0	0	0	0
CG4849-PA	FBpp0084626	111 kDa	0	0	0	0	0	0	0	0
CG34417-PC	FBpp0111615	97 kDa	0	0	0	0	0	0	0	0

Supplemental Table 4: Number of unique peptides identified in Osa-GFP IP-mass spectrometry (over 95% probability, min. 3 peptides, % coverage ≥4)

Identified Proteins	Accession Number	MW	Control 5	Sample 5	Sample 6	Control 7	Sample 7	Control 8	Sample 8	Control 9	Sample 9
mor-PB	FBpp0291706	125 kDa	0	36	7	0	4	0	0	0	0
osa-PB	FBpp0088543	284 kDa	0	0	0	0	0	0	0	0	0
brm-PC	FBpp0075278	185 kDa	0	0	0	0	0	0	0	0	0
dalao-PA	FBpp0071235	79 kDa	0	0	0	0	23	0	0	0	0
Bap55-PA	FBpp0086115	47 kDa	0	0	0	0	0	0	11	0	0
CG5033-PA	FBpp0088519	90 kDa	0	0	0	3	12	0	0	0	0
koi-PB	FBpp0292403	64 kDa	0	0	0	0	10	0	0	0	0
Ef1gamma-PB	FBpp0084761	49 kDa	0	0	0	0	0	0	0	0	9
rhea-PA	FBpp0076353	307 kDa	0	0	0	0	0	0	0	0	0
Snr1-PA	FBpp0078331	42 kDa	0	0	0	0	0	0	0	0	6
RpL3-PA	FBpp0081822	47 kDa	0	0	0	0	0	0	0	0	5
eIF4AIII-PA	FBpp0081324	46 kDa	0	0	0	0	0	0	0	0	7
Ald-PB	FBpp0084367	39 kDa	0	0	0	0	0	0	0	0	5
l(1)G0020-PA	FBpp0071217	113 kDa	0	0	0	0	5	0	0	0	0
CG12050-PB	FBpp0113107	120 kDa	0	0	0	0	5	0	0	0	0
pav-PA	FBpp0073083	101 kDa	0	0	0	0	5	0	0	0	0
CG17838-PA	FBpp0083365	63 kDa	0	0	0	0	0	0	0	0	0
CG3287-PB	FBpp0085490	52 kDa	0	0	0	0	3	0	0	0	0
CG6905-PA	FBpp0072468	93 kDa	0	0	0	0	3	0	0	0	0
CG8108-PA	FBpp0076068	103 kDa	0	0	4	0	0	0	0	0	0
CG4849-PA	FBpp0084626	111 kDa	0	0	0	0	5	0	0	0	0
CG34417-PC	FBpp0111615	97 kDa	0	0	0	0	3	0	0	0	0

Supplemental Table 5: Number of unique peptide identified in Osa-GFP IP-mass spectrometry (over 95% probability, min 2 peptides, % coverage ≥ 6.5)

Identified Proteins	Accession Number	MW	Control	Sample
mor-PA	FBpp0082692	131 kDa	0	41
brm-PC	FBpp0075278	185 kDa	0	39
osa-PB	FBpp0088543	284 kDa	0	40
dalao-PA	FBpp0071235	79 kDa	0	20
Bap60-PA	FBpp0073572	58 kDa	0	18
Bap55-PA	FBpp0086115	47 kDa	0	12
d4-PA	FBpp0085418	55 kDa	0	12
Snr1-PA	FBpp0078331	42 kDa	0	8
BCL7-like-PA	FBpp0071293	17 kDa	0	6
His2Av-PA	FBpp0084434	15 kDa	0	2
alphaTub84D-PA	FBpp0081062	50 kDa	0	4
tth-PB	FBpp0073680	45 kDa	0	2
Ccp84Ae-PA	FBpp0081192	21 kDa	0	5
mor-PB	FBpp0291706	125 kDa	0	2
Pabp2-PA	FBpp0087863	25 kDa	0	2
CG14235-PA	FBpp0074584	11 kDa	0	2

Supplemental Table 6: Number of unique peptides identified in Osa IP-mass spectrometry from wild type and brat mutant larval brain extracts (over 95% probability, min 3 peptides)

Identified Proteins	Accession Number	Molecular Weight	wild type	*brat* mutant
mor-PA	FBpp0082692	131 kDa	42	37
brm-PC	FBpp0075278	185 kDa	39	38
osa-PB	FBpp0088543	284 kDa	37	38
dalao-PA	FBpp0071235	79 kDa	19	21
Act5C-PA	FBpp0070787	42 kDa	15	12
Bap60-PA	FBpp0073572	58 kDa	21	17
Bap55-PA	FBpp0086115	47 kDa	15	13
Tsc1-PA	FBpp0083931	125 kDa	19	16
gig-PA	FBpp0074588	204 kDa	16	11
betaTub56D-PB	FBpp0085720	50 kDa	16	9
CG2950-PA	FBpp0077100	70 kDa	16	11
d4-PA	FBpp0085418	55 kDa	9	11
Snr1-PA	FBpp0078331	42 kDa	11	7
crp-PA	FBpp0080411	67 kDa	8	10
sub-PA	FBpp0086041	71 kDa	10	15
AGO2-PB	FBpp0075312	137 kDa	11	9
alphaTub84D-PA	FBpp0081062	50 kDa	10	4
wee-PA	FBpp0078999	69 kDa	6	13
CG2519-PA	FBpp0078408	147 kDa	17	0
sbb-PD	FBpp0290762	230 kDa	9	6
CG6455-PC	FBpp0288710	82 kDa	10	9
Ef1alpha48D-PA	FBpp0087142	50 kDa	10	4
eIF-4E-PC	FBpp0076216	28 kDa	6	3
fabp-PB	FBpp0099726	15 kDa	6	5
BCL7-like-PA	FBpp0071293	17 kDa	4	4
Lmpt-PG	FBpp0291919	64 kDa	6	5
Obp44a-PA	FBpp0087892	16 kDa	7	7
Eno-PB	FBpp0077571	54 kDa	9	4
CG8486-PE	FBpp0289561	307 kDa	7	3
Rapgap1-PD	FBpp0111515	101 kDa	7	0
CG4877-PB	FBpp0075144	125 kDa	4	5
Df31-PA	FBpp0085273	19 kDa	4	4
CG34325-PA	FBpp0111439	20 kDa	4	0
awd-PA	FBpp0085223	19 kDa	4	0
CG14985-PB	FBpp0288415	28 kDa	3	0
Ald-PB	FBpp0084367	39 kDa	4	0
Ef2b-PA	FBpp0085265	94 kDa	4	0
Argk-PA	FBpp0076270	61 kDa	5	0
blw-PA	FBpp0071794	59 kDa	5	0
CG10274-PA	FBpp0076726	59 kDa	0	3
Nlp-PA	FBpp0084918	17 kDa	3	0

Identified Proteins	Accession Number	Molecular Weight	wild type	*brat* mutant
l(3)03670-PA	FBpp0085107	24 kDa	3	0
smt3-PA	FBpp0078984	10 kDa	4	0
ATPsyn-beta-PA	FBpp0088250	54 kDa	3	0
Pdi-PA	FBpp0075401	56 kDa	3	0
CG2950-PD	FBpp0290163	83 kDa	3	0
FK506-bp2-PA	FBpp0085703	12 kDa	3	0
CG2852-PA	FBpp0071844	22 kDa	3	0

Supplemental Table 7: List of balanced genes in neuroblasts (balanced = show enrichment for both H3K4me3 and H3K27me3 mark)

Gene ID	Gene Symbol	H3K4me3 mark	H3K27me3 mark
FBgn0028400	Syt4	enriched	enriched
FBgn0036354	Poc1	enriched	enriched
FBgn0036277	CG10418	enriched	enriched
FBgn0014343	mirr	enriched	enriched
FBgn0036286	CG10616	enriched	enriched
FBgn0004882	orb	enriched	enriched
FBgn0031376	Der-1	enriched	enriched
FBgn0013954	FK506-bp2	enriched	enriched
FBgn0031732	CG11149	enriched	enriched
FBgn0019650	toy	enriched	enriched
FBgn0004880	scrt	enriched	enriched
FBgn0024836	stan	enriched	enriched
FBgn0040281	Aplip1	enriched	enriched
FBgn0035179	CG12038	enriched	enriched
FBgn0039808	CG12071	enriched	enriched
FBgn0004102	oc	enriched	enriched
FBgn0010238	Lac	enriched	enriched
FBgn0039588	CG12413	enriched	enriched
FBgn0035481	CG12605	enriched	enriched
FBgn0035086	CG12851	enriched	enriched
FBgn0031270	CG13689	enriched	enriched
FBgn0003866	tsh	enriched	enriched
FBgn0003720	tll	enriched	enriched
FBgn0034501	CG13868	enriched	enriched
FBgn0028999	nerfin-1	enriched	enriched
FBgn0011656	Mef2	enriched	enriched
FBgn0002733	HLH-mbeta	enriched	enriched
FBgn0010473	tutl	enriched	enriched
FBgn0038834	RpS30	enriched	enriched
FBgn0003430	slp1	enriched	enriched
FBgn0259938	cwo	enriched	enriched
FBgn0024245	dnt	enriched	enriched
FBgn0011202	dia	enriched	enriched
FBgn0010316	dap	enriched	enriched
FBgn0033159	Dscam	enriched	enriched
FBgn0037525	CG17816	enriched	enriched
FBgn0040778	CG17977	enriched	enriched
FBgn0032723	ssp3	enriched	enriched
FBgn0003300	run	enriched	enriched
FBgn0003093	Pkc98E	enriched	enriched
FBgn0039688	Kul	enriched	enriched
FBgn0039883	RhoGAP100F	enriched	enriched

Supplemental Table 7: List of balanced genes in neuroblasts (balanced = show enrichment for both H3K4me3 and H3K27me3 mark)

Gene ID	Gene Symbol	H3K4me3 mark	H3K27me3 mark
FBgn0000928	fs(1)Yb	enriched	enriched
FBgn0004567	slp2	enriched	enriched
FBgn0050015	CG30015	enriched	enriched
FBgn0016672	Ipp	enriched	enriched
FBgn0050296	RIC-3	enriched	enriched
FBgn0051140	CG31140	enriched	enriched
FBgn0261649	tinc	enriched	enriched
FBgn0051457	CG31457	enriched	enriched
FBgn0051637	CG31637	enriched	enriched
FBgn0052452	CG32452	enriched	enriched
FBgn0053017	CG33017	enriched	enriched
FBgn0085409	CG34380	enriched	enriched
FBgn0085432	pan	enriched	enriched
FBgn0038461	CG3678	enriched	enriched
FBgn0003391	shg	enriched	enriched
FBgn0038837	CG3822	enriched	enriched
FBgn0005624	Psc	enriched	enriched
FBgn0033793	CG3955	enriched	enriched
FBgn0023170	RpL39	enriched	enriched
FBgn0265047	fdy	enriched	enriched
FBgn0259927	CG42450	enriched	enriched
FBgn0263000	CG43308	enriched	enriched
FBgn0037024	CG4365	enriched	enriched
FBgn0263707	CG43659	enriched	enriched
FBgn0263995	cpo	enriched	enriched
FBgn0264090	CG43759	enriched	enriched
FBgn0264574	Glut1	enriched	enriched
FBgn0037849	CG4596	enriched	enriched
FBgn0032225	CG5022	enriched	enriched
FBgn0032229	CG5045	enriched	enriched
FBgn0032236	mRpS7	enriched	enriched
FBgn0034371	SP2637	enriched	enriched
FBgn0003330	Sce	enriched	enriched
FBgn0032210	CYLD	enriched	enriched
FBgn0038519	Prx3	enriched	enriched
FBgn0038401	CG5916	enriched	enriched
FBgn0010612	l(2)06225	enriched	enriched
FBgn0037802	Sirt6	enriched	enriched
FBgn0262742	Fas1	enriched	enriched
FBgn0263395	hppy	enriched	enriched
FBgn0037151	CG7130	enriched	enriched
FBgn0031952	cdc14	enriched	enriched

Supplemental Table 7: List of balanced genes in neuroblasts (balanced = show enrichment for both H3K4me3 and H3K27me3 mark)

Gene ID	Gene Symbol	H3K4me3 mark	H3K27me3 mark
FBgn0036499	CG7276	enriched	enriched
FBgn0015550	tap	enriched	enriched
FBgn0243512	puc	enriched	enriched
FBgn0038889	CG7922	enriched	enriched
FBgn0003714	tko	enriched	enriched
FBgn0033911	VGAT	enriched	enriched
FBgn0015299	Ssb-c31a	enriched	enriched
FBgn0036900	CG8765	enriched	enriched
FBgn0030706	CG8909	enriched	enriched
FBgn0030092	fh	enriched	enriched
FBgn0034564	CG9344	enriched	enriched
FBgn0031081	Nep3	enriched	enriched
FBgn0051603	tRNA:CR31603	enriched	enriched
FBgn0262108	CR42861	enriched	enriched

Supplemental Table 8: Enriched GO terms in genes that are balanced in NBs

GO-ID	corr p-value	Description
6357	1.81E-06	regulation of transcription from RNA polymerase II promoter
50794	1.81E-06	regulation of cellular process
48523	1.81E-06	negative regulation of cellular process
50789	8.26E-06	regulation of biological process
65007	8.26E-06	biological regulation
48519	9.95E-06	negative regulation of biological process
904	4.64E-05	**cell morphogenesis involved in differentiation**
80090	4.73E-05	regulation of primary metabolic process
31323	7.07E-05	regulation of cellular metabolic process
32989	8.66E-05	cellular component morphogenesis
19219	8.66E-05	regulation of nucleobase-containing compound metabolic process
45892	8.66E-05	negative regulation of transcription, DNA-dependent
51171	8.66E-05	regulation of nitrogen compound metabolic process
51253	9.79E-05	negative regulation of RNA metabolic process
51252	9.79E-05	regulation of RNA metabolic process
2000112	9.86E-05	regulation of cellular macromolecule biosynthetic process
10556	9.86E-05	regulation of macromolecule biosynthetic process
6355	9.86E-05	regulation of transcription, DNA-dependent
2001141	9.86E-05	regulation of RNA biosynthetic process
45934	9.86E-05	negative regulation of nucleobase-containing compound metabolic process
51172	9.86E-05	negative regulation of nitrogen compound metabolic process
7350	1.03E-04	blastoderm segmentation
31324	1.19E-04	negative regulation of cellular metabolic process
902	1.19E-04	cell morphogenesis
60255	1.28E-04	regulation of macromolecule metabolic process
42221	1.30E-04	response to chemical stimulus
31326	1.40E-04	regulation of cellular biosynthetic process
9889	1.40E-04	regulation of biosynthetic process
9880	1.40E-04	embryonic pattern specification
2000113	1.67E-04	negative regulation of cellular macromolecule biosynthetic process
10558	1.67E-04	negative regulation of macromolecule biosynthetic process
7411	1.69E-04	**axon guidance**
9890	1.81E-04	negative regulation of biosynthetic process
31327	1.81E-04	negative regulation of cellular biosynthetic process
10468	1.81E-04	regulation of gene expression
19222	1.92E-04	regulation of metabolic process
6935	2.16E-04	chemotaxis
122	2.40E-04	negative regulation of transcription from RNA polymerase II promoter
7409	2.40E-04	**axonogenesis**
50896	2.74E-04	response to stimulus
9790	2.74E-04	embryo development
70593	3.10E-04	**dendrite self-avoidance**

GO-ID	corr p-value	Description
9653	3.69E-04	anatomical structure morphogenesis
35282	3.87E-04	segmentation
10629	3.87E-04	negative regulation of gene expression
10605	4.15E-04	negative regulation of macromolecule metabolic process
48468	5.12E-04	cell development
9892	5.66E-04	negative regulation of metabolic process
30154	5.87E-04	**cell differentiation**
7399	6.47E-04	**nervous system development**
48812	6.77E-04	**neuron projection morphogenesis**
31175	6.80E-04	**neuron projection development**
48667	7.15E-04	**cell morphogenesis involved in neuron differentiation**
7156	7.48E-04	homophilic cell adhesion
42330	7.93E-04	taxis
48869	8.19E-04	cellular developmental process
48666	8.20E-04	**neuron development**
48699	8.82E-04	generation of neurons
31098	8.82E-04	stress-activated protein kinase signaling cascade
7423	1.01E-03	sensory organ development
48858	1.23E-03	cell projection morphogenesis
32990	1.23E-03	cell part morphogenesis
45165	1.78E-03	**cell fate commitment**
8056	1.78E-03	ocellus development
7369	2.26E-03	gastrulation
7365	2.48E-03	periodic partitioning
30182	2.76E-03	**neuron differentiation**
7275	3.05E-03	multicellular organismal development
16043	3.13E-03	cellular component organization
48731	3.13E-03	system development
19896	3.16E-03	**axon transport of mitochondrion**
48598	3.16E-03	embryonic morphogenesis
30030	3.35E-03	cell projection organization
48729	3.35E-03	tissue morphogenesis
32501	3.74E-03	multicellular organismal process
23052	3.74E-03	signaling
10604	3.81E-03	positive regulation of macromolecule metabolic process
9605	3.86E-03	response to external stimulus
9987	4.19E-03	cellular process
35287	4.20E-03	head segmentation
32502	4.25E-03	developmental process
71840	4.30E-03	cellular component organization or biogenesis
31328	4.30E-03	positive regulation of cellular biosynthetic process
9891	4.36E-03	positive regulation of biosynthetic process
71842	4.48E-03	cellular component organization at cellular level

Supplemental Table 8: Enriched GO terms in genes that are balanced in NBs

GO-ID	corr p-value	Description
7154	4.48E-03	cell communication
42067	4.48E-03	establishment of ommatidial planar polarity
7422	4.91E-03	peripheral nervous system development
60322	4.91E-03	head development
50793	5.20E-03	regulation of developmental process
71841	6.22E-03	cellular component organization or biogenesis at cellular level
1654	6.26E-03	eye development
51254	6.63E-03	positive regulation of RNA metabolic process
16318	6.63E-03	ommatidial rotation
16337	6.82E-03	cell-cell adhesion
7243	6.82E-03	intracellular protein kinase cascade
31325	6.82E-03	positive regulation of cellular metabolic process
10557	6.83E-03	positive regulation of macromolecule biosynthetic process
7389	7.04E-03	pattern specification process
7254	7.60E-03	JNK cascade
45935	7.60E-03	positive regulation of nucleobase-containing compound metabolic process
51173	7.60E-03	positive regulation of nitrogen compound metabolic process
9893	7.60E-03	positive regulation of metabolic process
8038	7.95E-03	neuron recognition
51403	8.12E-03	stress-activated MAPK cascade
8037	8.25E-03	cell recognition
60429	8.45E-03	epithelium development
7267	9.57E-03	cell-cell signaling
7165	9.69E-03	signal transduction
48646	9.84E-03	anatomical structure formation involved in morphogenesis
22008	9.86E-03	neurogenesis
9888	9.86E-03	tissue development

Supplemental Table 9: List of neuronal genes balanced in the NBs

Gene ID	Gene Symbol	H3K4me3 mark	H3K27me3 mark
FBgn0035179	CG12038	enriched	enriched
FBgn0030706	CG8909	enriched	enriched
FBgn0259927	CG42450	enriched	enriched
FBgn0031081	Nep3	enriched	enriched
FBgn0031952	cdc14	enriched	enriched
FBgn0032225	CG5022	enriched	enriched
FBgn0033159	Dscam	enriched	enriched
FBgn0010316	dap	enriched	enriched
FBgn0011656	Mef2	enriched	enriched
FBgn0024836	stan	enriched	enriched
FBgn0010238	Lac	enriched	enriched
FBgn0033793	CG3955	enriched	enriched
FBgn0033911	VGAT	enriched	enriched
FBgn0263395	hppy	enriched	enriched
FBgn0034501	CG13868	enriched	enriched
FBgn0050296	RIC-3	enriched	enriched
FBgn0035086	CG12851	enriched	enriched
FBgn0035481	CG12605	enriched	enriched
FBgn0004880	scrt	enriched	enriched
FBgn0028400	Syt4	enriched	enriched
FBgn0243512	puc	enriched	enriched
FBgn0037849	CG4596	enriched	enriched
FBgn0262742	Fas1	enriched	enriched
FBgn0261649	tinc	enriched	enriched
FBgn0038837	CG3822	enriched	enriched
FBgn0051140	CG31140	enriched	enriched
FBgn0003093	Pkc98E	enriched	enriched
FBgn0039688	Kul	enriched	enriched
FBgn0039808	CG12071	enriched	enriched
FBgn0039883	RhoGAP100F	enriched	enriched
FBgn0085432	pan	enriched	enriched
FBgn0019650	toy	enriched	enriched
FBgn0028999	nerfin-1	enriched	enriched
FBgn0010473	tutl	enriched	enriched
FBgn0040281	Aplip1	enriched	enriched
FBgn0085409	CG34380	enriched	enriched
FBgn0263995	cpo	enriched	enriched
FBgn0264574	Glut1	enriched	enriched